11-18-2011

INTEGRATION OF PLANT-BASED CANOPY SENSORS FOR SITE-SPECIFIC NITROGEN MANAGEMENT

Luciano S. Shiratsuchi
University of Nebraska-Lincoln, shozo@huskers.unl.edu

INTEGRATION OF PLANT-BASED CANOPY SENSORS FOR SITE-SPECIFIC NITROGEN MANAGEMENT

by

Luciano Shozo Shiratsuchi

A DISSERTATION

Presented to the Faculty of

The Graduate College at the University of Nebraska

In Partial Fulfillment of Requirements

For the Degree of Doctor of Philosophy

Major: Agronomy

Under the Supervision of Professors Richard Ferguson and John Shanahan

Lincoln, Nebraska

November, 2011

INTEGRATION OF PLANT-BASED CANOPY SENSORS FOR SITE-SPECIFIC NITROGEN MANAGEMENT

Luciano S. Shiratsuchi, Ph.D.

University of Nebraska, 2011

Advisors: Richard B. Ferguson and John F. Shanahan

The soil's nitrogen (N) supply can vary drastically in the field, spatially as well as temporally making any soil prediction difficult even with very detailed mapping. Consequently, a plant-based approach wherein the measured canopy can indicate the N needs in a reactive and spatially-variable way can be a better approach than mapping, because integrate the soil N supply and translate the crop need on-the-go. The first experiment evaluated the performance of various spectral indices for sensing N status of corn, where spectral variability might be confounded by water-induced variations in crop reflectance. We found that water and previous crops effects on vegetation indices (VI) must be considered, and also that some VIs are less susceptible to water with good ability for N differentiation. In the second experiment, the objective was to develop an approach that relies on local soil conditions as well as on active canopy sensor measurements for real-time adjustment of N application rate. We found that local variations in plant N availability must be considered to determine the optimal N rate on-the-go, and that the localized reference incorporated the spatial variability of the N-rich plot. Next, we

determined the correlation between active canopy sensors assessments of N availability and ultrasonic sensor measurements of canopy height at several growth stages for corn. We found strong correlations between both sensors and that they had similar abilities to distinguish N-mediated differences in canopy development. The integrated use of both sensors improved the N estimation compared to the isolated use of either sensor. Based on these strong correlations, we developed an N recommendation algorithm based on ultrasonic plant height measurements to be used for on-the-go variable rate N application. Lastly, we evaluated the crop water status using infrared thermometry integrated with optical and ultrasonic sensors, we concluded that the integration of sensors was beneficial to detect water-stressed zones in the field, affecting yield and possibly promising to delineate zones for N and water management.

ACKNOWLEDGEMENTS

First of all, I would like to give special thanks for my advisers Drs. Richard Ferguson and John Shanahan and also Dr. Viacheslav Adamchuk for all initial and continuous support that they provided for me since the beginning of my first steps in experiencing a new life style here in Lincoln. They were much more than academic supervisors and they are still providing attention and care for us since the day that we met. I would also like to thank Dr. Donald Rundquist for not only being a member of my Scientific Committee, but also helping me to organize my remote sensing concepts and being an example of gracious conduct and effective teacher.

I would like to thank also Dennis Francis, Mike Schlemmer and Jim Schepers who made my stay in USA to be one of the best times of life as researcher, and also for countless hours of great moments of thinking. I believe that all their recommendations and feelings about agricultural research conduct are impossible to describe with words. Dennis, Richard and their families showed unconditional love for our family since we met, so many thanks to them would not be enough.

Special thanks go to all ARS – USDA and South Central Agricultural Laboratory (SCAL) crew that made possible the execution of what I had envisioned as the perfect on-farm research and I had thought that this was almost impossible. They showed that team work can really be effective when affinity between members exist. I was fortunate to meet Glen Slater whose coordination work at SCAL provided me all the resources and logistics to work at the experimental station independently. Without his help and others

(Dave, Perry, Irv, Terry, Cassy, Ryan and Nick) none of my field work would have been possible.

I am grateful to the staff of the ARS and UNL team: Aaron Bereuter, Jeff Shanle, Myron Coleman, Paul Koerner, Luke Pesek, Jamie Pesek, Chris Bauer, Dan Walters, Anatoly Gitelson, Dave Marx, Brian Leavitt, Ahmad, Tri Setiyono, Jessica Torrion for all their help in all aspects and also for tremendous contributions to my professional career.

Many Thanks to Kyle Holland that always provided several types of optical sensors making feasible and smooth the steps of this research program. Special thanks to Collin Lutz and Scot that helped me tremendously to put together the "bike system" (software and hardware), that was the major sensor platform for most experiments. Thanks to the farmers: Evan Brandes, Brandon Hunnicut, Ed Rathje and others that were always available and helpful allowing us to interfere in their regular operation. They are the major reason that justifies the conduction of this type of on-farm research.

I wish to grateful acknowledge the Brazilian Agricultural Research Corporation (EMBRAPA) for all the resources, that made possible for my professional dream to come true. Thanks to Edemar Corazza and Special thanks go to Dr. Edson Sano who supported me with advices and tips on how to make my stay in the USA the best possible.

I also would like to thank the graduate students: Darrin Roberts, Akwasi Abunyewa, Brian Krienke, Atefeh Hosseini, Nabaraj Banjara, Chris Proctor and Nick Ward for their company and laughs during my hard times. Special thanks to Krienke family (Brian and Abbey) who showed sincerely their friendship and the Vossler family (Greg, Cindy, Ethan and Colton) who made me feel at home with their hospitality in my great team roping experiences in Nebraska.

Lastly, the most important thanks goes to my entire family though physically separated by great distance were always present, especially thanks to my wife Simone and my son Kevin who encouraged me with their love and faith, during our great stay here in Lincoln. Without them I could do nothing.

Finally, *eu gostaria de agradecer de joelhos à Deus e ao nosso Senhor Jesus Cristo por nos guiar e proteger durante toda nossa jornada terrestre.* So, I say to you: Ask and it will be given to you; seek and you will find; knock and the door will be opened to you (Luke11:9).

TABLE OF CONTENTS

GENERAL INTRODUCTION

Nitrogen Use Efficiency (NUE)

Given its transformations and mobility in the soil profile, nitrogen (N) is the most dynamic nutrient in agricultural systems. Normally, it is the most limiting nutrient for the achievement of high yield. This complexity makes for uncertainty in its recommendation, based on traditional soil analysis. This dynamic characteristic of N in the soil suggests a need for research and development of new management practices or devices to predict when, where, and how much N is required (Schepers and Raun, 2008).

Current practices for applying N have resulted in low nitrogen use efficiency (NUE) mainly because uniform applications disregard spatial and temporal variability in the soil and crop and also the use of N rates above the crop needs (Raun and Johnson, 1999). Increasing the problem, the risk of N loss (through denitrification, volatilization, surface runoff, leaching, etc.) can be considerably higher if the N fertilizer application timing and procedure are inadequate.

One of the major causes for low NUE is the poor synchrony of soil N supply and crop demand (Shanahan et al., 2008). Normally, N application takes place before the time of N uptake from crops, for practical and operational reasons. When the method and timing of N application is not ideal, related high losses can occur.

In most of the American corn crop production, the N fertilizers have been applied at preplant in early spring or in the late fall. Normally, the high N uptake for crops is two

to six months later in the middle of growing season, with an N uptake peak around VT (Abendroth et al., 2011). This approach causes a delay that can be responsible for a major loss of N to the environment. In the U.S. Corn Belt, an estimated 75% of the N application occurs prior to planting and only 25% after planting, with rates around 150 kg/ha (Shanahan et al, 2008). Considering that only 30% is utilized by crop production, farmers are applying 105 kg N ha^{-1} in each season uniformly to the environment following current management practices.

Nitrogen Management Strategies Using Precision Agriculture

Using the concept of precision agriculture wherein the spatial variability of crops is considered three approaches are available for applying nitrogen fertilizers: (i) map-based (adjusting the N rate according to previous maps); (ii) real time or on-the-go (deciding on the N rate electronically using a device/sensor to measure some characteristic before variable rate application); or (iii) integrated (using a combination of sensor and map) (Adamchuk et al., 2011).

In the effort to increase the NUE in crop systems, many researchers have proposed techniques and procedures involving soil spatial variability based on soil analysis and sensor readings. Examples include: (i) the use of grid sampling to adjust the N fertilizer application (Ferguson et al, 2002); (ii) the use of soil conductivity maps to address different soil types and zones in the field with different N demand (Eigenberg et al, 2006, Heiniger et al., 2003, Perry and Roberts, 2008); and (iii) the use of aerial images or other types of remote sensing techniques to estimate the N and water stress in corn

(Clay et al, 2006 and Hong et al., 2006). All these techniques require some type of mapping approach to be able to vary the N fertilizers in the field. However, the ideal should be to apply the fertilizer in real time or near to that. But how can we measure N demand and apply fertilizers in accordance with crop needs considering the spatial and temporal variability of N in the plant in real time?

Plant-Based Active Canopy Sensors

One promising technique involves the use of proximal remote sensing based on plant-based active canopy sensors (ACS) that can vary the N rate on-the-go without the need for maps to control the application. These sensors have their own light source and they are not influenced by sunlight. The sensors use the crop canopy reflectance in certain wavebands resulting from chlorophyll content in the leaves. This chlorophyll content correlates highly with N content in the plant.

In previous studies with hand-held chlorophyll meters, researchers found that these sensors can detect the onset N stress in many cases before it is visible to the human eye (Schepers et al., 2006). This is early enough to correct N deficiency without reducing yields (Samborski et al., 2009). For the ACS, the recommended in-season N application must be done between V8-V12 to properly address the sensor sensibility for N demand in corn (Martin et al., 2007). Using ACS, Solari et al (2008) found that vegetative stages around V11 and V13 are the best for predicting the N requirement for corn, and that it is possible to use these sensors to address different N rates on-the-go.

In an effort to refine the readings of ACS, Sui & Thomasson (2006) measured relationships between sensors and plant height in cotton. They used one ultrasonic sensor to measure plant height integrated with passive optical sensors. They concluded it is possible to use this integration of sensors to divide the N status into two categories deficiency and non-deficiency with 90% accuracy. In corn forage, Freeman et al. (2007) measured plant height using conventional measurement techniques and found strong relationships between plant height, biomass, yield, N uptake, and optical readings. They concluded that the integration of optical readings and plant height may be used to refine the midseason fertilizer N rates based on expected N removal and by-plant measurements at or before V10. Recently, Yin et al. (2011) showed that plant height can be used for in-season prediction of corn yield. This prediction provides a physiological basis for the use of high-density plant height measurements to guide variable-rate fertilizer N applications within the field and to more accurately estimate crop yield. Individually or together, plant height and vegetation indices can be used to estimate N availability during the corn growing season; consequently their use represents an attractive option for in-season N management.

Vegetation Indices for Crop Canopy Assessment

Active canopy sensors measure the reflectance of the crop canopy in certain wavelengths. Using these vegetation indices (VI), the N fertilizer requirement can be calculated based on the estimated plant N status. Since the 1960's, scientists have extracted and modeled vegetation biophysical variables using remotely sensed data from

these VIs. These are dimensionless, radiometric measures that indicate relative abundance and activity of green vegetation, including leaf-area-index (LAI), percentage green cover, chlorophyll content, green biomass, and absorbed photosynthetically active radiation (APAR) (Jensen, 2007). A vegetation index should: (i) maximize sensitivity to plant biophysical parameters; (ii) normalize or model external effects, such as sun angle, viewing angle, and the atmosphere for consistent spatial and temporal comparisons; (iii) normalize internal effects such as canopy background variations, including topography, soil variations, and differences in senesced or woody vegetation; and (iv) be coupled to some specific measurable biophysical parameter such as biomass, LAI, or APAR as part of the validation effort and quality control (Running et al., 1994). In general these indices are extremely efficient measurements that can be used to retrieve plant vigor, including N nutrition and crop water status. Green plant leaves typically exhibit very low reflectance and transmittance in the visible parts of the spectrum (400-700nm), due to strong absorptance by photosynthetic plant pigments (Chappelle et al., 1992). Leaves absorb mainly blue (~450nm) and red (~660nm) and reflect green (~550nm) wavelengths. By contrast, they reflect and transmit a high portion of the near infrared (NIR) region of the spectrum (~700-1400nm). Innumerous VIs are developed with various purposes, some functionally equivalent as well as some that can provide unique biophysical information (Qi et al., 1995; Zygielbaum et al., 2009). Most are based in the inverse relationship between red and NIR reflectance that are associated with healthy green vegetation. The most famous is the Normalized Difference Vegetation Index (NDVI) that uses the ratio of NIR and red to assess vegetation cover (Rouse et al., 1974). Others are more suitable for high LAI environments due to non-saturation of the red band, including Chlorophyll

Index based Indices (CI) (Gitelson et al., 2005) and others for chlorophyll assessment by orbital platforms such as the Meris Terrestrial Chlorophyll Index (MTCI) (Dash and Curran, 2004). The following conceptual model proposed by Gitelson et al. (2003, 2005) is important to understand and will be used for most indices in the following chapters:

$$[R(\lambda_1)^{-1} - R(\lambda_2)^{-1}] R(\lambda_3) \alpha \text{ pigment}$$

In this model, $R(\lambda_1)^{-1}$ is the inverse reflectance at a wavelength λ_1 which is intended to be maximally sensitive to the pigment of interest; $R(\lambda_2)^{-1}$ is the inverse reflectance at a wavelength that is minimally sensitive to the pigment of interest; and $R(\lambda 3)^{-1}$ is the reflectance at a wavelength that is insensitive to the pigment.

Each VI has its limitation and application, but all have in common the ability to non-destructively enhance the canopy response for some characteristic of interest in this case, for nitrogen and water management.

A Brief History of the ACS Algorithms and Approaches Developed in Nebraska

The first approach for calculating N recommendations based on an optical sensor resulted from a study using chlorophyll meters (Varvel et al., 2007). This study was conducted to develop a plant-based technique to detect and correct N deficiencies in-season using a contact device that clipped the leaf and made readings of chlorophyll absorption using the red (660nm) and near infrared bands (940nm) (SPAD 502, Konica Minolta Sensing Inc., Osaka, Japan). Researchers found high linear correlations between

the sufficiency index (SI) and relative grain yield, showing that both responded similarly to N fertilizer application. This sensor normalization technique (SI) is the ratio of a sensed crop property to the same measurement from a known or standard crop (reference), and is described mathematically as SI = VI of a sensed crop / VI of the reference crop (Holland and Schepers, 2010). The reference crop in this case is a non-limited N crop. Relationships between N rate and SI were described by quadratic models and a function was developed to describe the amount of N to maximize yield. In essence, the researchers used historical yield response functions to determine the N rate that maximized relative grain yield and then subtracted the N rate by the estimated plant N using the hand-held chlorophyll meter, and the difference was the N recommendation. The combined model is: $SI = 0.8073 + 0.002(Nrate) - 0.0000056(Nrate)^2$, assuming $R^2 = 0.70$.

With the advent of ACS technology that did not require contact with the leaf allowing on-the-go measurements of plant N status and application in real time Solari et al., (2006, 2008 and 2010) stepped forward to supply the first algorithm in Nebraska to use with this new generation of sensors. They developed an algorithm for ACS based on the linear relationship between ACS sensor SI and SPAD SI, employing the same quadratic equation determined from Varvel et al. (2007) and based on the good correlation between both sensors: N recommended = $317\sqrt{0.97 - SI}$, where SI is the ACS sensor readings in real time. Even when based on chlorophyll meter data, the algorithm developed provided reasonable estimates of N recommendations for maximizing yields (Solari et al., 2010; Roberts, 2009; Roberts et al., 2010).

Finally, Holland and Schepers (2010) derived a variable rate N application model that is a mathematical procedure to describe the general shape of an N fertilizer response function (sensor index vs. N rate) and the relationship between N rate and in-season crop vegetation index data acquired with the use of sensors. The major difference from the previous algorithm is that the new algorithm allows the user to input parameters that can change the N recommendation. For example, given the N rate that should maximize yield for the specific site and previous experiences from the producer and if the possible N response and the sensor reading threshold are below some specific SI, the N recommended will be reduced. In general, the new algorithm offers more flexibility, since it has not embedded an N rate that maximizes yield as the previous algorithm. On the other hand this algorithm offers more sources for human error if the inputs are not properly selected by the user. The recent algorithm model is being validated and incorporated on sensors firmware. Continuous advances are being made to improve the utility of these ACS for in-season N application. The algorithm is:

$$N\,rec = (Nopt - Npre - Ncrd + Ncomp)\sqrt{\frac{(1 - SI)}{\Delta SI(1 + 0.1e^{m(SItreshold - SI)})}}$$

In this model, N rec is the N rate that should be applied in kg ha^{-1} ; Nopt is the economic optimum nitrogen rate (EONR) or the maximum N rate prescribed by producers; Npre is the N rate applied before sensing; Ncrd is the N credit for the previous season's crop, nitrate in the water, or manure application; Ncomp is the N in excess of Nopt required by the crop under soil limiting conditions at a given growth stage; SI is the sufficiency

index; m is the back-off rate variable (0<m<100); and SI treshold is the back-off cut-on point.

Influence of Detailed Topography in Crop N and Water Demand

Another factor that can be used to fine-tune any algorithm or approach to variable N application is the influence of topography features in the N availability for the corn plant. Previous research has shown that slope is correlated with yield and nutrient availability. Plant roots absorb nutrients better at low slope; high water-holding capacity in these areas results in higher-yielding areas. However, apparent electrical conductivity (EC) could better explain the yield response than elevation features alone (Kitchen et al., 2003). Other studies show that topographical features can result in high- and low-yielding areas, depending on rainfall in that year. High slope normally tends to diminish the infiltration rate and the soil water-holding capacity (Kaspar et al., 2003, Kravchenko et al., 2005). Numerous properties influence the suitability of soil as a medium for crop growth and yield. These include soil water-holding capacity, water infiltration rate, texture, structure, bulk density, organic matter, pH, fertility, soil depth, topography features, the presence of soil restrictive layers, and the quantity and distribution of crop residues. These properties are complex and vary spatially as well as temporally within fields (Kitchen et al., 2003). Use of Real Time Kinematic Global Positioning Systems (RTK GPS) to make detailed maps of the topography could provide a valuable layer of information for refining the N application and evaluating the crop water status. Several

variations of N response and corn yield using ACS can be found in the literature, but no investigations attempt to correlate sensor responses to detailed topographic features.

Influence of Previous Crop and Irrigation Level in N Requirement for Corn

Given changes resulting from the previous crop and the irrigation level in the system, can the N estimation by ACS be the same for different rotations and water levels? Long-term experiments evaluating the soybean nitrogen contribution to corn and sorghum in western Corn Belt rotations showed that corn in the rainfed and irrigated fields obtained around 65 kg N ha^{-1} $year^{-1}$ from soybean in a two year rotation with soybean, and rainfed sorghum obtained 80 kg N ha^{-1} $year^{-1}$ from soybean in a soybean-sorghum rotation (Varvel and Wilhelm, 2003). Researchers concluded that these credits must be considered when N fertilizer recommendations are formulated otherwise, excessive N applications take place, increasing the N available for loss either through leaching or denitrification.

Eck (1984) showed that because of the opportunity for better N management, the interactions between N rates and water level must be taken into consideration when assessing corn production. However, it is very difficult to separate those factors in practical conditions. Al-Kaisi & Yin (2003) showed that reducing water level by 20% (from 100% ET to 80% ET) had no effect on corn yield.

Studies show that water can have more effect on plant reflectance than N stress (Elwadie et al., 2005). Schlemmer et al., (2005) found that chlorophyll meter readings were also affected by water treatments, but research is needed to assess the influence of

previous crop and different water levels and N supply in the vegetation indices key for the algorithms used for the on-the-go N application using ACS. How do these VI calculated from ACS vary with different water levels and previous crops that contribute to indigenous N? Is there any way to optimize the crop sensing to separate N from water influence? Can canopy temperature help improve the ability to separate N and water?

RESEARCH OBJECTIVES

The general objective of this research program was to develop in-season N management strategies to optimize the on-the-go N application in irrigated cornfields by the integration of plant-based canopy sensors. The specific objectives are described in the following chapters:

Chapter 1

Investigate the performance of various spectral indices for sensing the N status of corn, where spectral variability might be confounded by water-induced variations in crop reflectance.

Chapter 2

Develop an approach that relies on local soil conditions as well as on active canopy sensor measurements for real-time adjustment of N application rate; evaluate the correlations between localized plant status and soil attributes in variable landscapes.

Chapter 3

Determine the correlation between active optical reflectance crop canopy sensors assessments of N availability and ultrasonic sensor measurements of canopy height at several growth stages for corn; test the ability of both sensors to distinguish N-mediated differences in canopy development; and evaluate benefits of the integrated use of both sensors.

Chapter 4

Develop an N recommendation algorithm based on ultrasonic plant height measurements to be used for in-season and on-the-go variable rate N application; validate and compare the algorithm proposed with other approaches for in-season N fertilization.

Chapter 5

Evaluate the crop water status using infrared thermometry integrated with optical and ultrasonic sensors considering detailed topographical features.

REFERENCES

Abendroth, L.J., R.W. Elmore, M.J. Boyer, and S.K. Marlay. 2011. Corn Growth and Development. PMR 1009. Iowa State University Extension, Ames, IA.

Adamchuk, V.I., Viscarra Rossel, R.A., Sudduth, K.A., Schulze Lammers, P. 2011. Sensor fusion for precision agriculture. In: Thomas, C., editor. Sensor Fusion - Foundation and Applications. Croatia: In-Tech. p. 27-40.

Al Kaisi, M.M; Yin, X. 2003. Effects of Nitrogen rate, irrigation rate, and plant population on corn yield and water use efficiency. Agron. J. 95:1475-1482

Chapelle, E.W., Kim, M.S., McMurtrey, J.E. 1992. Ratio analysis of reflectance spectra (RARS). An algorithm for the remote estimation of the concentrations of chlorophyll-a, chlorophyll-b, and carotenoids in soybeans leaves. Remote Sensing of Environment, 39: 239-247.

Ciganda, V.; Gitelson, A.; Scheppers, J. 2008. Vertical profile and temporal variation of chlorophyll in maize canopy: quantitative “crop vigor” indicator by means of reflectance-based techniques. Agron. J. 100: 1409-1417

Clay, D.E.; Kim, K.; Chang, J.; Clay, S.A.; Dalsted, K. 2006. Characterizing water and nitrogen stress in corn using remote sensing. Agron. J. 98:579-587

Dash, J. and Curran, P.J. 2004. The MERIS terrestrial chlorophyll index. International Journal of Remote Sensing 25: 5403-5413.

Eck, H. 1984. Irrigated corn yield response to nitrogen and water. Agron. J. 76:421-428

Elwadie, M.E., F.J. Pierce, and J. Qi. 2005. Remote sensing of canopy dynamics and biophysical variables estimation of corn in Michigan. Agron. J. 97:99–105

Eigenberg, R. A., Nienaber, J. A., Woodbury, B.L., Ferguson, R.B. 2006. Soil Conductivity as a Measure of Soil and Crop Status—A Four-Year Summary. Soil Science Society of America Journal 70, 1600-1611.

Eigenberg, R.A.; Nienaber, J.A.; Woodbury, B.L.; Ferguson, R.B. 2006. Soil conductivity as a measure of soil and crop status – a four year summary. Soil Sci. Soc. Am. J. 70: 1600-1611.

Freeman, K.W.; Girma, K.; Arnall, D.B.; Mullen, R.W.; Martin, K.L.; Teal, R.K.; Raun, W.R. 2007. By-plant prediction of corn forage biomass and nitrogen uptake at various growth stages using remote sensing and plant height. Agron. J. 99:530-536

Ferguson, R.B., Hergert, G.W., Schepers, J.S., Gotway, C.A., Cahoon, J.E., Peterson, T.A. 2002. Site-specific nitrogen management of irrigated maize: Yield and soil residual Nitrate Effects. Soil Science Society of America Journal 66, 544-553.

Gitelson, A.A., A. Viña, T.J. Arkebauer, D.C. Rundquist, G. Keydan, and B. Leavitt. 2003. Remote estimation of leaf area index and green leaf biomass in maize canopies. Geophys. Res. Lett. 30(5):1248 doi:10.1029/2002Gl016450.

Gitelson, A.A., Vina, A., Ciganda, V., Rundquist, D.C., Arkebauer, T.J. 2005. Remote estimation of canopy chlorophyll content in crops. Geophysical Research Letters 32: 4-7.

Heege, H.J.; Reusch, S.; Thiessen, E. 2008. Prospects and results for optical systems for site-specific on-the-go control of nitrogen-top-dressing in Germany. Agron. J. 9:115-131

Heiniger, R.W., McBride, R.G., Clay, D.E. 2003. Using Soil Electrical Conductivity to Improve Nutrient Management. Agron. J. 95, 508-519.

Holland, K.H., Schepers, J.S. 2010. Derivation of a Variable Rate Nitrogen Application Model for In-Season Fertilization of Corn. Agron. J. 102: 1415-1424.

Hong, N., White, J.G., Weisz, R., Crozier, C.R., Gumpertz, M.L., Cassel, D. K. 2006. Remote Sensing-Informed Variable-Rate Nitrogen Management of Wheat and Corn. Agron. J. 98, 327-338.

Jensen, J.R. 2007. Remote Sensing of the environment: an earth resource perspective. Upper Saddle River: Prentice Hall. 592p.

Kaspar, T.C., T.S. Colvin, D.B. Jaynes, D.L. Karlen, D.E. James, D.W. Meek. 2003. Relationship Between Six Years of Corn Yields and Terrain Attributes. Precision Agriculture. 4: 87-101.

Kitchen, N.R., Drummond, S.T., Lund, E.D., Sudduth, K.A., Buchleiter, G.W. 2003. Soil Electrical Conductivity and Topography Related to Yield for Three Contrasting Soil–Crop Systems. Agron. J. 95: 483-495.

Kravchenko, A.N., Robertson, G.P., Thelen, K.D., Harwood, R.R. 2005. Management, topographical, and weather effects on spatial variability of crop grain yields. Agron. J. 97: 514-523.

Martin, K.L., K. Girma, K.W. Freeman, R.K. Teal, B. Tubana, D.B. Arnall, B. Chung, O. Walsh, J.B. Solie, M.L. Stone, and W.R. Raun. 2007. Expression of variability in corn as influenced by growth stage using optical sensor measurements. Agron. J. 99: 384–389.

Perry, E.M., Roberts, D. A. 2008. Sensitivity of Narrow-Band and Broad-Band Indices for Assessing Nitrogen Availability and Water Stress in an Annual Crop. Agron. J. 100: 1211-1219.

Qi, J., Moran, M.S., Dedieu, G. 1995. Biophysical parameter estimations using multidirectional spectral measurements. Remote Sensing of Environment. 53: 188-198.

Raun, W.R.; Solie, J.B.; Stone, M.L.; Martin, K.L.; Freeman, K.W.; Mullen, R.W; Zhang, H. Scheppers, J.S.; Johnson, G.V. 2005. Commun. In Soil Sci. and Plant An. 36:2759-2781

Rouse, J. W., Hass, R.W., Schell, J. A., Deering, D. W., Harlan, J.C. 1974. Monitoring the vernal advancement of retrogradation of natural vegetation. Greenbelt, Md.: NASA Goddard Space Flight Center.

Running, S.W., Justice, C.O., Solomonson, V., Hall, D., Barker, J., Kaufmann, Y.J., Strahler, A.H., Huete, A.R., Muller, J.P. Vanderbilt, V., Wan, Z.M., Teilett, P.,

Carneggie, D. 1994. Terrestrial remote sensing science and algorithms planned for EOS/MODIS. International Journal of Remote Sensing. 15: 3587 – 3620.

Samborski, S.M., Tremblay, N., Fallon, E. 2009. Strategies to Make Use of Plant Sensors-Based Diagnostic Information for Nitrogen Recommendations. Agron. J. 101: 800-816

Shanahan, J.F.; Kitchen, N.R.; Raun, W.R.; Schepers, J.S. 2008. Responsive in-season nitrogen management for cereals. Computers and Electronics in Agriculture 61(1): 51-62

Schepers, J.S., D. Francis, and G. Varvel. 2006. Chlorophyll meters. USDA- ARS, Gov. Print. Offi ce, Washington, DC.

Schepers, J.S., and W.R. Raun. 2008. Nitrogen in agricultural systems. ASA, CSSA, and SSSA, Madison, WI.

Schlemmer, M.R., D.D. Francis, J.F. Shanahan, and J.S. Schepers. 2005. Remotely measuring chlorophyll content in corn leaves with diff ering nitrogen levels and relative water content. Agron. J. 97:106–112

Solari, F. 2006. Developing a crop based strategy for on-the-go nitrogen management in irrigated cornfields. PhD Dissertation, University of Nebraska, Lincoln. 157p.

Solari, F.; Shanahan, J.F.; Ferguson, R.B.; Scheppers, J.S.; Gitelson, A. 2008. Active sensor reflectance measurements of corn nitrogen status and yield potential. Agron. J. 100(3):571-579

Solari, F., Shanahan, J.F., Ferguson, R.B., Adamchuk, V.I. 2010. An Active Sensor Algorithm for Corn Nitrogen Recommendations Based on a Chlorophyll Meter Algorithm. Agron. J. 102, 1090-1098.

Sui, R.; Thomasson, J.A. 2006. Ground-based sensing system for cotton nitrogen status determination. Transactions of the ASABE 49(6): 1983-1191

Varvel, G.E., Wilhelm, W.W., Shanahan, J.F., Schepers, J.S. 2007. An Algorithm for Corn Nitrogen Recommendations Using a Chlorophyll Meter Based Sufficiency Index. Agron. J. 99, 701-706.

Varvel, G.E. and Wilhelm, W.W. 2003. Soybean Nitrogen Contribution to Corn and Sorghum in Western Corn Belt Rotations. Agron. J. 95, 1220-1225.

Yin, X., Mcclure, M.A., Jaja, N., Tyler, D.D., Hayes, R.M. 2011. In-Season Prediction of Corn Yield Using Plant Height under Major Production Systems. Agron. J. 103, 923-929.

Zhang, J., Blackmer, A.M., Ellsworth, J.W., Koehler, K.J. 2008. Sensitivity of Chlorophyll Meters for Diagnosing Nitrogen Deficiencies of Corn in Production Agriculture. Agron. J. 100: 543-550.

Zygielbaum, A.I., Gitelson, A. a, Arkebauer, T.J., Rundquist, D.C. 2009. Non-destructive detection of water stress and estimation of relative water content in maize. Geophysical Research Letters 36, 2-5.

CHAPTER 1

COMPARISON OF SPECTRAL VEGETATION INDICES DERIVED FROM ACTIVE CROP CANOPY SENSORS FOR CORN (*Zea mays, L.)* GROWN UNDER DIFFERENT CROP ROTATIONS AND IRRIGATION LEVELS

ABSTRACT

Much of the previous evaluation of active crop canopy sensors for in-season assessment of crop nitrogen (N) status has occurred in environments without water stress. The impact of concurrent water and N stress on the use of active crop canopy sensors for in-season N management is unknown. The objective of this study was to evaluate the performance of various spectral indices for sensing N status of corn, where spectral variability might be confounded by water-induced variations in crop reflectance. The study was conducted in 2009 and 2010 with experimental treatments of irrigation level (100 and 70% ET), crop rotation (corn - corn or soybean-corn) and N fertilizer rate (0, 75, 150 and 225 kg N ha^{-1}). Crop canopy reflectance was measured from V11 to R4 stage using two active sensors – a two band (880 and 590nm) and a three band (760, 720 and 670 nm). Among the indices, the vegetation index studied by Datt et al. (1999) (DATT) and Meris Terrestrial Chlorophyll Index (MTCI) were the least affected by water stress, with good ability to differentiate N rate with both crop rotations. The Chlorophyll Index using amber band (CI), Normalized Difference Vegetation Index using Red Edge band (NDVI_RE) and the Normalized Vegetation Index using the Red band (NDVI_Red) showed more variation due to water supply, and had only moderate ability to differentiate N rates.

Abbreviations List: ACS: active crop canopy sensors, CC: irrigated corn after corn; CS: irrigated corn after soybean; NSI:nitrogen sufficiency index; ET: evapotranspiration. NIR: near infrared; CI: chlorophyll index vegetation index using amber and NIR; CIRE: chlorophyll index vegetation index using red edge and NIR; DATT: vegetation index calculated using NIR, red edge and red bands published by Datt et al. (1999); MTCI: Meris terrestrial chlorophyll index; NDVI_RE: normalized difference vegetation index using the red edge band; NDVI_Red: normalized difference vegetation index using the red band.

INTRODUCTION

In-season nitrogen (N) management for corn using active crop canopy sensors (ACS) relies on the use of algorithms that can trigger on-the-go N fertilization in the field based on crop canopy reflectance. Optical sensing equipment that employs this approach is commercially available and these sensors rely on some version of a vegetation index to express crop reflectance (Shanahan et al., 2008; Eitel et al., 2008) and prescribe N rate application.

There are different approaches and vegetation indices used to determine N rate based on these sensors, but the majority of algorithms use the N sufficiency index (NSI) approach previously proposed for chlorophyll meter readings (Varvel et al., 1997). For example: when the ratio between a targeted region in the field and a well-fertilized reference in the same field reaches a certain level, N fertilizer is needed according to a function that describes the relationship between yield and NSI readings (Bausch and Duke, 1996). Some N rate recommendation algorithms utilize yield potential that is determined by growing degree days and an estimate of biomass at the day of sensing

(Raun et al., 2002). Several additional vegetation indices have been used to calculate N rate for corn and wheat using active canopy sensors, such as the Green Normalized Difference Vegetation Index (GNDVI) (Dellinger et al., 2008), and the Chlorophyll Index (CI) (Solari et al., 2008).

Regardless of the approach used, an understanding of how these indices may be influenced by water stress and previous crop is needed. Previous work by Eitel et al. (2008) investigated the impact of water availability and N stress on leaf area index (LAI) in wheat using a multispectral radiometer and a chlorophyll meter. They showed that the ratio of the Modified Chlorophyll Absorption Ratio Index to the second Modified Triangular Vegetation Index (MCARI/MTVI2) is sensitive to N and less susceptible to variable LAI caused by water stress. Another example of interaction between water and N stress in corn using remote sensing was the work done by Clay et al. (2006), where broad band widths were used to calculate different indices (NDVI, GNDVI, NDWI (Normalized Difference Water Index) and NRI (N reflectance index), with the major conclusion being that water and N had additive effects on yield and optimum N rates (100 – 120 kg N ha^{-1}) were similar across different water levels. There are other examples of indices used specifically to detect water stress (Zygelbaum et al., 2009), to determine chlorophyll content, and to estimate gross primary productivity (Lemaire et al, 2004; Inoue et al., 2008, Wu et al., 2009). All these indices were developed using spectral radiometers or other passive sensors. The same approaches can be used with active crop canopy sensors to calculate vegetation indices for in-season N management. However, the degree they are influenced by water stress and previous crop in corn production is unknown.

The objectives of this study were: (i) to compare the performance of various spectral indices for measuring N status in corn at different irrigation levels and crop rotations; (ii) determine the potential of these indices to differentiate N rate at different crop stages; (iii) compare the correlation of indices collected during vegetative growth stages with grain yield.

MATERIAL AND METHODS

Experimental Design and Site Description

The experimental site was located at the University of Nebraska South Central Agricultural Laboratory (40.57012368 º N, -98.14329432 º W, 558 m above mean sea level, Map Datum WGS 84) near Clay Center during the 2009 and 2010 growing seasons. The soil at this site is predominantly Crete silt loam (fine, smectitic, mesic Pachic Argiustolls), 0-1% slope and previously for 3 years in continuous corn. Experimental treatments consisted of two irrigation levels (70 and 100% of estimated evapotranspiration - ET), two crop rotations (corn after corn - CC and corn after soybean - CS), and four N rates (0, 75, 150 and 225 kg Nha^{-1}). The experimental design was a randomized complete block split split plot, with irrigation level as the main plot, previous crop as the subplot, and fertilizer N rate as sub-subplots. The irrigation treatments were delivered using a linear-move sprinkler system that varied travel speed to change water application rate. Climatological data were recorded on-site for both growing seasons using an automated weather station. Planting dates, plant population and row spacing

were similar both years (Table 1). Soil sampling and analysis was done each spring to characterize soil fertility where the experiments were conducted (Table 2). Soil pH was determined according to Watson and Brown (1998); extractable P and K were determined by Mehlich I (Sims, 1989), organic matter was estimated by loss-on-ignition method (Nelson and Sommers, 1996) and the micronutrients by routine of certified laboratory procedures. The previous soybean crop was planted during the 2008 growing season to start the crop rotation. Crops were planted and managed using best management practices for high yielding corn, optimizing the supply of all crop nutrients other than N (Table 2).

Crop Canopy Sensing

Crop canopy reflectance was measured for corn during the following growth stages V11, V13, V15, R2, R3 and R4 (Abendroth et al., 2011) using two active canopy sensors – a two-band sensor (880 and 590 nm, Crop Circle 210), and a three band sensor (760, 720, and 670 nm, Crop Circle 470) (Holland Scientific, Lincoln, Nebraska, USA). The platform used for sensor data acquisition consisted of a bicycle modified to support two optical sensors, a GeoXT GPS receiver (Trimble Navigation, Ltd., Sunnyvale, California, USA) and a netbook computer (Figure 1).

The platform provided the ability to maintain a distance of at least 60 cm between the sensors and the top of the crop canopy when acquiring readings throughout the growing season and avoiding soil compaction near the row and additional damage that could occur if high clearance machinery were used. Each plot (9.14 x 6.09 m) consisted of 8 rows, and rows 3 and 6 were sensed at each growth stage with about 30 sensor

output mean values recorded per plot. Both optical sensors were mounted together to measure the crop reflectance at about the same target (sensor were mounted 0.3 m apart). In order to sense rows 3 and 6, two passes were made through each plot. Approximately 12 readings from each sensor were averaged to record with each geographical location. With the typical speed traveled through plots, and one GPS location recorded per second, approximately 30 geographic locations were recorded for each plot. Sensors measurements were collected and integrated (averaged) using customized LabView software (National Instruments, Austin, Texas, USA), filtered using MathLab (Mathworks, Natick, Massachusetts, USA), Microsoft Excel and ArcGIS 9.3 (ESRI, Redlands, California, USA) to eliminate the plot-border effect and some GPS inaccuracies. Collected and filtered data were used for statistical data analysis (SAS 9.2) (SAS, Cary, North Carolina, USA).

Vegetation Indices

Six vegetation indices (CI, CIRE, DATT, MTCI, NDVI_RE and NDVI_Red) were evaluated in terms of their potential to differentiate N rates with both irrigation levels and crop rotations (Table 3). The criteria for index selection for N assessment was guided by previous successful use in cereal crops (CI and NDVI); possibility of use with satellite imagery (MTCI) and by the ranking proposed by Lemaire (2004), where the root mean square error (RMSE) was minimized and the agreement with the PROSPECT Model (Jacquemoud and Baret, 1990) was maximized for chlorophyll estimation (it was the case for the DATT index)

All vegetation index values were normalized (actual index value divided by the index value of the highest N rate) to facilitate comparison among indices and to perform statistical analysis. The normalization was cited in previous work as the Sufficiency Index (SI) and is used to minimize factors that can affect vegetation indices, including N rate, hybrid, stages of growth, and environmental conditions. (Schepers et al., 1992; Schepers, 1994; Varvel et al., 1997).

Soil Moisture Measurement and Crop Yield Assessment

Soil moisture content was monitored hourly during the growing season by means of Watermark soil moisture sensors (Irrometer Co, Riverside, California, USA) installed at 30, 61 and 91 cm depths in plots with 225 kg Nha^{-1} for the two different water levels (70 and 100 % ET) and crop rotations (CC and CS). For comparison between irrigation levels, the soil matric potential was averaged by day for each depth.

Grain yield for each plot was measured with a plot combine Gleaner K (2 rows) using the Harvest Master System (Juniper Systems Inc., Logan, Utah, USA) and corrected to an average grain moisture content of 15.5 g kg^{-1}.

Statistical Analyses

To evaluate treatment effects on grain yield, the two years of data were analyzed by the PROC MIXED procedure of SAS for ANOVA and means separation using the Duncan's Multiple Range Test ($p<0.1$), Year, irrigation levels, crop rotations, as well as

replications were considered random effects. The effects of treatments on vegetation indices also used repeated measures ANOVA (time-repeated measures analysis) with PROC MIXED since several growth stages were measured for each of the six vegetation indices evaluated both years, under different crop rotations, irrigation levels and N rates. Again, only two levels of irrigation were tested, Year was included as a random effect and was considered a replication of irrigation level in the statistical analysis. To test the ability of the vegetation indices to differentiate N rates under different rotations the Duncan Multiple Range Test ($p<0.10$) was used disregarding irrigation effects. The vegetation indices were tested for the effects of irrigation levels comparing the variance between the vegetation indices considering variation caused by two irrigation levels (70 and 100% ET) using the Barlett's test. The vegetation indices were ranked by Pairwise F test comparison from the least to the most affected by irrigation levels, considering the variation caused by irrigation levels for each index during 2 years. Lastly to measure the relationship between vegetation indices, chlorophyll meter and grain yield PROC GLM and MANOVA (Multivariate Analysis of Variance) were used to obtain partial correlations adjusting for irrigation levels and crop rotations.

RESULTS AND DISCUSSION

Rainfall and temperature history, along with application amounts for the 100% ET irrigation treatment, are shown in Figure 2 for both growing seasons. Overall climatic conditions were near normal for this location, although 2009 was slightly warmer and drier in the early season than the same period in 2010. Consequently, irrigation was

initiated earlier in 2009 (around V10) than in 2010 (around V13) (Figure 2). The soil-moisture content at V11 and V13 was lower for the 70% ET treatment compared to 100% ET, even without the irrigation which was implemented in 2010 (Figure 3), likely due to irrigation limitation a imposed in the previous season.

Treatment Effects on Grain Yield

Irrigation Level

There was no effect of irrigation levels (70 and 100% ET) on corn grain yield, and neither of the two-way interactions of interest (Rotation*Irrigation and N*Irrigation) were significant. Al-Kaisi and Yin (2003), studying the effects of irrigation, plant population and N rate on corn yield, observed similar results where application of water at 80 % and 100 % ET had no difference in water extraction from the soil profile and also no yield advantage for 100% ET. Such results suggest that reducing irrigation level (e.g., 80 % ET) can save water with little impact on grain yield.

In 2009, grain yield for irrigation levels were significantly different, with the 100% ET treatment yielding 591 kg ha^{-1} more than the 70% ET treatment. However, in 2010 there were no statistically significant differences in grain yield with irrigation level, though the difference was still 487 kg ha^{-1}. In 2009, the average grain yield was higher and optimized by irrigation. Yield differences due to water levels can vary due to several factors, such as irrigation timing. Payero et al. (2009) showed that corn yield with the same level of water supply can vary with different timing of irrigation application.

During both years, and by grouping water levels (disregarding the previous crop), the difference between 70 and 100 % ET treatment yields were 538 kg ha^{-1}, with 10846 and 11385 kg ha^{-1} for 70 and 100 % ET, respectively (Figure 4). For the CC rotation, yields were 9322 kg ha^{-1} and 9323 kg ha^{-1} for 70 and 100 % ET respectively, showing no yield advantage due to the higher irrigation level (Figure 5). For the CS rotation, yields were 12370 and 13447 kg ha^{-1} for 70 and 100 % ET with a difference of 1,077 kg ha^{-1} (significant at $p < 0.1$, Duncan's Multiple Range Test) (Figure 5).

Previous Crop and Nitrogen Rate

The N x Rotation interaction was statistically significant, indicating that yield responses to N were different between the two crop rotations (Table 4 and Figure 4).

Average yield differences between crop rotations were considerable (3585 kg ha^{-1}). This shows how legumes as a previous crop can improve crop productivity, with greater access to mineralized soil N due to the low C:N ratio of the soybean residue. In 2009, at the 70 % ET irrigation level, yield differences between CC and CS were 2924 kg ha^{-1} ($p < 0.01$), with yields of 10763 kg $ha^{-1}$and 13688 kg ha^{-1}respectively. For the 100% ET irrigation level, the differences were similar (2,963 kg ha^{-1}), but yield levels were higher (11334 and 14294 kg ha^{-1}).

All N fertilization rates significantly increased corn yield in the CC rotation, showing almost linear response to N. On the other hand, fertilizer N rate higher than 150 kg N ha^{-1}did not increase grain yield when the previous crop was soybean in 2009 (Figure 4).

For the CS rotation in 2010, there were higher yields with the 100% ET treatment compared to the 70% ET treatment, and greater yield response to N at lower N rates (Figure 5).

Treatments Effects on Vegetation Indices

Water Effects on Vegetation Indices

The amount of water available to plants began to be limiting around V11 in 2009 and past V13 in 2010, when irrigation commenced and there were differences in soil-moisture levels between irrigation treatments (Figures 2 and 3). Due to rainfall patterns, the effect of irrigation level on vegetation indices were evaluated at later growth stages than the time window recommended for N application. Treatments were evaluated when soil moisture levels were different between irrigation levels (V11and R4 growth stages in 2009 and R4 in 2010). Only spectral reflectance data collected at the V11-R4 growth stages were included in the analysis of variance (Table 5). The analysis of variance for vegetation indices indicated that during the period of V11 through R4, there were no incidences of statistically significant four- and three-way interactions of treatment effects on vegetation indices. Of primary interest then are the significant two-way interactions involving growth stage, previous crop and N rate. For example, the N*Rotation interaction was significant for all indices. The effect of irrigation level on vegetation indices varied between the two years, as expected.

Vegetation Index values were normalized (actual index value divided by the index value of the highest N rate) to facilitate comparison among indices (Figures 6 and 7).

Before testing the response of vegetation indices to irrigation level, we evaluated the impacts of site characteristics (background soil fertility, historical management) on vegetation indices early in the growing season when there was no water stress. For both years, there was no influence of site characteristics (soil organic matter differences, soil texture, residual soil N, residue) on canopy reflectance (data not shown), so we can assume that the variations in vegetation indices were influenced primarily by irrigation water level and fertilizer N rate.

The Barlett's Test showed significant differences due to the variance caused by irrigation levels on the six vegetation indices (again there were six, not two, variances being compared with Bartlett's)analyzing all vegetation indices together (degrees of freedom = 5; Chi square = 26.71; $p < 0.05$).Using a F test to separate pairwise variances the vegetation indices were ranked accordingly to the variance caused by irrigation level (Table 6).

Among all indices tested, the DATT index was least influenced by irrigation level and showed the lowest mean square error and standard error (Table 6, Figures 6 and 7). This may be particularly important in environments where water stress is likely to be confounded with N stress, but its response to N rates was smaller during the window for in-season N management for both years compared to MTCI or CIRE. The DATT vegetation index was first validated for sensitivity to chlorophyll content in uncorrected as well as the scatter-corrected spectra, showing that this index can enhance the

chlorophyll absorption in reflectance by removing the interferences caused by variations in leaf scatter that can be affected by water stress and leaf and architecture (Datt, 1999).

The MTCI was the second least influenced by irrigation level, but it had a higher standard error for fertilizer N rate than the DATT index (Figures 6 and 7). However, the N response was better in the sense of showing less saturation with an increase of N rate, and it displayed better distinguishing ability with regard to differences in N supply. The vegetation indices CI and CIRE showed good responses to N rates but they were the most affected by water level at V11 and R4 (Table 6, Figure 6 and 7).

The NDVI_RE was the third best index in terms of identifying N stress independent of irrigation level, but it plateaued beyond 75 kg ha^{-1}ha of fertilizer N in 2009, limiting its utility for N fertilizer application and compromising its ability to differentiate N rates in that particular year. It is important to point out that the slope of response for N rates was smaller (as expected) when NDVI was used to estimate chlorophyll content or biomass due to saturation at high leaf area index (LAI) at those corn stages (Gitelson, et al, 1996). So, the expected saturation of the NDVI (Gitelson, 2004) also occurred in this experiment at these growth stages (Figure 6K and 6L, and 7K and 7L).

In general, we observed that corn plants under water stress (70% ET) had changes in leaf structure rather than LAI, but only at later stages (after VT). As reported earlier, impacts of water stress will vary with growth stage, but water stress at early growth stages will affect LAI the most (Çakir, 2004). Normally, in this region of the Great Plains, irrigation commences between V14 and VT growth stages, depending on stored soil water and precipitation. Consequently, irrigation effects on vegetation indices may

not be evident until after the VT growth stage (Figure 7). During vegetative stages, there were more pronounced effects of irrigation level only at (V11) in 2009, as it was a drier season than 2010.

Ability of the Vegetation Indices to Differentiate N Rates

Among the indices proposed for assessment of crop N status, CIRE, MTCI and NDVI_RE did not have a significant N*Stage interaction, indicating that these indices did not require a specific growth stage within this window (V11 until R4) to differentiate N rates. All other N management indices need adjustments for specific growth stage to be used for managing N within the window studied. All indices had similar responses, but CI, CIRE and NDVI_Red had significant N*Rotation*Stage interactions, indicating that those indices may vary in their ability to differentiate the impact of N rate at these growth stages.

In 2009 the CI, CIRE, DATT and MTCI indices could differentiate fertilizer rates of 0, 75 and 150 kg N ha^{-1} for the CC rotation at V11 until R6 (table 8), while the NDVI_RE index was only able to differentiate 0 kg ha^{-1} from the other N rates at the R6 growth stage (all averaged over irrigation level). The NDVI_Red index could differentiate N rates at V13, R2 and R4. The DATT and MTCI indices could differentiate fertilizer rates of 0, 75 and 150 kg N ha^{-1} with the CS rotation at V15 (Table 7). The CIRE and NDVI_RE indices could only differentiate zero from the other N rates at vegetative stages betweenV11 and V15 with CS rotation. The CI, DATT and MTCI

indices were able to separate N rates after tasseling until R6 but NDVI_RE and NDVI_Red separated N rates only at R6 with CS rotation in 2009.

In 2010, with the CC rotation, all indices could differentiate N rates from V7 until R3. The NDVI_Red could not differentiate 75 kg N ha^{-1} from 150 kg N ha^{-1} during R3, R4 and R6 (Table 8). With CS rotation, the CI, CIRE, MTCI and DATT indices could differentiate N rates during most of the vegetative growth stages. The NDVI_Red index could not differentiate N rates after V15. Except for R6 all indices could at least separate 0 kg ha^{-1} form the orher N rates. Similar results were found in another long term CC experiment where a two band sensor (Crop Circle 210) was used to differentiate N rates in small plots, where in a growing season with high N response the sensor could differentiate most N rates (0, 75, 150 and 300 kg Nha^{-1}), and in another growing season they could distinguish only 0 kg ha^{-1} from other N rates using CI (Shiratsuchi et al., 2009).

Among all indices tested, the MTCI and DATT indices were found to have the best ability to differentiate the effect of fertilizer N rate on crop canopy status, across different levels of irrigation and previous crop. For this reason, these indices were used to illustrate the difference in vegetation-index response with different previous crops (Figure 8). It is important to stress that MTCI and DATT were minimally affected by irrigation level and therefore could be better indices to sense for N variances in situations where N deficiency and water stress occurs simultaneously.

In dry environments where irrigation is imposed and the water management is near optimal, the DATT and MTCI could perform better for site-specific N management than the other vegetation indices tested, because they showed better sensitivity to N rate

and less variability due to irrigation levels. If the previous crop was soybean in a rain fed environment, these indices are preferable preferred due to their ability to separate N rates with CS rotation.

Relationships between Vegetation Indices and Grain Yield

In 2009, at the V11, V13 and V15 growth stages, all vegetation indices showed a high partial correlation with final grain yield (Figure 9) adjusting for water and rotation. The NDVI_RE, CIRE, MTCI and DATT indices showed high, and similar, correlations at all growth stages studied, even higher than the chlorophyll meter (SPAD). The NDVI_Red index had a lower correlation with final grain yield at V11 and V13 growth stages compared to other indices. All correlations showed the same trend of stronger relationships at later growth stages except for SPAD. Due to sampling procedures (amount and method) and practicality, the chlorophyll meters may be biased due to human error during data gathering. Chlorophyll meters may need a specific growth stage and should be sampled at the ear leaf (after silking) for best performance (Costa et al., 2001), but they are less sensitive to variations in canopy structure that causes changes in reflectance.

The same trend of increasing correlation between vegetation index and grain yield with growth stage was observed in 2010. All vegetation indices showed relatively high partial correlations with grain yield at V7, V9 and V11 growth stages (Figure 10). The NDVI_Red and SPAD had the lowest correlations, though still relatively high and significant. The CIRE, CI, MTCI and DATT indices had the highest correlation with

grain yields. The good associations between grain yield and these types of indices at early growth stages (V7, V9 and V11) bode well for the many applications of this technology to better meet crop N demand in-season, reducing N loss and protecting the environment.

SUMMARY AND CONCLUSIONS

This study investigated how crop canopy reflectance, measured by different vegetation indices (NSI), was influenced with different levels of irrigation, fertilizer N rate and crop rotation. We investigated the ability of these indices to differentiate fertilizer N rate under various conditions, and the correlation of indices collected during various growth stages with grain yield. Among the indices studied, the MTCI and DATT indices were the least affected by irrigation level, and by inference, water stress, with ability to differentiate fertilizer N rates with both continuous corn and corn following soybean. The CI, CIRE, $NDVI\_RE_e$ and NDVI_Red indices showed more variation due to irrigation level, and low ability to distinguish fertilizer N rate with corn following soybean. The ranking from the least affected by irrigation level to the most affected were DATT, MTCI, NDVI_RE, NDVI_Red, CIRE and CI. Comparing the vegetation indices for N differentiation, again DATT and MTCI had the best ability to separate N rates, so these two indices are more appropriate if low variance for water stress and high ability to distinguish N rates across crop rotations is needed. All vegetation indices had good correlation with final grain yield when sampled between V11 and V15, where MTCI and DATT again were stronger across years. The results suggest that careful attention should be given to how water

stress and previous crop can affect the ability of these vegetation indices to determine crop N status.

REFERENCES

Abendroth, L.J., R.W. Elmore, M.J. Boyer, and S.K. Marlay. 2011. Corn Growth and Development. PMR 1009. Iowa State University Extension, Ames, IA.

Al-kaisi, M.M., X. Yin, 2003. Effects of Nitrogen Rate , Irrigation Rate , and Plant Population on Corn Yield and Water Use Efficiency. Agron. J. 95: 1475-1482.

Bausch, W.C., and H.R. Duke. 1996. Remote sensing of plant nitrogen status in corn. Trans. ASAE. 39: 1869-1875.

Çakir, R. 2004. Effect of water stress at different development stages on vegetative and reproductive growth of corn. Field Crops Research. 89: 1-16.

Clay, D.E., K.I. Kim, J. Chang, S. Clay, K. Dalsted. 2006 Characterizing Water and Nitrogen Stress in Corn Using Remote Sensing. Agron. J. 98: 579-587.

Costa, C., L. Dwyer, P. Dutilleul, D. Stewart, B. Ma, D. Smith. 2001 Inter-Relationships of Applied Nitrogen, Spad, and Yield of Leafy and Non-Leafy Maize Genotypes. Journal of Plant Nutrition, 248: 1173-1194.

Datt, B. 1999. Visible/near infrared reflectance and chlorophyll content in Eucalyptus leaves. International Journal of Remote Sensing, 2014: 2741– 2759

Dash, J.; and P.J. Curran. 2004. The MERIS terrestrial chlorophyll index. International Journal of Remote Sensing, 2523: 5403-5413.

Dellinger, A.E., J.P. Schmidt, D.B. Beegle. 2008. Developing nitrogen fertilizer recommendations for corn using an active sensor. Agron. J. 100: 1546-1552.

Eitel, J.U.H., D.S. Long, P.E. Gessler, E.R. Hunt. 2008. Combined spectral index to improve ground-based estimates of nitrogen status in dry land wheat. Agron. J. 100: 1694-1702.

Gitelson, A.A., A. Viña, V. Ciganda, D.C. Rundquist, T.J. Arkebauer. 2005. Remote estimation of canopy chlorophyll content in crops. Geophysical Research Letters 32, L08403, doi: 10.1029/2005GL022688

Gitelson, A.A., and M.N. Merzlyak. 1996. Signature analysis of leaf reflectance spectra: algorithm development for remote sensing. Journal of Plant Physiology 148: 493–500.

Gitelson, A.A. 2004. Wide Dynamic Range Vegetation Index for remote quantification of biophysical characteristics of vegetation. Journal of plant physiology, 161: 165-173.

Inoue,Y., J. Penuelas, A. Miyata, M. Mano 2008. Normalized difference spectral indices for estimating photosynthetic efficiency and capacity at a canopy scale derived from hyperspectral and CO2 flux measurements in rice. Remote Sensing of Environment. 112: 156-172.

Jacquemoud, S., and Baret, F. 1990. PROSPECT: A model of leaf optical properties. Remote Sensing of Environment, 34: 75–91.

Lemaire, G., C. François, E. Dufrêne. 2004. Towards universal broad leaf chlorophyll indices using PROSPECT simulated database and hyperspectral reflectance measurements. Remote Sensing of Environment. 84: 1-28.

Nelson, D.W., and L.E. Sommers. 1996. Total carbon, organic carbon and organic matter. p. 961-1010. In D.L. Sparks, A.L. Page, P.A. Helmke, R.H. Loeppert, P.N. Soltanpour, M.A. Tabatabai, C.T. Johnson, and M.E. Sumner (ed.) Methods of soil analysis. Part 3 – Chemical methods. Soil Sci. Soc. Am. Book Ser. 5. SSSA, Madison, WI.

Payero, J.O., D. Tarkalson, S. Irmak,D. Davison, J.L. Petersen. 2009. Effect of timing of a deficit-irrigation allocation on corn evapotranspiration, yield, water use efficiency and dry mass. Agricultural Water Management. 96: 1387-1397.

Raun, W.R., J.B. Solie, G.V. Johnson, M.L. Stone, R.W. Mullen, K.W. Freeman, W.E. Thomason, and E.V. Lukina. 2002. Improving nitrogen use efficiency in cereal grain production with optical sensing and variable rate application. Agron. J. 94: 815–820.

Rouse, J.W., R.H. Haas, J.A. Schell, D.W. Deering, J.C. Harlan. 1974. Monitoring the vernal advancements and retrogradation of natural vegetation. In: NASA/GSFC, Final Report, Greenbelt, MD, USA, pp. 1–137.

Schepers, J.S., D.D. Francis, M.F. Vigil, and F.E. Below. 1992. Comparison of corn leaf nitrogen concentration and chlorophyll meter readings. Commun. Soil Sci. Plant Anal. 23: 2173–2187.

Schepers, J.S. 1994. New diagnostic tools for tissue testing. Commun. Soil Sci. Plant Anal. 25: 817–826.

Shanahan, J.F., N. R. Kitchen, W.R., Raun, J.S. Schepers. 2008. Responsive in-season nitrogen management for cereals. Comput. Eletron. Agric. 6: 51-62.

Shiratsuchi, L.S., R.B. Ferguson, V.I. Adamchuck, J.F. Shanahan, G.P. Slater. 2009 Integration of ultrasonic and active canopy sensors to estimate the in-season nitrogen content for corn. In: North Central Extension-Industry Soil Fertility Conference, Des Moines, IA, Nov. 18-19, 2009. PPI, Brookings, SD.

Sims, J.T. 1989. Comparison of mehlich 1 and mehlich 3 extractants for P, K, Ca, Mg, Mn, Cu and Zn in Atlantic coastal plain soils. Commun. Soil Sci. Plant Anal. 20:1707–1726. doi:10.1080/00103628909368178

Solari, F., J.F. Shanahan, R.B. Ferguson, J.S. Schepers, A.A. Gitelson. 2008. Active sensor reflectance measurements of corn nitrogen status and yield potential. Agron. J. 100: 571-579.

Varvel, G.E., J.S. Schepers, D.D. Francis. 1997. Ability for in-season correction of nitrogen deficiency in corn using chlorophyll meters. Soil Sci. Soc. Am. J. 6: 1233-1239.

Watson, M.E., and J.R. Brown. 1998. pH and lime requirement. p. 13–16. In J.R. Brown (ed.) Recommended chemical soil test procedures for the north central region. NCR Res. Publ. 221. Univ. of Missouri, Columbia, MO.

Wu,C., Z. Niu, Q. Tang, W. Huang,B. Rivard, J. Feng. 2009. Remote estimation of gross primary production in wheat using chlorophyll-related vegetation indices. Agricultural and Forest Meteorology. 149: 1015-1021.

Zygelbaum, A.I., A.A. Gitelson, T.J. Arkebauer, D.C. Rundquist. 2009. Non-destructive detection of water stress and estimation of relative water content in maize. Geophysical Research Letters 36. L12403, doi: 10.1029/2009GL03890.

Figure 1. Platform for data acquisition (bicycle equipped with 2 optical sensors, DGPS, laptop computer and batteries.

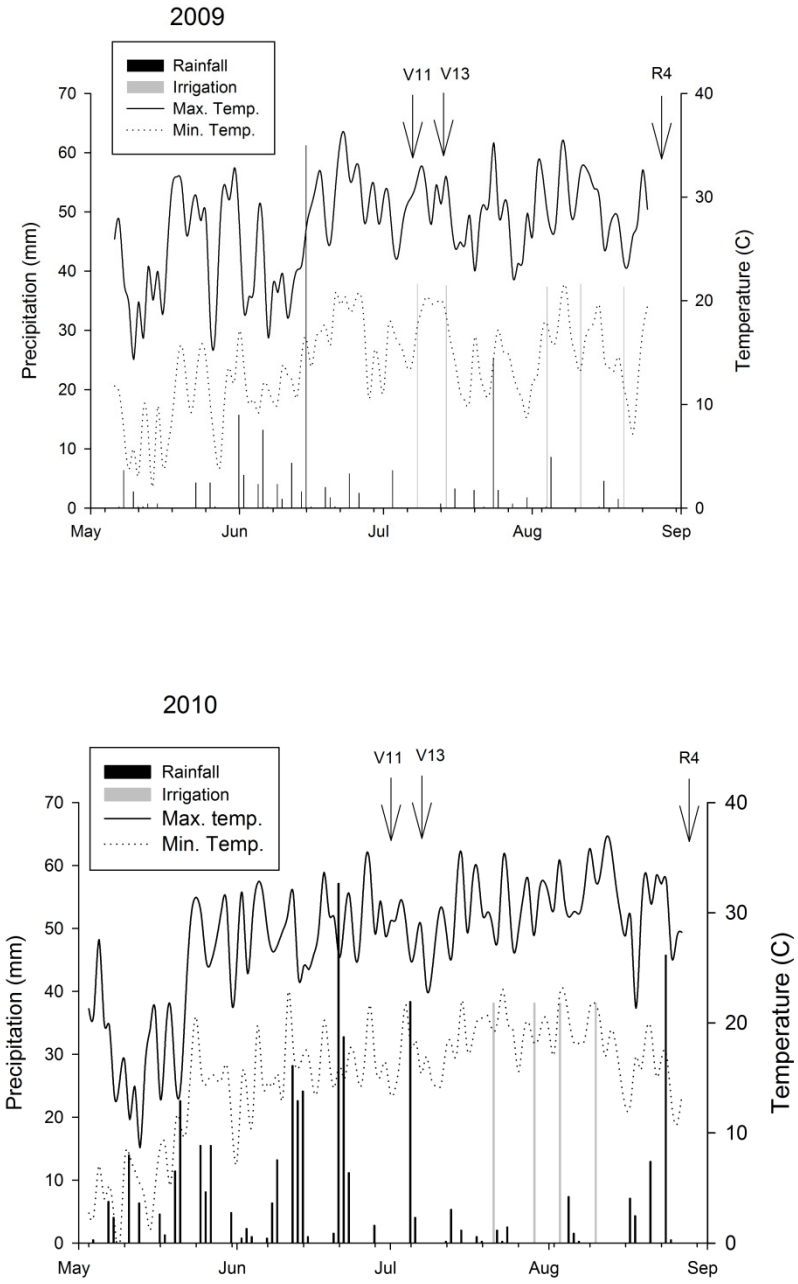

Figure 2. Daily rainfall, irrigation and air temperatures for the 2009 and 2010 growing seasons at the South Central Agricultural Laboratory.

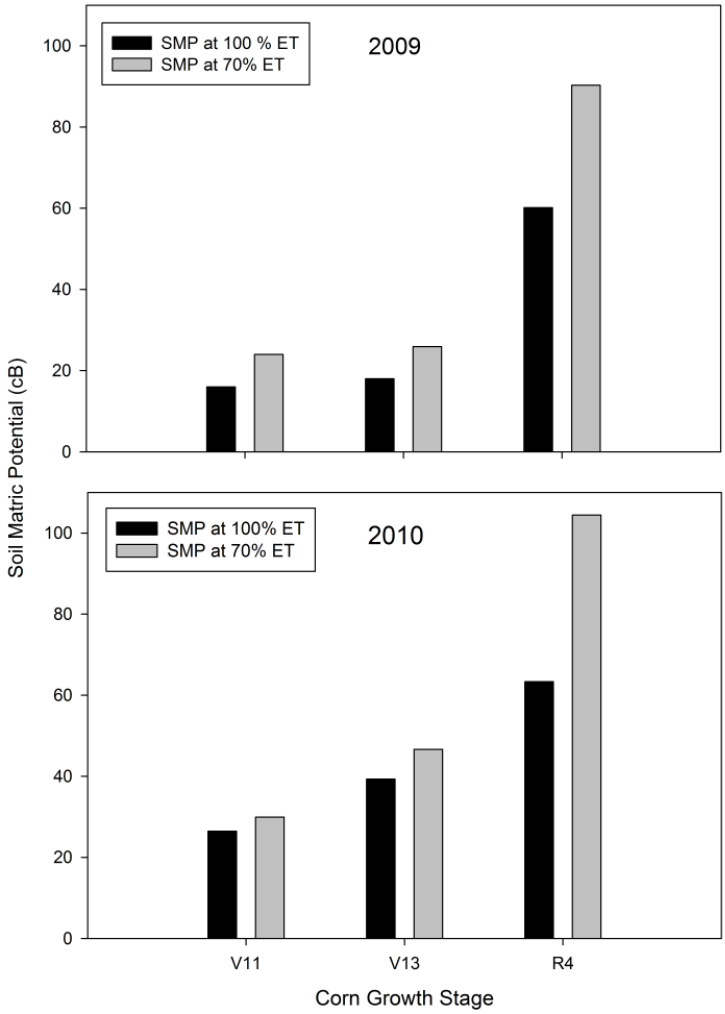

Figure 3. Soil matric potential (SMP) measured by Watermark sensors at V11, V13 and R4 growth stages at 61 cm soil depth.

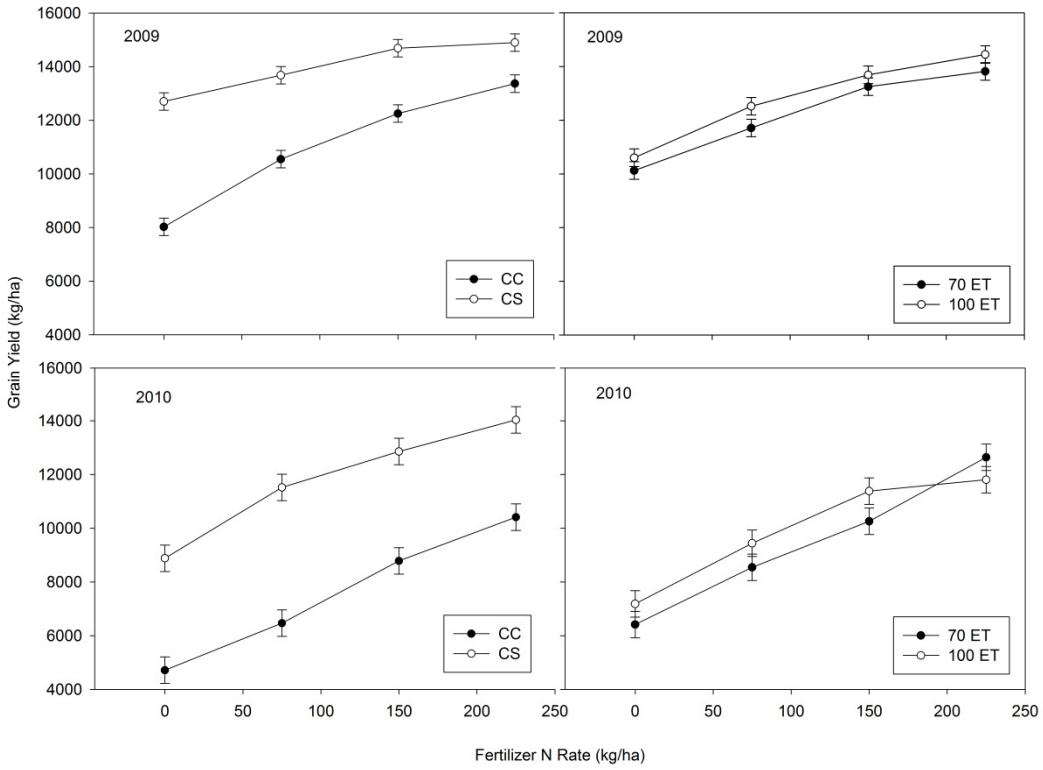

Figure 4. Grain yield as influenced by N rate, croprotations and water levels during 2009 and 2010. Errors bars represent standard error.

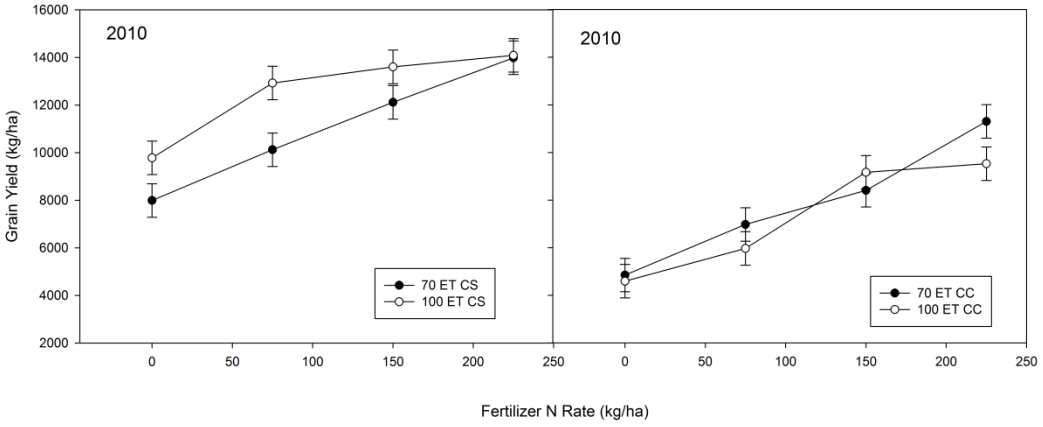

Figure 5. Grain yield as influenced by N rate, under different water levels with different crop rotation (CC and CS). Errors bars represent standard error.

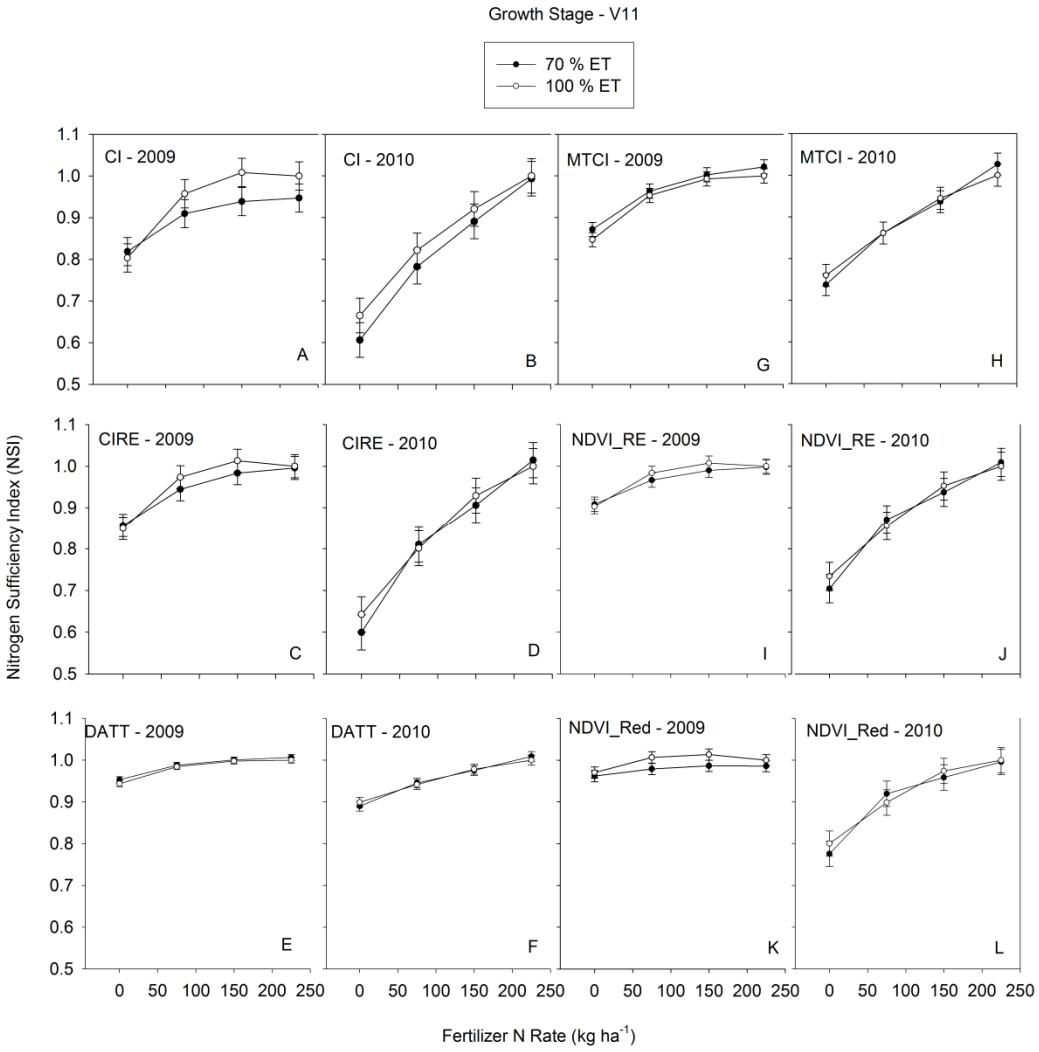

Figure 6. Vegetation indices response to fertilizer N rate and irrigation level, at the V11 growth stage during 2009 and 2010 growing seasons. Error bars represent standard error.

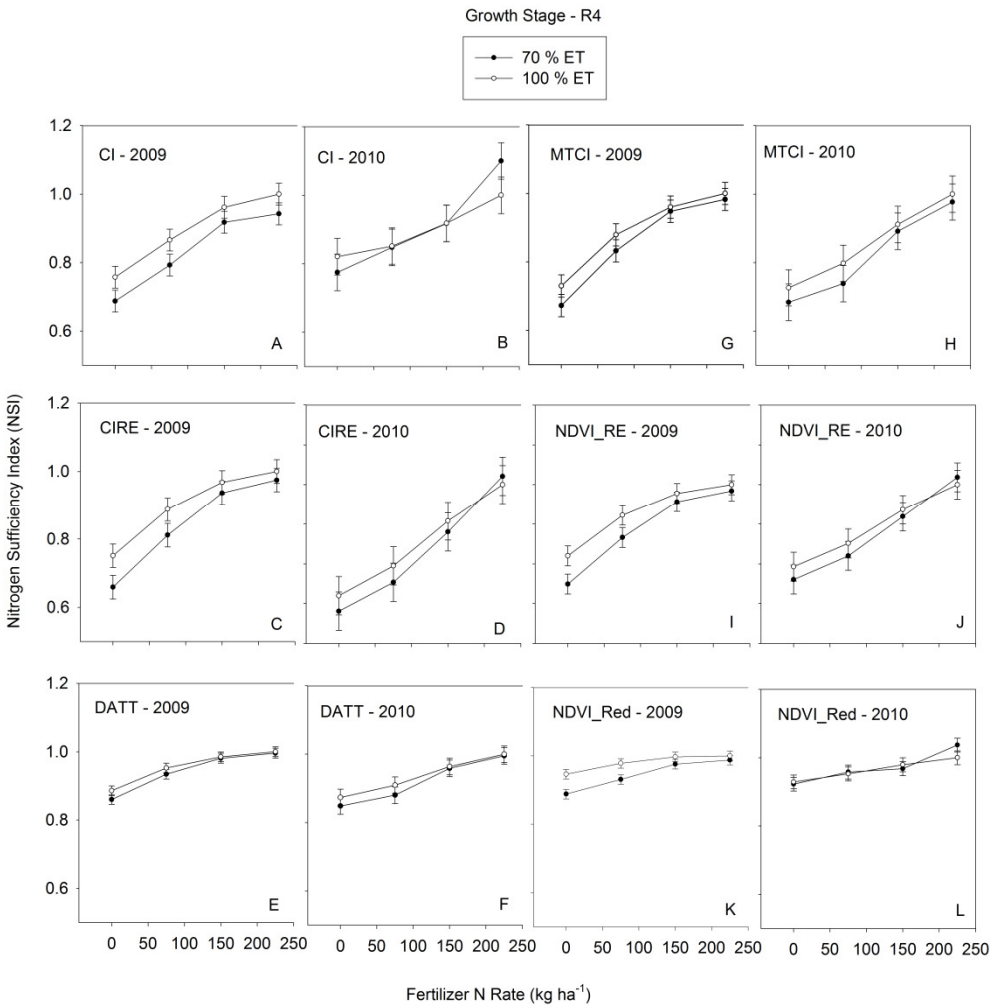

Figure 7. Vegetation indices response to fertilizer N rate and irrigation level, at the R4 growth stage during 2009 and 2010 growing seasons. Error bars represent standard error.

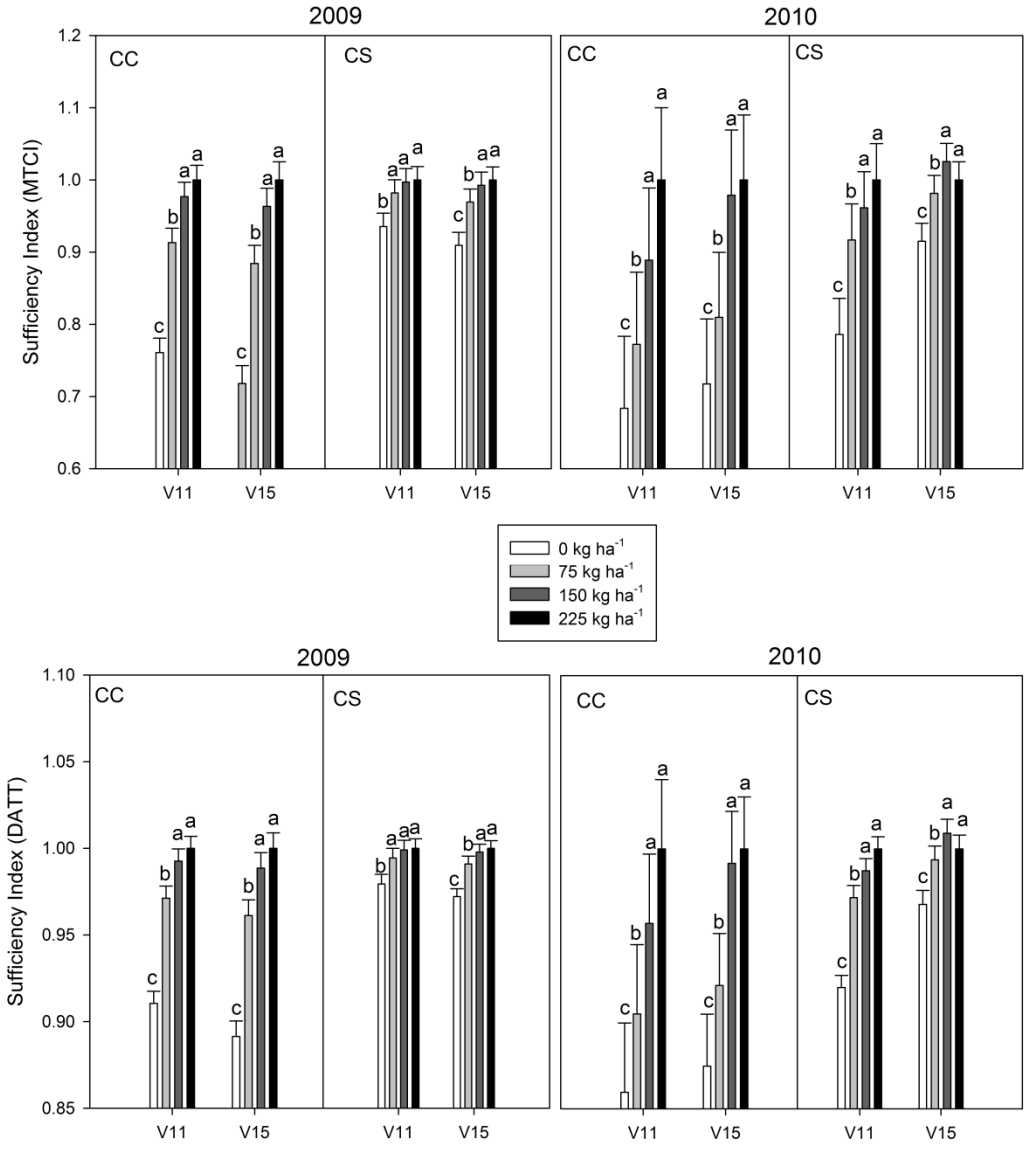

Figure 8. The effect of crop rotation (CC and CS) and growth stage on crop canopy reflectance using two vegetation indices, MTCI and DATT, averaged across water level for 2009 and 2010. Errors bars represent standard error and letters the statistically significant differences according to Duncan's Multiple Range Test ($p<0.10$).

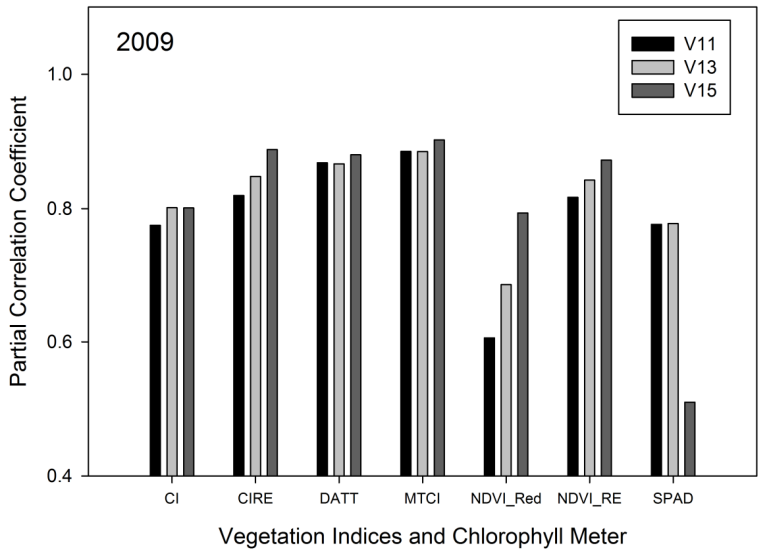

Figure 9. Partial correlation coefficient values between vegetation indices and grain yield for three growth stages in 2009 accounting for irrigation levels and crop rotations. All correlations were significant with $p < 0.01$

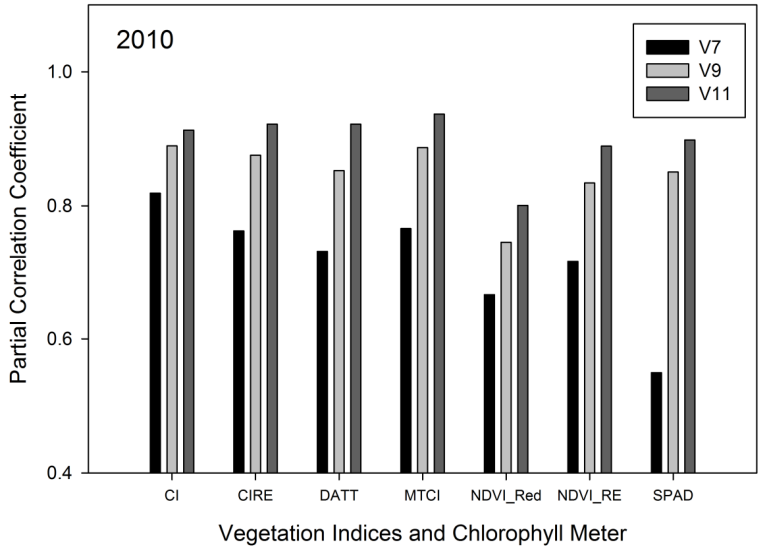

Figure 10. Partial correlation coefficient values between vegetation indices and grain yield for three growth stages in 2010 accounting for irrigation levels and crop rotations. All correlations were significant with $p < 0.01$

Table 1. Planting date and crop characteristics.

	2009	2010
Planting date	May 6	April 29
Hybrid	Pioneer 33H29	Pioneer 1395XR
Plant population	72,610 plants/ha	72,610 plants/ha
Row Spacing	76.2 cm	76.2 cm

Table 2. Soil test analysis results for the study sites in 2009 and 2010.

Soil parameter	2009	2010
	0-20 cm	0-20 cm
Soil pH	6.6	6.6
Organic matter (%)	3	3.3
Nitrate - N (mg kg^{-1})	6.7	4.5
Bray-1 P (mg kg^{-1})	25.5	24.3
K (mg kg^{-1})	364	405
CEC	13.3	15.3
Fe (mg kg^{-1})	52	58.3
S (mg kg^{-1})	6.6	8.2
Mn (mg kg^{-1})	7.8	15.4
Ca (mg kg^{-1})	1838	2156
Mg (mg kg^{-1})	210	227
Na (mg kg^{-1})	12	25

Table 3. Vegetation index formulas and wavebands used in this study.

Indices	Wavebands* (nm)	Formula	Source
CI	880, 590	CI= $(R_{880}/R_{590}) - 1$	Gitelson et al, 2005
CIRE	760, 720	CIRE= $(R_{760}/R_{720}) - 1$	Gitelson et al, 2005
DATT	760, 720, 670	DATT = $(R_{760}-R_{720})/(R_{760}-R_{670})$	Datt et al, 1999
NDVI_Red	760, 670	NDVI_Red = $(R_{760}-R_{670})/(R_{760}+R_{670})$	Rouse et al, 1974
NDVI_RE	760, 720	NDVI_RE= $(R_{760}-R_{720})/(R_{760}+R_{720})$	Rouse et al, 1974
MTCI	760, 720, 670	MTCI = $(R_{760}-R_{720})/(R_{720}-R_{670})$	Dash & Curran, 2004

* For our calculation, we used the bands 880 and 590nm (Crop Circle, Model 210 sensor), 760, 720, 670 nm (Crop Circle, Model 470 sensor) because these were the wavebands collected by the respective sensors.

Table 4. Analysis of variance of corn yield (2009 and 2010) for 70 and 100 % ET under different crop rotations (CC and CS).

Source of Variation	Num DF	Den DF	F value	Pr > F
Irrigation	1	9	2.19	0.1733
Rotation	1	10	123.26	<.0001
Rotation*Irrigation	1	10	2.78	0.1264
N	3	60	106.43	<.0001
N*Irrigation	3	60	1.28	0.2903
N*Rotation	3	60	4.6	0.0058
N*Rotation*Irrigation	3	60	0.26	0.8575

Table 5. Analysis of variance of six vegetation indices calculated from active canopy sensor reflectance at different irrigation levels (70 and 100% ET) and different crop rotations (CC and CS) between growth stages V11 and R4.

Source of variation		CI	CIRE	DATT	MTCI	NDVI RE	NDVI Red
Effect	Num DF	Pr > F					
Irrigation	1	0.179	0.2972	0.5847	0.5341	0.3894	0.4446
Rotation	1	<.0001	<.0001	<.0001	<.0001	<.0001	<.0001
Rotation*Irrigation	1	0.104	0.0924	0.0755	0.0621	0.1373	0.5467
N	3	<.0001	<.0001	<.0001	<.0001	<.0001	<.0001
N*Irrigation	3	0.749	0.6557	0.8788	0.8425	0.7532	0.899
N*Rotation	3	<.0001	<.0001	0.0008	0.0041	<.0001	0.0011
N*Rotation*Irrigation	3	0.9535	0.7933	0.8833	0.8268	0.8548	0.9711
Stage	4	<.0001	<.0001	<.0001	<.0001	<.0001	<.0001
Stage*Irrigation	4	0.5524	0.6846	0.191	0.1626	0.4712	0.4473
Stage*Rotation	4	<.0001	<.0001	0.3835	0.043	0.0008	<.0001
Stage*Rotation*Irrigation	4	0.6904	0.836	0.469	0.5019	0.934	0.8897
Stage*N	12	0.0038	0.1772	0.0974	0.3744	0.5884	0.0004
Stage*N*Irrigation	12	0.9748	0.9997	0.9994	0.9999	0.9986	0.9985
Stage*N*Rotation	12	0.0209	0.0271	0.7407	0.6584	0.0146	0.0009
Stage*N*Rotation*Irrigation	12	0.9999	0.9979	0.9999	0.9998	0.9996	0.9783

Table 6. Ranking of variation to irrigation levels analyzed during 2009 and 2010 growing seasons. Values followed by the same letter are not significantly different (p<0.10).

Rank	Vegetation Index	Mean Squared Error	F test *p < 0.10*
Least affected			
1	DATT	0.00006199	c
2	MTCI	0.00017699	b
3	NDVI_RE	0.00036718	b
4	NDVI_Red	0.00044026	b
5	CIRE	0.00058541	ab
6	CI	0.00163116	a
Most affected			

Table 7. Nitrogen Sufficiency Index for the vegetation indices during several growth stages and N rates under CS rotation. Means followed by the same letter are not significantly different (p<0.10).

Corn - Soybean (CS)	N rate	2009						2010					
NSI	kg ha^{-1}	V11	V13	V15	R2	R3	R4	V11	V13	V15	R2	R3	R4
CI	0	0.99a	0.98a	0.92a	0.88c	0.84c	0.83c	0.75c	0.78c	0.91c	0.89b	0.85c	0.69b
	75	1.02a	1.00a	0.96a	0.96b	0.93b	0.94b	0.92b	0.90b	1.01b	0.97a	0.93b	0.77a
	150	1.03a	1.01a	0.98a	0.99a	0.97a	1.02a	0.97a	0.96a	1.18a	1.05a	1.00a	0.83a
CIRE	0	0.97b	0.96b	0.91b	0.86c	0.84b	0.81c	0.74c	0.76c	0.92c	0.81c	0.80c	0.66c
	75	1.02a	1.00a	0.98a	0.95b	0.95a	0.95b	0.91b	0.90b	1.00b	0.91b	0.90b	0.76b
	150	1.02a	1.02a	1.00a	1.00a	0.98a	1.02a	0.96a	0.96a	1.08a	0.98a	0.96a	0.86a
DATT	0	0.98b	0.98b	0.97c	0.95c	0.95c	0.93c	0.92c	0.91c	0.97c	0.92c	0.91c	0.85c
	75	0.99a	0.99a	0.99b	0.98b	0.98b	0.99b	0.97b	0.97b	0.99b	0.96b	0.95b	0.90b
	150	1.00a	1.00a	1.00a	1.00a	1.00a	1.01a	0.99a	0.99a	1.01a	0.99a	0.98a	0.97a
MTCI	0	0.94b	0.94b	0.91c	0.85c	0.83c	0.80c	0.79c	0.76c	0.92c	0.79c	0.77c	0.68c
	75	0.98a	0.98a	0.97b	0.94b	0.94b	0.96b	0.92b	0.90b	0.98b	0.90b	0.88b	0.78b
	150	1.00a	1.00a	0.99a	0.99a	0.99a	1.02a	0.96a	0.96a	1.03a	0.96a	0.94a	0.92a
NDVI_RE	0	0.98b	0.98b	0.95b	0.92c	0.90b	0.87b	0.84c	0.85c	0.95c	0.88c	0.87c	0.75c
	75	1.01a	1.00a	0.99a	0.97b	0.97a	0.97a	0.95b	0.94b	1.00b	0.94b	0.94b	0.82b
	150	1.01a	1.01a	1.00a	1.00a	0.99a	1.01a	0.98a	0.98a	1.04a	0.99a	0.97a	0.90a
NDVI_Red	0	1.02a	1.01a	0.99b	0.99b	0.97b	0.95b	0.93b	0.96c	0.99b	0.98b	0.99a	0.90a
	75	1.02a	1.01a	1.00a	1.00a	1.00ab	0.98b	0.98a	0.99b	1.01b	0.99b	1.00a	0.93a
	150	1.02a	1.01a	1.00a	1.00a	0.99ab	1.00a	1.00a	1.00a	1.04a	1.01a	1.00a	0.93a

Table 8. Nitrogen Sufficiency Index for the vegetation indices during several growth stages and N rates under CC rotation. Index for the vegetation indices during several growth stages and N rates under CS rotation. Means followed by the same letter are not significantly different (p<0.10).

Corn - Corn (CC)	N rate	2009						2010					
NSI	kg ha^{-1}	V11	V13	V15	R2	R3	R4	V11	V13	V15	R2	R3	R4
CI	0	0.68c	0.67c	0.66b	0.65c	0.65c	0.65c	0.50c	0.58c	0.61c	0.71c	0.75c	0.85b
	75	0.89b	0.87b	0.86a	0.83b	0.81b	0.76b	0.67b	0.72b	0.72b	0.84b	0.85b	0.86b
	150	0.97a	0.94a	0.92a	0.95a	0.91a	0.91a	0.84a	0.86a	1.02a	0.93a	0.95a	0.93a
CIRE	0	0.73c	0.70c	0.63c	0.63c	0.58c	0.60c	0.46c	0.54c	0.60c	0.69c	0.69c	0.73b
	75	0.90b	0.87b	0.83b	0.78b	0.77b	0.76b	0.66b	0.70b	0.73b	0.81b	0.82b	0.78b
	150	0.98a	0.96a	0.94a	0.87a	0.90a	0.91a	0.85a	0.87a	1.00a	0.93a	0.92a	0.91a
DATT	0	0.91c	0.89c	0.87c	0.85c	0.83c	0.82c	0.86c	0.85c	0.87c	0.88c	0.87c	0.88b
	75	0.97b	0.96b	0.95b	0.94b	0.91b	0.90b	0.90b	0.90b	0.92b	0.92b	0.92b	0.89b
	150	0.99a	0.99a	0.98a	0.98a	0.96a	0.96a	0.96a	0.96a	0.99a	0.97a	0.96a	0.96a
MTCI	0	0.76c	0.72c	0.66c	0.63c	0.59c	0.59c	0.68c	0.66c	0.72c	0.73c	0.72c	0.75b
	75	0.91b	0.88b	0.84b	0.82b	0.76b	0.75b	0.77b	0.76b	0.81b	0.81b	0.81b	0.78b
	150	0.98a	0.96a	0.94a	0.94a	0.89a	0.90a	0.89a	0.89a	0.98a	0.91a	0.90a	0.91a
NDVI_RE	0	0.89b	0.87b	0.83b	0.84b	0.80c	0.81a	0.58c	0.66c	0.71c	0.78c	0.77c	0.79b
	75	0.98b	0.97b	0.95b	0.95b	0.94b	0.92a	0.76b	0.79b	0.81b	0.87b	0.88b	0.83b
	150	1.01a	1.01a	1.01a	1.01a	0.99a	1.00a	0.90a	0.92a	1.00a	0.95a	0.95a	0.94a
NDVI_Red	0	0.93b	0.92c	0.90b	0.92c	0.89b	0.89c	0.64c	0.78c	0.81c	0.91c	0.90b	0.92c
	75	0.98a	0.97b	0.97a	0.97b	0.95a	0.94b	0.83b	0.89b	0.89b	0.97b	0.98a	0.95b
	150	1.00a	0.99a	0.99a	1.00a	0.98a	0.98a	0.94a	0.96a	1.02a	1.00a	1.00a	0.98a

CHAPTER 2

LOCAL REFERENCE: AN APPROACH FOR SITE-SPECIFIC NITROGEN FERTILIZATION USING ACTIVE CANOPY SENSORS

ABSTRACT

Active crop canopy sensors have been used to guide nitrogen (N) fertilization based on the status of crop with respect to a reference strip (N-rich). Localized reference strips that account for variable growing conditions can provide more accurate N fertilization need estimates than other methods that rely on averaged values of N-rich strips. The objectives of this study are: (i) to develop an approach that relies on local soil conditions as well as on active canopy sensor measurements for real-time adjustment of N application rate; (ii) to compare the method developed against other approaches in different field conditions and (iii) evaluate the correlations between localized plant status and soil attributes in variable landscapes. The experiment was conducted during 2009 and 2010 growing season in three different production fields each year. In each site, two experiments were conducted: (i) A set of replicated field-long strip treatments comparing the traditional University-recommended N method versus the sensor-based approaches with either average reference strip or the localized reference method, and (ii) 250 small plots with 0, 75, 100, 150, 200 and 250 kg N/ha application rates were established covering different landscape positions and soil types. The small plots were arranged using a spatial design

to have equidistance between the centroids of the plots to interpolate sensor responses for different fertilizer N rates and simulate plant and soil conditions on sidedress N application and then compare different approaches across the variable landscape. Generally it was found that the Local approach could identify regions in the field where the plant status is a better predictor and potentially increase the N use efficiency, while maximizing grain yield and maintaining the partial factor productivity.

Abbreviations List: EC: apparent soil electrical conductivity; RTK: real time kinematic GPS; NUE: nitrogen use efficiency; ACS: active optical crop canopy sensors; SI: sufficiency index; CI: chlorophyll index.

INTRODUCTION

The current nitrogen (N) management practices for corn production systems typically include significant quantities of N applied at field uniform rates. These conventional practices do not consider the spatial variability of the soil N supply, thus often resulting in low N use efficiency (NUE) (Shanahan, 2008). It was shown in previous studies that N fertilization needs can vary according to differences in soil, topographical features and weather influencing corn yield response to N fertilization (Franzen et al., 1999; Kaspar et al., 2003, Erskine et al., 2007). The soil N supply can very drastically in fields in a spatial and temporal way, making any soil prediction and mapping difficult even with a very detailed map (Shahandeh et al. 2005). Consequently the use of map-based approaches to determine the N rates for in-season site-specific N application is often ineffective. In this scenario, a plant based approach where the

measured canopy status can indicate the crop N needs in a reactive and spatially-variable way may be a better option, because it integrates the soil N supply and translates this into crop N need on-the-go. There are several commercial systems available that use crop canopy reflectance using active light sensors for N estimation in the plant. One advantage compared to conventional passive sensors is that these systems do not depend on sunlight because they have their own light source, enabling easier comparisons between measurements, allowing the farmer to work night and day. These active crop canopy sensors (ACS) have been used to guide N fertilization based on the status of crop with respect to a N-rich strip located in some part of the farmer's field, and then all measurements were normalized against this reference where plant N is considered non-limited. This approach uses an overall average number acquired from the ACS, but it is known that the well fertilized plots will respond differently in different areas of the field due to the spatial variability of soils. However, localized reference strips that account for variable growing conditions in the same location where the sensor measurement is being collected can provide more accurate fertilization need estimates than other methods that rely on an averaged value of N-rich strip. The objectives of this study are: (i) to develop an approach that relies on local plant status as well as on active canopy sensor measurements for real-time adjustment of N application rate; (ii) to compare the method developed against other approaches in different field conditions and (iii) evaluate the correlations between localized plant status and soil attributes in variable landscapes.

MATERIAL AND METHODS

On Farm Research Fields

The experiment was conducted during 2009 and 2010 growing seasons in three different production fields each year representing different soil types and agroecosystems across Nebraska (6 site years) (Figure 1). The producer fields were strategically located to better represent the variability of soils and sprinkler irrigated corn systems in the state, ranging from sandy to clay loam, high to low soil organic matter (SOM), and having differences in elevation and rainfall patterns. In terms of landscape, generally the relief varies from less than 3 meter for some sites (BR09, HU09) and 5 to 12 meters in others (RT09, BR10, HU10 and BL10), with substantial changes in topography. The BL10 field was the only production field owed by University of Nebraska and not by cooperating producers. It is located nearby Brule, Nebraska (West portion of the State) and it has a different elevation (500 meters higher than the other fields that are about 500 m above sea level). The weather pattern in this region is considerable dryer than the others located in Central Nebraska. The corn hybrids, plant population, cropping systems were chosen by the cooperating farmers (Table 1). They also managed the irrigation and general fertilization accordingly to common best management practices to avoid deficiencies other than N. The soils were predominantly silt and clay loam fields (HU09, RT09, HU10) and sandy fields (BR09, BR10, BL10) with gradients in topography and soil variability (Table 1 and 1a).

Equipments and Field Variability Characterization

The crop, soil and landscape information collected to address the objectives were SOM, elevation, apparent soil electrical conductivity (EC) and crop canopy reflectance. All information were georeferenced to a common geographical coordinate system (Geographic using decimal degrees and map datum WGS84 or Universal Transverse Mercator (UTM), Spheroid GRS80, Zone 14N and map datum WGS84) using ArcGIS 9.3 (ESRI, Redlands, CA). Soil sampling and active crop canopy sensors were positioned using a Global Navigation Satellite System (GNSS) receiver with differential correction from the Wide Area Augmentation System (WAAS). The Differential GNSS used was a Trimble GeoXT (Trimble Navigation, Ltd., Sunnyvale, CA) with sub meter accuracy. Detailed elevation and EC measurements were collected using Veris 3100 (Veris Tech Inc., Salinas, KS) coupled with a real-time kinematic GNSS (RTK) Trimble AgGPS 442 (Trimble Navigation, Ltd., Sunnyvale, CA), that is able to receive Global Positioning System (GPS – operated by United States) and Global Navigation Satellite System (GLONASS – operated by Russia) signals; with circular error probability less than 1 centimeter horizontal and 2.5 cm vertical using a local base station. The differential correction for the RTK system was done using a mobile base station installed in each field during the EC mapping. Measurements of EC have been used successfully to measure soil salinity, depth of soil horizons, cation exchange capacity, water content (Lesch et al., 1998; Kitchen et al., 2003; Sudduth et al., 2010), may be helpful in predicting N response for crops.

Soil sampling was done early Spring each year using directed soil sampling scheme for the fields based on soil types GIS layer from the Soil Survey Geographic Database (SSURGO) (Natural Resources Conservation Service, NRCS-USDA) and historical EC, or grain yield maps. The point density (2.5 acre grid size) was targeted to have the ability to interpolate the samples and generate a confident SOM map for each of the fields. A hand probe was used to collect soil samples from 0-20 cm for soil nutrient determination.

Active crop canopy sensor readings were collected from each field during the side-dress N application around V11 and later at R4 using a high clearance machine and a modified bicycle platform to accommodate the sensors and GPS. The optical sensor was a Crop Circle Model ACS-210 (Holland Scientific, Inc., Lincoln, NE), that generates modulated light in the visible and near infrared (NIR) parts of the electromagnetic spectrum and measures canopy reflectance with visible (590nm) and NIR detectors (880nm). Careful attention was kept to acquire sensors readings 0.5 m above the crop canopy positioning the sensor over the corn row in V11 and also avoiding tassels during R4 growth stage.

Nitrogen Recommendations Algorithm

The sensor reflectance's in the visible and NIR were used to calculate the Chlorophyll Index (CI) that is a vegetation index proposed by Gitelson et al. (2002, 2005) and is being widely used in irrigated corn production. The CI uses the following equation:

$$CI = \left(\frac{NIR}{VIS}\right) - 1$$

Where NIR is the sensor reflectance at 880nm and VIS is the reflectance at 590nm.

The Sensor-based algorithms tested in this study require that all the sensor readings outputted as CI have to be converted to a Sufficiency Index (SI). SI is a normalization procedure calculating the ratio of the real time sensor reading for the area being assessed to the sensor reading from a reference plot considered to be non-N limited (N-rich). Many studies have reported that a SI expression is better than an absolute reading for assessing crop N status, because it normalizes the difference between cultivars, canopy structure (i.e., growth stage and leaf architecture), and different fields and types of crop (Peterson et al., 1993; Hussain et al., 2000; Biggs et al., 2002; Debaeke et al., 2006; Holland and Schepers, 2010; Zhu et al., 2011). The SI used was calculated by:

$$SI = \frac{CI\_target}{CI\ N\_rich}$$

Where: CI_target is the CI being assessed in real time at the target of the sensor fingerprint and CI N_rich is the CI from the N-rich or a non-N limiting crop location.

The algorithm used for corn N recommendations in this study was an active sensor algorithm based on a chlorophyll meter using the formula proposed by Solari et al., 2010:

$$Nrec = 317 * \sqrt{0.97 - SI}$$

Where: N rec is the N rate recommended in kg ha^{-1} and SI is the sufficiency index calculated from a N rich reference strip value.

Local and Average Approaches

Local approach (Local) refers to the real-time and site-specific N fertilization method based on the SI calculated from a localized N-rich reference. In this study it was the reference strip closer than 6 meter. The N rate for the N-rich plot for this study in all fields was 250 kg N ha^{-1} (75 kg N ha^{-1} applied at planting and 175 kg N ha^{-1} applied at side-dress around V11 growth stage).

Average approach (Average) refers to the real-time and site-specific N fertilization method based on the SI calculated from a reference strip or plot located in some place in the field, not necessarily close to the area that is being sensed. Currently it is the most commonly used approach in farmer's fields.

Experimental Treatments

In each field, two sets of complimentary experiments were conducted to test the Local and the Average approaches:

Experiment 1 - Field long strips

In this experiment several field long strips across the center pivots were used to test different approaches: (i) Uniform N fertilization method from the traditional university

based algorithm recommendation (UNL), (ii) N-rich strip using the highest N rate to have a non-N limited treatment (Reference), (iii) Sensor Based Average approach using an CI average value that came from the N-rich strip (Average) and (iv) Sensor based Local approach using a localized CI that came from the closest N-rich reference (Local) (Figure 2). Operationally, for all fields, all three replications of the Reference (250 kg N ha^{-1}) and the Local strips were sensed first using a high clearance machine equipped with active canopy sensors. The sensor data was downloaded to a laptop PC in the field and ArcGIS was used to calculate the average value of CI for each of 6x15 m plots in the long strip for the reference and local strips (Table 6). In each of the 3 replications for the Local approach, the CI from each of the plots were divided by the neighbor N-rich plot, to calculate the localized SI that was used to variable rate fertilization after mapping. For the Average approach, average value from the 3 replicates was used to calculate the SI before the variable rate fertilization.

The UNL algorithm was calculated using the formula:

$$\text{N rec} = 35 + (1.2 * EY) - (8 * NO_3) - (0.14 * EY * OM) - CRD$$

Where: N rec is the N rate recommended in lb/acre; EY is the expected grain yield, NO_3 is the soil nitrate content in ppm; OM is the organic matter in percent and CRD is other credits in lb/acre. The N rec was converted to kg N ha^{-1} and represented the total N applied in all replications.

The final grain yield, N rates and Partial Factor Productivity (PFP) were measured as response variable. PFP is the ratio between grain yield divided by the amount of N per area used (Cassman et all., 1996; Olk et al., 1999). In this case it used yield in kg ha^{-1} and

N rate in kg N ha^{-1}. The PFP is a good parameter to determine the Nitrogen use efficiency (NUE) and profitability. For the field long strips the yield data was recorded by a combine equipped with yield monitor using differential GNSS and then submitted to filtering process using the software Yield Editor (Sudduth and Drummond, 2007; USDA-ARS, Columbia, MO). The filtered yield data was used to average grain yield points for each plot (6x15 m) inside each treatment strip. It averaged about 10-15 yield points for each plot depending on the combine speed.

Experiment 2 – Small Plots

For the second experiment a particular design of 250 small plots with 0, 75, 100, 150, 200 and 250 kg N ha^{-1} application rates were established covering different landscape positions and soil types (Table 1a). The small plots were arranged using a spatial experimental design that utilizes equidistance between the centroids of the plots (6 x 15 m) with the same N rate. This was done to interpolate sensor responses for different fertilizer N rates and to simulate crop N status from various side-dress N applications and compare different sensor-based approaches (Local and Average) across the landscape (Figure 2). This procedure allows flexibility to simulate different N rates that will be used to calculate N fertilizer rates for the Local and Average approaches and evaluate the grain yield and SI responses across the landscape. All small plots received 75 kg N ha^{-1} at planting and then the other rates were completed on side-dress (V11 growth stage). Later in the season (R4 growth stage) when the N rates had time to have effect on plots, they were sensed using ACS for simulations using different approaches.

Grain yield and CI for each N rate was modeled using semivariogram scaled to the sample variance. This allowed the semivariograms from different fields to be compared and a better model to be developed to interpolate the variables (CI and Yield) for each N rate. The CI and yield surfaces originating from the equidistant plot design were interpolated by kriging using the software GS+ (Gamma Design Software, Plainwell, Michigan - USA) giving a 1x 1 m spatial resolution and then exported as point text files for ArcGIS to make map surfaces in a raster format. Grain yield was determined by hand harvest for each of the small plots and then for each N rate a different yield map was generated. This allows one to calculate a yield response quadratic function for every pixel. The N rates calculated for the sensor-based algorithm were extracted from the raster map surface of SI at 75 kg N ha^{-1} (SI_75N) to simulate the same procedure for side-dress application that was done for the long strips (Experiment 1) where 75 kg N ha^{-1} was applied at planting. The SI_75N was determined by map algebra dividing the CI map using 75 kg N ha^{-1} (CI_75N) by a CI map using 250 kg N ha^{-1} (CI_250N). This procedure was used to calculate a localized SI for every pixel inside the small plot area. Similarly SI for all the other rates 0, 150, and 200 kg N ha^{-1} were calculated to generate a SI quadratic function for each pixel. After creating the surface map of CI and Yield for each N rate, one transect was selected (39 to 49 points equidistant from 15 m) in the center of the small plot area in each field to adjust the yield and SI quadratic equations. The grain yield for each N rate was then calculated for the Local or Average approaches (Table 12-17). The yield response and SI quadratic equations were modeled only for the central replicate, assuming that the yield spatial variation is the same all over in the small

plot area. The final grain yield, N rates and Partial Factor Productivity (PFP) were measured as response variables for the Local and Average approach.

For all fields and experiments, there were common layers of information (i.e. EC, RTK elevation, SOM), that were mapped using different resolutions. For example: The soil EC and RTK elevation mapped with the Veris 3100 were done before planting in the whole field using a different pass width, so to have EC values and elevation data for each plot. Interpolated map surfaces were created with a 1x1 m resolution to extract an averaged value for each plot. The same procedure was done for SOM analysis that was mapped in a 1 ha grid size, with a 1x1m resolution. Interpolated surface were used to average the value for each plot, bringing all layers of information's (EC, RTK, SOM) for the same spatial resolution.

Statistical Analysis

Experiment 1 – Field Long Strips

To evaluate treatment effects on grain yield, N rates and PFP, the six-site years were analyzed as randomized complete block design (RCBD) by the PROC MIXED procedure of SAS for ANOVA and means separation using the Duncan's Multiple Range Test ($p<0.05$), with 3 replicates (each one representing one pass from one side to another in the center pivot divided in about 40 to 50 plots across the variable landscape). The replications and different producer's fields were considered random effects.

Experiment 2 – Small Plots

To compare the two approaches (Local and Average) three random transects were selected for each field with 39 points each to represent 3 replicates of the N rates calculated using the different approaches (Figure 3). The response variables (grain yield, N rate and PFP) were used for a RCBD using the same statistical analysis of the Experiment 1 for each producer field and between fields. Lastly, Spearman rank correlation coefficients were calculated between variables in the small plot area to study how the landscape spatial variability of soil attributes (EC, soil organic matter, RTK elevation and RTK relative elevation to the highest point in the field) influences CI, SI and grain yield in all six fields.

RESULTS AND DISCUSSION

The rainfall patterns and irrigation amounts are shown in Figure 4 for both growing seasons (2009 and 2010). All fields received between 150-330 mm additional irrigation applied by center pivots using the farmer's irrigation schedule. Overall climatic conditions were slightly different between the two seasons where 2009 was warmer until VT growth stage than 2010, and irrigation was initiated earlier. Due to a warmer season in early Spring in 2009 there was a higher chance for better N mineralization and less immobilization in the beginning of the season improving the crop productivity that year compared to 2010. All fields in 2009 had higher yields compared to fields in 2010. The elevation varied from 516 to 1062 meters above sea level. Only BL10 was in the 1000 m

range and the others fields were around 500 m. SOM varied from 5 to 34 g kg^{-1} and grain yields from 4.123 to 19.613 Mg ha^{-1} (Table 2).

Experiment 1 – Field Long Strips

Results from the analysis of variance (ANOVA) of grain yields indicated that the field BL10 was the only one that it did not have a significant effect between treatments (Table 3). This could be related to N leaching earlier in the growing season in the Reference and UNL treatments for this location where those treatments were imposed earlier than the others Sensor Based (Local and Average) that were side-dressed around V10-V11 growth stages. The soil type in this field could be prone to N loss by several pathways since course gravels are mixed with silt loam and sandy across the different soil types and the variable topography can enhance the possibility of N loss. If the N applied in the Reference (250 kg N ha^{-1}) was used by the crop, one would expect differences between treatments to be significant, since lower side-dress N rates were applied on the other treatments. In general, it could be seen that the BL10 field had the lowest grain yield across years (~ 9 Mg ha^{-1}) (Figure 5). On the other hand, the RT09 field showed significant indigenous N contribution to the grain yield. However, even with statistical significant for grain yield, it did not show differences for both sensor based approaches (Figure 5). Nitrogen rates and yield response to N for the Reference strip showed that higher yield generally is obtained with more N applied. Comparing the UNL recommendation approach with the Reference, 4 of 6 fields yielded more for Reference than for UNL (BR09, BR10, HU10 and BL10). Fields HU09 and RT09 did not show

differences in yield but the UNL recommendation used less N than Reference in all cases as expected. Comparing the Average and the Local approaches, the grain yield was similar in 4 of 6 fields (Figure 5). In fields BR09 and BR10 the results were opposite, showing significant higher yield for the Average approach in BR09 and significant higher yield for Local Approach in BR10. It is important to point out that the Average recommendation applied much more N than the Local approach for BR09. At BR10 the N rates were the same but higher yields were observed for the Local, indicating that this sensor based approach should be more beneficial.

In terms of PFP, results from ANOVA indicated that the N application rates and grain yields using different approaches had an effect on PFP in all fields. As expected Reference had the lowest PFP observed across years, varying from 38 to 59 (Table 4), followed by UNL that varied from 41 to 81 kg grain (kg N applied)$^{-1}$. PFP is sensitive when very low rates are applied and low rates are very common with sensor-based approaches. For this reason the extreme lows and no N application were excluded from the PFP analysis as done by Roberts et al. (2009) when comparing the UNL and Reference approaches with the Sensor based Local and Average approaches, otherwise there always would be an advantage for the sensor-based approaches. The criteria for PFP outlier's exclusion for the sensor based approaches were: (i) values lower than the averaged PFP for the Reference (PFP ~ 30) and (ii) values higher than PFP ~ 300, that represents applications of about 50 kg N ha^{-1} to produce 15000 kg grain ha^{-1}, which can happen frequently when sensors are being used. Generally the PFP Average and Local were similar, but Local was superior on fields BR09 and HU09 with a PFP advantage of

9 and 15 kg grain (kg N applied)$^{-1}$ respectively. Overall, the grain yield and N rates were not significantly different, but in terms of PFP there was advantage for Local (Table 5).

Results from ANOVA for CI indicated that the plant N status sensed by active sensors were significantly different in all fields (Table 3). The CI index on the Reference varied from 3.22 to 4.88, giving SI values from 0.77 to 1.05 for all treatments in the time of sensing (side dress application) at V11 growth stage (Table 6). One explanation for higher yields with the Average approach over the Local approach is that the SI in the Local strips were 1.05, meaning that on average the CI in the Local strips were higher than the Average strips, consequently lower N rates were applied to the Local strips, as observed, yielding less than the Average approach (Table 6). On the other field were Local was superior than Average (BR10) the SI at side-dress was higher for the Local than for the Average, but the N rates were not different, but the Local yielded considerable more (~1.3 Mg ha^{-1}).

Experiment 2 – Small Plots

Geostatistical Analysis

Adjusting the semivariograms scaled to sample variance using the GS+ software, it was observed that semivariance increased linearly with distance for CI and Yield at some N rates. This was probably due to trends in the data. When the scaled to sample semivariance ratio is superior to 1 indicates that the variance increasing with distance between measurements is higher than the average semivariance in the lag range for each

field. For dense point data collection such as those collected (CI and yield data), semivariances higher than the average for the whole field make no sense with the kriging interpolation procedure. For this reason it was decided to standardized the model to Spherical. This represents a linear model with short ranges and plateaus when the experimental range (Ao) is reached. The range for each field was considered when the scaled semivariance reached 1, or Sill value (Co+C) equaled 1, when using the model and criteria for range determination, the parameters that changed from field to field and between N rates, were the intercept (Co) and the range (Ao). The models showed that the range for CI increases as N rate increase, and they varied from 45 – 360 m, depending on the field (Tables 18 and 19). Generally the fields in 2009 showed lower ranges for lower N rates compared to 2010, representing a less uniform field in short distances. The same trend was observed with grain yield with ranges varying from 50-350 m. Again, this is an indication that when there is low N supply in the soil, there are more variability in CI and grain yield, as expected. However, for some fields, HU09 and RT09, there were smaller ranges for the highest N rates suggesting that high and low yields can be found close together. This could be explained by high plant stand failure on those high N plots or spatial variability between plots that is often observed in fields. Overall, the ranges for CI and Yield across N rates were 184 and 172 m, respectively. This finding give some basis for future plot design to avoid points far from 30% of the range distance to generate representative sampling for comparisons, as proposed by Isaaks and Srivastava (1989).

Localized Yield and SI Response Equations

Using the central transect (with about 39 – 49 points depending on the field) from the 3 replications in each field it was decided to adjust the Yield considering only the quadratic model, assuming that this model could fit the yield and SI response in all parts of the field. Between the 538 quadratic equations generated, only a few did not fit or had low R^2 (Tables 12 – 17). Generally the equations fit the data well, with high R^2 and reasonable good Yield and SI predictions when the N rate was zero. There are some outliers that were excluded when the analysis for the Local and Average approaches were done using simulated grain yield calculated from the N rate determined by the sensor based algorithm. One example is when the 0 kg N ha^{-1} resulted in grain yields much below the average for 40 kg N ha^{-1}, which is unreal in most agricultural fields. All these equations where replaced by the average equation for the specific field. One good use for these equations could be the simulation of Yield and SI response for different N rates generated from different sensor based algorithms. These equations came from small plots that received 75 kg N ha^{-1} at planting and the supplement 25, 75, 100, 125 and 175 kg N ha^{-1} at side-dress, assuming that minimal N was lost before time of sensing. The only drawback is that the CI values were collected at later stages of corn (R4) in order to be able to sense the crop after response to N. As such, they may not represent the same differences as the small plots sensed from V11 until VT (when side-dress N occurs). Si was used to model the equations and it was expected that normalization would reduce the effect of growth stage as reported by Holland and Schepers (2010).

Treatment Effect on Grain Yield and PFP

Analysis of variance for grain yield indicates that all fields had significant treatment effect on grain yield for the small plots (Table 7). Even though the BL10 field had similar yield between treatments, the Reference and/or UNL yielded more than the sensor based approaches, justifying this significance (Figure 6). Different results were obtained compared with the Long Strips treatments, where in the BL10 there were no treatment effects. Another indication that N was lost from the Reference strips from time of application to time of sensing for the Experiment 1 is that the Reference for the Local plots (250 kg N ha^{-1}) in Experiment 2 yielded more than the sensor based treatments. Comparing the grain yield between treatments UNL and Reference, the RT09 and BL10 fields did not have differences, but in both cases UNL had much less N applied (30-50 kg N ha^{-1}) as expected because Reference had excess N applied. UNL yielded more than both of the sensor based treatments for all fields but used considerable more N. Between the sensor based treatments (Local and Average), the Local had higher yields in 4 of 6 fields, but also had higher N applied. The RT09 field had the highest yield of all fields but again did not have differences between sensor approaches and between UNL and Reference, confirming the results on the field long strips. The HU09 field also had the same results for sensor based approaches but the Reference approach yielded more than the UNL treatments (Figure 6).

In terms of PFP, the Reference treatments had the lowest, followed by the UNL approach that range from 48.8 to 100 kg grain (kg N applied)$^{-1}$ (Table 8). Comparing the

sensor based approaches, the Average had higher PFP than Local in 5 of 6 fields, but the differences were around 12 kg grain (kg N applied)$^{-1}$. In the RT09 field the Local approach was superior to the Average by 49 kg grain (kg N applied)$^{-1}$, probably due to the high indigenous N in this field. Combining all fields, the grain yields were the same between the sensor-based approaches, but the Local had more N applied, but not enough to have higher PFP, showing that Local and Average were similar in terms of profitability (Table 9). The UNL had 36% less PFP than the sensor based approaches, showing disadvantages in terms of NUE.

It is interesting to note that the method of the yield prediction based on quadratic equations from yield and SI with N rates interpolated from surfaces did not have issues as encountered in the field long strips (where for the BR09 field the CI in the Local strip at time of sensing was higher than the reference strips, causing low N application in the Local, that resulted in lower yields), because they use the same SI for both approaches (Table 10), enabling a fair comparison between sensor based approaches considering the same spatial variability for Yield and SI response. These equations covered a broad range of soil types, climate conditions, crop management (previous crop, plant population, hybrids) and could be used to simulate yield and SI response for several other algorithms available to the public (Tables 12-17). Another advantage of using spatial response equations is that it is not required to have a check plot (0 kg N ha^{-1}) to adjust an equation and then obtain a SI(0) or a Yield(0) from the equation if there is N response in the field.

Correlation of ACS with Detailed Soil Attributes

Analyzing landscape variability of soil attributes (EC, soil organic matter, RTK elevation) in the 6 fields at the small plot level generally low correlations were found between final grain yield (Y_250N) and soil attributes (Table 11). This maybe due to the high variability encountered in each of the fields (Table 2). The highest correlations were found for ECdp and Y_250N (0.53) and Y_0N (0.50). RTK elevation showed low correlation with grain yield (- 0.36) and where the elevation was normalized to the highest point for each field (RTK_rel) the correlations were not significant across fields. These results did not confirm the findings of Kaspar et al. (2003) where corn yield was negatively correlated with relative elevation, slope and curvature in dryer seasons. This may be due to combining two different seasons in our study (one dryer than the other, but both did not have excess of water, and that is uncommon where the experiments were conducted). Soil organic matter was high correlated with ECsh, but both had low correlation with final grain yield. On the other hand, SI in the check plot (SI_0N) had high correlations with Y_75N and Y_250N, 0.70 and 0.67 respectively, indicating that sensor readings can estimate better grain yield than soil attributes (Table 11).

Overall, it was identified that the spatial variability between fields and the rank of importance for soil attributes on grain yield varied from field to field, as also observed by Roberts (2010), where only for fine-textured soils with eroded slopes. The management zone delineation based on soil attributes integrated with the same sensor algorithm using the Average approach resulted in N savings around (40 – 120 kg N ha^{-1}). For course

textured fields and high N demand, the current sensor based N application algorithm may require further calibration. But as shown in the previous results for the small plots areas the Local Approach using a localized reference can integrate all plant N demand and improve the ability of the sensor based approach if the same algorithm is used.

Comparing the Average and Local Approaches it was observed in general that the Local approach could identify regions in the field where the CI is higher and potentially increase the yield in these regions. This was observed in field BR10, but more N was required (Figure 7). This greater use by sensor recommendation was also observed by Roberts et al. (2010), when comparing the N rates prescribed with the use of ACS and the farmer's N rates. However, in general the results support sensor-based N applications for environmental benefits. Evaluating the N rates applied using the Local approach minus the N rate using Average approach (L-A_N) showed high correlations between these regions (potentially high yielding sites) with CI_0N, CI_75N and CI_250N, indicating that the Local approach could identify high yielding sites across the landscape (Table 11).

Recently a new variable rate N application model has been published (Holland and Schepers, 2010):

$$N\ rec = (Nopt - Npre - Ncrd + Ncomp)\sqrt{\frac{(1 - SI)}{\Delta SI(1 + 0.1e^{m(SItreshold - SI)})}}$$

Where: N rec is the N rate that should be applied in kg ha^{-1} ; Nopt is the economic optimum nitrogen rate (EONR) or the maximum N rate prescribed by producers; Npre is the N rate applied before sensing; Ncrd is the N credit for the previous season's crop, nitrate in the water or manure application, Ncomp is the N in excess of Nopt required by the crop under soil limiting conditions at a given growth stage; SI is the sufficiency index; m is the back-off rate variable (0<m<100); and SItreshold is the back-off cut-on point.

In this algorithm framework, the SI response is an input (they used one parameter called Δ SI, that is the SI where N rate is zero and this influences the N rates prescribed (Figure 8). The other inputs (Nopt, Npre, Ncrd, Ncomp and threshold SI value) also change the N rec, sometimes for the same SI there were differences as great as 85 kg N ha^{-1} for the Nrec (Figures 8-10).

The algorithm accounts for variation in SI for calculation of N rate, and is consistent with our results on the small plot areas, where high negative correlation was found between Δ SI calculated from the SI response equations with CI_0N, CI_75N, SI_0N and SI_75N (Figure 11). This indicates the possibility for estimation of a "Spatial Δ SI" for using on-the-go in conjunction with the Local approach. In the same way others inputs in the algorithm (total N sources accordingly to historical N response in the field and SI threshold) can also be used spatially using the Local Approach. This shows the probability of using a more flexible algorithm, such as Holland and Schepers (2010) in conjunction with the virtual reference approach (Holland and Schepers, 2011), in estimating a local reference CI without the need of N-rich plot. Using this approach in conjunction with spatial information's about the N rate that maximize yield, Δ SI, and threshold values for SI, will enhance the advantage of the Local approach against the Average approach, without the need of previous soil maps or management zones delineation.

SUMMARY AND CONCLUSIONS

This study evaluated: (i) the use of a localized N-rich reference strip (Local Approach) that accounts for variable growing conditions compared to an approach that account for averaged values of a given plot disregarding any spatial variability (Average); (ii) the comparison of sensor approaches with the conventional uniform N application (UNL); and (iii) how landscape soil spatial variability can influence the Local Approach. The study was conducted in two experiments: Experiment 1 – Field long strips: where long strips with different approaches under farmers conditions were evaluated; Experiment 2- Small Plots: using a spatial design to generate layers of different N application rates and simulate the same treatments of Experiment 1.

In the field long strips, mixed results were observed in 4 of 6 fields. The Local and Average approaches performed similar in terms of yield and only in one field was the Local approach superior compared to the Average approach. In one field where the Average approach yielded more than the Local it was found that a higher averaged CI in the Local strip at time of sensing reduced considerably the N rate applied compared to the Average approach. In terms of PFP the Average and Local approaches were similar in 4 of 6 fields, but Local was superior on the other 2 fields. In the Small plot experiments the spatial variability of CI and Yield were analyzed using semivariograms scaled to sample variance. It was found that the plots had spatial dependence with smaller ranges for the smaller N rates when Yield or CI were evaluated. This finding show that the spatial resolution used in the study was assured by the spatial dependence and that experiments of this nature can be designed for similar purposes. Surface raster maps of Yield and CI

were generated and SI and Yield equations with N rates were calculated using a transect in each field. This generated a valuable data base for algorithm testing and simulation of site-specific N application where yield potential and soil conditions change with the landscape. In this simulation study the Local approach yielded considerable more in 4 of 6 fields compared to Average approach, but applied more N on most of the fields. Overall, the Local approach had the same PFP as the Average approach, followed by UNL and Reference strip. It was found that the Local approach could identify regions in the field where the plant status was better at time of sensing (CI is higher) and potentially higher yields on those regions. Analyzing how the landscape RTK elevation and soil attributes influenced the sensor readings, showed that low correlations were obtained and that a plant-based sensor approach can more likely do a better job of accounting for yield spatial variability. Finally, the Local Sensor Based approach could maximize grain yield and have the same PFP of the Average Sensor Based Approach, showing potential for a better NUE.

REFERENCES

Cassman KG, Gines GC, Dizon MA, Samson MI, Alcantara JM. 1996. Nitrogen-use efficiency in tropical lowland rice systems: contributions from indigenous and applied nitrogen. Fields Crops Res 47: 1–12

Debaeke, P., P. Rouet, and E. Justes. 2006. Relationship between the normalized SPAD index and the nitrogen nutrition index: Application to durum wheat. J. Plant Nutr. 29:75–92.

Erskine, R.H., Green, T.R., Ramirez, J. A, MacDonald, L.H. 2007. Digital Elevation Accuracy and Grid Cell Size: Effects on Estimated Terrain Attributes. Soil Science Society of America Journal 71: 1371-1380.

Franzen, D.W., Hofman, V.L., Cihacek, L.J., Swenson, L.J. 1999. Soil Nutrient Relationships with Topography as Influenced by Crop. Precision Agriculture 1: 167-183.

Gitelson, A.A. Remote estimation of canopy chlorophyll content in crops. 2005. Geophysical Research Letters 32: 4-7.

Gitelson, Anatoly A; Kaufman, Y.J.; Stark, Robert; Rundquist, D. 2002. Novel algorithms for remote estimation of vegetation fraction. Remote Sensing of Environment 80: 76-87.

Holland, K.H. and Schepers, J.S. 2010. Derivation of a Variable Rate Nitrogen Application Model for In-Season Fertilization of Corn. Agron. J. 102: 1415-1418.

Holland, K.H., and J.S. Schepers. 2011. Active-crop sensor calibration using the virtual reference concept. P. 469-479. In J.V. Stafford (ed.) Precision Agriculture 2011. Czech Centre for Science and Society, Prague, Czech Republic.

Hussain, F., K.F. Bronson, S. Yadvinder, S. Bijay, and S. Peng. 2000. Use of chlorophyll meter suffi ciency indices for nitrogen management of irrigated rice in Asia. Agron. J. 92:875–879.

Isaaks, E. H. and R.M. Srivastava. 1989. An Introduction to Applied Geostatistics, Oxford University Press, New York, USA.

Kaspar, T.C., T.S. Colvin, D.B. Jaynes, D.L. Karlen, D.E. James, D.W. Meek. Relationship Between Six Years of Corn Yields and Terrain Attributes. Precision Agriculture 4, 87-101 (2003).

Kitchen, N.R., Drummond, S.T., Lund, E.D., Sudduth, K.A., Buchleiter, G.W. 2003. Soil Electrical Conductivity and Topography Related to Yield for Three Contrasting Soil–Crop Systems. Agron. J. 95: 483-495.

Lesch, S.M., J. Herrero, and J.D. Rhoades. 1998. Monitoring for temporal changes in soil salinity using electromagnetic induction techniques. Soil Sci. Soc. Am. J. 62:232–242.

Olk, D.C.; K.G. Cassman; G. Simbahan, P.C. Santa Cruz; S. 1999. Abdulrachman, R. Nagarajan, P.S. Tan, S. Satawathananont. Interpreting fertilizer-use efficiency in relation to soil nutrient-supplying capacity, factor productivity, and agronomic efficiency. Nutrient Cycling in Agroecosystems 35-41.

Peterson, T.A., T.M. Blackmer, D.D. Francis, and J.S. Schepers. 1993. Using a chlorophyll meter to improve N management. NebGuide G93–1171-A. Univ. of Nebraska Ext., Lincoln.

Roberts, D.F. 2009. An Integrated Crop- and Soil-Based Strategy for Variable-Rate Nitrogen Management in Corn. PhD Dissertation, University of Nebraska, Lincoln..

Roberts, D.F., Kitchen, N.R., Scharf, P.C., Sudduth, K.A. 2010. Will Variable-Rate Nitrogen Fertilization Using Corn Canopy Reflectance Sensing Deliver Environmental Benefits? Agron. J. 102: 85-90.

Shahandeh, H., Wright, A.L., Hons, F.M., Lascano, R.J. 2005. Spatial and Temporal Variation of Soil Nitrogen Parameters Related to Soil Texture and Corn Yield. Agron. J. 97: 772-782.

Shanahan, J., Kitchen, N., Raun, W., Schepers, J. 2008. Responsive in-season nitrogen management for cereals. Computers and Electronics in Agriculture 61: 51-62.

Solari, F., Shanahan, J.F., Ferguson, R.B., Adamchuk, V.I. 2010. An Active Sensor Algorithm for Corn Nitrogen Recommendations Based on a Chlorophyll Meter Algorithm. Agron. J. 102: 1090-1098.

Sudduth, K.A., N.R. Kitchen, D.B. Myers, S.T. Drummond. 2010. Mapping Depth to Argillic Soil Horizons Using Apparent Electrical Conductivity. Journal of Environmental and Engineering Geophysics 15: 135-146.

Zhu, J., Tremblay, N., Liang, Y. 2011. A Corn Nitrogen Status Indicator Less Affected by Soil Water Content. Agron. J. 103: 890-898.

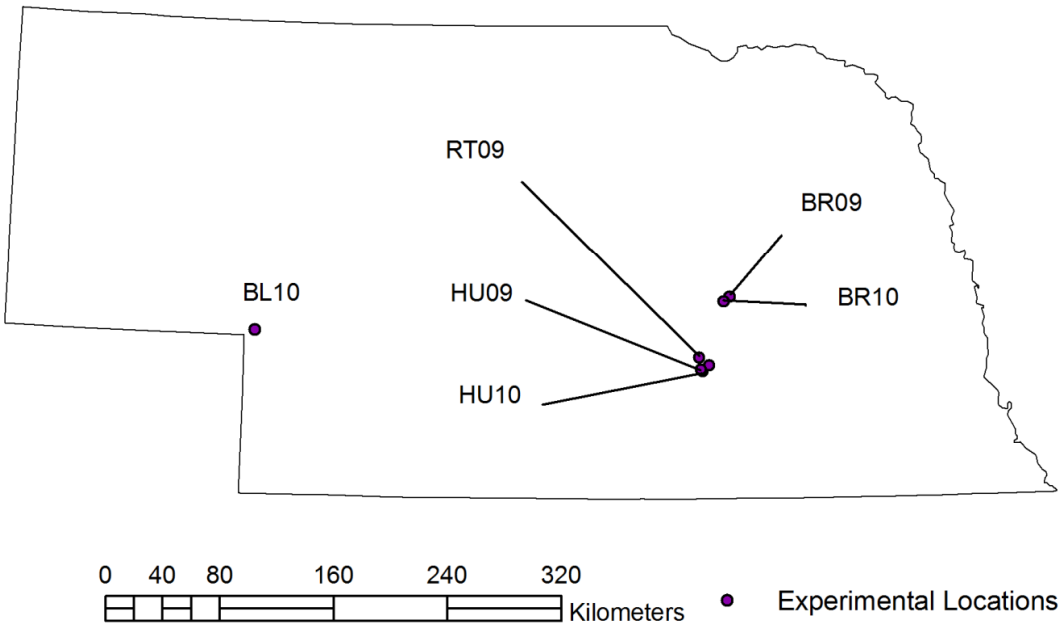

Figure 1. Localization of the different experimental fields during 2009 and 2010 growing seasons.

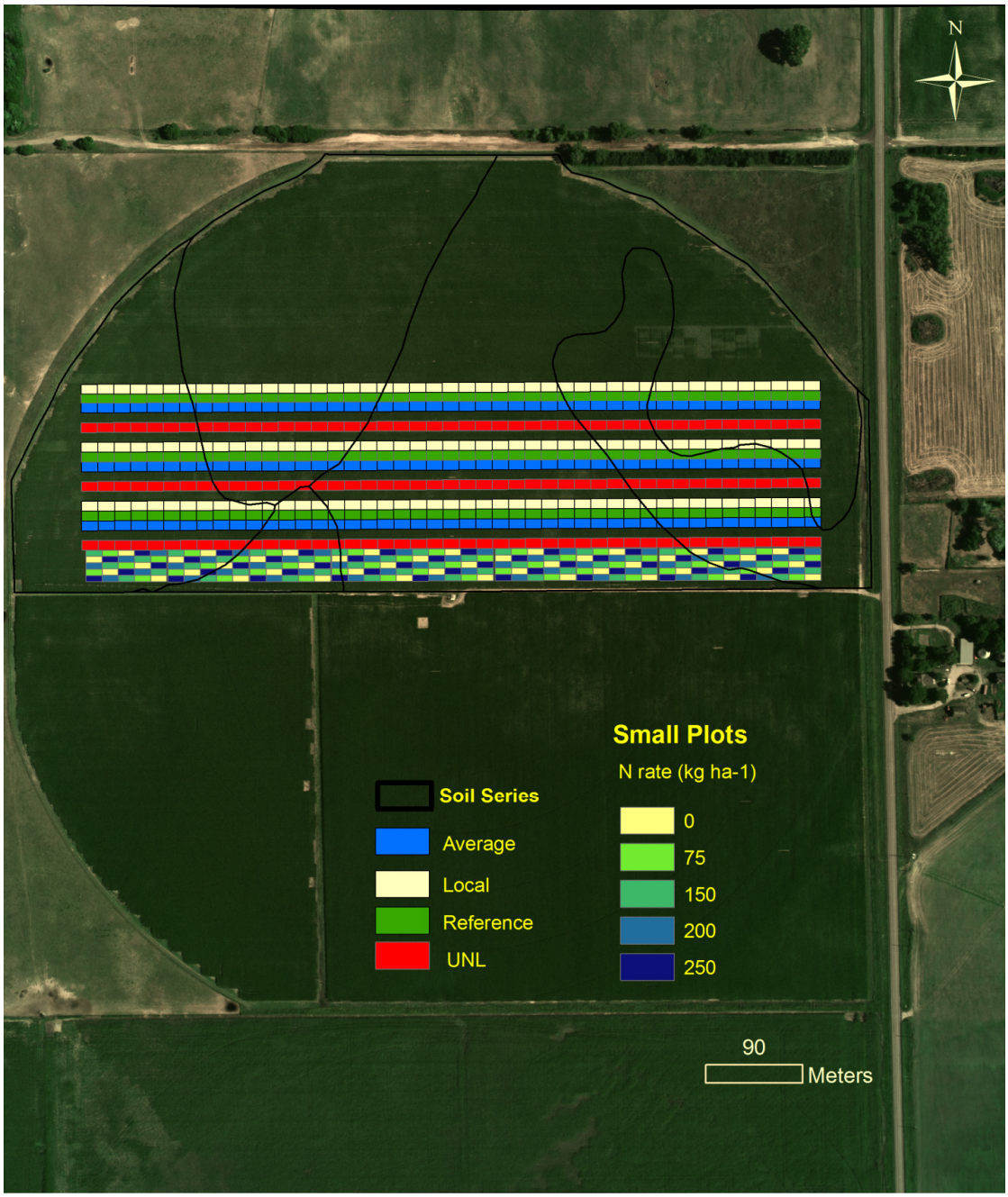

Figure 2. Experimental design for the Field Long Strips (Experiment 1) and Small Plots (Experiment 2), where a spatial design were adjusted for data interpolation. Example of the BR09 field.

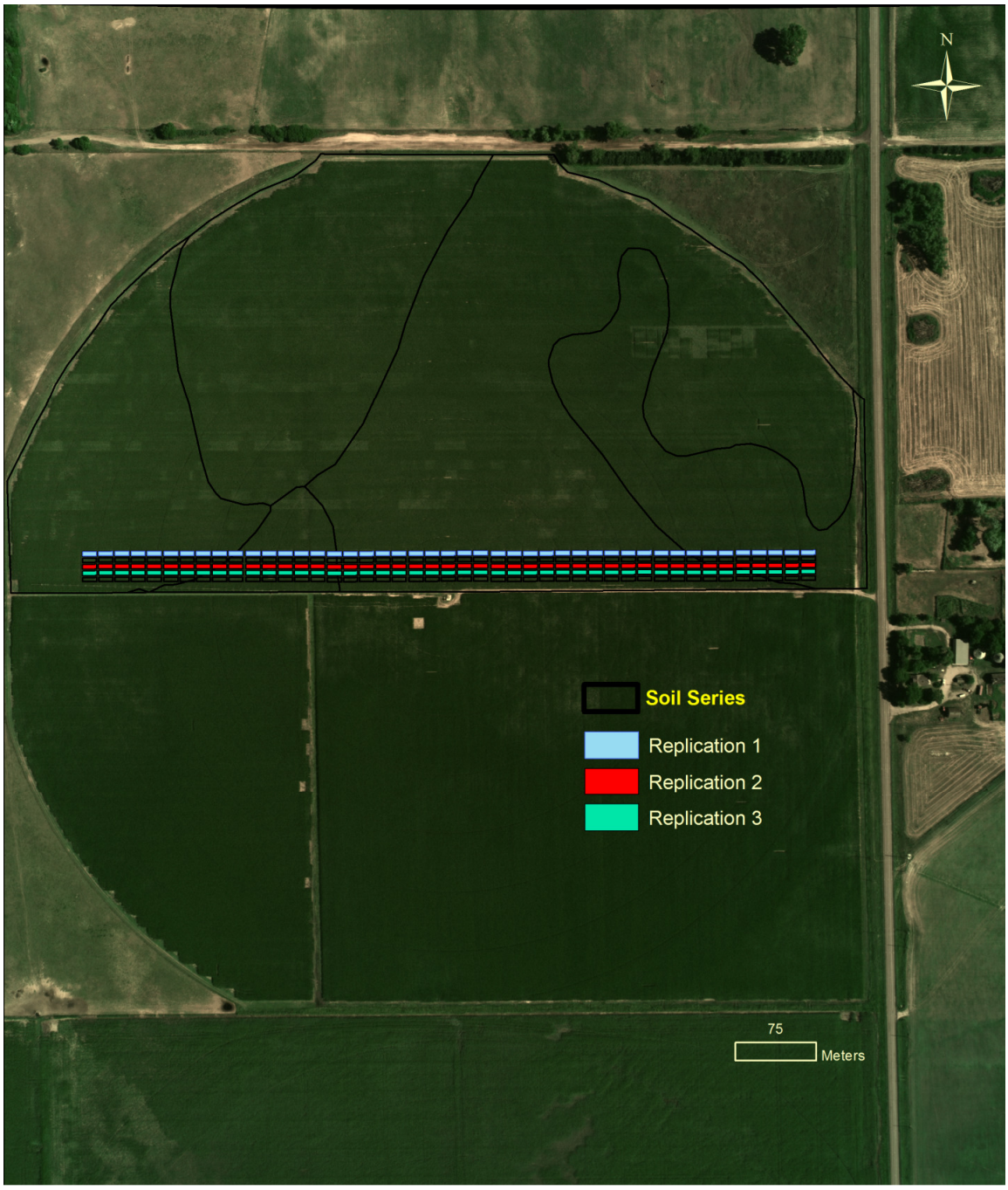

Figure 3. Randomization of the Experiment 2 (Small Plots) inside the area where the spatial design was imposed. Example of the BR09 field.

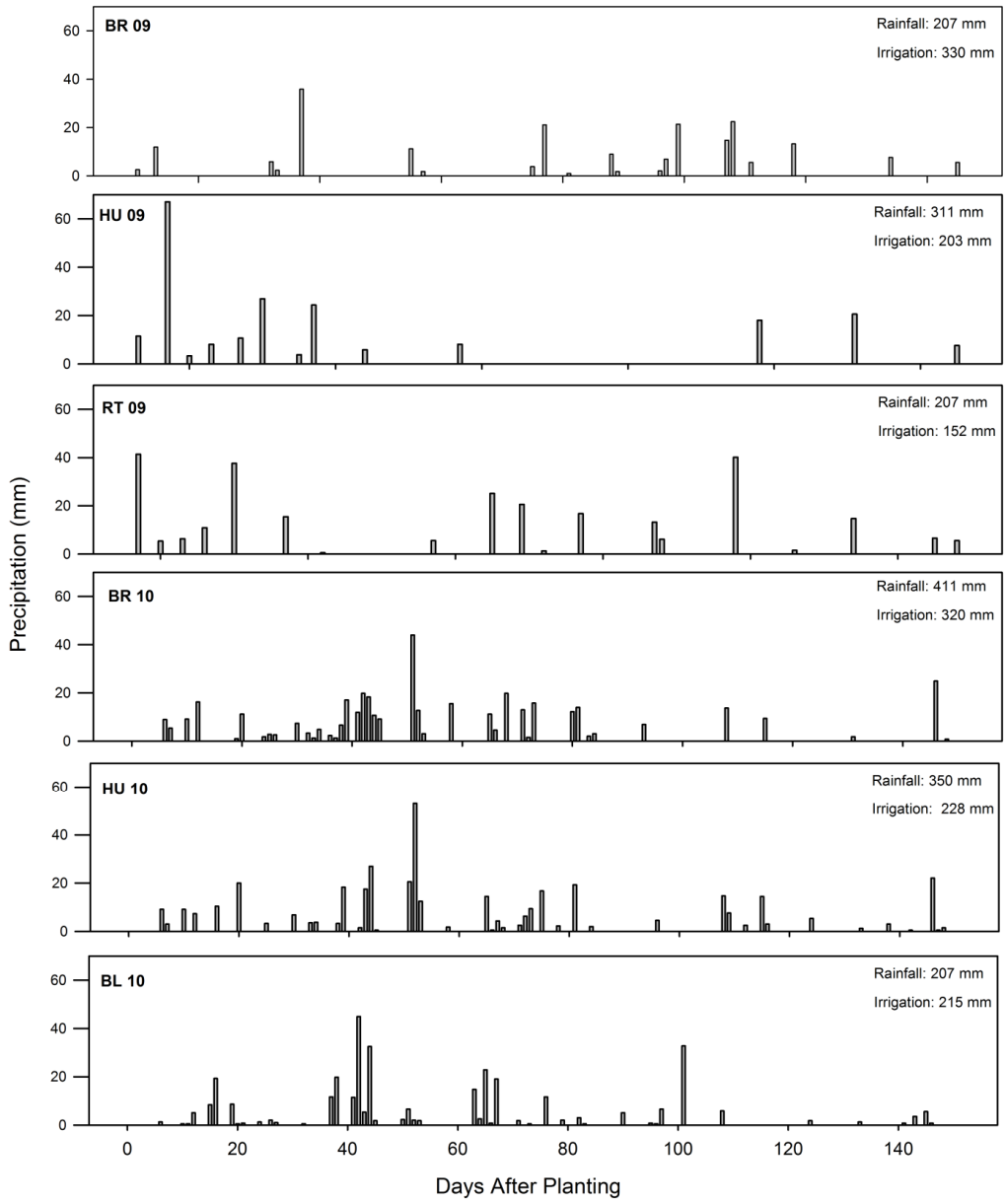

Figure 4. Rainfall and irrigation amount during the growing season for all producer's fields.

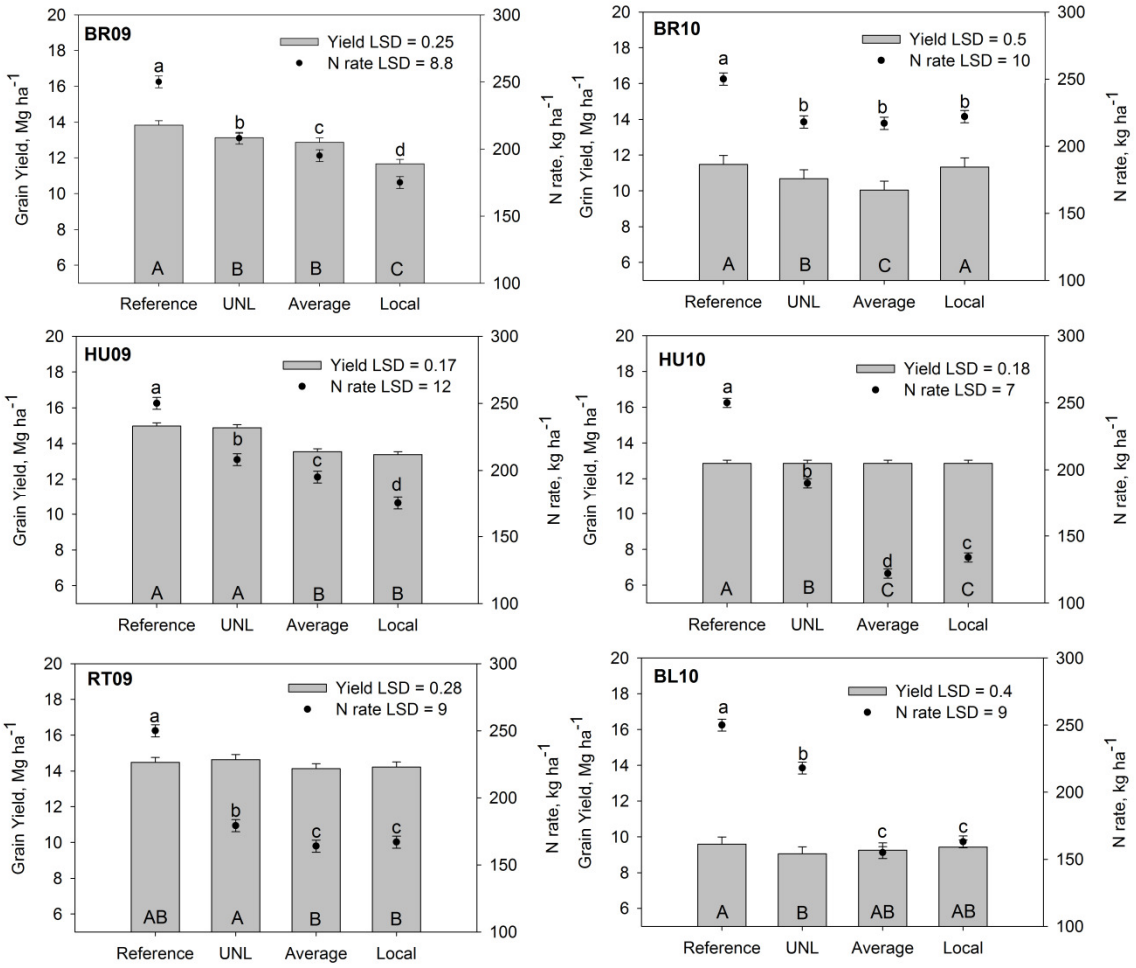

Figure 5. Average grain yield and N applied resulted from the treatments at the Field Long Strips. Least significant difference (LSD) was calculated for treatment within each field. Treatment mean groupings are indicated for yield (uppercase letters) and N rate (lowercase letters) for each field. Error bars indicate standard error for each treatment.

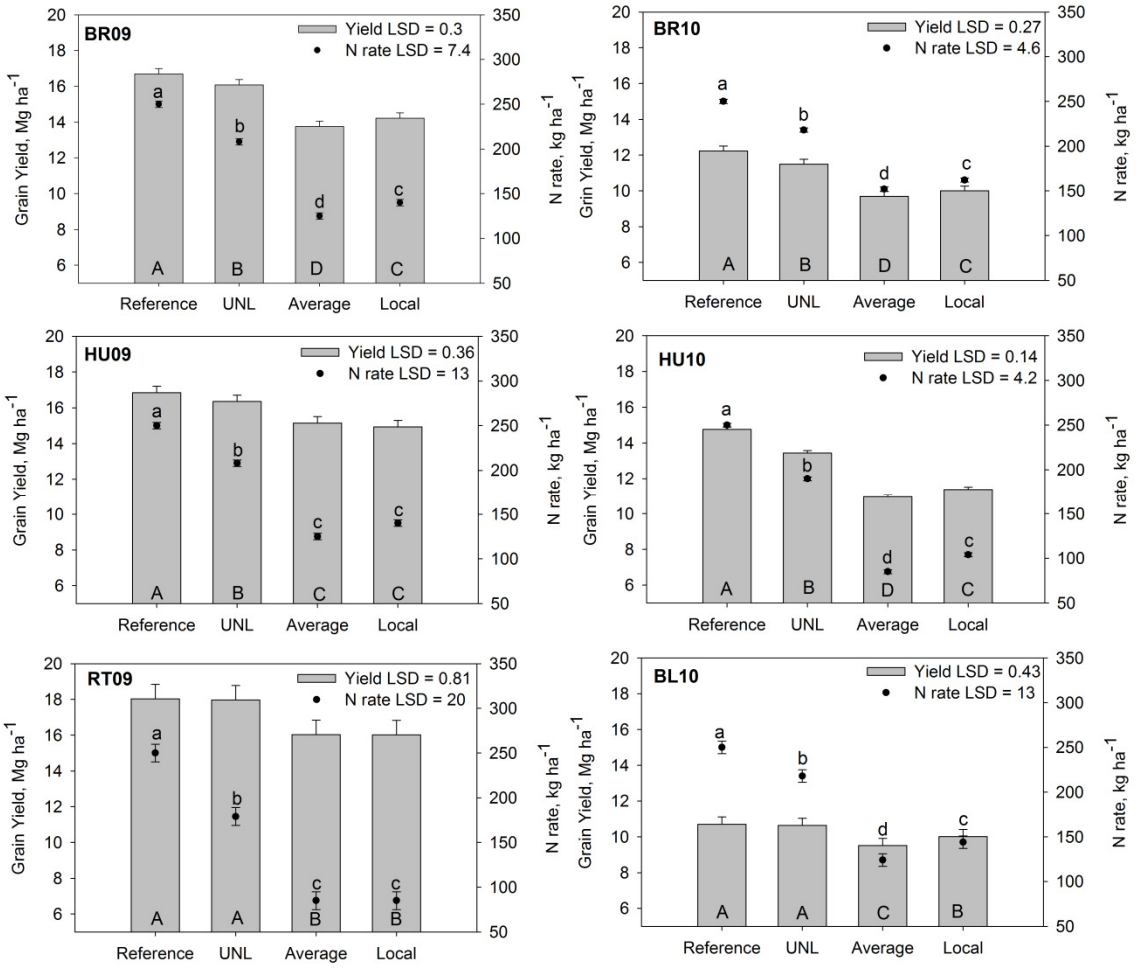

Figure 6. Average grain yield and N applied resulted from the treatments at the Small Plots. Least significant difference (LSD) was calculated for treatment within each field. Treatment mean groupings are indicated for yield (uppercase letters) and N rate (lowercase letters) for each field. Error bars indicate standard error for each treatment.

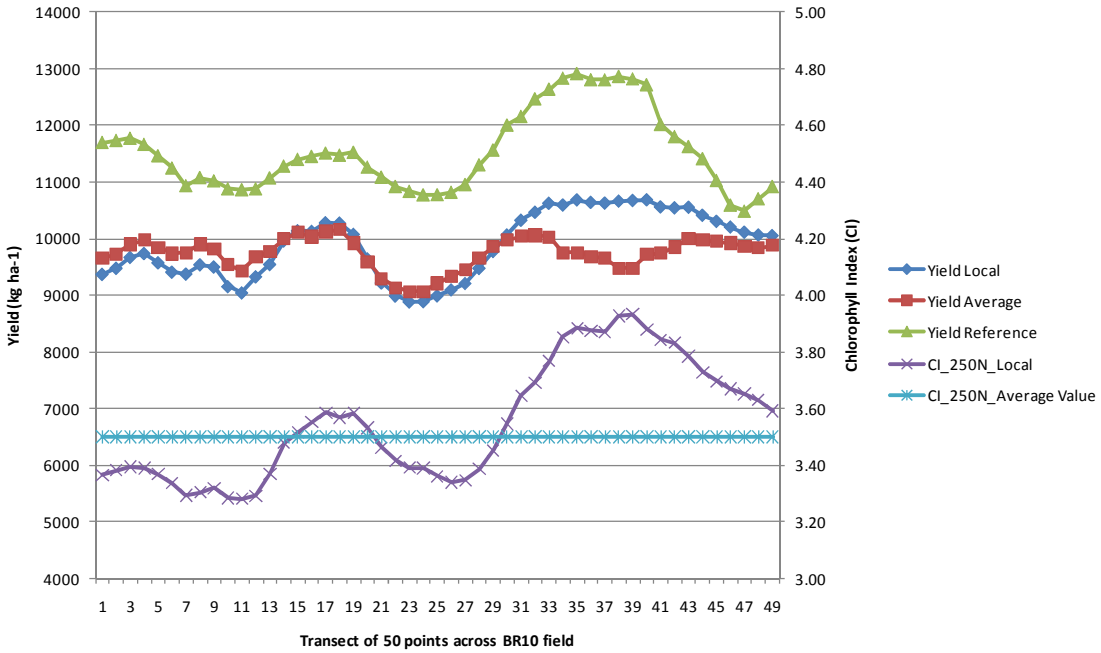

Figure 7. Transect for the BR10 field showing the spatial variation of grain yield when different approaches (Local and Average) were imposed to calculate N rates. Yield Reference is the final yield obtained in the N-rich strip (250 kg n ha^{-1}). CI_250N_Local is the CI for each point of the transect when 250 kg N ha^{-1} was applied and CI_250N_Average Value is the average for the whole transect.

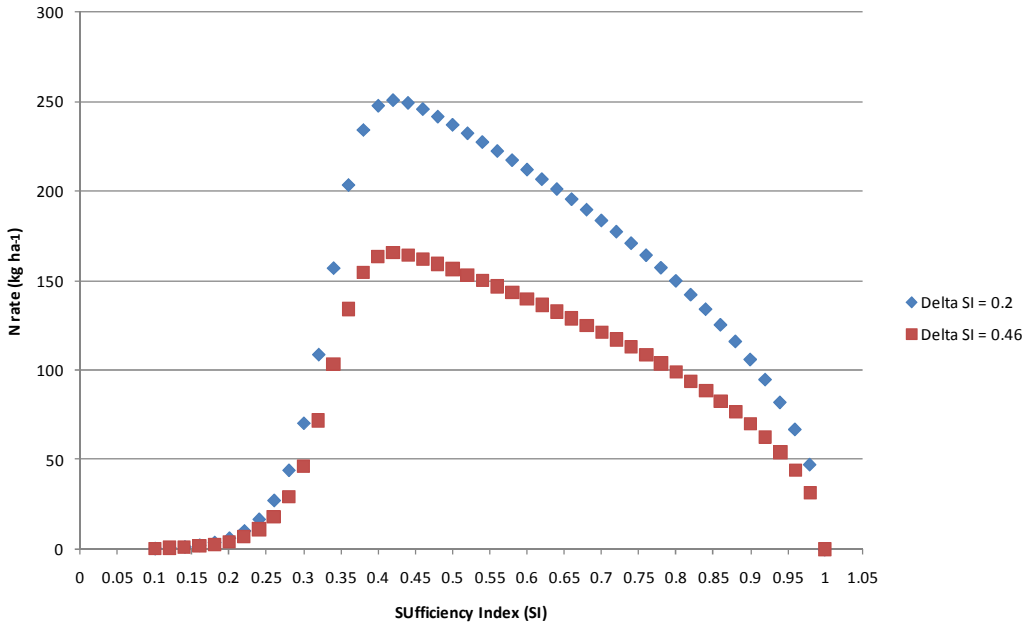

Figure 8. Effect of the N rate prescription changing at various SI when two different values of Delta SI (Δ SI).are used.

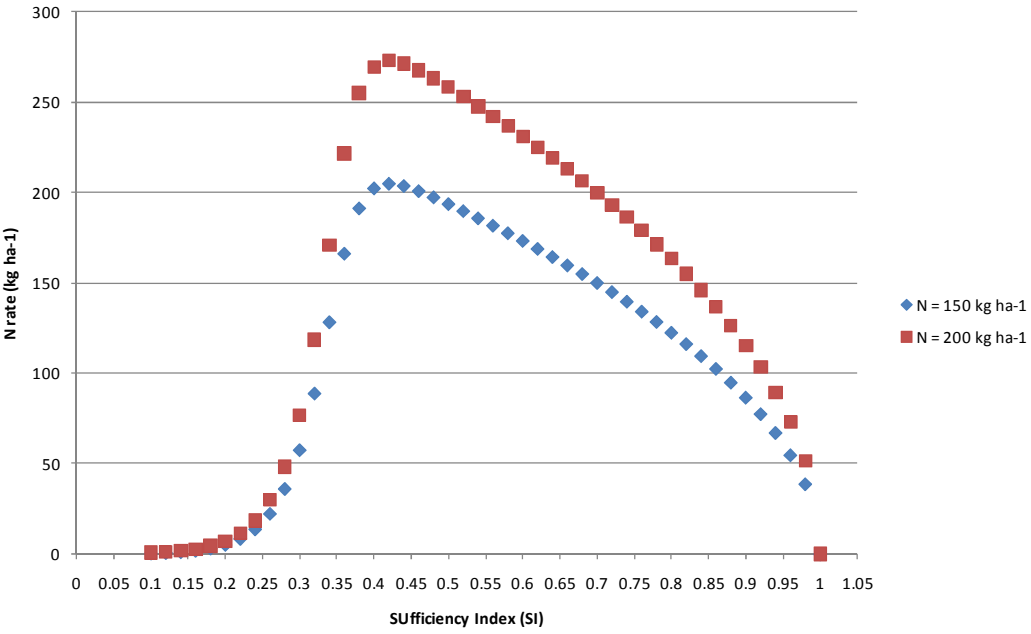

Figure 9. Effect of the N rate precription changing at various SI when two different values of nitrogen rate that maximizes the yield.are used.

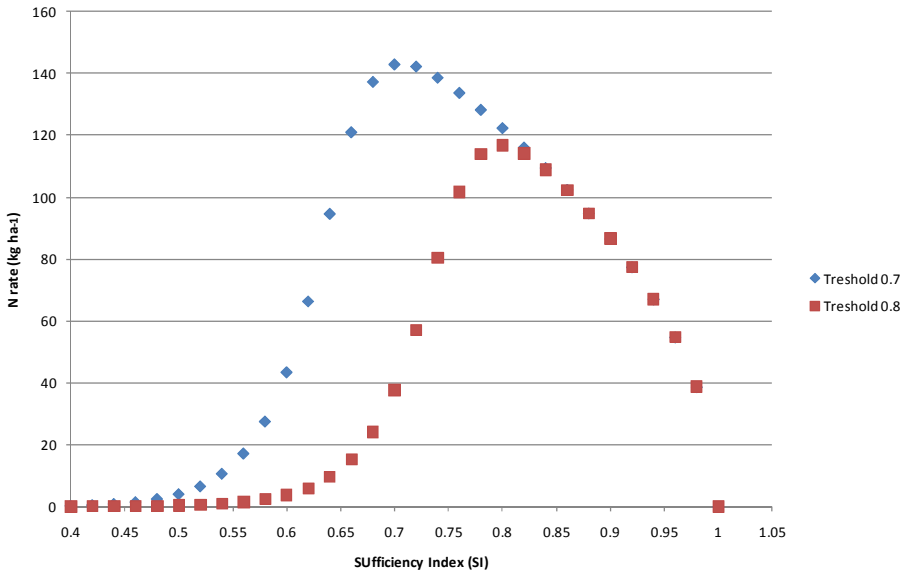

Figure 10. Effect of the N rate precription changing at various SI when two different values of SI treshold are used.

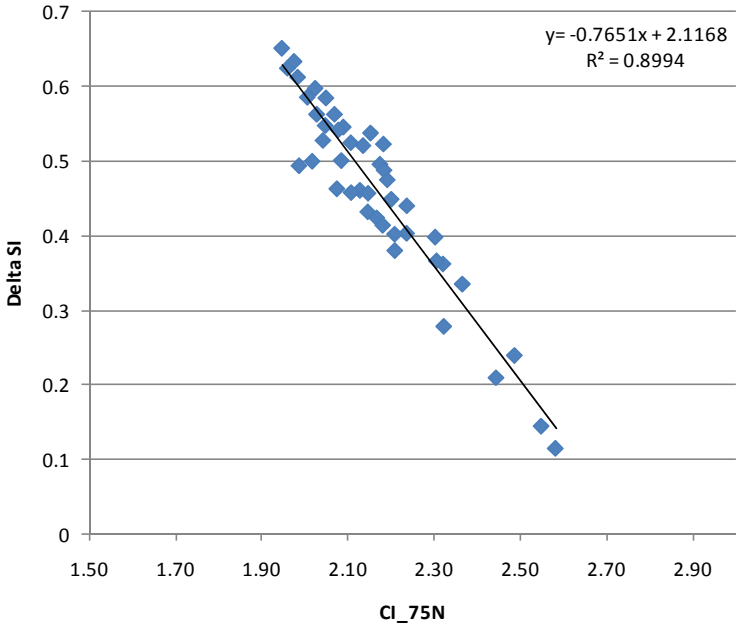

Figure 11. Correlation between the Δ SI and chlorophyll index using 75 kg N ha^{-1} (CI_75N) for the BR09 field.

Table 1. Previous crop, row spacing, N rates used in the small plots area, crop system and predominant soil series at experimental fields conducted during 2009 and 2010.

Site	Previous Crop	Corn Hybrid	N rates (kg ha^{-1})	Crop System	Soil Series
BR09	Soybeans	Pioneer 32T84	75, 100, 150, 200, 250	No tillage	Ipage Fine Sand
HU09	Corn	Dekalb 65-63VT3	75, 100, 150, 200, 250	Strip Till	Hastings Silt Loam
RT09	Soybeans	Pioneer 32B11	75, 100, 150, 200, 250	No tillage	Hord Silt Loam
BR10	Soybeans	Pioneer 33D47	0,75,150,200,250	No tillage	Libory Fine Sand
HU10	Corn (Popcorn)	Excel 5995YGVT3	0,75,150,200,250	No tillage	Hastings Clay Loam
BL10	Corn	Dekalb DKC5259	0,75,150,200,250	No tillage	Satanta Loam

Table 1a. Detailed soil information with the percent of area that was covered with different soil taxonomic class in each field (% Area) and slope.

Field	Series	Slope	% Area	Taxonomic Class
BR09	Novina sandy loam	1 to 3%	19.30	Coarse-loamy, mixed, superactive, mesic Fluvaquentic Haplustolls
	Thurman loamy fine sand	0 to 2%	22.30	Sandy, mixed, mesic Udorthentic Haplustolls
	Thurman loamy fine sand	2 to 6%	13.40	Sandy, mixed, mesic Udorthentic Haplustolls
	Ipage loamy fine sand	0 to 3%	45.20	Mixed, mesic Oxyaquic Ustipsamments
HU09	Hastings silt loam	0 to 1%	55.70	Fine, smectitic, mesic Udic Argiustolls
	Hastings silt loam	1 to 3%	22.50	Fine, smectitic, mesic Udic Argiustolls
	Hastings silty clay loam	3 to 7%	21.70	Fine, smectitic, mesic Udic Argiustolls
RT09	Uly silt loam	3 to 6%	1.20	Fine-silty, mixed, superactive, mesic Typic Haplustolls
	Hord silt loam	1 to 3%	11.00	Fine-silty, mixed, superactive, mesic Cumulic Haplustolls
	Hastings silt loam	0 to 1%	17.50	Fine, smectitic, mesic Udic Argiustolls
	Thurman fine sandy loam	2 to 11%	22.10	Sandy, mixed, mesic Udorthentic Haplustolls
	Hord silt loam	1 to 3%	48.10	Fine-silty, mixed, superactive, mesic Cumulic Haplustolls
BR10	Libory loamy fine sand	0 to 3%	49.40	Sandy over loamy, mixed, superactive, mesic Oxyaquic Haplustolls
	Valentine fine sand	3 to 9%	26.20	Mixed, mesic Typic Ustipsamments
	Valentine fine sand	9 to 24%	24.40	Mixed, mesic Typic Ustipsamments
HU10	Hastings silt loam	1 to 3%	34.00	Fine, smectitic, mesic Udic Argiustolls
	Hastings silt loam	3 to 7%	22.50	Fine, smectitic, mesic Udic Argiustolls
	Hastings silty clay loam	7 to 11%	43.50	Fine, smectitic, mesic Udic Argiustolls
BL10	Bankard loamy sand	1 to 3%	14.80	Sandy, mixed, mesic Ustic Torrifluvents
	Bayard very fine sandy loam	1 to 3%	23.70	Coarse-loamy, mixed, superactive, mesic Torriorthentic Haplustolls
	Satanta loam	3 to 6%	41.80	Fine-loamy, mixed, superactive, mesic Aridic Argiustolls
	Satanta-Dix complex	3 to 9%	19.70	Fine-loamy, mixed, superactive, mesic Aridic Argiustolls

Table 2. Descriptive statistics for yield, CI, SI, RTK Elevation, RT_ rel, EC and SOM across all sites in the small plots transects.

Descriptive Statistics

Variable	N	Mean	Std Dev	Median	Minimum	Maximum
Yield_0N (kg ha^{-1})	264	9938	4146	9797	4123	19439
Yield_75N (kg ha^{-1})	264	11137	3979	10777	3419	18283
Yield_250N (kg ha^{-1})	264	14497	2913	14537	8476	19613
CI_0N	264	2.44	0.40	2.40	1.52	3.98
CI_75n	264	2.59	0.38	2.58	1.60	3.75
CI_250n	264	3.26	0.48	3.13	2.44	4.50
SI_0N	264	0.75	0.11	0.75	0.54	1.20
SI_75n	264	0.80	0.08	0.80	0.55	1.02
Elevation (m)	264	633	190	563	516	1062
EC_shallow (mS m^{-1})	264	3.98	3.32	3.77	0.38	12.46
EC_deep (mS m^{-1})	264	27.96	26.21	11.18	1.06	74.96
SOM (g kg^{-1})	264	22.1	9.5	26.4	5.0	34.3
RTK_rel	264	0.99	0.00	0.99	0.98	1.00

Table 3. Analysis of variance results for grain yield, partial factor productivity (PFP) in kg grain (kg N applied^{-1}) and chlorophyll index using 75 kg N ha^{-1} at time of sensing across all fields for the long strips treatments.

Field				**Yield (kg ha^{-1})**		**PFP**		**CI**	
	Rep	Num df	Den DF	F Value	Pr > F	F Value	Pr > F	F Value	Pr > F
BR09	2	3	534	66.32	<.0001	23.94	<.0001	84.95	<.0001
HU09	2	3	666	135.29	<.0001	141.05	<.0001	149.03	<.0001
RT09	2	3	462	3.57	0.0142	39.86	<.0001	13.21	<.0001
BR10	2	3	594	9.4	<.0001	10.69	<.0001	13.21	<.0001
HU10	2	3	594	19.35	<.0001	216.8	<.0001	44.59	<.0001
BL10	2	3	510	1.74	0.1584	74.81	<.0001	14.94	<.0001

Table 4. Mean separation grouping for average partial factor productivity (PFP) in kg grain (kg N applied^{-1}) in each field for the long strips treatments (LSD, α=0.05).

PFP	**BR09**	**HU09**	**RT09**	**BR10**	**HU10**	**BL10**
Local	78.4a	119.2a	100.9a	59.6a	105.2a	70.6a
Average	69.8b	104.4b	100.4a	56.2a	109.5a	69.2a
UNL	62.9c	80.0c	81.6b	48.9b	66.1b	41.5b
Reference	55.3c	59.9d	57.9c	45.9b	51.4c	38.3b

Table 5. Mean separation grouping for average grain yield, N rate and partial factor productivity (PFP) across all fields for the long strips treatments (LSD, α=0.05).

PFP	Grain Yield Mg ha^{-1}	N rate kg ha^{-1}	PFP kg grain(kg N)$^{-1}$
Local	12.031c	133.9c	89.8a
Average	12.018c	140.6c	85.4b
UNL	12.537b	199.9b	63.7c
Reference	12.917a	250.0a	51.6d

Table 6. Average sensor data (SI and CI) for each field using the localized and averaged reference approaches for the long strips.

Field	Long Strips		
	SI_Local	SI_Average	CI_ref
BR09	1.05	0.83	4.01
HU09	1.00	0.92	4.88
RT09	0.91	0.87	4.81
BR10	0.80	0.77	3.52
HU10	0.95	0.95	4.16
BL10	0.92	0.96	3.22

Table 7. Analysis of variance results for grain yield and partial factor productivity across all fields for the small -plots treatments.

Field			**Yield**		**PFP**	
	Rep df	Trt df	F Value	Pr > F	F Value	Pr > F
BR09	2	3	159.39	<0.0001	118.7	<0.0001
HU09	2	3	51.53	<0.0001	63.05	<0.0001
RT09	2	3	15.46	<0.0001	35.98	<0.0001
BR10	2	3	149.22	<0.0001	76.14	<0.0001
HU10	2	3	1249.15	<0.0001	298.22	<0.0001
BL10	2	3	12.89	<0.0001	37.84	<0.0001

Table 8. Mean separation grouping for average partial factor productivity (PFP) in kg grain (kg N applied^{-1}) in each field for the small plots treatments (LSD, α=0.05).

PFP	BR09	HU09	RT09	BR10	HU10	BL10
Local	102.8b	132.1a	197.5a	61.9b	110.3b	71.5b
Average	112.7a	133.8a	148.4b	65.0a	133.5a	92.7a
UNL	77.2c	87.9b	100.3c	52.7c	70.7c	48.8c
Reference	33.7d	67.3c	72.1d	48.9d	59.0d	42.8c

Table 9. Mean separation grouping for average grain yield, N rate and partial factor productivity (PFP) across all fields for the small plots treatments (LSD, α=0.05).

PFP	**Grain Yield Mg ha^{-1}**	**N rate kg ha^{-1}**	**PFP kg grain(kgN)$^{-1}$**
Local	12.762c	112.14d	113.8c
Average	12.513c	109.4c	114.3c
UNL	14.327b	199.8b	72.9b
Reference	14.878a	250.0a	59.5a

Table 10. Average sensor data (SI and CI) for each field using the localized and averaged reference approaches for the small plots.

Field	Small Plots		
	SI_Local	SI_Average	CI_ref
BR09	0.77	0.77	2.80
HU09	0.82	0.82	3.01
RT09	0.87	0.87	3.33
BR10	0.71	0.71	3.55
HU10	0.87	0.87	2.97
BL10	0.76	0.76	3.87

Table 11. Spearman rank correlation between grain yield (Y), chlorophyll index (CI), sufficiency index (SI), Delta SI (Δ SI) and GPS RTK elevation (RTK), Relative RTK elevation (RTK_rel), apparent soil electrical conductivity (EC) at shallow (ECsh) and deep (ECdp), soil organic matter (SOM) and the difference between N rates prescribed for the Local minus the Average (L-A_N) across all sites in the small plots transects. The BL10 field ECdp measurements were discarded due to issues in the data collection.

	Yield_0N	Y_75N	Y_250N	CI_0N	CI_75N	CI_250N	SI_0N	SI_75N	RTK	ECsh	ECdp	SOM	RTK_rel	Δ SI	L–A_N
Y_0N	1.00														
Y_75N	0.94***	1.00													
Y_250N	0.91***	0.89***	1.00												
CI_0N	0.32***	0.33***	0.19***	1.00											
CI_75N	0.09	0.13	-0.06	0.80***	1.00										
CI_250N	-0.30***	-0.27***	-0.38***	0.56***	0.67***	1.00									
SI_0N	0.73***	0.70***	0.67***	0.47***	0.14***	-0.41***	1.00								
SI_75N	0.50***	0.53***	0.42***	0.29***	0.38***	-0.39***	0.71***	1.00							
RTK	-0.12*	-0.12**	-0.30***	0.27***	0.52***	0.30***	-0.08	0.32***	1.00						
ECsh	0.34***	0.32***	0.25***	0.19***	0.37***	-0.14**	0.36***	0.68***	0.61***	1.00					
ECdp	0.50***	0.44***	0.53***	0.11*	0.12**	-0.37***	0.56***	0.67***	0.14***	0.80***	1.00				
SOM	0.42***	0.41***	0.30***	0.45***	0.57***	0.08	0.45***	0.68***	0.58***	0.77***	0.67***	1.00			
RTK_rel	-0.08	-0.09	-0.06	-0.23***	-0.39***	-0.26***	-0.02	-0.16**	-0.20**	-0.38***	-0.31***	-0.46***	1.00		
Δ SI	-0.35***	-0.30***	-0.28***	-0.74***	-0.52***	-0.19***	-0.64***	-0.50***	-0.32***	-0.45***	-0.50***	-0.63***	-0.19**	1.00	
L–A_N	0.11*	0.11*	0.08	0.54***	0.53***	0.62***	-0.03	-0.10	0.11*	0.15**	0.14**	0.21***	0.11*	-0.37***	1.00

*Statistical significance at *p<0.10*
**Statistical significance at *p<0.05*
***Statistical significance at *p<0.001*

Table 12.Yield (kg ha^{-1}) and Sufficiency Index (SI) predicted equations to evaluate the N response (kg ha^{-1}) for the transect made in the small plots area at the BR09.

Long	Lat	ID	Yield Response Equation	R2	SI response Equation	R2
-97.99215123	41.27476437	1	Yield = -0.3415N2 + 145N + 463	R² = 0.963	SI = -5E-06N2 + 0.0034N + 0.4726	R² = 0.9826
-97.99196077	41.27476437	2	Yield = -0.3415N2 + 199N + 478.05	R² = 0.9456	SI = -3E-06N2 + 0.0025N + 0.5397	R² = 0.9808
-97.99178441	41.27476437	3	Yield = 0.0001N2 + 32.982N + 9685.4	R² = 0.9028	SI = -4E-07N2 + 0.0018N + 0.5682	R² = 0.9926
-97.99160099	41.27475026	4	Yield = 0.007N2 + 28.519N + 10194	R² = 0.9208	SI = 5E-06N2 - 2E-05N + 0.7225	R² = 0.997
-97.99141758	41.2747432	5	Yield = -0.0298N2 + 40.13N + 9109.3	R² = 0.9931	SI = 8E-06N2 - 0.0014N + 0.8569	R² = 0.8677
-97.99123416	41.2747432	6	Yield = 0.0852N2 - 9.0342N + 13910	R² = 0.9485	SI = 4E-06N2 + 1E-04N + 0.761	R² = 0.7854
-97.9910578	41.27475026	7	Yield = 0.1705N2 - 43.858N + 17469	R² = 0.9411	SI = 2E-07N2 + 0.0014N + 0.6382	R² = 0.9451
-97.99088144	41.27475731	8	Yield = 0.0547N2 - 0.8378N + 13801	R² = 0.7935	SI = -5E-07N2 + 0.0018N + 0.597	R² = 0.9907
-97.99070508	41.27475731	9	Yield = -0.1111N2 + 58.279N + 8661.2	R² = 0.8309	SI = -3E-06N2 + 0.0029N + 0.4795	R² = 0.9544
-97.99051461	41.27475731	10	Yield = -0.1874N2 + 89.247N + 5684.8	R² = 0.7931	SI = -3E-06N2 + 0.0028N + 0.475	R² = 0.9666
-97.9903312	41.2747432	11	Yield = -0.1009N2 + 60.332N + 7874.4	R² = 0.8599	SI = 6E-06N2 - 0.0006N + 0.7918	R² = 0.9401
-97.99015484	41.27475026	12	Yield = -0.0647N2 + 44.534N + 9258.8	R² = 0.9894	SI = 8E-06N2 - 0.0016N + 0.8863	R² = 0.7309
-97.98996437	41.27475026	13	Yield = -0.0866N2 + 55.147N + 7911.9	R² = 0.9799	SI = -3E-07N2 + 0.0017N + 0.5988	R² = 0.9629
-97.98976685	41.27475026	14	Yield = -0.3415N2 + 135.99N + 470	R² = 0.9714	SI = -6E-06N2 + 0.0039N + 0.4377	R² = 0.983
-97.9896046	41.27475026	15	Yield = -0.3415N2 + 115.99N + 400	R² = 0.9862	SI = -7E-06N2 + 0.0041N + 0.4374	R² = 0.9187
-97.98941413	41.27475026	16	Yield = -0.3415N2 + 145N + 375	R² = 0.9969	SI = -1E-05N2 + 0.005N + 0.402	R² = 0.9515
-97.98923777	41.27475731	17	Yield = -0.3415N2 + 145.99N + 495	R² = 0.9798	SI = -1E-05N2 + 0.0058N + 0.3484	R² = 0.992
-97.98906846	41.27476437	18	Yield = -0.2544N2 + 109.23N + 4190.5	R² = 0.9608	SI = -1E-05N2 + 0.0056N + 0.3663	R² = 0.984
-97.98887799	41.27476437	19	Yield = -0.1674N2 + 78.762N + 6672.9	R² = 0.963	SI = -1E-05N2 + 0.0054N + 0.4156	R² = 0.9883
-97.98870163	41.27476437	20	Yield = -0.1482N2 + 70.515N + 7528.3	R² = 0.9861	SI = -1E-05N2 + 0.0045N + 0.5048	R² = 0.9295
-97.98851117	41.27476437	21	Yield = -0.2444N2 + 104.62N + 4778.7	R² = 1	SI = -1E-05N2 + 0.0052N + 0.477	R² = 0.8841
-97.98834186	41.27475731	22	Yield = -0.1672N2 + 88.239N + 5291.9	R² = 0.9923	SI = -1E-05N2 + 0.0051N + 0.4625	R² = 0.9285
-97.98815845	41.27476437	23	Yield = -0.0135N2 + 41.026N + 8740.1	R² = 0.9828	SI = -7E-06N2 + 0.0036N + 0.5609	R² = 0.9376
-97.9879962	41.27476437	24	Yield = -0.0825N2 + 61.066N + 7533.9	R² = 0.9878	SI = -7E-06N2 + 0.0035N + 0.5517	R² = 0.9959
-97.98780573	41.27476437	25	Yield = -0.3415N2 + 125N + 380	R² = 0.941	SI = -9E-06N2 + 0.0044N + 0.4543	R² = 0.9978
-97.98760115	41.27476437	26	Yield = -0.3415N2 + 141N + 478.05	R² = 0.9724	SI = -7E-06N2 + 0.0038N + 0.5128	R² = 0.9249
-97.98743184	41.27476437	27	Yield = -0.1069N2 + 63.162N + 7784.9	R² = 0.9795	SI = -5E-06N2 + 0.0029N + 0.6029	R² = 0.8056
-97.98724137	41.27476437	28	Yield = 0.0074N2 + 21.905N + 11105	R² = 0.7353	SI = -4E-06N2 + 0.0023N + 0.6656	R² = 0.7345
-97.98706502	41.27476437	29	Yield = -0.0083N2 + 30.666N + 9753.1	R² = 0.7719	SI = -5E-06N2 + 0.0027N + 0.6343	R² = 0.8562
-97.98686749	41.27476437	30	Yield = -0.1218N2 + 73.077N + 5984.7	R² = 0.9506	SI = -6E-06N2 + 0.0035N + 0.525	R² = 0.9012
-97.98669819	41.27476437	31	Yield = -0.1644N2 + 83.641N + 5638.9	R² = 0.9981	SI = -7E-06N2 + 0.0039N + 0.4582	R² = 0.9511
-97.98652888	41.27476437	32	Yield = -0.2632N2 + 107.45N + 4745.9	R² = 0.8656	SI = -8E-06N2 + 0.0046N + 0.3872	R² = 0.9623
-97.98634547	41.27475026	33	Yield = -0.3276N2 + 125.51N + 3533.8	R² = 0.8916	SI = -7E-06N2 + 0.0041N + 0.414	R² = 0.9371
-97.986155	41.27475026	34	Yield = -0.2476N2 + 107.81N + 3804	R² = 0.9934	SI = -8E-06N2 + 0.0042N + 0.4527	R² = 0.9343
-97.98595747	41.27475026	35	Yield = -0.1775N2 + 87.181N + 5101.2	R² = 0.9935	SI = -7E-06N2 + 0.0039N + 0.499	R² = 0.921
-97.98576701	41.27475026	36	Yield = -0.1204N2 + 66.113N + 7059.8	R² = 0.991	SI = -8E-06N2 + 0.004N + 0.5436	R² = 0.8767
-97.98560476	41.27475026	37	Yield = -0.0422N2 + 43.247N + 8491.4	R² = 0.9937	SI = -7E-06N2 + 0.0035N + 0.5763	R² = 0.8382
-97.98542134	41.27475026	38	Yield = -0.0688N2 + 58.145N + 6750.7	R² = 0.9876	SI = -5E-06N2 + 0.0032N + 0.5378	R² = 0.9645

-97.98523793	41.27475026	39	Yield = -0.1158N2 + 75.712N + 5144.7	R² = 0.9879	SI = -5E-06N2 + 0.0032N + 0.5064	R² = 0.9919
-97.98504746	41.2747432	40	Yield = -0.1311N2 + 75.287N + 5735.8	R² = 0.9866	SI = -6E-06N2 + 0.0036N + 0.5003	R² = 0.9844
-97.9848711	41.2747432	41	Yield = -0.0842N2 + 51.194N + 8455	R² = 0.9908	SI = -7E-06N2 + 0.0036N + 0.5863	R² = 0.7815
-97.98470179	41.2747432	42	Yield = -0.0189N2 + 29.777N + 10165	R² = 0.9887	SI = -5E-06N2 + 0.0028N + 0.6209	R² = 0.8075
-97.98451132	41.2747432	43	Yield = -0.0103N2 + 30.503N + 9707.1	R² = 0.9954	SI = -5E-06N2 + 0.0033N + 0.5426	R² = 0.9242
-97.98433496	41.27473615	44	Yield = -0.1572N2 + 82.942N + 5111.6	R² = 0.9959	SI = -1E-05N2 + 0.006N + 0.3752	R² = 0.9522
	Average Equation		**Yield = -0.1309N2 + 71.447N + 6748**	**R² = 0.995**	**SI = -5E-06N2 + 0.0032N + 0.5397**	**R² = 0.947**

Table 13. Yield (kg ha^{-1}) and Sufficiency Index (SI) predicted equations to evaluate the N response (kg ha^{-1}) for the transect made in the small plots area at the HU09.

Long	Lat	ID	Yield Response Equation	R2	SI response Equation	R2
-98.16755961	40.8416722	1	Yield = -0.0355N2 + 11.326N + 15958	R² = 0.0491	SI = -6E-07N2 + 0.0009N + 0.8125	R² = 0.9938
-98.1673843	40.84167698	2	Yield = -0.036N2 + 21.168N + 14360	R² = 0.9132	SI = 3E-06N2 - 0.0004N + 0.9135	R² = 0.9759
-98.16720519	40.84166661	3	Yield = -0.0543N2 + 32.371N + 13113	R² = 0.9997	SI = 7E-06N2 - 0.0023N + 1.1089	R² = 0.4758
-98.16702995	40.84166535	4	Yield = -0.0666N2 + 37.969N + 12569	R² = 0.9986	SI = 1E-06N2 - 0.0004N + 1.0158	R² = 0.1029
-98.16684261	40.84167609	5	Yield = -0.0434N2 + 30.912N + 13137	R² = 0.965	SI = -6E-06N2 + 0.0026N + 0.7513	R² = 0.8925
-98.16665937	40.8416778	6	Yield = -0.0145N2 + 19.333N + 14368	R² = 0.8534	SI = -3E-06N2 + 0.0018N + 0.7384	R² = 0.9505
-98.16647624	40.84167042	7	Yield = 0.0004N2 + 11.385N + 15332	R² = 0.8134	SI = 3E-07N2 + 0.0009N + 0.7555	R² = 0.9494
-98.16629307	40.84166607	8	Yield = -0.0768N2 + 31.932N + 14079	R² = 0.9457	SI = 3E-06N2 + 0.0003N + 0.726	R² = 0.8961
-98.16612572	40.84167091	9	Yield = -0.1549N2 + 58.002N + 11920	R² = 0.9799	SI = 3E-06N2 - 0.0003N + 0.8554	R² = 0.9646
-98.16593455	40.84166953	10	Yield = -0.1463N2 + 61.232N + 11130	R² = 0.9015	SI = -5E-07N2 + 0.0007N + 0.8671	R² = 0.9928
-98.16575931	40.84166827	11	Yield = -0.0719N2 + 35.818N + 13069	R² = 0.8808	SI = -2E-07N2 + 0.001N + 0.7711	R² = 0.9575
-98.16558407	40.841667	12	Yield = -0.0706N2 + 35.531N + 12865	R² = 0.9887	SI = 4E-06N2 - 0.0003N + 0.8364	R² = 0.964
-98.16541278	40.84166878	13	Yield = -0.128N2 + 59.518N + 10391	R² = 0.9948	SI = 7E-06N2 - 0.0016N + 0.9298	R² = 0.9852
-98.16522161	40.8416674	14	Yield = -0.1957N2 + 84.903N + 8106.6	R² = 0.9963	SI = 4E-06N2 - 0.0008N + 0.9306	R² = 0.9983
-98.16505028	40.84167221	15	Yield = -0.1985N2 + 86.874N + 7872.6	R² = 0.9929	SI = -3E-06N2 + 0.0017N + 0.7885	R² = 0.9505
-98.16487496	40.84167699	16	Yield = -0.0056N2 + 19.221N + 13033	R² = 0.7799	SI = 4E-07N2 + 0.0007N + 0.791	R² = 0.9795
-98.16468781	40.84167261	17	Yield = 0.1125N2 - 23.096N + 16570	R² = 0.6243	SI = 1E-05N2 - 0.0029N + 0.9528	R² = 0.996
-98.16451652	40.8416744	18	Yield = 0.0928N2 - 18.812N + 16519	R² = 0.4961	SI = 1E-05N2 - 0.0035N + 0.98	R² = 0.9911
-98.16432519	40.84168511	19	Yield = 0.0731N2 - 18.526N + 17235	R² = 0.1592	SI = 4E-06N2 - 0.0005N + 0.8678	R² = 0.9861
-98.16414203	40.84168076	20	Yield = 0.0462N2 - 4.7174N + 15604	R² = 0.3342	SI = -8E-06N2 + 0.0036N + 0.638	R² = 0.764
-98.16393891	40.84167929	21	Yield = -0.0046N2 + 26.182N + 11283	R² = 0.8013	SI = -1E-05N2 + 0.0049N + 0.4565	R² = 0.8323
-98.1637796	40.84167813	22	Yield = 0.0025N2 + 30.844N + 9767	R² = 0.8784	SI = -9E-06N2 + 0.0044N + 0.4051	R² = 0.8694
-98.16359636	40.84167983	23	Yield = -0.1109N2 + 53.681N + 10013	R² = 0.9282	SI = -7E-06N2 + 0.004N + 0.3962	R² = 0.9124
-98.1634251	40.84167859	24	Yield = 0.0025N2 + 30.844N + 9500	R² = 0.9825	SI = -1E-05N2 + 0.0065N + 0.2815	R² = 0.8794
-98.16324588	40.84167729	25	Yield = -0.1109N2 + 53.681N + 10013	R² = 0.9855	SI = -2E-05N2 + 0.0094N + 0.17	R² = 0.9173
-98.16304663	40.84168491	26	Yield = -0.0169N2 + 13.749N + 13619	R² = 0.5221	SI = -1E-05N2 + 0.0064N + 0.3242	R² = 0.9486
-98.16287147	40.84167759	27	Yield = -0.0169N2 + 13.749N + 13300	R² = 0.6454	SI = 6E-06N2 - 0.0006N + 0.7274	R² = 0.8015
-98.16268819	40.84168231	28	Yield = -0.0169N2 + 13.749N + 13360	R² = 0.7178	SI = 1E-05N2 - 0.0038N + 1.0219	R² = 0.9955
-98.16251681	40.84169014	29	Yield = 0.0159N2 + 11.382N + 12580	R² = 0.7122	SI = 7E-06N2 - 0.0014N + 0.9671	R² = 0.6
-98.16232955	40.84169483	30	Yield = -0.1109N2 + 53.681N + 10013	R² = 0.61	SI = -1E-05N2 + 0.0043N + 0.558	R² = 0.976
-98.16214631	40.84169653	31	Yield = -0.1603N2 + 77.347N + 7340.6	R² = 0.8144	SI = -1E-05N2 + 0.0062N + 0.3306	R² = 0.9424
-98.16198302	40.84169534	32	Yield = -0.0943N2 + 61.796N + 7635.9	R² = 0.9361	SI = -5E-06N2 + 0.0032N + 0.4897	R² = 0.9806
-98.16182378	40.84168814	33	Yield = -0.1053N2 + 66.545N + 7251.2	R² = 0.9157	SI = 3E-06N2 + 0.0002N + 0.7826	R² = 0.9508
-98.16159677	40.84168649	34	Yield = 0.0025N2 + 30.844N + 9785	R² = 0.654	SI = -8E-06N2 + 0.003N + 0.752	R² = 0.6163
-98.16144531	40.84169446	35	Yield = 0.0025N2 + 30.844N + 9767	R² = 0.6252	SI = -2E-05N2 + 0.0069N + 0.5134	R² = 0.8134
-98.16125422	40.84168702	36	Yield = -0.0947N2 + 43.126N + 10424	R² = 0.5013	SI = -9E-06N2 + 0.0038N + 0.6432	R² = 0.8581
-98.16108281	40.84169787	37	Yield = -0.0046N2 + 26.182N + 11283	R² = 0.8666	SI = 9E-06N2 - 0.0016N + 0.8663	R² = 0.9965
-98.16089574	40.84168744	38	Yield = -0.0046N2 + 26.182N + 10280	R² = 0.8042	SI = 1E-05N2 - 0.0035N + 0.9495	R² = 0.9981

-98.1607205	40.84168616	39	Yield = -0.0046N2 + 26.182N + 11083	R^2 = 0.7415	SI = 8E-06N2 - 0.0014N + 0.8783	R^2 = 0.9832
	Average Equation		**Yield = -0.0504N2 + 32.604N + 11988**	**R^2 = 0.8969**	**SI = -1E-06N2 + 0.0013N + 0.7319**	**R^2 = 0.979**

Table 14. Yield (kg ha^{-1}) and Sufficiency Index (SI) predicted equations to evaluate the N response (kg ha^{-1}) for the transect made in the small plots area at the RT09.

Long	Lat	ID	Yield Response Equation	R2	SI response Equation	R2
-98.2478725	40.89312812	1	Yield = -0.0434N2 + 3.8922N + 18953	R² = 0.7322	SI = 4E-05N2 - 0.012N + 1.6501	R² = 0.8334
-98.24787406	40.89299096	2	Yield = 0.0321N2 - 12.588N + 19464	R² = 0.2487	SI = 2E-05N2 - 0.0062N + 1.2102	R² = 0.9948
-98.24787553	40.89286066	3	Yield = 0.0599N2 - 14.239N + 18892	R² = 0.7676	SI = 1E-05N2 - 0.0025N + 0.9422	R² = 0.9135
-98.24787708	40.8927235	4	Yield = -0.0139N2 + 10.088N + 16919	R² = 0.7364	SI = 2E-05N2 - 0.0051N + 1.1706	R² = 0.9452
-98.24787879	40.89257262	5	Yield = -0.1096N2 + 39.927N + 14722	R² = 0.8407	SI = 3E-05N2 - 0.0086N + 1.4661	R² = 0.9631
-98.24788946	40.89242866	6	Yield = -0.1398N2 + 45.631N + 14636	R² = 0.6755	SI = 2E-05N2 - 0.0064N + 1.305	R² = 0.9949
-98.24789094	40.89229836	7	Yield = -0.0935N2 + 32.481N + 15509	R² = 0.5277	SI = 6E-06N2 - 0.0013N + 0.9427	R² = 0.8793
-98.24788338	40.892168	8	Yield = -0.1146N2 + 45.81N + 13981	R² = 0.9654	SI = 1E-06N2 + 0.0003N + 0.8484	R² = 0.891
-98.24789404	40.89202404	9	Yield = -0.2415N2 + 91.951N + 10117	R² = 0.9321	SI = 8E-06N2 - 0.0024N + 1.0724	R² = 0.8421
-98.24787744	40.89189362	10	Yield = -0.3781N2 + 140.31N + 6145.7	R² = 0.8828	SI = 1E-05N2 - 0.0047N + 1.2367	R² = 0.7079
-98.24789179	40.8917442	11	Yield = -0.3302N2 + 120.41N + 8034.8	R² = 0.9195	SI = 1E-05N2 - 0.0031N + 1.0972	R² = 0.695
-98.24788745	40.89161688	12	Yield = -0.1807N2 + 68.729N + 12264	R² = 0.9151	SI = -1E-06N2 + 0.0013N + 0.7459	R² = 0.9721
-98.24788325	40.89147639	13	Yield = -0.1195N2 + 50.633N + 13456	R² = 0.837	SI = -1E-05N2 + 0.0052N + 0.4944	R² = 0.9206
-98.24789774	40.89134111	14	Yield = -0.156N2 + 60.244N + 12972	R² = 0.8511	SI = -8E-06N2 + 0.0029N + 0.7639	R² = 0.9796
-98.24788813	40.89120902	15	Yield = -0.1819N2 + 65.618N + 12759	R² = 0.8361	SI = 6E-06N2 - 0.0019N + 1.1148	R² = 0.2518
-98.24789706	40.89107423	16	Yield = -0.1482N2 + 50.456N + 14223	R² = 0.766	SI = 7E-06N2 - 0.0019N + 1.0691	R² = 0.2402
-98.24789495	40.89093375	17	Yield = -0.0911N2 + 32.825N + 15468	R² = 0.619	SI = -2E-06N2 + 0.0015N + 0.796	R² = 0.3601
-98.24788911	40.89079606	18	Yield = -0.0886N2 + 36.71N + 14735	R² = 0.8409	SI = -8E-06N2 + 0.0034N + 0.7101	R² = 0.2514
-98.24789427	40.89066687	19	Yield = -0.1038N2 + 42.511N + 14186	R² = 0.8339	SI = 1E-06N2 - 0.0006N + 1.1156	R² = 0.0549
-98.24790327	40.89052647	20	Yield = -0.1012N2 + 43.212N + 13992	R² = 0.8354	SI = 2E-05N2 - 0.0087N + 1.6701	R² = 0.6084
-98.24790109	40.89039161	21	Yield = -0.0921N2 + 41.823N + 13875	R² = 0.9038	SI = 3E-05N2 - 0.0088N + 1.5074	R² = 0.588
-98.24791002	40.89025683	22	Yield = -0.0125N2 + 14.482N + 15861	R² = 0.8426	SI = 1E-05N2 - 0.0022N + 0.9299	R² = 0.7258
-98.24790797	40.89011073	23	Yield = 0.0747N2 - 19.13N + 18647	R² = 0.4181	SI = -1E-05N2 + 0.006N + 0.3766	R² = 0.8474
-98.24789843	40.88997302	24	Yield = 0.0192N2 + 0.2825N + 16905	R² = 0.5078	SI = -2E-05N2 + 0.0062N + 0.5502	R² = 0.9696
-98.24789246	40.88984656	25	Yield = -0.0643N2 + 34.601N + 13554	R² = 0.9778	SI = 1E-06N2 - 0.0005N + 1.0096	R² = 0.0112
-98.24789405	40.88970611	26	Yield = -0.0427N2 + 31.292N + 13234	R² = 0.9853	SI = 1E-05N2 - 0.0027N + 0.9235	R² = 0.9214
-98.24789564	40.88956566	27	Yield = 0.0621N2 + 2.3858N + 14787	R² = 0.9763	SI = -4E-07N2 + 0.0025N + 0.4472	R² = 0.8758
-98.24788596	40.88943918	28	Yield = 0.0596N2 + 7.4965N + 13889	R² = 0.9817	SI = -2E-05N2 + 0.0096N - 0.008	R² = 0.7945
-98.24789493	40.88930158	29	Yield = -0.085N2 + 51.187N + 10699	R² = 0.9929	SI = -3E-05N2 + 0.0129N - 0.0811	R² = 0.9091
-98.24790019	40.88916397	30	Yield = -0.2012N2 + 87.275N + 7992.8	R² = 0.996	SI = -1E-05N2 + 0.0058N + 0.3581	R² = 0.8747
-98.2478907	40.88902063	31	Yield = -0.2782N2 + 116.57N + 5426.4	R² = 0.9859	SI = -2E-06N2 + 0.0027N + 0.4125	R² = 0.9248
-98.24788473	40.88889418	32	Yield = -0.3198N2 + 131.06N + 4094.1	R² = 0.9678	SI = -1E-05N2 + 0.0071N + 0.0968	R² = 0.9895
-98.24788626	40.88875934	33	Yield = -0.3061N2 + 123.54N + 4853.8	R² = 0.9849	SI = -3E-05N2 + 0.0125N - 0.1431	R² = 0.8139
-98.24788045	40.88861884	34	Yield = -0.2776N2 + 110.35N + 6226	R² = 0.9971	SI = -3E-05N2 + 0.0096N + 0.2268	R² = 0.8386
-98.2478932	40.88847285	35	Yield = -0.2075N2 + 87.208N + 8178.5	R² = 0.9934	SI = 9E-06N2 - 0.0022N + 0.9719	R² = 0.5689
-98.24788034	40.8883014	36	Yield = -0.063N2 + 43.754N + 11436	R² = 0.9591	SI = 2E-05N2 - 0.0065N + 1.0961	R² = 0.7918
-98.24789661	40.88817228	37	Yield = 0.0496N2 + 5.9774N + 14547	R² = 0.9085	SI = 2E-05N2 - 0.0043N + 0.9243	R² = 0.9551
-98.24789421	40.88805709	38	Yield = 0.1084N2 - 21.621N + 17376	R² = 0.6496	SI = 1E-05N2 - 0.0028N + 0.9127	R² = 0.9423

-98.24790339	40.88789983	39	Yield = 0.0285N2 - 8.1816N + 17368	R^2 = 0.0113	SI = 1E-05N2 - 0.0035N + 1.1131	R^2 = 0.5123
	Average Equation		**Yield = -0.1049N2 + 46.025N + 13087**	**R^2 = 0.9599**	**SI = -4E-06N2 + 0.0002N + 0.8473**	**R^2 = 0.9409**

Table 15. Yield (kg ha^{-1}) and Sufficiency Index (SI) predicted equations to evaluate the N response (kg ha^{-1}) for the transect made in the small plots area at the BR10.

Long	Lat	ID	Yield Response Equation	R2	SI response Equation	R2
-98.03985575	41.24391477	1	Yield = -0.0162N2 + 36.122N + 4225.8	R² = 0.9158	SI = 8E-07N2 + 0.0011N + 0.6806	R² = 0.9742
-98.03967141	41.24391928	2	Yield = -0.0173N2 + 36.873N + 4205.7	R² = 0.9132	SI = 1E-07N2 + 0.0014N + 0.6779	R² = 0.9365
-98.03947916	41.24391768	3	Yield = -0.0217N2 + 38.932N + 4155	R² = 0.9016	SI = -7E-07N2 + 0.0016N + 0.6769	R² = 0.8846
-98.03930302	41.24391016	4	Yield = -0.0284N2 + 40.71N + 4120.5	R² = 0.8891	SI = -1E-06N2 + 0.0018N + 0.6754	R² = 0.8668
-98.03911085	41.24390251	5	Yield = -0.0319N2 + 40.349N + 4142.3	R² = 0.8922	SI = -1E-06N2 + 0.0019N + 0.6661	R² = 0.8982
-98.03893453	41.24390709	6	Yield = -0.0367N2 + 40.368N + 4156.5	R² = 0.8913	SI = -2E-06N2 + 0.0019N + 0.6612	R² = 0.9359
-98.03875839	41.24389957	7	Yield = -0.045N2 + 41.953N + 4012.5	R² = 0.878	SI = -1E-06N2 + 0.0018N + 0.6643	R² = 0.939
-98.03857414	41.24389803	8	Yield = -0.0465N2 + 42.356N + 4120.9	R² = 0.8743	SI = -2E-06N2 + 0.0018N + 0.6636	R² = 0.9325
-98.038398	41.24389051	9	Yield = -0.0466N2 + 41.815N + 4130.5	R² = 0.8821	SI = -1E-06N2 + 0.0017N + 0.6637	R² = 0.9257
-98.03822168	41.24389509	10	Yield = -0.0432N2 + 41.302N + 3791.8	R² = 0.8978	SI = -1E-06N2 + 0.0017N + 0.6644	R² = 0.918
-98.03802556	41.2438918	11	Yield = -0.0366N2 + 39.415N + 3782.6	R² = 0.9077	SI = -2E-06N2 + 0.002N + 0.6535	R² = 0.9126
-98.03784483	41.2438998	12	Yield = -0.0461N2 + 42.336N + 3733.6	R² = 0.8958	SI = -3E-06N2 + 0.0022N + 0.6443	R² = 0.8904
-98.03766631	41.2438999	13	Yield = -0.0461N2 + 43.369N + 3766.7	R² = 0.8991	SI = -3E-06N2 + 0.0024N + 0.6352	R² = 0.8922
-98.03748577	41.24389522	14	Yield = -0.0447N2 + 44.226N + 3823.6	R² = 0.8893	SI = -2E-06N2 + 0.0022N + 0.6181	R² = 0.9027
-98.03730942	41.24389057	15	Yield = -0.0455N2 + 45.591N + 3725.6	R² = 0.8871	SI = -3E-06N2 + 0.0023N + 0.6074	R² = 0.9029
-98.03712472	41.24388269	16	Yield = -0.0429N2 + 45.457N + 3680.8	R² = 0.8895	SI = -3E-06N2 + 0.0023N + 0.6035	R² = 0.9131
-98.03694401	41.2438891	17	Yield = -0.0403N2 + 45.065N + 3715.5	R² = 0.888	SI = -2E-06N2 + 0.0022N + 0.5979	R² = 0.9123
-98.03674662	41.24388745	18	Yield = -0.037N2 + 44.354N + 3684.1	R² = 0.8833	SI = -2E-06N2 + 0.0023N + 0.5945	R² = 0.8969
-98.03658285	41.24388449	19	Yield = -0.0307N2 + 42.204N + 3734.6	R² = 0.902	SI = -2E-06N2 + 0.0023N + 0.5908	R² = 0.9177
-98.0364128	41.2438799	20	Yield = -0.0247N2 + 39.193N + 3657.2	R² = 0.9202	SI = -2E-06N2 + 0.0023N + 0.5867	R² = 0.9276
-98.03622171	41.2438783	21	Yield = -0.013N2 + 34.78N + 3659.1	R² = 0.9302	SI = -2E-06N2 + 0.0023N + 0.58	R² = 0.9445
-98.03602639	41.24387825	22	Yield = -0.0054N2 + 31.175N + 3781.5	R² = 0.9168	SI = -2E-06N2 + 0.0022N + 0.573	R² = 0.9565
-98.03585217	41.24387204	23	Yield = -0.0111N2 + 31.862N + 3811.2	R² = 0.9054	SI = -2E-06N2 + 0.0023N + 0.5684	R² = 0.9694
-98.0356716	41.24386894	24	Yield = -0.008N2 + 30.492N + 3925.4	R² = 0.8939	SI = -1E-06N2 + 0.0021N + 0.5674	R² = 0.9683
-98.03548051	41.24386734	25	Yield = -0.003N2 + 30.134N + 3765.1	R² = 0.8965	SI = -2E-07N2 + 0.0017N + 0.5773	R² = 0.9407
-98.03532301	41.24386602	26	Yield = -0.0169N2 + 33.502N + 3764.8	R² = 0.9476	SI = -3E-07N2 + 0.0017N + 0.584	R² = 0.9294
-98.03512763	41.24387072	27	Yield = -0.0175N2 + 34.501N + 3762.3	R² = 0.9534	SI = 9E-08N2 + 0.0016N + 0.5986	R² = 0.9278
-98.03495543	41.24386928	28	Yield = -0.0284N2 + 37.555N + 4002.9	R² = 0.9646	SI = -1E-06N2 + 0.0018N + 0.6111	R² = 0.942
-98.03476644	41.2438677	29	Yield = -0.0249N2 + 38.312N + 4022.2	R² = 0.9489	SI = -1E-06N2 + 0.002N + 0.6067	R² = 0.9403
-98.03459224	41.24385989	30	Yield = -0.0287N2 + 40.035N + 4297.9	R² = 0.95	SI = -2E-06N2 + 0.002N + 0.6101	R² = 0.9599
-98.03442002	41.24386004	31	Yield = -0.0365N2 + 42.969N + 4246.8	R² = 0.9521	SI = -1E-06N2 + 0.002N + 0.6033	R² = 0.9689
-98.03422055	41.24385678	32	Yield = -0.0359N2 + 42.982N + 4500.3	R² = 0.9555	SI = -1E-06N2 + 0.002N + 0.6201	R² = 0.9651
-98.03401896	41.24385509	33	Yield = -0.0372N2 + 42.792N + 4797.5	R² = 0.952	SI = -2E-06N2 + 0.002N + 0.639	R² = 0.9352
-98.03383837	41.24385357	34	Yield = -0.03N2 + 40.691N + 5012.2	R² = 0.9584	SI = -2E-06N2 + 0.002N + 0.6498	R² = 0.9263
-98.033662	41.24385051	35	Yield = -0.0292N2 + 40.956N + 5030.2	R² = 0.959	SI = -2E-06N2 + 0.002N + 0.658	R² = 0.8949
-98.03349608	41.2438507	36	Yield = -0.0375N2 + 44.172N + 4743.5	R² = 0.9506	SI = -2E-06N2 + 0.002N + 0.6717	R² = 0.8623
-98.03332177	41.24385082	37	Yield = -0.0359N2 + 42.972N + 4994.6	R² = 0.9398	SI = -2E-06N2 + 0.0019N + 0.6929	R² = 0.8322
-98.0331306	41.24385397	38	Yield = -0.0322N2 + 41.993N + 5147.4	R² = 0.9113	SI = -2E-06N2 + 0.0019N + 0.6958	R² = 0.8444

-98.03295213	41.24385089	39	Yield = -0.0354N2 + 42.682N + 5119.3	R² = 0.9051	SI = -2E-06N2 + 0.0019N + 0.6922	R² = 0.8666
-98.03276786	41.2438317	40	Yield = -0.0259N2 + 40.767N + 5025.4	R² = 0.8764	SI = -2E-06N2 + 0.0021N + 0.6765	R² = 0.8599
-98.03257413	41.24383998	41	Yield = -0.0518N2 + 45.051N + 4925.4	R² = 0.853	SI = -3E-06N2 + 0.0023N + 0.6642	R² = 0.8906
-98.03241011	41.24383613	42	Yield = -0.0499N2 + 44.329N + 4761	R² = 0.8432	SI = -3E-06N2 + 0.0023N + 0.6482	R² = 0.8828
-98.03223289	41.24383712	43	Yield = -0.0602N2 + 45.789N + 4812	R² = 0.8505	SI = -4E-06N2 + 0.0025N + 0.6361	R² = 0.8892
-98.03206239	41.24382825	44	Yield = -0.0636N2 + 47.096N + 4543.2	R² = 0.8426	SI = -5E-06N2 + 0.0029N + 0.6213	R² = 0.8865
-98.03187204	41.24382913	45	Yield = -0.0765N2 + 48.875N + 4527.2	R² = 0.8263	SI = -5E-06N2 + 0.0029N + 0.6246	R² = 0.8837
-98.03168509	41.2438226	46	Yield = -0.0908N2 + 50.817N + 4510.9	R² = 0.8068	SI = -5E-06N2 + 0.0029N + 0.6311	R² = 0.8812
-98.03149147	41.24382345	47	Yield = -0.0925N2 + 50.586N + 4523.2	R² = 0.8064	SI = -5E-06N2 + 0.0028N + 0.6442	R² = 0.8711
-98.03132741	41.24382207	48	Yield = -0.0839N2 + 49.018N + 4545.5	R² = 0.8202	SI = -5E-06N2 + 0.0027N + 0.6582	R² = 0.8506
-98.03113711	41.24382047	49	Yield = -0.0776N2 + 48.424N + 4544.9	R² = 0.8278	SI = -4E-06N2 + 0.0026N + 0.6775	R² = 0.8205
	Average Equation		**Yield = -0.0381N2 + 41.373N + 4234.1**	**R² = 0.9069**	**SI = -2E-06N2 + 0.0021N + 0.6348**	**R² = 0.9238**

Table 16. Yield (kg ha^{-1}) and Sufficiency Index (SI) predicted equations to evaluate the N response (kg ha^{-1}) for the transect made in the small plots area at the HU10.

Long	Lat	ID	Yield Response Equation	R2	SI response Equation	R2
-98.23484555	40.81271388	1	Yield = -0.0999N2 + 51.952N + 6930.7	R² = 0.9915	SI = -7E-06N2 + 0.0027N + 0.7652	R² = 0.8292
-98.23464984	40.81271258	2	Yield = -0.0923N2 + 50.585N + 6981.2	R² = 0.991	SI = -8E-06N2 + 0.0031N + 0.7469	R² = 0.9748
-98.23447761	40.81271144	3	Yield = -0.0911N2 + 50.247N + 7016.2	R² = 0.9907	SI = -9E-06N2 + 0.0034N + 0.7358	R² = 0.9507
-98.23429763	40.8127043	4	Yield = -0.0917N2 + 50.248N + 7033	R² = 0.9898	SI = -9E-06N2 + 0.0035N + 0.7403	R² = 0.9071
-98.23410975	40.81270305	5	Yield = -0.0948N2 + 50.666N + 7038.6	R² = 0.9886	SI = -8E-06N2 + 0.003N + 0.7314	R² = 0.9695
-98.23392956	40.81271375	6	Yield = -0.1052N2 + 52.192N + 7036.5	R² = 0.988	SI = -8E-06N2 + 0.0032N + 0.7258	R² = 0.9588
-98.23374957	40.81270661	7	Yield = -0.0883N2 + 46.865N + 7478.8	R² = 0.9831	SI = -9E-06N2 + 0.0036N + 0.7125	R² = 0.8938
-98.23358518	40.81270551	8	Yield = -0.0777N2 + 44.634N + 7554.1	R² = 0.973	SI = -9E-06N2 + 0.0036N + 0.7231	R² = 0.8943
-98.23339737	40.81269832	9	Yield = -0.077N2 + 44.338N + 7575.4	R² = 0.9726	SI = -7E-06N2 + 0.0028N + 0.7413	R² = 0.9597
-98.23321731	40.81269712	10	Yield = -0.0747N2 + 43.674N + 7616.9	R² = 0.9674	SI = -5E-06N2 + 0.0022N + 0.7329	R² = 0.8607
-98.23302943	40.81269587	11	Yield = -0.0699N2 + 42.446N + 7673.6	R² = 0.9675	SI = -6E-06N2 + 0.0025N + 0.709	R² = 0.9929
-98.23285721	40.81269473	12	Yield = -0.05N2 + 35.51N + 8220.8	R² = 0.9613	SI = -7E-06N2 + 0.0029N + 0.7	R² = 0.9631
-98.23267716	40.81269353	13	Yield = -0.0447N2 + 33.8N + 8271.7	R² = 0.949	SI = -5E-06N2 + 0.0024N + 0.7284	R² = 0.9994
-98.23248152	40.81268628	14	Yield = -0.0581N2 + 37.777N + 8169.1	R² = 0.9342	SI = -3E-06N2 + 0.0017N + 0.7599	R² = 0.8567
-98.23231719	40.81267924	15	Yield = -0.0417N2 + 33.706N + 8280	R² = 0.9407	SI = -3E-06N2 + 0.0016N + 0.7715	R² = 0.9929
-98.2321291	40.81269583	16	Yield = -0.0359N2 + 33.619N + 8287.9	R² = 0.9376	SI = -3E-06N2 + 0.0016N + 0.7767	R² = 0.9575
-98.23194919	40.81268274	17	Yield = -0.0167N2 + 27.284N + 8809.9	R² = 0.9138	SI = -3E-06N2 + 0.0018N + 0.7677	R² = 0.8869
-98.23175348	40.81268144	18	Yield = -0.0099N2 + 26.16N + 8961.3	R² = 0.9339	SI = -4E-06N2 + 0.0018N + 0.7894	R² = 0.935
-98.23158126	40.81268029	19	Yield = -0.0293N2 + 32.2N + 8623.9	R² = 0.9416	SI = -3E-06N2 + 0.0015N + 0.7985	R² = 0.9634
-98.23140903	40.81267914	20	Yield = -0.0216N2 + 28.374N + 9085.1	R² = 0.9371	SI = -2E-06N2 + 0.0013N + 0.7824	R² = 0.9637
-98.23122898	40.81267794	21	Yield = -0.0159N2 + 25.689N + 9355.2	R² = 0.9185	SI = -2E-06N2 + 0.0014N + 0.7902	R² = 0.966
-98.23105676	40.81267679	22	Yield = -0.0581N2 + 37.777N + 8169.1	R² = 0.9317	SI = -3E-06N2 + 0.0017N + 0.789	R² = 0.9038
-98.23086105	40.81267549	23	Yield = -0.0417N2 + 33.706N + 8280	R² = 0.92	SI = -3E-06N2 + 0.0016N + 0.8054	R² = 0.9031
-98.23067317	40.81267424	24	Yield = -0.0359N2 + 33.619N + 8287.9	R² = 0.9317	SI = -2E-06N2 + 0.0012N + 0.8227	R² = 0.6717
-98.23049312	40.81267304	25	Yield = -0.0167N2 + 27.284N + 8809.9	R² = 0.8443	SI = -3E-06N2 + 0.0015N + 0.8272	R² = 0.8387
-98.23032872	40.81267194	26	Yield = -0.0099N2 + 26.16N + 8961.3	R² = 0.8396	SI = -4E-06N2 + 0.0018N + 0.8202	R² = 0.8306
-98.23014084	40.81267069	27	Yield = -0.0293N2 + 32.2N + 8623.9	R² = 0.7491	SI = -6E-06N2 + 0.0022N + 0.8245	R² = 0.7987
-98.22996079	40.81266949	28	Yield = -0.0216N2 + 28.374N + 9085.1	R² = 0.7659	SI = -6E-06N2 + 0.0024N + 0.806	R² = 0.808
-98.22979646	40.81266244	29	Yield = -0.0159N2 + 25.689N + 9355.2	R² = 0.8256	SI = -6E-06N2 + 0.0024N + 0.8101	R² = 0.8392
-98.22960075	40.81266113	30	Yield = -0.0361N2 + 25.617N + 9610.7	R² = 0.8111	SI = -4E-06N2 + 0.0016N + 0.8096	R² = 0.7653
-98.22941287	40.81265988	31	Yield = -0.0276N2 + 23.351N + 9714.7	R² = 0.7717	SI = -3E-06N2 + 0.0016N + 0.7996	R² = 0.9096
-98.22924065	40.81265873	32	Yield = -0.0308N2 + 22.781N + 9888.4	R² = 0.7273	SI = -4E-06N2 + 0.0019N + 0.7949	R² = 0.9329
-98.22905277	40.81265747	33	Yield = -0.027N2 + 22.272N + 9999.6	R² = 0.7129	SI = -3E-06N2 + 0.0016N + 0.801	R² = 0.9439
-98.2288962	40.81265643	34	Yield = -0.0596N2 + 32.146N + 9545.6	R² = 0.7804	SI = -2E-06N2 + 0.0012N + 0.8099	R² = 0.8876
-98.22868497	40.81264312	35	Yield = -0.0117N2 + 23.488N + 9770.4	R² = 0.8987	SI = -2E-07N2 + 0.0008N + 0.8067	R² = 0.9309
-98.22852058	40.81264202	36	Yield = -0.0059N2 + 21.749N + 9843.6	R² = 0.8909	SI = -5E-07N2 + 0.001N + 0.8017	R² = 0.974
-98.22832487	40.81264071	37	Yield = 0.0325N2 + 11.216N + 10247	R² = 0.8729	SI = -3E-06N2 + 0.0019N + 0.7769	R² = 0.5875
-98.22813699	40.81263945	38	Yield = 0.037N2 + 11.49N + 10119	R² = 0.8898	SI = -4E-06N2 + 0.0022N + 0.7609	R² = 0.5918

-98.22795694	40.81263825	39	Yield = 0.0197N2 + 17.956N + 9516.9	R² = 0.9268	SI = -1E-06N2 + 0.0012N + 0.7846	R² = 0.976
-98.22778471	40.8126371	40	Yield = 0.0577N2 + 9.9789N + 9227.6	R² = 0.9092	SI = -2E-06N2 + 0.0013N + 0.7936	R² = 0.9805
-98.22758894	40.81264173	41	Yield = 0.024N2 + 20.269N + 8771.3	R² = 0.8924	SI = -2E-06N2 + 0.0014N + 0.7729	R² = 0.9466
-98.22743237	40.81264069	42	Yield = 0.0459N2 + 14.336N + 8840.4	R² = 0.8415	SI = -2E-06N2 + 0.0015N + 0.7585	R² = 0.9557
-98.22723666	40.81263937	43	Yield = 0.0463N2 + 15.439N + 8619.7	R² = 0.8455	SI = -3E-06N2 + 0.0018N + 0.7536	R² = 0.9558
-98.22706444	40.81263822	44	Yield = 0.0261N2 + 23.208N + 7949	R² = 0.8693	SI = -3E-06N2 + 0.0016N + 0.7444	R² = 0.9403
-98.22689221	40.81263707	45	Yield = 0.0195N2 + 25.043N + 7801.9	R² = 0.8626	SI = -4E-06N2 + 0.0021N + 0.7384	R² = 0.938
-98.22671216	40.81263586	46	Yield = 0.0167N2 + 26.025N + 7732.1	R² = 0.8659	SI = -4E-06N2 + 0.0023N + 0.727	R² = 0.8784
-98.22651645	40.81263455	47	Yield = 0.0125N2 + 26.881N + 7768.2	R² = 0.8753	SI = -3E-06N2 + 0.002N + 0.7342	R² = 0.9322
-98.2263364	40.81263334	48	Yield = 0.0011N2 + 29.073N + 7763.8	R² = 0.8731	SI = -4E-06N2 + 0.0021N + 0.7586	R² = 0.8889
-98.22614845	40.81263803	49	Yield = -0.01N2 + 31.376N + 7728.6	R² = 0.8702	SI = -4E-06N2 + 0.002N + 0.7864	R² = 0.8581
	Average Equation		**Yield = -0.0279N2 + 29.95N + 8674.4**	**R² = 0.9507**	**SI = -4E-06N2 + 0.002N + 0.7704**	**R² = 0.9566**

Table 17. Yield (kg ha^{-1}) and Sufficiency Index (SI) predicted equations to evaluate the N response (kg ha^{-1}) for the transect made in the small plots area at the BL10.

Long	Lat	ID	Yield Response Equation	R2	SI response Equation	R2
-101.965521	41.02846617	1	Yield = -0.0877N2 + 28.689N + 6263	R² = 0.6205	SI = -6E-07N2 + 0.001N + 0.7977	R² = 0.8978
-101.9653304	41.02846617	2	Yield = -0.1092N2 + 37.115N + 7185.1	R² = 0.6582	SI = 3E-07N2 + 0.0009N + 0.7683	R² = 0.9278
-101.9651399	41.02846617	3	Yield = -0.0945N2 + 37.829N + 7353	R² = 0.9249	SI = -7E-07N2 + 0.0013N + 0.72	R² = 0.9724
-101.9649652	41.02847411	4	Yield = -0.1059N2 + 42.505N + 7610.6	R² = 0.9351	SI = -2E-06N2 + 0.0018N + 0.6924	R² = 0.9954
-101.9647984	41.02847411	5	Yield = -0.1128N2 + 44.678N + 8046.6	R² = 0.8949	SI = -3E-06N2 + 0.0021N + 0.6804	R² = 0.9846
-101.9646079	41.02847411	6	Yield = -0.0864N2 + 40.68N + 7926.7	R² = 0.9874	SI = -3E-06N2 + 0.0021N + 0.6802	R² = 0.9939
-101.9644332	41.02845823	7	Yield = -0.0529N2 + 34.815N + 7369.7	R² = 0.9929	SI = -5E-06N2 + 0.0028N + 0.6269	R² = 0.9245
-101.9642426	41.02848205	8	Yield = -0.0111N2 + 25.773N + 6743.3	R² = 0.8891	SI = -8E-06N2 + 0.0041N + 0.5195	R² = 0.9305
-101.9640679	41.02847411	9	Yield = 0.0021N2 + 22.415N + 6406.7	R² = 0.8378	SI = -1E-05N2 + 0.0046N + 0.509	R² = 0.9471
-101.9639012	41.02847411	10	Yield = -0.0611N2 + 33.383N + 6928.1	R² = 0.9917	SI = -8E-06N2 + 0.0037N + 0.6033	R² = 0.9675
-101.9637186	41.02847411	11	Yield = -0.097N2 + 40.495N + 7079.4	R² = 0.9508	SI = -3E-06N2 + 0.0023N + 0.645	R² = 0.9933
-101.963536	41.02848205	12	Yield = -0.0928N2 + 40.197N + 6877.9	R² = 0.9851	SI = -2E-06N2 + 0.0019N + 0.6417	R² = 0.9957
-101.9633454	41.02847411	13	Yield = -0.1278N2 + 48N + 6715.3	R² = 0.9389	SI = -3E-06N2 + 0.002N + 0.6739	R² = 0.9974
-101.9631787	41.02848205	14	Yield = -0.1004N2 + 43.149N + 6093.5	R² = 0.9935	SI = -2E-06N2 + 0.0019N + 0.6516	R² = 0.9956
-101.9629802	41.02846617	15	Yield = -0.0556N2 + 34.72N + 5462.8	R² = 0.9349	SI = -2E-06N2 + 0.0024N + 0.5712	R² = 0.9884
-101.9628055	41.02846617	16	Yield = -0.0447N2 + 33.175N + 4970.6	R² = 0.9353	SI = -6E-06N2 + 0.0034N + 0.5475	R² = 0.9571
-101.9626229	41.02846617	17	Yield = -0.0842N2 + 41.239N + 4685.8	R² = 0.9928	SI = -1E-05N2 + 0.0045N + 0.5388	R² = 0.9276
-101.9624561	41.02847411	18	Yield = -0.0951N2 + 42.707N + 4585.2	R² = 0.9739	SI = -2E-05N2 + 0.006N + 0.5236	R² = 0.8852
-101.9622655	41.02847411	19	Yield = -0.0448N2 + 32.097N + 3979.5	R² = 0.9227	SI = -2E-05N2 + 0.0079N + 0.5066	R² = 0.7557
-101.9620829	41.02847411	20	Yield = 0.0136N2 + 20.167N + 3480.6	R² = 0.8023	SI = -2E-05N2 + 0.0079N + 0.4667	R² = 0.6727
-101.9618844	41.02846617	21	Yield = 0.019N2 + 18.829N + 3630.7	R² = 0.8175	SI = -1E-05N2 + 0.0061N + 0.4397	R² = 0.7034
-101.9616939	41.02846617	22	Yield = -0.0002N2 + 22.367N + 4188.8	R² = 0.8409	SI = -8E-06N2 + 0.0045N + 0.4823	R² = 0.725
-101.9615271	41.02846617	23	Yield = -0.0195N2 + 25.634N + 5054.7	R² = 0.8746	SI = -3E-06N2 + 0.003N + 0.5241	R² = 0.8282
-101.9613524	41.02846617	24	Yield = -0.0861N2 + 39.65N + 6091.4	R² = 0.9948	SI = -6E-07N2 + 0.002N + 0.5458	R² = 0.9914
-101.9611619	41.02847411	25	Yield = -0.1318N2 + 49.91N + 6852.6	R² = 0.9425	SI = -2E-07N2 + 0.0016N + 0.5901	R² = 0.971
-101.9609872	41.02847411	26	Yield = -0.1365N2 + 51.376N + 7166.5	R² = 0.9846	SI = -5E-07N2 + 0.0016N + 0.6176	R² = 0.9841
-101.9608125	41.02847411	27	Yield = -0.1525N2 + 54.606N + 7390.5	R² = 0.9797	SI = -1E-06N2 + 0.0017N + 0.6231	R² = 0.9764
-101.9606219	41.02847411	28	Yield = -0.1594N2 + 54.143N + 7760.7	R² = 0.9756	SI = -1E-06N2 + 0.0017N + 0.6494	R² = 0.9725
-101.9604552	41.02847411	29	Yield = -0.1482N2 + 51.181N + 7640.7	R² = 0.9913	SI = -5E-06N2 + 0.0025N + 0.6551	R² = 0.9787
-101.9602726	41.02848205	30	Yield = -0.1236N2 + 45.96N + 7074	R² = 0.9885	SI = -9E-06N2 + 0.0036N + 0.6473	R² = 0.9992
-101.96009	41.02848205	31	Yield = -0.0588N2 + 32.133N + 6237.9	R² = 0.7792	SI = -1E-05N2 + 0.0047N + 0.685	R² = 0.8372
-101.9598994	41.02846617	32	Yield = -0.0181N2 + 21.573N + 5735.9	R² = 0.6114	SI = -9E-06N2 + 0.0039N + 0.6441	R² = 0.6792
-101.9597247	41.02846617	33	Yield = -0.0167N2 + 19.97N + 5779.8	R² = 0.6484	SI = -6E-06N2 + 0.0032N + 0.6228	R² = 0.7253
-101.9595262	41.02848205	34	Yield = -0.0339N2 + 23.202N + 6020.5	R² = 0.8101	SI = -1E-05N2 + 0.005N + 0.6989	R² = 0.7725
-101.9593595	41.02848205	35	Yield = -0.0472N2 + 27.451N + 6030.1	R² = 0.9018	SI = -1E-05N2 + 0.005N + 0.6864	R² = 0.8197
-101.9591848	41.02848205	36	Yield = -0.0503N2 + 29.577N + 6124.1	R² = 0.9129	SI = -7E-06N2 + 0.0032N + 0.6556	R² = 0.8301
-101.9590101	41.02846617	37	Yield = -0.0423N2 + 27.937N + 6439.7	R² = 0.871	SI = -3E-06N2 + 0.0022N + 0.6762	R² = 0.8239
-101.9588275	41.02846617	38	Yield = -0.0523N2 + 29.374N + 7132.8	R² = 0.9254	SI = -2E-06N2 + 0.0019N + 0.6838	R² = 0.9107

-101.9586449	41.02846617	39	Yield = -0.0956N2 + 38.019N + 7887	R² = 0.9776	SI = -2E-06N2 + 0.0018N + 0.686	R² = 0.9989
-101.9584464	41.02845823	40	Yield = -0.0806N2 + 34.93N + 8028	R² = 0.9927	SI = -1E-06N2 + 0.0016N + 0.6804	R² = 0.9989
-101.9582717	41.02846617	41	Yield = -0.0548N2 + 29.547N + 8019.5	R² = 0.9677	SI = 1E-07N2 + 0.0013N + 0.6801	R² = 0.9857
-101.9581049	41.02846617	42	Yield = -0.0408N2 + 25.921N + 8173.5	R² = 0.9028	SI = 3E-07N2 + 0.0012N + 0.6956	R² = 0.9714
-101.9579144	41.02847411	43	Yield = -0.0646N2 + 29.207N + 8664.1	R² = 0.9442	SI = -2E-06N2 + 0.0016N + 0.7474	R² = 0.9832
-101.9577397	41.02847411	44	Yield = -0.1098N2 + 37.475N + 9055.6	R² = 0.9828	SI = -7E-06N2 + 0.0025N + 0.8102	R² = 0.9598
	Average Equation		**Yield = -0.0717N2 + 35.086N + 6544.2**	**R² = 0.9878**	**SI = -6E-06N2 + 0.003N + 0.6316**	**R² = 0.934**

Table 18. Semivariograms used to interpolate the chlorophyll index (CI) and grain yield (Y) surfaces at different N rates for the 2009 fields. The semivariograms were scaled to sample variance.

Field	CI and Yield	Model	Co	Co+C	Ao	r2	RSS
BR09	CI_75N	Spherical	0.2200	1.00	45.00	0.69	0.26300
	CI_100N	Spherical	0.2000	1.00	78.00	0.80	0.15000
	CI_150N	Spherical	0.0024	1.00	200.00	0.71	3.50000
	CI_200N	Spherical	0.0027	1.00	120.80	0.76	0.00007
	CI_250N	Spherical	0.0004	1.00	248.00	0.98	0.00002
	Y_75N	Spherical	0.3000	1.00	80.00	0.48	0.71000
	Y_100N	Spherical	0.2000	1.00	90.00	0.47	0.75500
	Y_150N	Spherical	0.0011	1.00	150.00	0.74	8.48000
	Y_200N	Spherical	0.0020	1.00	119.30	0.66	0.82000
	Y_250N	Spherical	0.0011	1.00	150.00	0.83	2.48000
HU09	CI_75N	Spherical	0.2200	1.00	85.00	0.47	2.17000
	CI_100N	Spherical	0.2800	1.00	200.00	0.63	0.79000
	CI_150N	Spherical	0.0019	1.00	300.00	0.90	0.52200
	CI_200N	Spherical	0.2498	1.00	110.00	0.68	2.54000
	CI_250N	Spherical	0.1500	1.00	156.00	0.74	1.23000
	Y_75N	Spherical	0.0015	1.00	52.50	0.54	0.78000
	Y_100N	Spherical	0.0007	1.00	70.90	0.68	9.88000
	Y_150N	Spherical	0.0006	1.00	300.00	0.85	0.39000
	Y_200N	Spherical	0.0002	1.00	320.00	0.85	0.38000
	Y_250N	Spherical	0.0009	1.00	235.00	0.87	2.04000
RT09	CI_75N	Spherical	0.0376	1.00	220.00	0.97	0.03330
	CI_100N	Spherical	0.0007	1.00	300.00	0.88	0.77000
	CI_150N	Spherical	0.0022	1.00	320.00	0.85	1.54000
	CI_200N	Spherical	0.3230	1.00	200.00	0.58	0.92000
	CI_250N	Spherical	0.2400	1.00	367.00	0.67	0.10000
	Y_75N	Spherical	0.0027	1.00	126.00	0.94	0.14700
	Y_100N	Spherical	0.0007	1.00	300.00	0.92	0.89700
	Y_150N	Spherical	0.0012	1.00	220.00	0.83	2.35000
	Y_200N	Spherical	0.0005	1.00	300.00	0.83	1.23000
	Y_250N	Spherical	0.1500	1.00	78.00	0.43	0.66000

Table 19. Semivariograms used to interpolate the chlorophyll index (CI) and grain yield (Y) surfaces at different N rates for the 2010 fields. The semivariograms were scaled to sample variance.

Field	CI and Yield	Model	Co	Co+C	Ao	r2	RSS
BR10	CI_0N	Spherical	0.0018	1.00	170.00	0.90	1.69000
	CI_75N	Spherical	0.0024	1.00	180.00	0.90	0.95000
	CI_150N	Spherical	0.0014	1.00	250.00	0.99	0.18000
	CI_200N	Spherical	0.0008	1.00	204.50	0.98	0.19600
	CI_250N	Spherical	0.0023	1.00	213.40	0.98	0.21500
	Y_0N	Spherical	0.0039	1.00	250.00	0.89	1.28000
	Y_75N	Spherical	0.0024	1.00	156.00	0.90	1.23000
	Y_150N	Spherical	0.0027	1.00	224.00	0.85	2.06000
	Y_200N	Spherical	0.0009	1.00	120.00	0.92	1.95000
	Y_250N	Spherical	0.0020	1.00	156.00	0.90	1.81000
HU10	CI_0N	Spherical	0.0035	1.00	250.00	0.88	1.25000
	CI_75N	Spherical	0.0010	1.00	170.00	0.91	0.68000
	CI_150N	Spherical	0.0008	1.00	120.00	0.87	2.85000
	CI_200N	Spherical	0.0001	1.00	185.00	0.90	0.90000
	CI_250N	Spherical	0.0007	1.00	196.20	0.90	0.33100
	Y_0N	Spherical	0.0008	1.00	300.00	0.91	1.07000
	Y_75N	Spherical	0.0013	1.00	200.00	0.98	0.43400
	Y_150N	Spherical	0.0054	1.00	150.00	0.78	3.53000
	Y_200N	Spherical	0.0015	1.00	350.00	0.95	0.32000
	Y_250N	Spherical	0.0031	1.00	100.00	0.79	4.43000
BL10	CI_0N	Spherical	0.1804	1.00	100.00	0.65	3.09000
	CI_75N	Spherical	0.0033	1.00	119.60	0.77	2.60000
	CI_150N	Spherical	0.0023	1.00	150.00	0.85	6.44000
	CI_200N	Spherical	0.0006	1.00	165.60	0.96	1.10000
	CI_250N	Spherical	0.0040	1.00	104.10	0.63	3.15000
	Y_0N	Spherical	0.0007	1.00	150.00	0.97	1.23000
	Y_75N	Spherical	0.0020	1.00	98.70	0.72	1.74000
	Y_150N	Spherical	0.0006	1.00	122.80	0.86	1.17000
	Y_200N	Spherical	0.0008	1.00	99.60	0.68	1.14500
	Y_250N	Spherical	0.0007	1.00	109.90	0.76	0.91800

CHAPTER 3

INTEGRATION OF ULTRASONIC AND OPTICAL REFLECTANCE SENSORS TO ESTIMATE THE IN-SEASON NITROGEN AVAILABILITY FOR CORN

ABSTRACT

Different approaches for in-season N management based on sensors are being used and different arrangements and apparatus can be used. Optical reflectance crop canopy sensors (ACS) are being used with success for N estimation and on-the-go N fertilization. Recently, some studies indicate that plant height could be used to estimate yield potential and probably indicate the plant N status. In this scenario the objectives of this research were to: (i) determine the correlation between ACS assessments of N availability and ultrasonic sensor measurements of canopy height at several growth stages for corn receiving varying amounts of N fertilization, (ii) test the ability of both sensors to distinguish N-mediated differences in canopy development and (iii) evaluate benefits of the integrated use of both sensors. This experiment was conducted with varying N rates in two small plots experiments and at six farmer's fields during 2008, 2009 and 2010. Plant height, crop canopy reflectance (NIR and visible portions of the spectrum) and geographic position using a DGPS receiver were recorded during different phenological stages. Results showed that there were strong relationships between plant height (H) and chlorophyll index (CI), with correlation coefficients ranging from 0.24 to 0.98. Higher levels of correlations were observed at V10 through V15 growth stages. Both sensors

were able to separate different N rates from V8 to V15 in 2008 and 2010 but they didn't have the same ability for 2009, where only at V13 both sensors could separate N rates. The integration of optical and ultrasonic sensors increased the ability to predict N fertilization rates and grain yield compared to each one in separate.

Abbreviations List: H: plant height measured by ultrasonic distance sensors; CI: chlorophyll index; NSI: nitrogen sufficiency index derived from the calculation of a vegetation index; HSI: plant height sufficiency index using the sufficiency index concept for plant height measurement using ultrasonic sensors.

INTRODUCTION

Since early 1950s, increased food production was a priority in agricultural areas around the World, the largest increase in the use of agricultural inputs was for N fertilizer due to the largest impact on yield as compared to other nutrients. Adding the fact that nowadays the population is increasing exponentially and more food will be needed in a couple of decades, consequently the need for N will increase and more efficient ways to apply N fertilizer is needed. It was reported that the N use efficiency (NUE) worldwide has remained at a stagnant 33% (Raun and Johnson, 1999). So, it is clear that all agricultural techniques that lead to increase the NUE should be in priority for researchers, farmers and extension educators. The major causes for low NUE are poor synchrony between soil N supply and crop demand, uniform application rates of fertilizer N to spatially-variable agricultural fields and failure to account for temporally variable influences on crop N needs (Shanahan et al., 2008). Procedures to determine N content in soil directly would be adequate if they could take place immediately before each

fertilization. However, this is normally not economically feasible due to the temporal changes of N content caused by several transformations among different forms of N. Therefore, the use of active optical reflectance crop canopy sensor (ACS) to assess corn canopy N status to guide spatially variable in-season N applications has been proposed as a means for improving NUE and decreasing environmental waste (Solari et al., 2008).

Previous studies have shown that canopy chlorophyll content is correlated to biophysical parameters such as leaf area index and plant height (Freeman et al, 2007; Jones et al., 2007). Sui & Thomasson (2006) noted that both crop spectral reflectance (measured using ACS) and plant height (measured using ultrasonic plant height sensor) were correlated with crop N status. Recently, Yin et al. (2011) showed that plant height could be used for in-season prediction of corn yield and this prediction provides a physiological basis for the use of high-density plant height measurements to guide variable-rate fertilizer N applications within the field and to more accurately estimate crop yield. Since plant height and vegetation indices, either individually or together, can be used to estimate N availability during the corn growing season, their use represent an attractive option for in-season N management. Several vegetation indices have been proposed for N management using ACS (NDVI - Raun et al., 2005; GNDVI - Dellinger et al., 2008; Chlorophyll Index – Solari et al., 2008) but the integration of these indices with other measurements even with the use of passive sensors (Temperature – Babar et al., 2006; plant height – Jones et al., 2007) is recent and rare in the literature. Some limitations have been reported for the use of optical sensors. For example, at reproductive stages of corn the ability of the optical sensor to detect canopy variation could be limited by the presence of tassels (Solari et al., 2008); leaves sampled at different growth stages

using chlorophyll meters (Zhang et al., 2007) can cause variations in the readings; high N rate at planting in high clay content soils can lead to enough N being supplied to the crop until the time of sensing (Turner and Jund, 1991) and plant chlorophyll content can also be influenced by herbicides (Reeves et al., 1993).

Different approaches for in-season N management based on sensors are being used and different arrangements and apparatus can be used. ACS are being used with success for N estimation and on-the-go N fertilization. Recently, some studies indicate that plant height could be used to estimate yield potential and probably indicate the plant N status. In this scenario the objectives of this research were to: (i) determine the correlation between active optical reflectance crop canopy sensor assessments of N availability and ultrasonic sensor measurements of canopy height at several growth stages for corn receiving varying amounts of N fertilization, (ii) test the ability of both sensors to distinguish N-mediated differences in canopy development and (iii) evaluate benefits of the integrated use of both sensors.

MATERIAL AND METHODS

A replicated small plot experiment was conducted in two irrigated experimental sites located at the South Central Agricultural Laboratory (SCAL) of the University of Nebraska at Clay Center (BN and MS sites). The BN study is a long-term N experiment conducted since 1986 with different N rates and the MS site represented the same experiment mounted in 2008. The other sites were on-farm research plots laid on 7 center

pivot-irrigated sites on cooperating farmers (HU08, HU09, HU10, BR09, BR10, RT09, BL10) during 2008, 2009 and 2010 (Table 1) (Figure 1).

The platform used for sensor data collection at several growth stages of corn was a bicycle modified to support an optical sensor (Crop Circle, model ACS-210, measuring wavelengths of 590 and 880 nm) (Holland Scientific, Lincoln, Nebraska, USA), an ultrasonic distance sensor (Senix model TS30S1) (Senix, Bristol, Virginia, USA), a GPS receiver (Trimble GeoXT) (Trimble Navigation, Ltd., Sunnyvale, California, USA) and a laptop computer. A distance of at least 60 cm was maintained between sensors and the top of the crop canopy throughout the season. In the BN and MS sites, plant height and canopy reflectance were recorded during several phenological stages (Table 1). The Chlorophyll Index (CI) (Gitelson, 2003) was calculated from spectral reflectance data. CI = (NIR/VIS) – 1, where NIR is near infrared at 880 nm and VIS is the visible band at 590 nm. Because of sidedress N application at the V10 growth stage in the farmers' fields in 2009, crop sensing was done at later stages (VT and R4) (Table 1). The N application in the farmer's field was done using a high clearance machine equipped with valve control and mapping capabilities and using plot fertilizer spreader at SCAL.

Different experiments with various N rates were sensed in experimental station (SCAL) and farmer's fields (Figure 2). The on-farm research experiments consisted of 250 small plots of 6 by 15 m across the center pivots with various N rates. The data collected by optical and ultrasonic sensors were filtered using MatLab (The MathWorks, Inc., Natick, Massachusetts, USA) software and later processed and analyzed using ArcGIS (ESRI, Redlands, California, USA). The experimental sites at SCAL were harvested with plot combine Gleaner K (2 rows) using the Harvest Master System

(Juniper Systems Inc., Logan, Utah, USA) and in the farmers field all 250 plots in each site were hand harvested (2 center rows of 3.5 m length), then all data were adjusted to an fixed grain moisture content of 155 g kg^{-1}.

Statistical Analysis

Pearson correlation coefficients were used to evaluate the relationships between sensor measurements, N rates and grain yield. Treatment mean separation was done for the plots using Duncan Multiple Range Test using a $p<0.05$. Multiple linear regression analysis using minimizing Akaike's Information Criteria (AIC) (Akaike, 1973) and other heuristic models (Forward, backward and stepwise regression procedures) were performed to evaluate the integration of sensors and to determine the best model for N rates and yield prediction. The model is described by the general equation:

$$y=\beta_0 + \beta_1 NSI + \beta_2 HSI + \beta_3 NSI*HSI$$

Where: NSI is the nitrogen sufficiency index, HSI is the plant height sufficiency index and NSI*HSI is the multiplication of NSI and HSI.

All statistical analysis and graphics were done using SAS (SAS Institute, Inc., Cary, North Carolina, USA) and Sigma Plot (Systat Software, Inc., San Jose, California, USA) software.

RESULTS AND DISCUSSION

Generally, all years had good growing conditions in all sites, but the rain pattern varied significantly for the 2009 growing season with about half of the total precipitation

for 2008 and 2010 and higher temperatures. The 2008 growing season had more rain, which was well distributed, and there was little need for irrigation. The 2009 had higher temperature and less precipitation in the beginning. The 2010 growing season repeated the pattern of 2008 but with less precipitation during mid-season (about 80 days after planting) (Figure 1 and 2). The irrigation commenced earlier in 2009 compared to 2008 and 2010 and in general all sites received about 127 to 300 mm of irrigation water.

The grain yield response for the N rates was higher during 2008 and 2010 as compared to 2009, which showed little response to N across BN09, BR09, and RT09 sites (Figure 4). The corn grain yield for all N rates was considerable higher for 2009 mainly due to a greater level of mineralization caused by higher temperature in the beginning of the season and less N leaching due a relatively low rainfall during mid-season.

For the BN site in 2008, CI (averaged over N rates) increased steadily to the V8 growth stage then tended to plateau. The same pattern occurred for 2010 but with plateau around V13 (Figure 2). In 2009, CI increased until V10, and then declined slightly. These results suggest that CI generally is maximized around V8 or V10. The trend in plant height (H) was linear from V6 until V13. The integrated measure of CI*H had a linear response of increasing as the growth stages progresses (Figure 5). The oscillation of CI values from V8 until V15 can be problematic and unpredictable limiting its application for yield or N prediction, especially considering spatially inconsistent crop maturity stage. On the other hand, the linear response of plant height during these stages can be easily modeled and make good yield and N prediction functions. For example, if a vegetation index decreases after certain growth stage the NDVI divided by growing

degree days proposed by Raun et al. (2005) cannot be used as a reliable predictor of grain yield for corn, unless if plant height measurements are integrated with the optical measurements. CI*H showed that combine the better response of CI in the beginning with the linearity and consistent increase of plant height in the end of the vegetative stage (Figure 5).

Correlation between Optical and Ultrasonic Sensors and Their Ability to Separate N Rates

For the SCAL sites (BN and MS), there were significant correlations between CI and H in all years from V10 until V15 (Figure 6). CI and H were also strongly correlated with N rate and grain yield between V10 and V15 growth stages (Figures 7 and 8). The correlations between HxN and CIxN were similar in 2008 and 2010, but did differ considerably for 2009 (Figure 7), suggesting that the soil N supply was greater early in the season during 2009 as compared to 2008 and 2010. The declining in correlation between H and N or yield at V15 could be due to lower quality of measurements by ultrasonic sensor used at a later growth stages (high and difficult to control distance above ground and lower apparent area of the top of crop required for an ultrasonic proximity measurements). Therefore, more noise was observed when filtering ultrasonic sensor data starting at V15 until maturity. The declining in correlations between CI and N or yield at these growth stages was not observed.

For the producer fields (Table 2), correlations between CI and H were relatively high for vegetative stages, but lower in reproductive stages, another reason other than

noise in the ultrasonic sensor data is the ability of plants under lower N rates reach the same height of high N rates at later stages. The relationship between either CI or H and N rate varied with the year and site, For most site-years, both CI and H were related to N rate as well as grain yield, but for a couple of site-years (HU10, BR09, BR10 and BL10), CI was stronger correlated with N rate and Yield than H. In the HU08 site H was stronger correlated with N and yield than CI. Also, H had stronger correlation with N at RT09 site during R4.

To illustrate the spatial correlation between CI and H one of the three farmers fields mapped during 2010 growing season on a bulk area (uniform N application by the farmer) around the experimental plots is illustrated in Figure 9. The field was mapped using the prototype system (software and hardware) developed for variable rate N based on CI or H.

In 2008 and 2010 both sensors were able to distinguish N rates beginning at V8 (Figures 9 and 10); the term CI*H did have similar results (Figure 11). The sensors were able to separate different N rates at V8, V10 and V13 growth stages in 2008 and 2010. However, in 2009 sensors were only able to distinguish 0 lb/ac from the other rates at V10, V11 and V15 growth stages. In 2009 only during V13 both sensors were able to separate N rates (Figure 9 and 10).

For the BN and MS sites during 3 years, CI increased with growth stage until V8 (Figure 4). The Nitrogen Sufficiency Index or relative index (NSI = CI for a specific N rate/reference CI, here = 300 kgN/ha) showed the same trend of N separation as CI. Plant height (H) increased continuously during the period of sensor measurements. When a vegetation index was used in conjunction with reference area of non limited N supply, the

differences between hybrids, soil, and other environmental conditions are normalized and the relationship is made stronger (Blackmer et al., 1996; Varvel et.al., 1997; Daughtry at.al., 2000; Shanahan et al., 2001; Solari et al, 2008).

Normalized plant height (to the 300 kgN/ha rate), Height Sufficiency Index (HSI) showed the same trend as NSI. In 2008 and 2010 both sensors were able to separate 0 from 75, 75 from 150 and 150 from 300 kgN/ha at V8, V10 and V13 growth stages using actual sensor readings. Normalized H (HSI) didn't show the same ability to separate N rates as the actual value of H measured by the ultrasonic sensor.

At the BN and MS site in 2009, CI increased until approximately V8 or 10 respectively and then declined (Figure 4). Plant height again increased continuously. Sensors were not able to separate 75 from 150 kg/ha and 150 from 300 kgN/ha in 2009, using either actual sensor or normalized values. Generally NSI and CI were able to separate only 0 kgN/ha from other N rates at V10-V15 growth stages, using an LSD test with $p < 0.05$. HSI was also able to separate 0 lb/ac from other N rates only at V10.

Evaluating the Integration of Optical and Ultrasonic Sensors

Evaluating the different sensors measurements (optical and ultrasonic) and the product of measurements, it was observed that the integration of CI and H (CI*H) resulted in similar results in terms of correlation with N rates or yield and the ability to distinguish N rates compared to CI or H individually.

The results for the multiple regression analysis using N rates and yield as dependent variable and CI, H and CI*H normalized by the reference plot (NSI, HSI and

CIHSI) as independent variables, indicated that the best model for either N or relative grain yield prediction included the integration of the optical (NSI) and the (HSI) ultrasonic.

Analyzing the integration in terms of N rate prediction, the backward regression resulted in the equation: N rate (kg N ha^{-1}) = -32.401182 + 405.42778NSI -367.82161 + 205.59746CIHSI with a RMSE of 64 kg N ha^{-1}. The stepwise and forward regression resulted in the equation N rate = -148.58725 + 592.077774NSI – 234.43655HSI. All methods used a $p<0.10$ for inclusion or exclusion of the variable from the model. The minimized AIC method resulted in the equation: N rate = 358.606 NSI – 405.981 HSI + 258.456 CIHSI with the same RMSE of 64 kg N ha^{-1}, but lower AIC compared to the others. The ranking of the top 14 models by AIC for N rate prediction is illustrated in Table 3. The models for NSI and HSI alone, with a reasonable RMSE and R^2 were in 12 and 13th place, showing that the integration can improve the prediction of N rate.

Analyzing optical and ultrasonic sensors in terms of relative grain yield prediction the results also indicated that integration was more beneficial than either optical or ultrasonic alone, as obtained also for N rates. The heuristic methods (forward, backward and stepwise regressions) resulted in the same equation RY = -0.15489 + 1.17123NSI – 0.19787 HSI with a RMSE of 0.12. For relative yield the product of CI*H was not included in the best model.

Conciliating all the methods used for model selection related previously, the best model for N rates estimation is described by the equation: N rate = 358.606 NSI – 405.981 HSI + 258.456 CIHSI with a RMSE of 64 kg N ha^{-1} (Table 3). The model that best describe relative grain yield was: RY = -0.15489 + 1.17123 NSI – 0.19787 HSI, with

a RMSE of 0.12 or plus and minus 12 % of the relative yield predicted by the model (Table 4).

This results corroborate with Jones et.al (2007) where NDVI x biomass provided the best estimate of chlorophyll content in spinach, and Freeman et al. (2007) where NDVI x Plant Height improved the prediction of grain yield potential in forage corn and concluded that can be used to refine mid-season fertilizer N rates based on expected N removal. Plant height can have a physiological basis to predict and estimate grain yield potential and if used properly certainly can also improve the INSEY approach proposed by Raun et al. (2005).

During these 3 years, in general, CI and H have similar ability to separate N rates. H continuously increase unlike CI, which plateaus or even declines at the end of vegetative stage.

The strong correlations between CI (optical sensors) and H (ultrasonic plant height sensor) showed that either sensor can be used to site-specific N management where N is the major limited nutrient. The integration of sensors was beneficial compared to the use of optical or ultrasonic alone.

More studies should be done with plant height sensors to control variable N application specially for crops that plant height can be a good indicator of yield potential and the reference high N strip is not always a good approach because the over application of N can induce excessive growth that will not affect the yield as for example for cotton, wheat, forage corn, and sugarcane. Another good application of the plant height approach could be in the subsistence/low income and small farms where the acquisition and use of

sensors is not viable economically and no sensor/equipment is needed to measure plant height using traditional measuring procedures.

SUMMARY AND CONCLUSIONS

The goal of this research was to evaluate the integration of an ultrasonic plant height sensor with an active light crop canopy sensor, to indirectly measure chlorophyll content of the canopy and estimate grain yield and N, allowing variable N rate application during the growing season. From V10 until V13 growth stages, plant height and CI were strongly correlated and both had the same ability to differentiate N rates. The integration of CI and H increased the ability for N rate or grain yield predictions. The differentiation of N rates by the use of optical and /or ultrasonic sensors were effective only after V7 growth stage. More studies are needed to investigate if only plant height could be used to predict yield potential or N requirement in the context of spatially variable environments.

REFERENCES

Akaike, H. 1973. Information theory and an extension of the maximum likelihood principle. In B.N. Petrov and F. Csaki (Eds.), International Symposium on Information Theory, 2: 267-281. Budapest: Academia Kiado.

Babar, M.A.; Reynolds, M.P., Ginkel, M. van; Klatt, R., Raun,W.R., Stone, M.L. 2006. Spectral Reflectance to Estimate Genetic Variation for In-Season Biomass, Leaf Chlorophyll, and Canopy Temperature in Wheat. Crop Science, 46: 1046.

Blackmer, T.M., J.S. Schepers, G.E. Varvel, and E.A. Walter-Shea. 1996. Nitrogen deficiency detection using reflected shortwave radiation from irrigated corn canopies. Agron. J. 88:1–5

Daughtry, C.S., C.L. Walthall, M.S. Kim, E.B. de Colstoun, and J.E. McMurtrey. 2000. Estimating corn leaf chlorophyll concentration from leaf and canopy refl ectance. Remote Sens. Environ. 74: 229–239

Dellinger,A.E.; Schmidt, J.P., Beegle, D.B. 2008. Developing Nitrogen Fertilizer Recommendations for Corn Using an Active Sensor. Agron. J. , 100: 1546-1552.

Freeman,K.W.; Girma, K.; Arnall, D.B.; Mullen, R.W.; Martin, K.L.; Teal, R.K.; Raun, W.R. 2007. By-plant prediction of corn forage biomass and nitrogen uptake at various growth stages using remote sensing and plant height. Agron. J., 99: 530-536.

Gitelson, A.A.; Gritz, Y.; Merzlyak, M.N. 2003. Relationships between leaf chlorophyll content and spectral reflectance and algorithms for non-destructive chlorophyll assessment in higher plant leaves. Journal of Plant Physiology, 160: 271-282.

Jones, C.L., Maness, N.O., Stone, M.L., Jayasekara, R. 2007. Chlorophyll estimation using multispectral reflectance and height sensing. Transactions of the ASABE, 50: 1867-1872.

Raun, W.R., Johnson, G.V. 1999. Improving nitrogen use efficiency for cereal production. AgronJ, 91:357-363.

Raun, W.R., Solie, J., Stone, M., Martin, K., Freeman, K., Mullen, R., Zhang, H., Schepers, J., Johnson, J. 2005. Optical Sensor-Based Algorithm for Crop Nitrogen Fertilization. Communications in Soil Science and Plant Analysis, 36: 2759-2781.

Raun,W.R., Solie, J.B., Johnson, G.V., Stone, M.L., Mullen, R.W., Freeman, K.W., Thomason, W.E., Lukina, E.V. 2002. Improving nitrogen use efficiency in cereal grain production with optical sensing and variable rate application. Agron. J. , 94: 815-820.

Reeves, D.W., P.L. Mask, W. Wood, and D.P. Delaney. 1993. Determination of wheat nitrogen status with a hand-held chlorophyll meter: Influence of management practices. J. Plant Nutr. 16:781–796.

Shanahan, J.F., J.S. Schepers, D.D. Francis, G.E. Varvel, W.W. Wilhelm, J.M. Tringe, M.R. Schlemmer, and D.J. Major. 2001. Use of remote-sensing imagery to estimate corn grain yield. Agron. J. 93:583–589

Shanahan,J.F., Kitchen, N., Raun, W., Schepers, J. 2008. Responsive in-season nitrogen management for cereals. Computers and Electronics in Agriculture, 61: 51-62.

Solari, F.; Shanahan, J.F.; Ferguson, R.B.; Schepers, J. 2008. Active sensor reflectance measurements of corn nitrogen status and yield potencial. Agron. J. , 100: 571-579.

Sui, R.; Thomasson, J.A. 2006. Ground-based sensing system for cotton nitrogen status determination. Transactions of the ASABE, 49: 1983-1991.

Turner, F.T., and M.F. Jund. 1991. Chlorophyll meter to predict nitrogen top-dress requirement for semi dwarf rice. Agron. J. 83:926–928

Varvel, G.E., J.S. Schepers, and D.D. Francis. 1997. Ability for in-season correction of nitrogen deficiency in corn using chlorophyll meters. Soil Sci. Soc. Am. J. 61:1233–1239

Yin,X.; Mcclure,M.A., Jaja,N., Tyler, D.D., Hayes, R.M. 2011. In-Season Prediction of Corn Yield Using Plant Height under Major Production Systems, Agron. J. , 103: 923-929.

Zhang, J., A.M. Blackmer, T.M. Blackmer, P.M. Kyveryga, and J.W. Ellsworth. 2007. Nitrogen deficiency and recovery in sustainable corn production as revealed by leaf chlorophyll measurements. Agron. Sustain. Dev. 27:313–319.

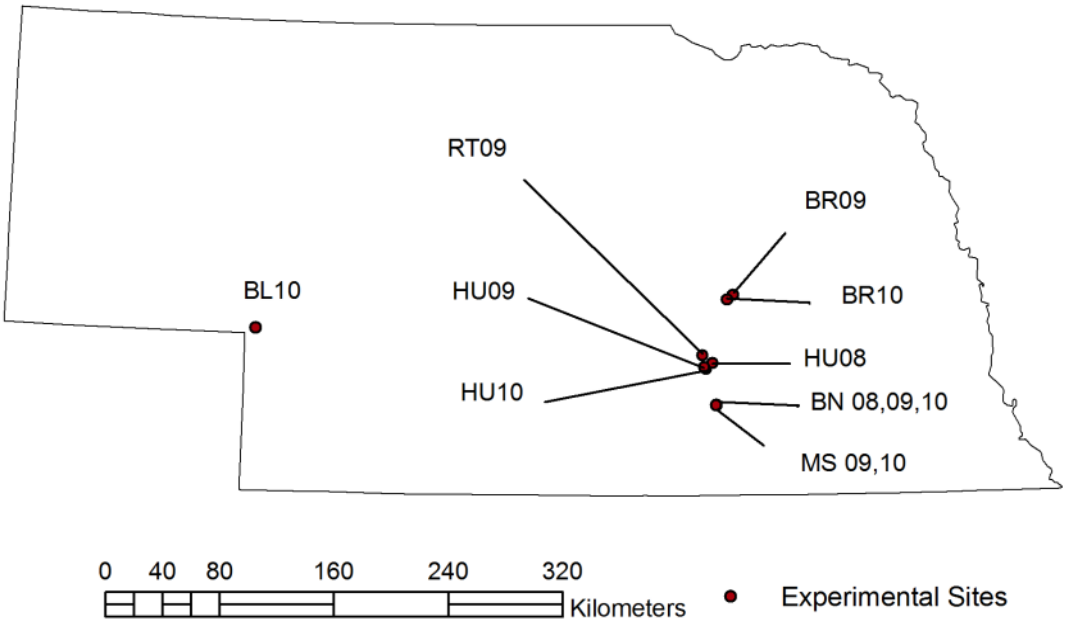

Figure 1. Experimental site locations

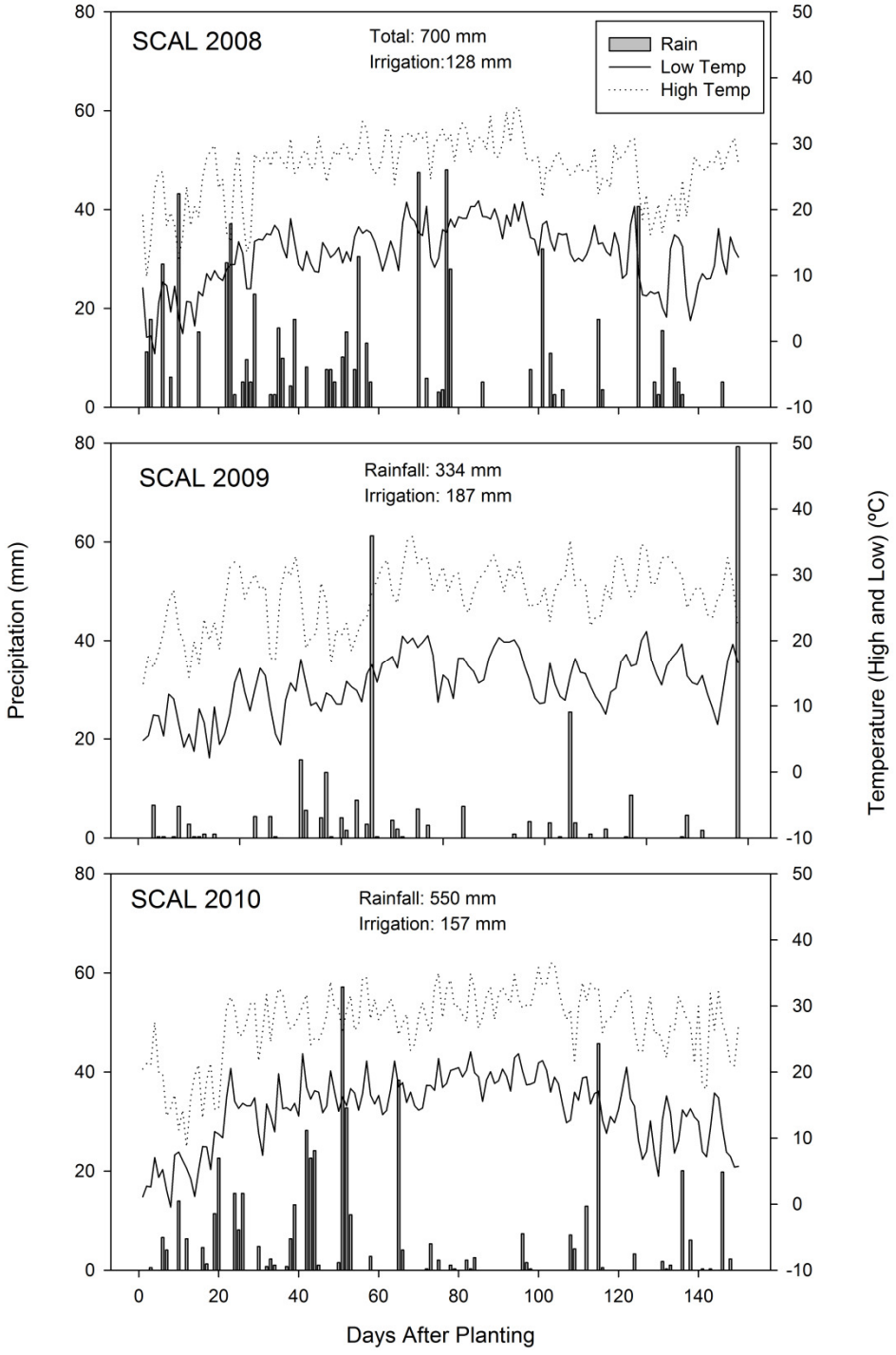

Figure 2. Daily rainfall (precipitation, mm) and temperature (ºC) for 2008, 2009 and 2010 growing seasons at SCAL.

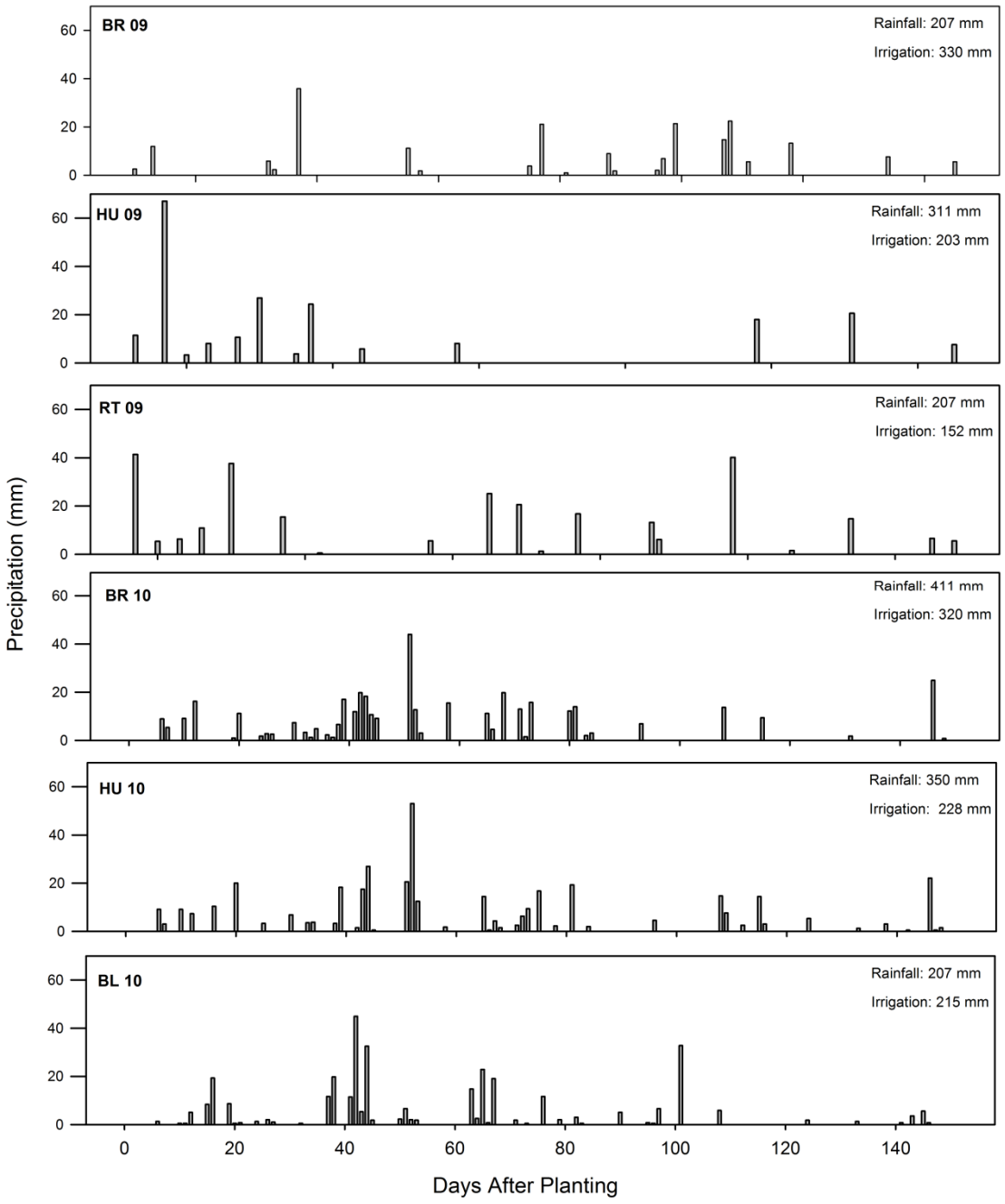

Figure 3. Daily rainfall (precipitation, mm) and temperature (ºC) for 2008, 2009 and 2010 growing seasons at on-farm research sites.

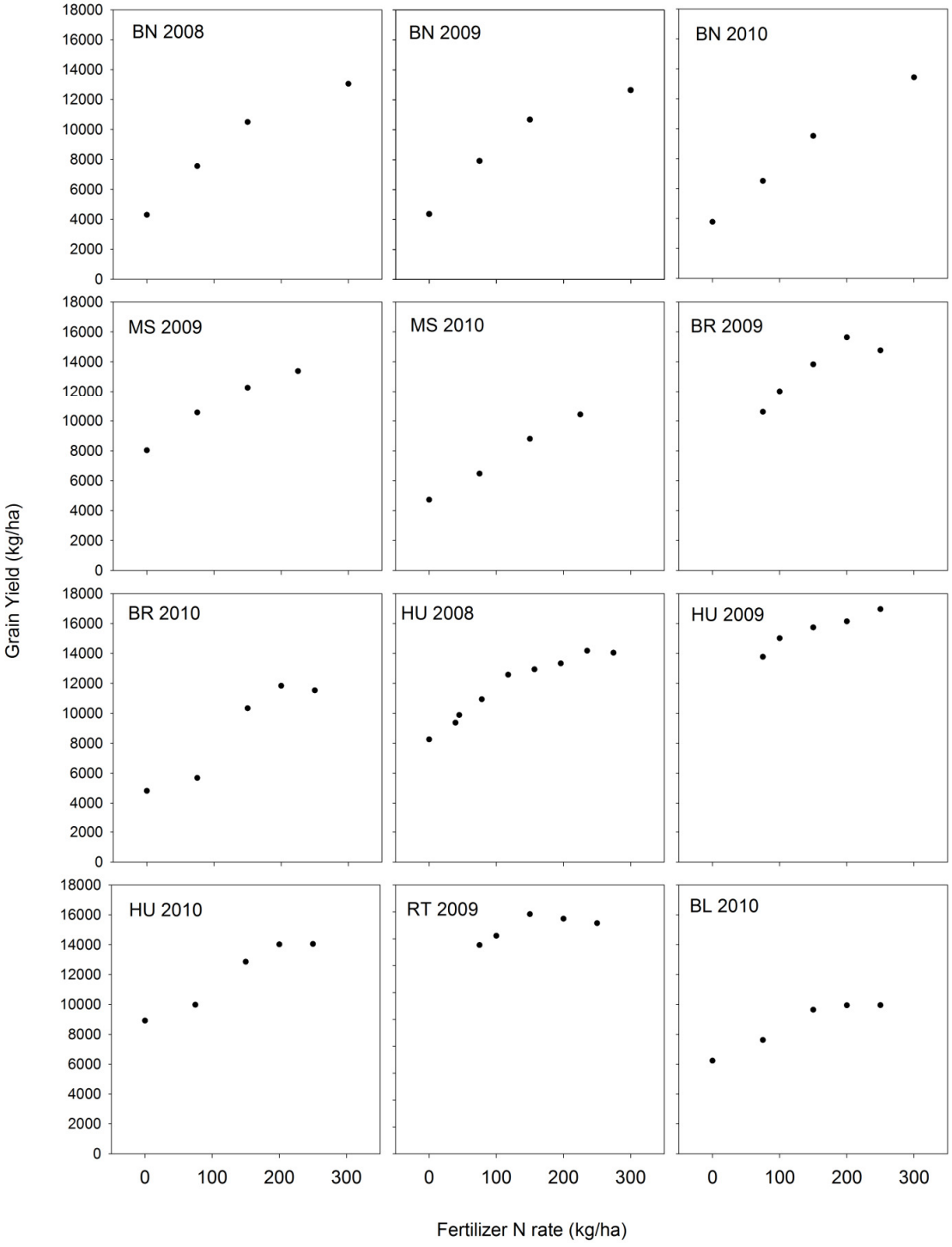

Figure 4. Grain yield response for N rates applied at experimental sites

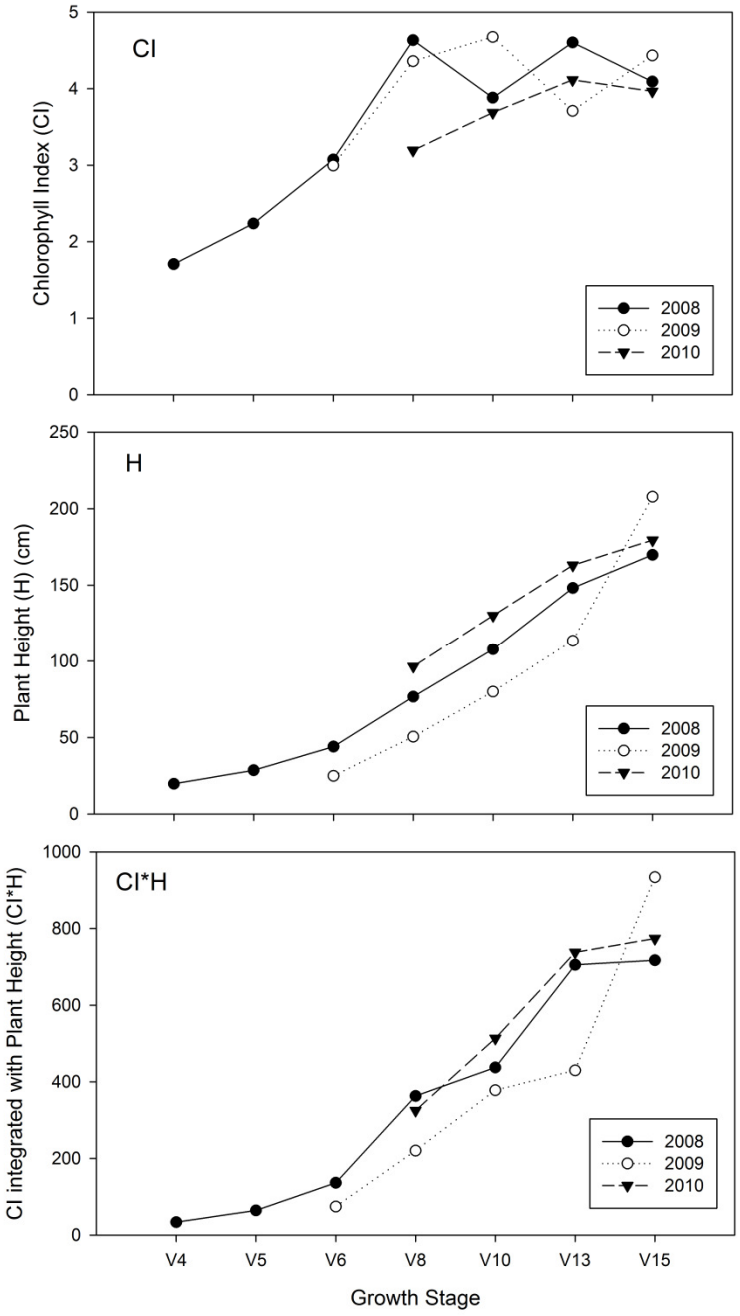

Figure 5. CI and H averaged across N rates for the BN small plots at SCAL during 2008, 2009 and 2010.

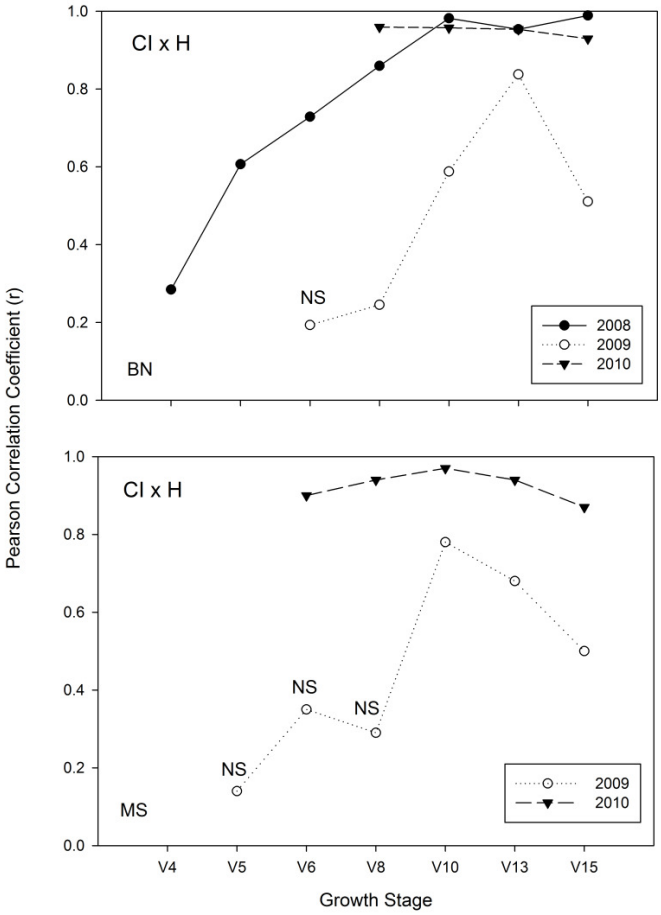

Figure 6. Pearson correlation coefficients (r) between chlorophyll index (CI) and plant height (H) for the BN and MS small plots at SCAL.

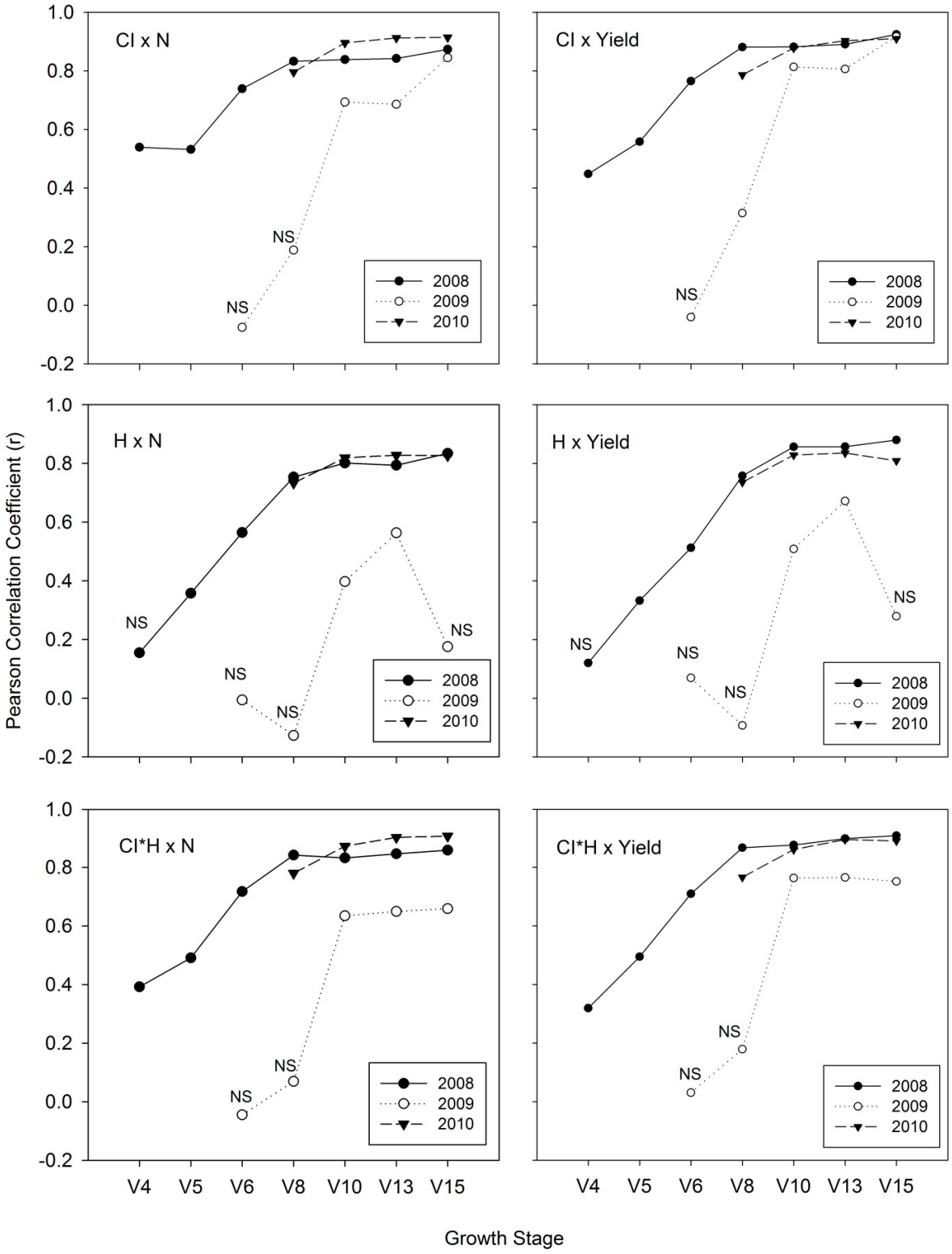

Figure 7. Pearson correlation coefficients (r) between CI, H and CI*H with N rate and yield at different growth stages for the BN Study.

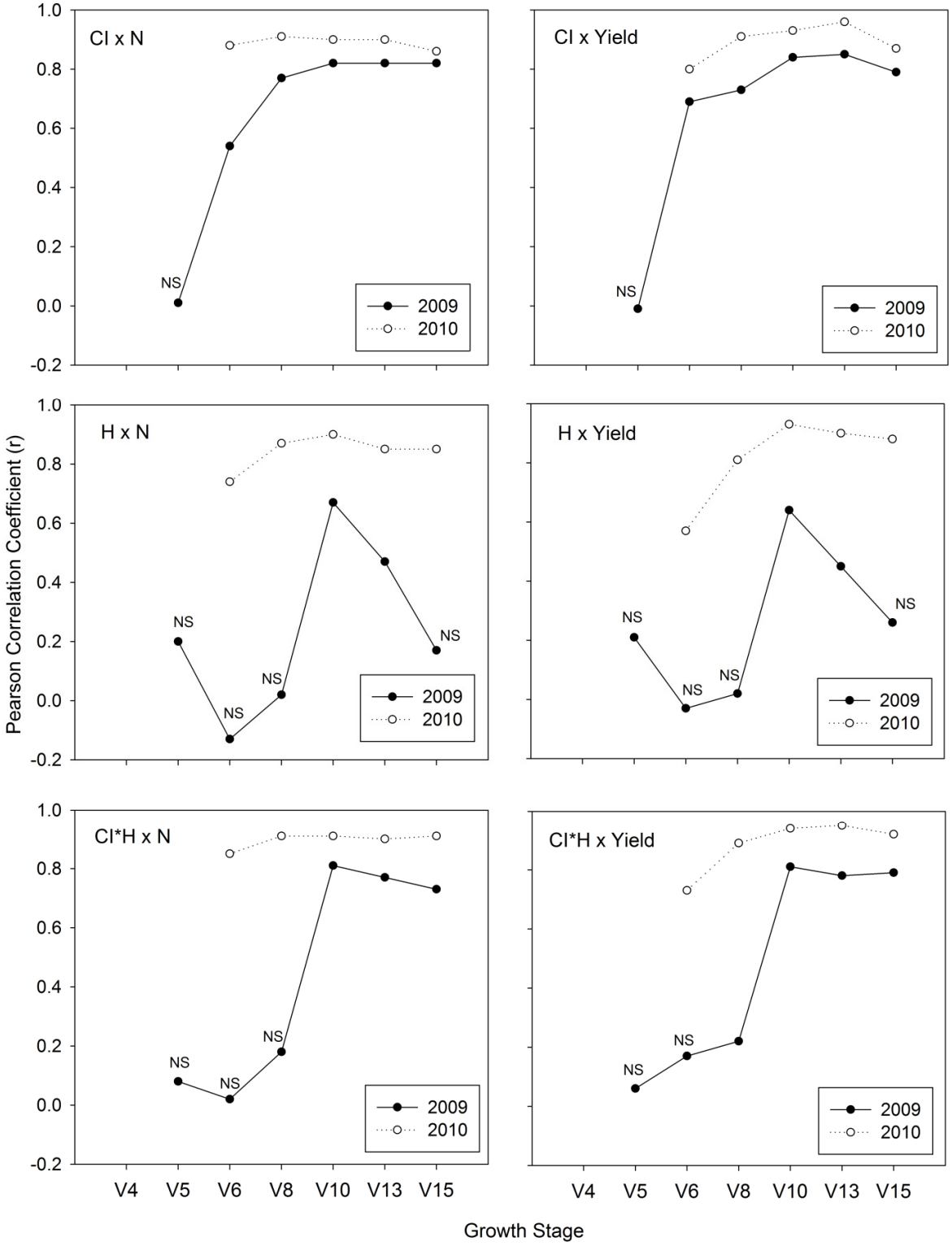

Figure 8. Pearson correlation coefficients (r) between CI, H and CI*H with N rate and yield at different growth stages for the MS Study.

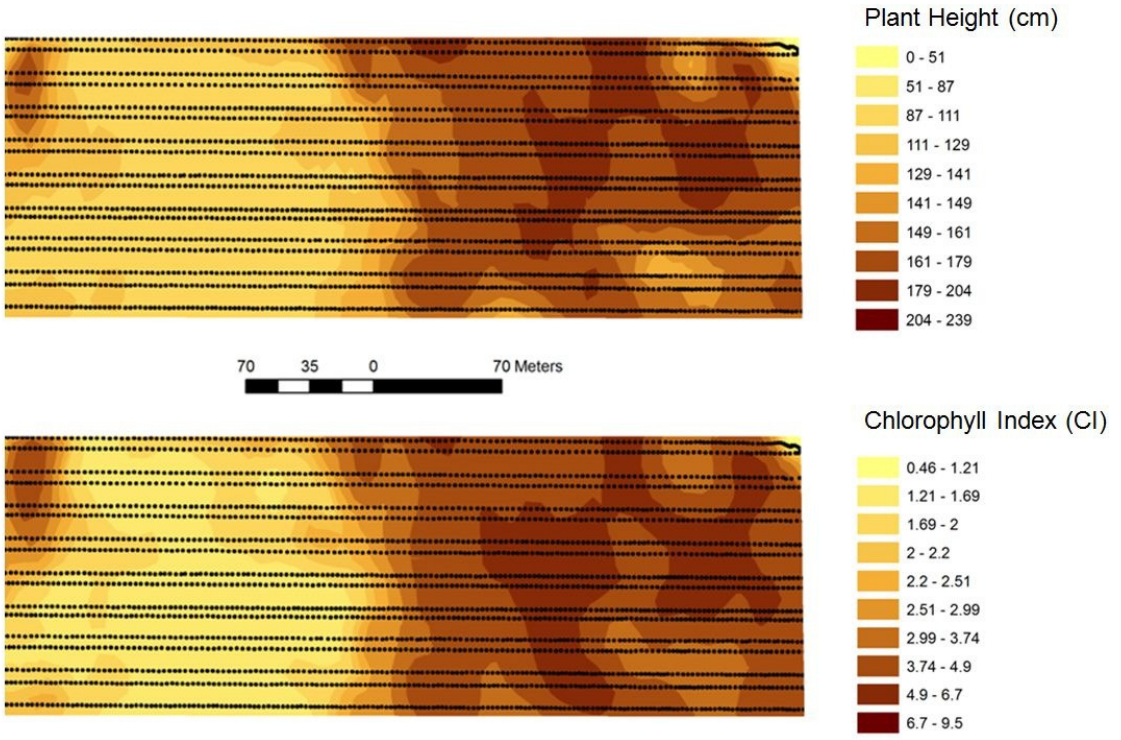

Figure 9. Plant Height and Chlorophyll Index maps generated from ultrasonic and active canopy sensors at one farmer field (BR10) in 2010 growing season.

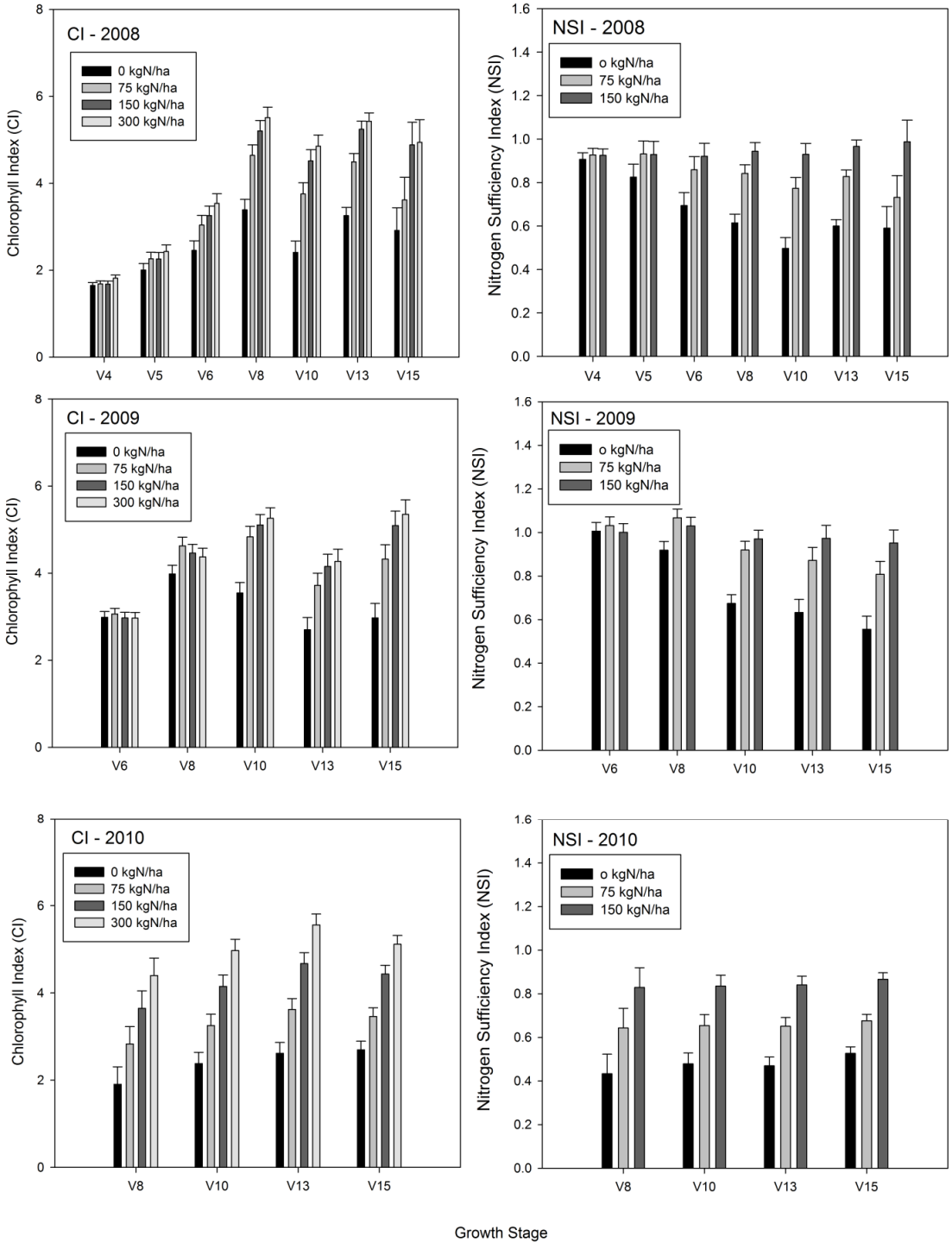

Figure 10. Chlorophyll Index (CI) and Nitrogen Sufficiency Index (NSI) by growth stage for different N rates, at SCAL, BN08, BN09 and BN10. NSI is the normalized CI relative to the 300 kg/ha N rate. Error bars represent Duncan LSD with $p < 0.05$.

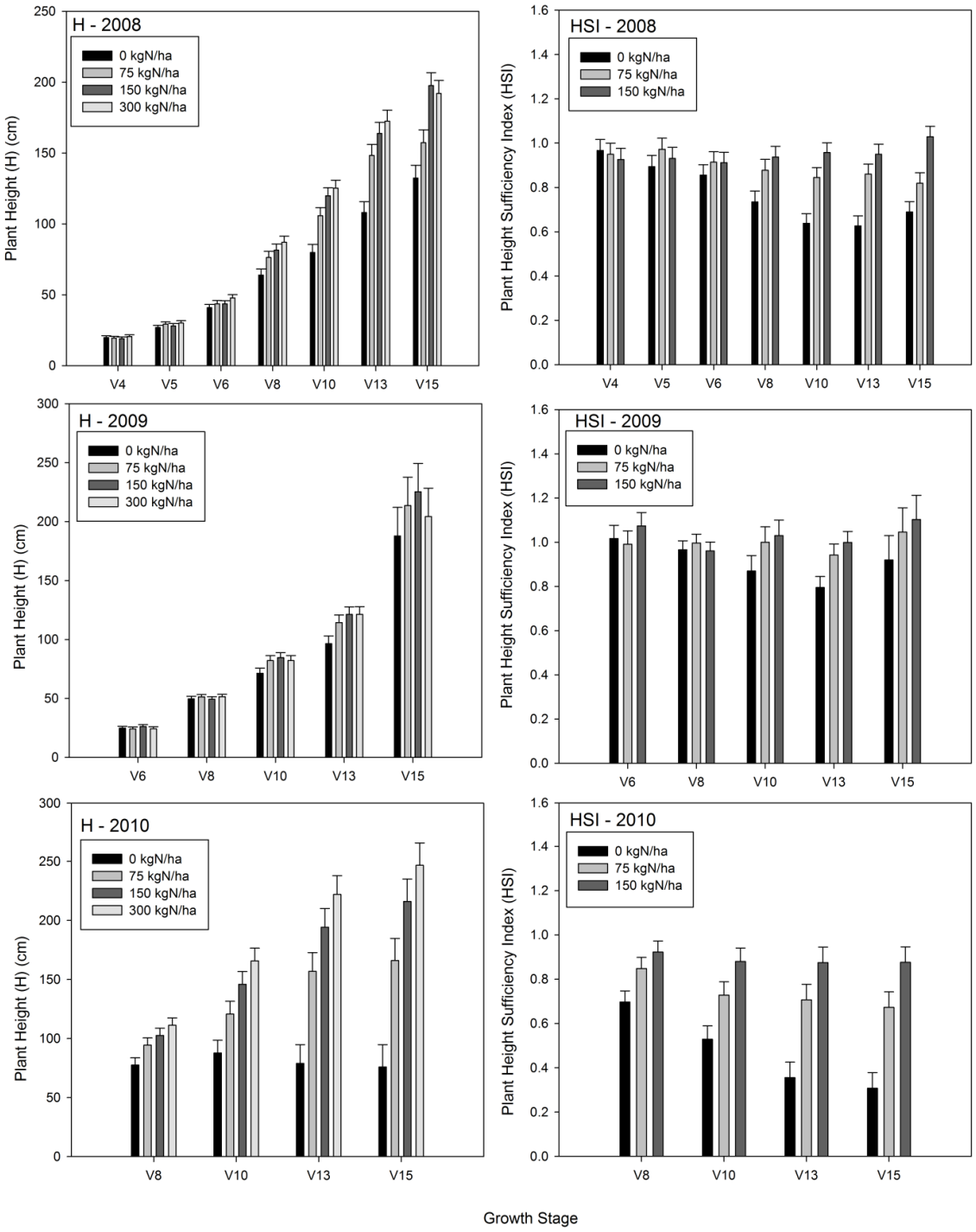

Figure 11. Plant Height (H) and Height Sufficiency Index (HSI) by growth stage for different N rates, at BN08, BN09 and BN10. HSI is the normalized H relative to the 300 kg/ha N rate. Error bars represent Duncan LSD with $p < 0.05$.

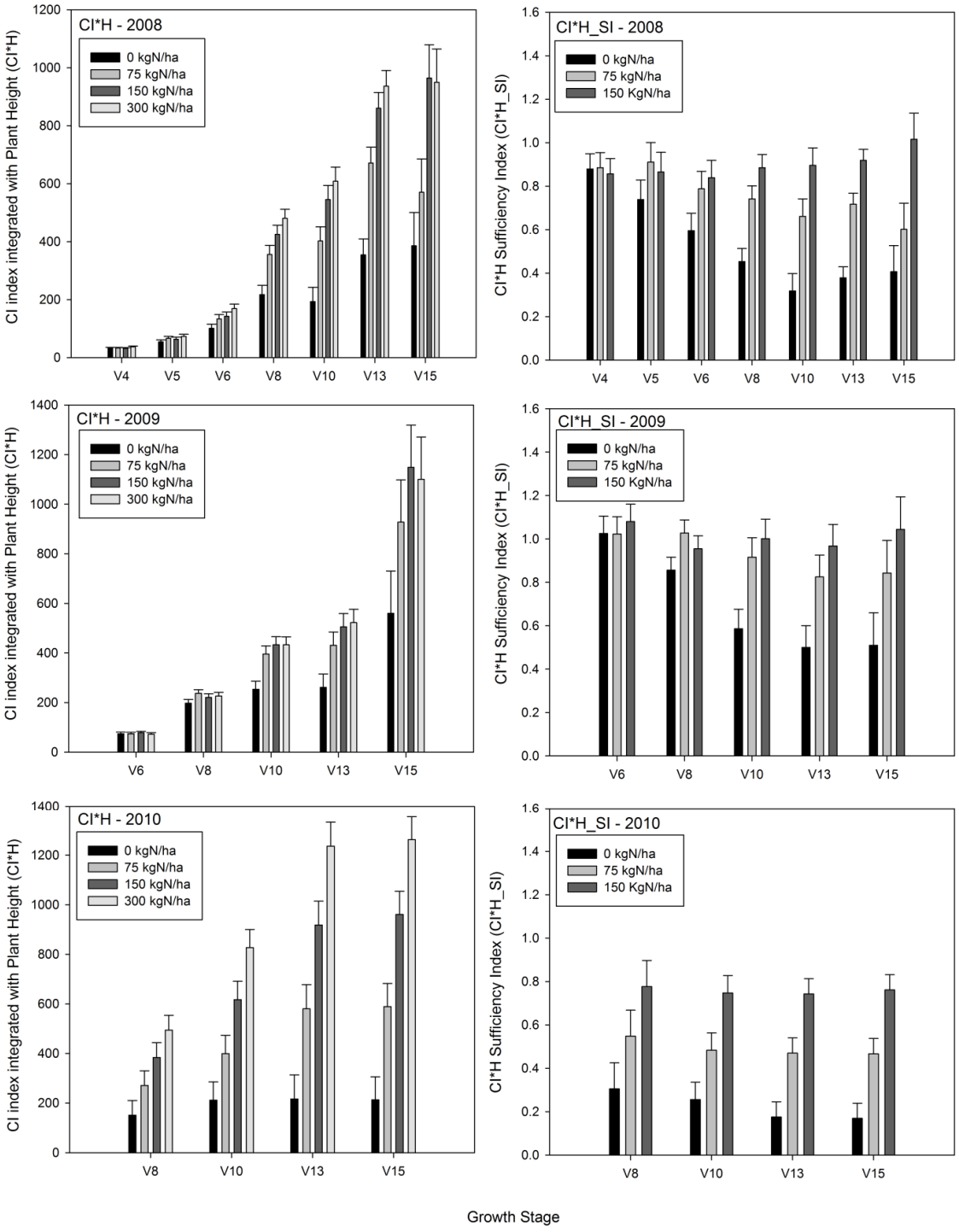

Figure 12. Chlorophyll Index (CI) integrated with Plant Height (H) (CI*H), and CI*H Sufficiency Index (CI*H_SI) by growth stage for different N rates, BN08, BN09 and BN10. CI*H_SI is the normalized CI*H relative to the 300 kg/ha N rate. Error bars represent Duncan LSD with $p < 0.05$.

Table 1. Corn phenological stages, N rates, Crop System and Predominant Soil Series at experimental sites conducted during 2008, 2009 and 2010. BN and MS are plots at experimental station (SCAL) and HU, BR, RT and BL are different farmer's fields. BN and MS had 3 replications and the farmers fields varied from 8 to 10 replications.

Site	Growth Stages	N rates (kg/ha)	Crop System	Soil Series
BN08	V4,5,6,8,10,11,13,15	0,75,150,300	No tillage	Crete Silt Loam
BN09	V6,8,10,11,13,15	0,75,150,300	No tillage	Crete Silt Loam
BN10	V8,10,11,13,15	0,75,150,300	No tillage	Crete Silt Loam
MS09	V5,6,8,10,13,15	0,75,150,225	Strip Till	Crete Silt Loam
MS10	V6,8,10,13,15	0,75,150,225	Strip Till	Crete Silt Loam
HU08	V8,10,13	0,75,150,225	Strip Till	Hastings Silt Loam
BR09	V15, R4	75, 100, 150, 200, 250	No tillage	Ipage Fine Sand
HU09	V15, R4	75, 100, 150, 200, 250	Strip Till	Hastings Silt Loam
RT09	V15, R4	75, 100, 150, 200, 250	No tillage	Hord Silt Loam
BR10	V15, R4	0,75,150,200,250	No tillage	Libory Fine Sand
HU10	V15, R4	0,75,150,200,250	No tillage	Hastings Clay Loam
BL10	V15, R4	0,75,150,200,250	No tillage	Satanta Loam

Table 2. Pearson correlation coefficients (r) between sensors readings for different on-farm research experimental sites.

Site/Year	Stage	CIxH	CIxN	HxN	(CI*H)xN	CIxYield	HxYield	(CI*H)xYield
HU 08	V8	0.82	0.14NS	0.18	0.16	0.18	0.29	0.21
	V10	0.91	0.32	0.34	0.32	0.46	0.49	0.47
	V13	0.73	0.35	0.23	0.33	0.37	0.11NS	0.28
HU 09	V15	0.84	0.02NS	0.01NS	0.03NS	0.02NS	0.08NS	0.10NS
	R4	0.92	0.11NS	0.01NS	0.11NS	0.05NS	-0.01NS	0.07NS
HU 10	V15	0.67	0.42	0.27	0.40	0.35	0.17	0.32
	R4	0.27	0.62	0.13	0.41	0.57	0.17	0.41
BR 09	V15	0.72	0.30	0.04NS	0.25	0.32	0.07NS	0.29
	R4	0.54	0.65	0.14	0.61	0.49	0.36	0.50
BR 10	V15	0.87	0.31	0.24	0.27	0.51	0.42	0.47
	R4	0.66	0.66	0.41	0.50	0.81	0.55	0.66
RT 09	V15	0.98	-0.02NS	-0.01NS	-0.03 NS	-0.01NS	-0.01NS	-0.01NS
	R4	0.43NS	0.16 NS	0.94	0.87	0.08NS	0.01NS	0.09NS
BL 10	V15	0.87	0.18	0.13	0.17	0.06NS	0.14	0.03NS
	R4	0.72	0.65	0.23	0.50	0.68	0.54	0.68

NS – non significant at $p < 0.05$

Table 3. Prediction models ranking using AIC criteria for N rate using normalized chlorophyll index - CI (NSI), normalized plant height - H (HSI) and the product of CI * H normalized (CIHSI). CI was measured by active optical canopy sensors and H measured by ultrasonic sensors. RMSE – root mean squared error; SSE – sum of squared error, RSQ – R squared; AIC – Akaike's Information Criteria.

Ranking	RMSE	Intercept	NSI	HSI	CIHSI	SSE	RSQ	AIC
1	64.8075	.	358.606	-405.981	258.456	957603.9	0.84773	1930.18
2	64.9272	-32.402	405.428	-367.822	205.597	956926.5	0.62982	1932.01
3	65.1036	-148.587	592.078	-234.437	.	966374.6	0.62616	1932.28
4	66.0797	181.048	.	-562.869	592.713	995568.2	0.61487	1939.16
5	66.4969	-286.724	690.574	.	-198.837	1008178	0.60999	1942.07
6	67.3583	-205.89	409.718	.	.	1039006	0.59807	1947.02
7	68.8007	.	.	-197.689	402.31	1083980	0.82763	1956.81
8	70.8265	.	660.509	-461.462	.	1148756	0.81733	1970.22
9	71.995	-73.244	.	.	270.164	1186972	0.54083	1977.78
10	75.166	.	-130.896	.	320.583	1293833	0.79426	1997.69
11	76.6137	.	.	.	184.185	1350021	0.78533	2005.51
12	83.3514	.	170.503	.	.	1597916	0.74591	2044.45
13	83.2015	-206.862	.	380.815	.	1585252	0.38675	2044.62
14	92.2079	.	.	153.442	.	1955528	0.68904	2091.11

Table 4. Prediction models ranking using AIC criteria for grain yield using normalized chlorophyll index - CI (NSI), normalized plant height - H (HSI) and the product of CI * H normalized (CIHSI). CI was measured by active optical canopy sensors and H measured by ultrasonic sensors. RMSE – root mean squared error; SSE – sum of squared error, RSQ – R squared; AIC – Akaike's Information Criteria.

Ranking	RMSE	Intercept	NSI	HSI	CIHSI	SSE	RSQ	AIC
1	0.12176	-0.15489	1.17123	-0.19787	.	3.38032	0.73924	-969.847
2	0.12178	.	0.93583	-0.37816	0.26259	3.38119	0.96699	-969.788
3	0.12242	-0.20326	1.01731	.	.	3.43206	0.73525	-968.338
4	0.12196	-0.08321	1.05608	-0.28016	0.12684	3.37672	0.73952	-968.093
5	0.12223	-0.27693	1.27326	.	-0.18121	3.40646	0.73722	-968.068
6	0.12501	.	1.24256	-0.43453	.	3.57851	0.96507	-958.686
7	0.12633	0.47279	.	-0.78823	1.13522	3.63892	0.71929	-952.819
8	0.12664	.	0.47987	.	0.32046	3.67292	0.96414	-952.671
9	0.13149	.	0.78115	.	.	3.97677	0.96118	-936.31
10	0.1324	0.11668	.	.	0.68353	4.01427	0.69034	-932.142
11	0.1361	.	.	0.1654	0.638	4.24183	0.95859	-919.405
12	0.13875	.	.	.	0.8205	4.42807	0.95677	-911.479
13	0.15917	-0.27017	.	1.0192	.	5.80207	0.55242	-847.051
14	0.16725	.	.	0.72224	.	6.43367	0.93719	-825.182

CHAPTER 4

NITROGEN RECOMMENDATION ALGORITHM FOR CORN BASED ON PLANT HEIGHT MEASURED BY ULTRASONIC DISTANCE SENSORS

ABSTRACT

The use of optical reflectance sensors (ACS) for on-the-go and site-specific application of nitrogen (N) in crops can improve nitrogen use efficiency (NUE), while improving grain yield response or reducing the amount of N applied in corn fields considering spatial variability. The objectives of this study were to: (i) develop an N recommendation algorithm based on ultrasonic plant height measurements to be used for in-season and on-the-go variable rate N application and (ii) validate and compare the algorithm proposed with other approaches for in-season N fertilization. To address objectives, ultrasonic plant height measurements were collected in two separate study sites during 2008, 2009 and 2010 growing season near Clay Center, NE. Plant height was measured at V10, V13 and V15 growth stages on plots that received 0, 75, 150, 225 and 300 kg N ha^{-1}, and final yield was measured. The algorithm was developed based on the relationship between relative grain yield, plant height and N rates. Since different N rates maximized yield when soybeans or corn were the previous crop, two different equations were generated to calculate the N recommendation for corn considering corn (CC) or soybeans (CS) as previous crop. The CC N recommendation (N_{rec}) equation is $N_{rec} = -2424HSI^2 + 3350HSI$

– 906 and the CS equation is N_{rec} = -2052HSI^2 + 2735HSI – 624. The first validation using a previous algorithm developed only with one year of data collection in CC in 2008 showed that adjustments had to be done to account for different previous crop since low N rates were applied compared to other treatments and consequently lower yields were obtained where the previous crop was soybean.

Abbreviations List: CC: corn after corn; CS: corn after soybeans; NSI: nitrogen sufficiency index derived from the sufficiency index calculation using a vegetative index; HSI: plant height sufficiency index derived from ultrasonic distance sensors; SB: sensor-based approach; AN: as needed approach.

INTRODUCTION

Currently, there are different options for in-season N prescription for corn fields. For example: side-dress applications based on crop history and N sources (Gagnon and Ziadi, 2010), side-dress application based on timing determined by chlorophyll meters (Scharf et al., 2006; Ruiz Diaz et al., 2008) and ultimately the use of on-the-go systems that use active optical reflectance sensors (ACS) that sense and apply N fertilizer in real time. The use of active crop canopy sensors for on-the-go and site-specific application of nitrogen (N) in crops can improve nitrogen use efficiency (NUE) compared to traditional uniform application, improving grain yield and reducing the amount of N applied considering spatial variability. Previous work has shown that these ACS can be used to estimate plant N status and prescribe N rates on-the-go with accuracy (Raun et al., 2005, 2007; Teal et al., 2006; Freeman et al., 2007 and Tubana et al., 2008, Dellinger et al, 2008). Chapter 3 we found that high correlations exist between these ACS and plant

height measured by ultrasonic distance sensors. Yin et al. (2011) found that plant height can be used to predict corn yield under major corn production systems. This entire context encourages the use of plant height as an option for an on-the-go sensor based system for N management. Normally, ACS require in their equations the sufficiency index approach (SI) to prescribe N; that is to normalize the sensor measurement by a non-limited N plant under a plot that receive enough N (N-rich) to not limit yield potential. This normalization reduces the effect of different cultivars, growth stages, crop history and soil conditions on sensor measurements. One limitation for the SI approach are crops such as cotton and sugarcane where excessive application of N can cause high vegetative growth that does not translate into yield, and the reflectance from these plots does not represent a good reference for the use of SI. On those situations plant height or its integration with optical sensors (Chapter 3) could be a better option. If plant height is a key indicator of plant growth and is linked to N nutrition during vegetative development of corn, the use of ultrasonic distance sensors to measure plant height at high spatial resolution to prescribe in-season N rates can be done. For optical sensors various algorithms and equations are available to translate crop reflectance into N rates (Dellinger et al., 2007; Solari et al., 2010; Holland and Schepers, 2010; Kitchen et al., 2010), but for plant height there is a need to generate one algorithm that can be used to prescribe N rates using ultrasonic sensors. The objectives of this study were to: (i) develop an N recommendation algorithm based on ultrasonic plant height measurements to be used for in season and on-the-go variable rate N application and (ii) validate and compare the algorithm proposed with other approaches for in-season N fertilization.

MATERIAL AND METHODS

This study was conducted at two experimental sites irrigated with a linear-move sprinkler system and located at the South Central Agricultural Laboratory (SCAL) of the University of Nebraska at Clay Center (BN and MS sites). The predominant soil at those sites are Crete silt loam (fine, smectitic, mesic Pachic Argiustolls), 0-1% slope. The BN site is a long-term experiment (since 1986) where different N rates, application time, use of a nitrification inhibitor and tillage methods are being evaluated. The MS site was designed in 2008 to initiate a soybean-corn rotation in one field where continuous corn had previously been grown.

To address the objectives, ultrasonic plant height measurements were collected using a bicycle modified to carry ultrasonic distance sensors. For the 2008 and 2009 growing seasons one ultrasonic sensor was mounted in the platform and for 2010, two sensors were mounted to collect a denser dataset. The sensors (Senix model TS30S1, Bristol, Virginia, USA) were integrated with a differentially corrected global positioning system (DGPS – Trimble GeoXT, Trimble Navigation Ltd., Sunnyvale, California) to record about 15 measurements per second about 60 cm over the top of corn rows. The on board collection software was programmed in LabView (National Instruments Corp., Austin, Texas, USA) and had the ability to record all data from the sensors. For every geographical coordinate recorded by each sensor we selected the maximum value among 15 measurements to represent the distance from the sensor to the highest point in the crop canopy. By difference with the sensor height to the ground level, we calculated plant

height. To start the system, the only input required from the user is the sensor height from the ground and a DGPS signal.

Plant height was measured at V10, V13 and V15 growth stages on plots that received 0, 75, 150, 225 and 300 kg N ha^{-1}. Final grain yield was measured with a plot combine (Gleaner K with 2rows) using the Harvest Master System (Juniper Systems Inc., Logan, UT), and corrected to an average grain moisture content of 155 g kg^{-1}.

Plant Height Algorithm Development

The algorithm was developed based on a previous framework for optical active canopy sensors developed by Solari (2006), who used quadratic equations to adjust the relationship between relative grain yield, sensor measurements and N rate. The general procedures for algorithm development were: (i) Determine the relationship of relative grain yield over years and N rates for each previous crop (CC and CS), and then calculate from the quadratic equation the N rate that maximized yield across 22 years of data for CC and 2 years for CS (Table 2); (ii) Determine the relationship between normalized plant height measurement to the highest N rate plot (HSI – analogous to SI) and N rates to adjust an equation that describes the estimated N supply in the crop by plant height over 5 site years, and (iii) Subtract from the N rate that maximizes yield in each system (CC and CS) from the estimated N supply in the plant, adjusting an equation to determine the N recommended rate.

Plant Height Algorithm Validation

The validation was conducted using a prototype plant height-based algorithm generated with data collected in 2008 from the long-term N study (BN) with CC (Figure 10).

For the validation we compared several approaches for in-season N fertilization:

1. 75 kg N ha^{-1} at planting + 150 kg N ha^{-1} at side-dress during V8 growth stage (V8)
2. 75 kg N ha^{-1} at planting + 150 kg N ha^{-1} at side-dress during V12 growth stage (V12)
3. 225 kg N ha^{-1} at planting (Reference)
4. 75 kg N ha^{-1} at planting + 150 kg N ha^{-1} at side-dress indicated when N was needed using chlorophyll meter approach with a threshold of 0.95 for SI – (AN)
5. Plant Height Based – (H)
6. Optical Sensor based – (SB)

In all treatments we used urea treated with Agrotain® to reduce the risk of ammonia volatilization. For SB treatment SI was calculated using the chlorophyll index proposed by Gitelson et al. (2005) as a vegetation index, using the formula CI = (NIR/VIS)-1, where NIR~880nm and VIS~ 590nm, integrated with the algorithm proposed by Solari et al. (2010). For the H treatment the normalized plant height (HSI) was used with measurements from the ultrasonic height sensors.

Experimental treatments consisted of two previous crops (CC and CS) and six approaches (V8, V12, AN, H, SB, Reference). The experimental design consisted of a

randomized complete block split-plot with previous crop as the main plot and approaches as subplots, consisting of 6 replications for each treatment. For the ANOVA we used the PROC GLM procedure and the Duncan Multiple Range Test for mean separation using $p<0.05$. Climatological data was recorded on-site for all growing seasons using an automated weather station and crops were managed to supply all nutrients other than N.

Grain yield and partial factor productivity (PFP) was measured to evaluate the different approaches. Partial Factor Productivity is the ratio between grain yield and the amount of N per area (Cassman et all., 1996; Olk et al., 1999). In this case we used yield in kg ha^{-1} and N rate in kg N ha^{-1}.

RESULTS AND DISCUSSION

Plant Height Algorithm Development

Analyzing the plant height and grain yield data, considering all experiments and growth stages, we found a high correlation between plant height sufficiency index (HSI) and relative grain yield (RY) (Figure 1), ensuring that the relationship between N rate and these two parameters are similar.

Starting with only CC, the relative yield and N rate relationship was explained by the equation: $RY= -0.00001N^2 + 0.005\ N + 0.4352$, ($R^2 = 0.9603$); which had an N rate that maximized yield at 250 kg N ha^{-1} across 22 years of data for the BN Study (Figure 2). The HSI and N rate relationship ($HSI = -0.000006N^2 + 0.003 + 0.6604$, ($R^2$=0.8054) also had the same N rate that maximized yield (250 kg N ha^{-1}), showing that HSI and

yield had the same N rate that maximizes yield (Figure 3). Subtracting 250 kg N ha^{-1} from the N rate determined from the equation of HSI, resulted in the equation that describes the N recommendation for the CC across growth stages (Figure 4).

We also analyzed the relationship across different growth stages, as differences among stages were reported previously for optical canopy sensors (Solari, 2006 and Varvel et al., 2007). We observed that for plant height the variation was smaller around the growth stages of V10, V13 and V15 (Figure 5), showing that the equation combining the growth stages in Figure 4 can be a good representation for the N recommendation for CC in a practical situation.

The N rate that maximized yield were different between the average relative yield for CC and CS (Figure 6). The N rate that maximized relative yield for CC (averaged across 22 years of data) and CS (averaged across 2 years) were 250 and 280 kg N ha^{-1}, respectively. This finding encouraged the use of two equations to calculate the N recommendation considering corn or soybeans as previous crop based on these rates and also, more importantly, in the relationship between HSI and N rate described in Figure 7.

To sum up, the CC equation was defined by $N_{rec} = -2424HSI^2 + 3350HSI - 906$ and the CS equation by $N_{rec} = -2052HSI^2 + 2735HSI - 624$ (Figure 8). Both equations required that a normalized plant height have to be used for N rate calculation.

Comparing equations developed for CC and CS with other algorithms previously evaluated using active canopy sensors, we observed over a range of SI that normally occurs in production fields (SI = 0.7 to 1.0) that all algorithms performed similarly except the Solari algorithm (Solari et al., 2010), using a N rate that maximized yield of 180 kg N ha^{-1}. All others included 250 kg N ha^{-1} as the N rate that maximized grain yield and

consequently it was expected that they would have similar trends (Figure 9). It is important to stress that HSI behaves differently compared to the SI from active canopy sensors that use different vegetation indices to calculate SI, so these equations generated here are only valid if the input is plant height measured by ultrasonic sensors, and plant height is normalized by plant height for the N-rich plot.

The need for a plant height algorithm is a reality since the use of ultrasonic sensors can be practical in a producer situation, and other studies have investigated the use of crop canopy height to improve optical sensor N estimation (Martin et al., 2010), to allow corn producers to market their corn grain earlier or predict yield spatially (Yin et al., 2011). Others studies have shown that plant height can be used for varying rate of plant growth regulators in cotton (Sharma et al., 2008) and to create an irrigation schedule when estimating evapotranspiration (Sammis et al., 1988). Finally, equations shown in Figure 8 provide the first algorithm to be implemented using ultrasonic distance sensors for on-the-go variable rate N fertilization, considering previous crop as an important variable for in-season N recommendation.

Plant Height Algorithm Validation

All validation was done comparing the first prototype plant height algorithm (Figure 10) generated from a N rate that maximized yield at 180 kg N ha^{-1} with other in-season N management approaches.

We found that grain yield and PFP were significantly different in the ANOVA performed for the treatments (Table 3). Year was significant showing that treatments

responded differently in different years. This could be explained by likely higher mineralization in 2009 compared to 2010 due to warmer temperatures early in the season. Since we had significant two and three-way interactions between N management approaches and previous crop, the treatment mean separation was done for both previous crop (CC and CS) for each year separately (Tables 4 and 5).

Analyzing grain yield for CC in 2009, the H yielded less than other treatments, but also the Reference treatment yielded less than other treatments, but equal to V8. The V12, SB, AN and V8 treatments had similar yields. Split application of N could be a major reason for better yields, since all split application treatments produced more yield than the reference where N was applied at planting (Table 4). This also could indicate that N was lost from the Reference applied at planting even with the use of Agrotain®. Randall et al. (2005) suggest that even with the use of an N inhibitor some N loss can occur comparing fall applications to early spring depending on rainfall patterns. In 2010 for CC there were no differences in grain yield among treatments.

For the CS in 2009 and 2010 only the H treatment produced less yield than the others treatments. All other approaches yielded similarly in both years. Generally split application was beneficial and the AN and SB approaches yielded similar to the Reference or other N application procedures. We observed that even late applications (V12) had better yields than at planting (Reference). Scharf et al. (2002) also found that delaying N applications until V12 – V16 resulted in yield loss of about 3%, but generally late applications had good yield response over 28 experiments with a single N application. There are some occasions where late applications may be of interest, for

example: spreading the work away from the planting season, remedying the N loss in wet years, or to allow use of in-season diagnostic tools as those related in this chapter.

Analyzing PFP for CC in 2009, the highest PFP of 82 kg grain (kg N applied)$^{-1}$ was for the H treatment, that was higher than for the SB treatment (74 kg grain (kg N applied)$^{-1}$) (Table 4). SB was superior to all other treatments that did not have differences in PFP, averaging around 60 kg grain (kg N applied)$^{-1}$. In 2010, SB had the lowest PFP but equal statistically to Reference, V12 and H treatments. The V8 and AN treatments were similar, since they were applied only a few days apart. Overall, the highest PFP for the H treatment in this study did not represent a better approach, but yield was maintained by indigenous N sources. This is strong evidence that justifies the need for an adjustment of the first prototype plant height algorithm. This was done in the first part of this Chapter in Figure 8, where higher N rates should be prescribed in general if the new proposed algorithm is used.

Overall, grain yield was higher for treatments where N was divided in two applications (75 kg N ha^{-1} at planting + 150 kg N ha^{-1} at side-dress), The ranking in terms of grain yield was V8, AN, V12, SB, REF and H. This indicates that split application performed better than total N at planting (Reference) as expected and that V8 (or AN applied at the same growth stage, but using chlorophyll meter threshold of 0.95 SI, as a decision criteria) tended to performed better than later at V12, though not statistically better. SB and H treatments had the lowest yields, but SB was not different from the other approaches that yielded more.

The first prototype algorithm tested based only on 1 year of data and specifically for CC seems weak to be used across previous crops; because it prescribed low N rates

for CS over years, producing less yield than other approaches. The new algorithm proposed shown in Figure 8 is a better option, since it accounts for previous crop and was developed using a higher N rate that maximized yield.

SUMMARY AND CONCLUSIONS

In this chapter an algorithm for in-season N fertilization based on plant height measured by an ultrasonic distance sensor was developed. We found that plant height measurements during V10-15 growth stages of corn can be a good indicator of in-season plant N status and can be used to prescribe N rate on-the-go similarly to the process used with active optical canopy sensors. Due to a different response of plant height to N rate and different N rate that maximized yield, we decided to generate an algorithm based on plant height that could prescribe N for irrigated corn considering the previous crop. The equations for different previous crops are: (i) $N_{rec} = -2424HSI^2 + 3350HSI – 906$ for corn after corn; and (ii) $N_{rec} = -2052HSI^2 + 2735HSI – 624$ for corn after soybeans. The new algorithm proposed, that accounts for previous crop and was developed using a N rate that maximized yield could be a reasonable option for in-season N management.

REFERENCES

Cassman KG, Gines GC, Dizon MA, Samson MI, Alcantara JM. 1996. Nitrogen-use efficiency in tropical lowland rice systems: contributions from indigenous and applied nitrogen. Fields Crops Res 47: 1–12

Dellinger, A.E., Schmidt, J.P., Beegle, D.B. 2008. Developing Nitrogen Fertilizer Recommendations for Corn Using an Active Sensor. Agron. J. 100: 1546-1552.

Freeman, K.W., Girma, K., Teal, R. K., Arnall, D. B., Tubana, B., Holtz, S., Mosali, J., Raun, W. R. 2007. By-Plant Prediction of Corn Forage Biomass and Nitrogen Uptake at Various Growth Stages Using Remote Sensing and Plant Height. Agron. J. 99: 530-536.

Gagnon, B., Ziadi, N. 2010. Grain Corn and Soil Nitrogen Responses to Sidedress Nitrogen Sources and Applications. Agron. J. 102: 1014-1022.

Gitelson, A.A., Vina, A., Ciganda, V., Rundquist, D.C., Arkebauer, T.J. Remote estimation of canopy chlorophyll content in crops. 2005. Geophysical Research Letters 32: 4-7.

Holland, K.H. , Schepers, J.S. 2010. Derivation of a Variable Rate Nitrogen Application Model for In-Season Fertilization of Corn. Agron. J. 102: 1415-1424.

Kitchen, N.R., Sudduth, K.A., Drummond, S.T., Scharf, P.C., Palm, H.L., Roberts, D.F., Vories, E.D. 2010. Ground-Based Canopy Reflectance Sensing for Variable-Rate Nitrogen Corn Fertilization. Agron. J. 102: 71-84.

Olk, D.C.; K.G. Cassman; G. Simbahan, P.C. Santa Cruz; S. Abdulrachman, R. Nagarajan, P.S. Tan, S. Satawathananont. 1999. Interpreting fertilizer-use efficiency in relation to soil nutrient-supplying capacity, factor productivity, and agronomic efficiency. Nutrient Cycling in Agroecosystems 35-41.

Raun, W., Solie, J., Stone, M., Martin, K., Freeman, K., Mullen, R., Zhang, H., Schepers, J., Johnson, G. 2005. Optical Sensor-Based Algorithm for Crop Nitrogen Fertilization*. Communications in Soil Science and Plant Analysis 36: 2759-2781.

Raun, W.R., Solie, J.B., Johnson, G.V., Stone, M.L., Mullen, R.W., Freeman, K.W., Thomason, W.E., Lukina, E.V. 2002. Improving nitrogen use efficiency in cereal grain production with optical sensing and variable rate application. Agron. J. 94: 815-820.

Randall, G.W., Vetsch, J.A. Corn Production on a Subsurface-Drained Mollisol as Affected by Fall versus Spring Application of Nitrogen and Nitrapyrin. Agron. J. 478, 472-478 (2005).

Ruiz Diaz, D.A., Hawkins, J.A., Sawyer, J.E., Lundvall, J.P. 2008. Evaluation of In-Season Nitrogen management Strategies for Corn Production. Agron. J. 100: 1711-1719.

Sammis, T.W., Smeal, D., Williams, S. 1988. Predicting Corn yield under limited irrigation using plant height. Transactions Of The Asabe 31: 830-838.

Scharf, P.C., Wiebold, W.J., Lory, J.A. 2002. Corn Yield Response to Nitrogen Fertilizer Timing and Deficiency Level. Agron. J. 94: 435-441.

Scharf, P.C., S.M. Brouder, and R.G. Hoeft . 2006. Chlorophyll meter readings can predict nitrogen need and yield response of corn in the north-central USA. Agron. J. 98:655–665.

Sharma, A., Dilawari, G., Taylor, R., Weckler, P., Banks, J C, Osborne, S. 2008. On-the-go Sensor System for Cotton Management for Application of Growth Regulators. ASAE Paper 0300.

Solari, F. 2006. Developing a crop based strategy for on-the-go nitrogen management in irrigated cornfields. PhD Dissertation, University of Nebraska, Lincoln, 157p.

Solari, F., Shanahan, J.F., Ferguson, R.B., Adamchuk, V.I. 2010. An Active Sensor Algorithm for Corn Nitrogen Recommendations Based on a Chlorophyll Meter Algorithm. Agron. J. 102: 1090-1098.

Teal, R.K., Tubana, B., Girma, K., Freeman, K. W., Arnall, D. B., Walsh, O., Raun, W. R. 2006. In-Season Prediction of Corn Grain Yield Potential Using Normalized Difference Vegetation Index. Agron. J. 98: 1488-1494.

Tubana, B.S., Arnall, D. B., Walsh, O., Chung, B., Solie, J. B., Girma, K., Raun, W. R. 2008. Adjusting Midseason Nitrogen Rate Using a Sensor-Based Optimization Algorithm to Increase Use Efficiency in Corn. Journal of Plant Nutrition 31: 1393-1419.

Varvel, G.E., Wilhelm, W.W., Shanahan, J.F., Schepers, J.S. 2007. An Algorithm for Corn Nitrogen Recommendations Using a Chlorophyll Meter Based Sufficiency Index. Agron. J. 99: 701-706.

Yin, X., Mcclure, M.A., Jaja, N., Tyler, D.D., Hayes, R.M. 2011. In-Season Prediction of Corn Yield Using Plant Height under Major Production Systems. Agronomy Journal 103: 923-929.

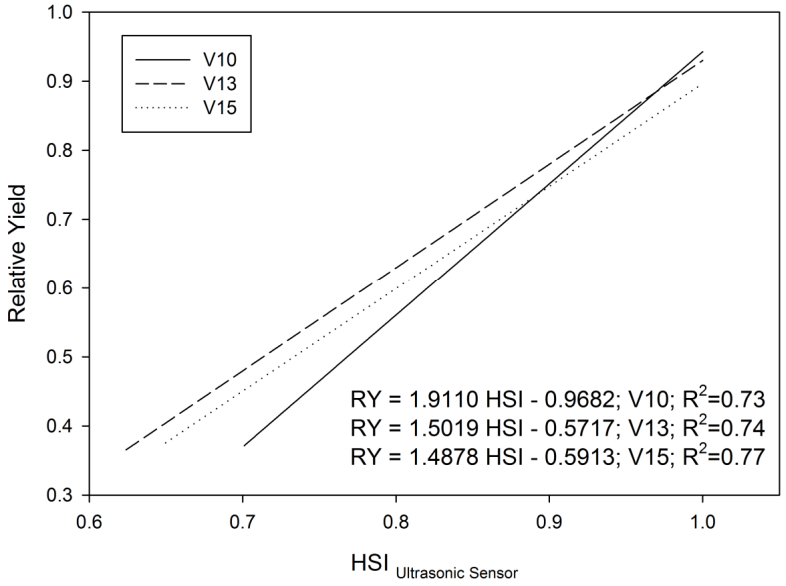

Figure 1. Relationship between relative grain yield and plant height normalized by the N-rich strip (HSI).

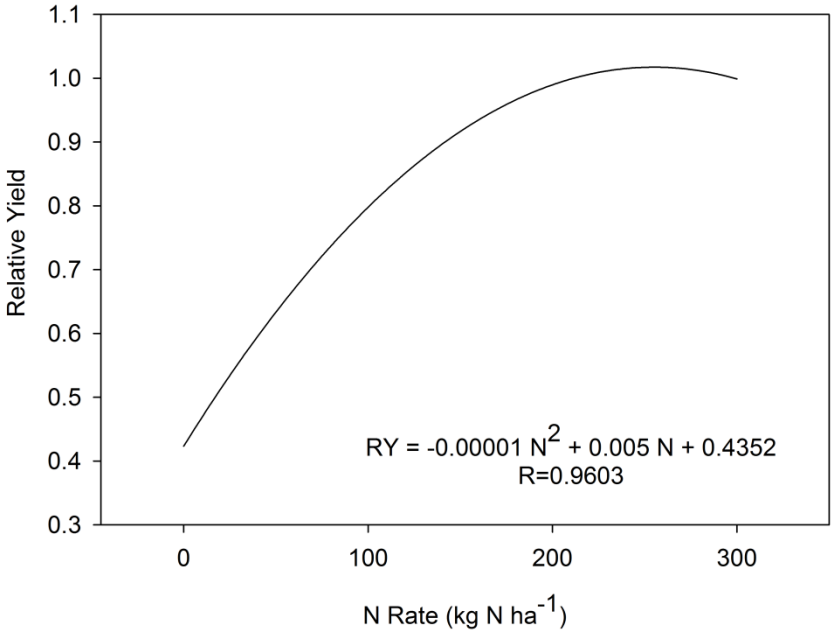

Figure 2. Relationship between relative grain yield and N rate across 22 years of data from the BN and MS study sites for CC.

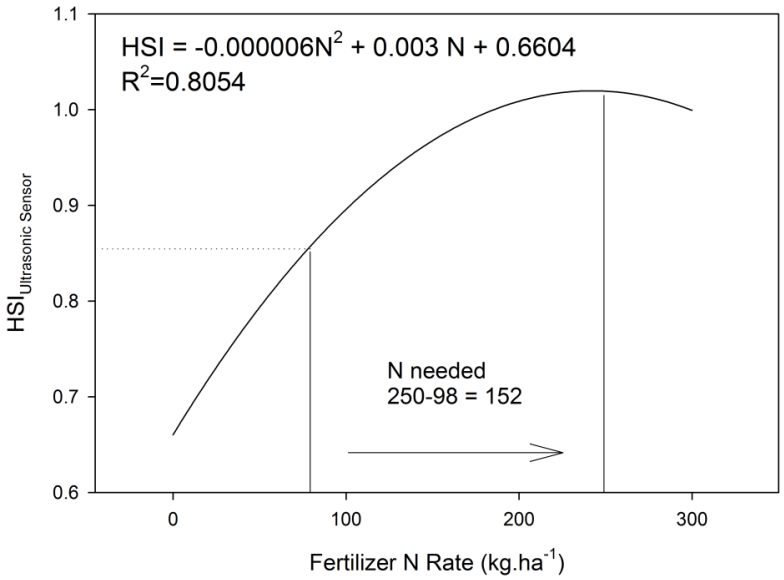

Figure 3. Relationship between HSI and N rates across 22 years of data from the BN and MS study sites for CC.

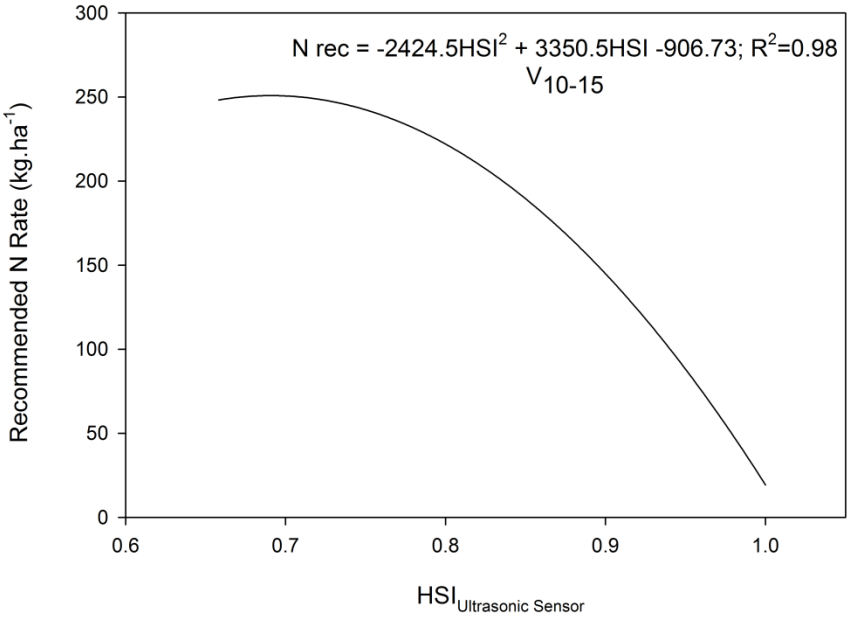

Figure 4. Recommended N rate for corn after corn (CC) across V11, V13 and V15 growth stages using an ultrasonic height sensor.

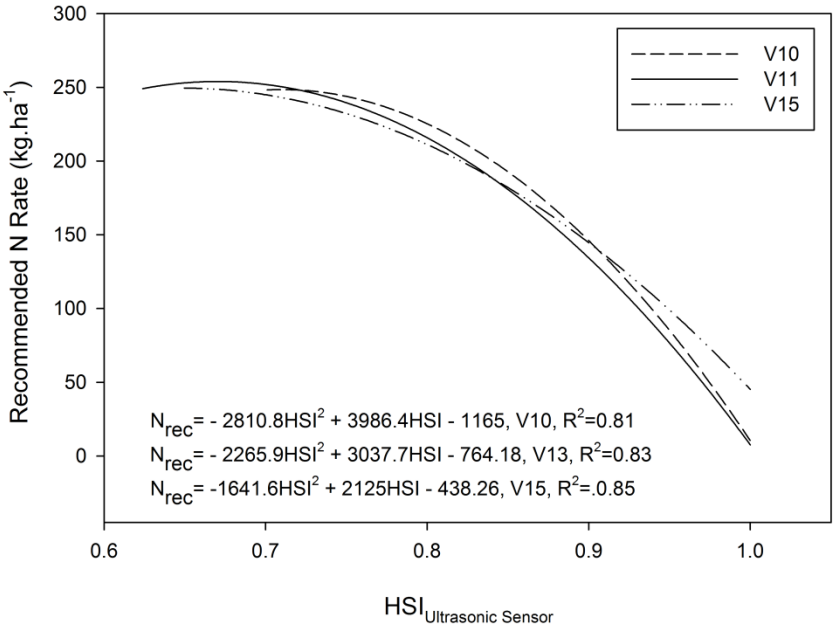

Figure 5. Recommended N rate for corn at different growth stages using an ultrasonic height sensor when the previous crop was corn (CC).

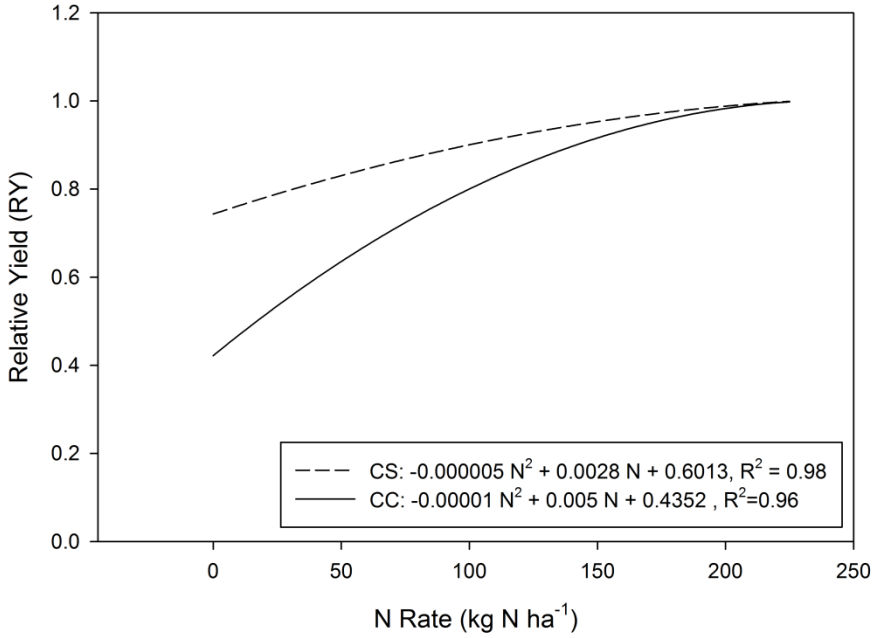

Figure 6. Relationship between relative grain yield and N rate for two different previous crop (CC and CS) for the BN and MS sites. BN includes 22 years of data and MS 2 years.

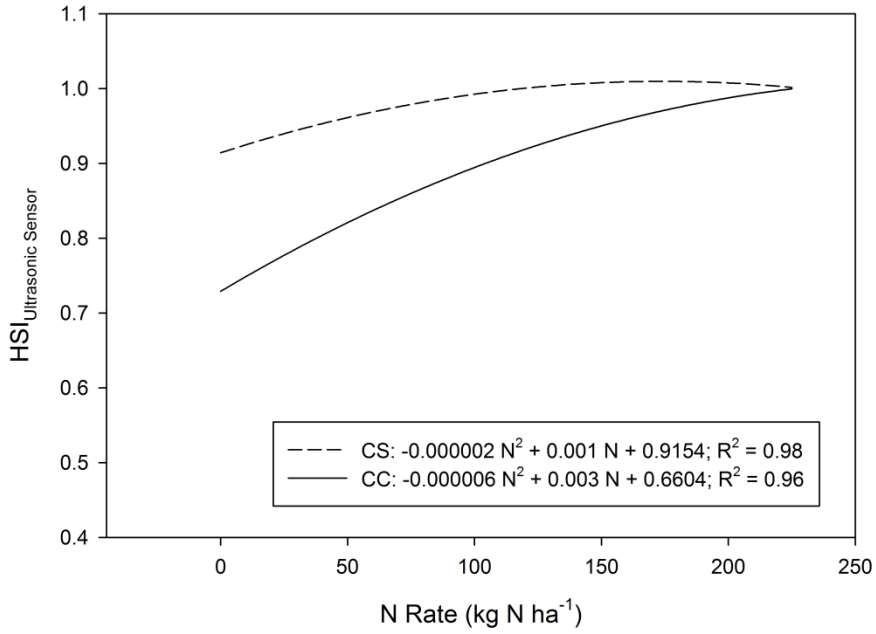

Figure 7. Relationship between HSI measured by ultrasonic sensor and N rates across 3 growth stages of data for the BN and MS study sites from 2008 until 2010.

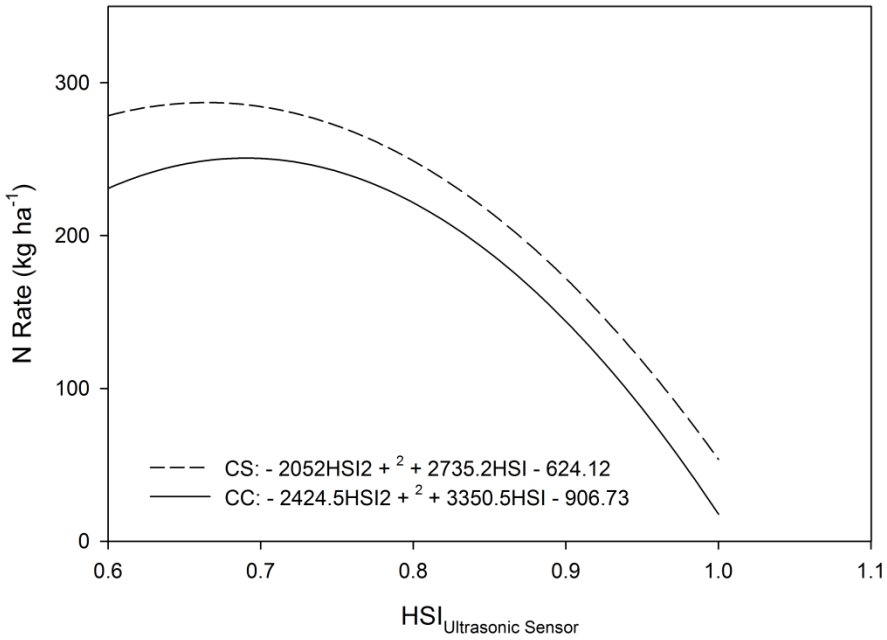

Figure 8. Recommended N rate for corn after corn (CC) and corn after soybeans (CS) across the V11, V13 and V15 growth stages using an ultrasonic height sensor.

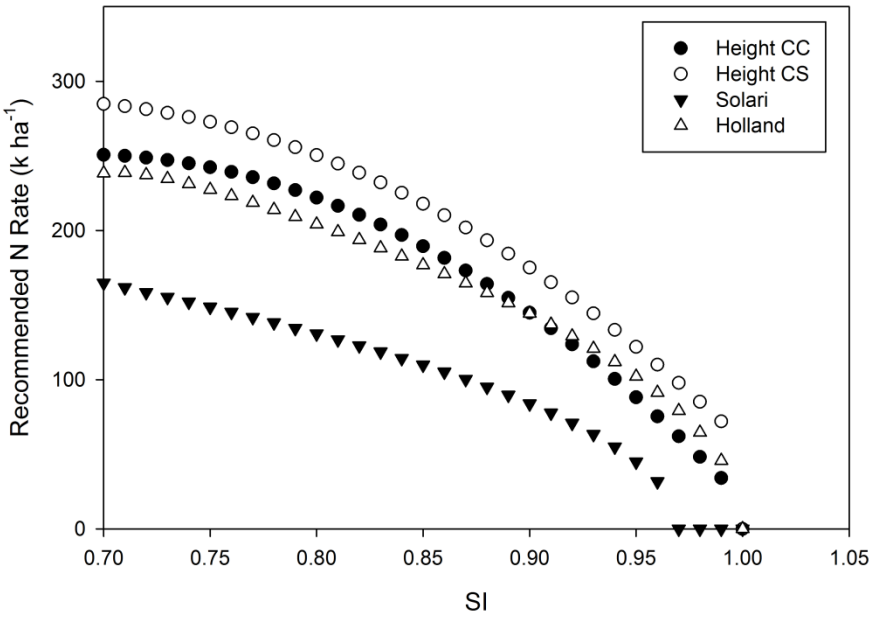

Figure 9. Comparison among algorithms developed to recommend N rate for corn using optical and ultrasonic sensors.

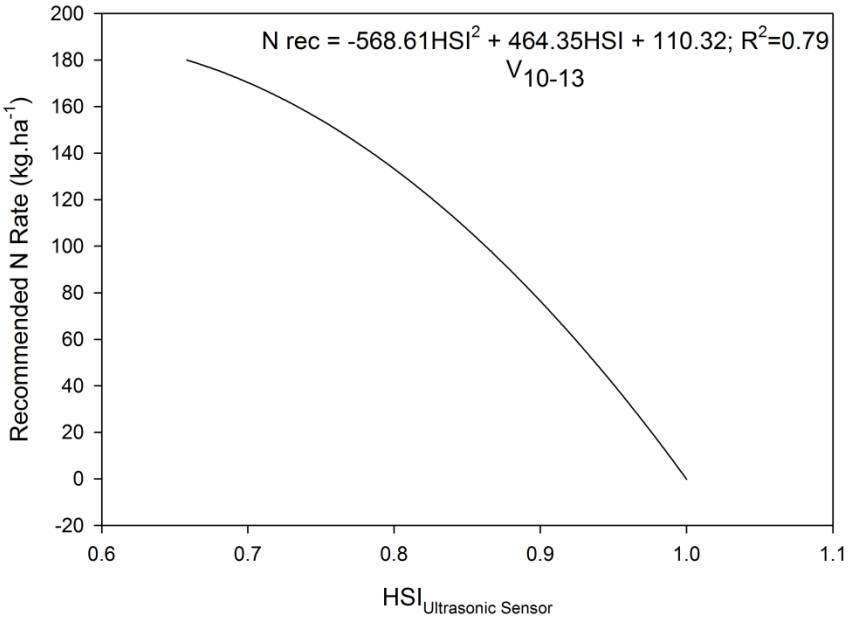

Figure 10. Prototype plant height algorithm developed for CC using only one site year of ultrasonic sensor collection during 2008 growing season. We used 180 kg N ha^{-1} as the N rate that maximized yield and ultrasonic sensor responses for one season data collection from V10, V11 and V13.

Table 1. Corn phenological stages, corn hybrid, N rates, crop system and predominant soil series at experimental sites conducted during 2008, 2009 and 2010. BN and MS are plots at experimental station (SCAL).

Site	Growth Stages	Corn Hybrid	N rates (kg/ha)	Crop System	Soil Series
BN08	V11,13,15	Pioneer 33H29	0,75,150,300	Strip Till	Crete Silt Loam
BN09	V11,13,15	Pioneer 33H29	0,75,150,300	Strip Till	Crete Silt Loam
BN10	V11,13,15	Pioneer 1395 XR	0,75,150,300	Strip Till	Crete Silt Loam
MS09	V10,13,15	Pioneer 33H29	0,75,150,225	Strip Till	Crete Silt Loam
MS10	V10,13,15	Pioneer 1395 XR	0,75,150,225	Strip Till	Crete Silt Loam

Table 2. Relative yield (RY) predicted equations to evaluate N response during 22 site years. The data from the BN study is from 1990 to 2010 and from MS Study (2009 and 2010). The Avg is the average equation across years. Study areas are less than 2 km apart.

Year	Equation	R^2
1990	$RY = -1E\text{-}05N^2 + 0.0044N + 0.5609$	$R^2 = 0.96$
1991	$RY = -1E\text{-}05N^2 + 0.0047N + 0.4824$	$R^2 = 0.9936$
1992	$RY = -1E\text{-}05N^2 + 0.0005N + 0.4516$	$R^2 = 0.9969$
1994	$RY = -8E\text{-}06N^2 + 0.0039N + 0.5460$	$R^2 = 0.9777$
1995	$RY = -1E\text{-}05N^2 + 0.0046N + 0.5248$	$R^2 = 0.9921$
1996	$RY = -1E\text{-}05N^2 + 0.0045N + 0.5168$	$R^2 = 1$
1997	$RY = -1E\text{-}05N^2 + 0.0061N + 0.4029$	$R^2 = 0.9983$
1998	$RY = -1E\text{-}05N^2 + 0.0052N + 0.4196$	$R^2 = 0.9973$
1999	$RY = -1E\text{-}05N^2 + 0.0051N + 0.4659$	$R^2 = 0.9884$
2000	$RY = -9E\text{-}06N^2 + 0.0041N + 0.5953$	$R^2 = 0.9962$
2001	$RY = -1E\text{-}05N^2 + 0.0061N + 0.3785$	$R^2 = 0.988$
2002	$RY = -8E\text{-}06N^2 + 0.0039N + 0.4983$	$R^2 = 0.9941$
2003	$RY = -7E\text{-}06N^2 + 0.0044N + 0.3507$	$R^2 = 0.9876$
2004	$RY = -3E\text{-}06N^2 + 0.0033N + 0.3312$	$R^2 = 0.9876$
2005	$RY = -5E\text{-}06N^2 + 0.0035N + 0.3775$	$R^2 = 0.9991$
2006	$RY = -1E\text{-}05N^2 + 0.0055N + 0.4147$	$R^2 = 0.9998$
2007	$RY = -1E\text{-}05N^2 + 0.0066N + 0.2550$	$R^2 = 0.994$
2008	$RY = -5E\text{-}06N^2 + 0.0038N + 0.3179$	$R^2 = 0.9952$
2009	$RY = -6E\text{-}06N^2 + 0.0033N + 0.5371$	$R^2 = 0.9991$
2010	$RY = -4E\text{-}06N^2 + 0.0030N + 0.4138$	$R^2 = 0.9989$
Avg	$RY = -9E\text{-}06N^2 + 0.0044N + 0.4451$	$R^2 = 0.9999$

Table 3. Analysis of variance (ANOVA) for the comparison among in-season N fertilization approaches.

Source	DF	Type I SS	Mean Square	F Value	Pr > F
Year	1	1.31E+09	1.31E+09	1259.43	<.0001
Approach	5	3.46E+08	69157470	66.51	<.0001
Year*Approach	5	66758807	13351761	12.84	<.0001
Previous crop	1	9.02E+08	9.02E+08	867.62	<.0001
Year*Previous crop	1	1.64E+08	1.64E+08	158.03	<.0001
Approach*Previous crop	5	61697744	12339549	11.87	<.0001
Year*Approach*Previous crop	5	1.28E+08	25605308	24.63	<.0001

Table 4. Treatment mean separation for grain yield and PFP (kg grain).(kg N applied)$^{-1}$ for the CC plots during 2009 and 2010 growing seasons.

Treatments	CC - 2009		CC - 2010	
	Yield ($kg.ha^{-1}$)	PFP ($kg.kg^{-1}$)	Yield ($kg.ha^{-1}$)	PFP ($kg.kg^{-1}$)
V8	13790ab	61c	12046a	53a
V12	14633a	65c	10725a	47ab
Reference	13367b	59c	10414a	46ab
AN	14205a	63c	11574a	51a
SB	14519a	74b	10807a	41b
H	12114c	82a	11141a	48ab

Table 5. Treatment mean separation for grain yield and PFP (kg grain).(kg N applied)$^{-1}$ for the CS plots during 2009 and 2010 growing seasons.

Treatments	CS - 2009		CS - 2010	
	Yield ($kg.ha^{-1}$)	PFP ($kg.kg^{-1}$)	Yield ($kg.ha^{-1}$)	PFP ($kg.kg^{-1}$)
V8	15084a	67c	13728a	61c
V12	14955a	66c	13938a	62c
Reference	14899a	66c	14035a	62c
AN	14981a	66c	13694a	60c
SB	14849a	165b	13459a	81b
H	13661b	180a	11983b	117a

CHAPTER 5

EVALUATION OF CROP WATER STATUS USING CANOPY SENSOR INTEGRATION

ABSTRACT

In the early 2000's, active optical crop canopy sensors began being used to manage in-season variable nitrogen (N) fertilization in cornfields, increasing the efficiency compared to preplant uniform rate N applications. There have also been initiatives of using ultrasonic sensors to measure plant height on-the-go for N application and crop water demand estimation, but no studies have integrated optical, ultrasonic and canopy temperature for crop water stress assessment. The objective of this chapter is to evaluate crop water status using infrared thermometry integrated with optical and ultrasonic canopy sensors. Specifics objectives are: (i) to evaluate corn canopy temperature under different previous crop, N rates and irrigation levels; (ii) test a procedure for water stress assessment in commercial cornfields using the integration of sensors, (iii) correlate plant based sensor measurements (N status, plant height and canopy temperature) with grain yield, soil attributes and detailed topographical features, and (iv) study the spatial dependence of canopy temperature. This study was conducted in one small plot study and on three producer's fields in 2010. The small plot experiment consisted of two irrigation levels (70 and 100% evapotranspiration – ET), two previous crops (corn after corn – CC and corn after soybeans – CS), and four N rates (0, 75, 150,

225 kg N ha^{-1}). Canopy temperature, optical reflectance and plant height were measured from R2 until R6 in the small plot study. At the producer's fields, three long strips across center pivots were used to have a non-limited N and water crop, and then continuous georeferenced sensors measurements were taken at the V11 growth stage in about 10 hectares in each field. In the small plot study the crop canopy temperature was influenced by irrigation levels and N rates. The procedure proposed could be used to identify zones in producer's field where water stress can be a yield-limiting factor. Inside the zones considered there were low correlations between plant height, plant N status and canopy temperature, indicating that the canopy temperature had more influence from water stress than vegetation cover. Concave landscape positions and lower elevation areas had higher yields compared to convex and high elevation portions indicating that detailed elevation mapping can be beneficial to delineate stables zones that possibly could be used with variable irrigation systems. The spatial dependence of canopy temperature was over 65 meters across producers' sites, suggesting that commercial high clearance applicator's swath width is adequate to obtain accurate maps of canopy temperature. The integration of canopy reflectance, plant height and canopy temperature was beneficial to detect water stressed zones in the field. Opportunities can be foreseen for on-the-go N fertilization using integration of these sensors because is likely that water stress can be confounded with differential N supply during the growing season and in different zones in the field.

Abbreviation list*:* IRT, infrared thermometers; NSI, nitrogen sufficiency index; HSI: Plant Height Sufficiency Index; CC, corn after corn; CS, corn after soybean; Tc-Ta, canopy temperature minus ambient temperature; Tc-Tr, canopy temperature minus canopy temperature of a well watered plot; CWSI, Crop Water Stress Index; MTCI, Meris Terrestrial Chlorophyll Index.

INTRODUCTION

Infrared thermometers (IRT) were introduced into agriculture more than 40 years ago as a hand-held tool to remotely measure the surface radiometric temperature of crops to characterize water stress in plants, predict yields and manage irrigation. Using optics and specialized detectors, these sensors were engineered to filter thermal radiation in the mid to far-infrared region (8 to 14 μm) converting to a digital temperature without direct physical contact between the leaf and the thermometer (Hatfield et al., 2008, O'Shaughnessy et al., 2011). Advances in IRTs have increased the options available for irrigation management available on the market at reasonable prices. The main goal of these IRT is to obtain crop canopy temperature to assess crop water status (Aston and Van Bavel, 1972; Idso et al., 1978; Idso et al., 1982). Several studies indicated that foliage temperature can be correlated with soil moisture content, plant water stress and plant transpiration rate (Idso et al., 1978, Howell et al., 1984, Jackson et al., 1981, González-Dugo et al., 2006). Vapor pressure deficit (VPD), net radiation and wind speed can influence canopy temperature (Sepulcre-Canto et al., 2006). Further studies demonstrated a linear relationship between vapor pressure deficit and foliage temperature, with one of the most important contributions for proper use of IRT being the crop water stress index (CWSI) developed at the USDA-ARS Water Conservation Laboratory, Phoenix, Arizona (Jackson et al. 1981). They also showed that canopy temperature (Tc) minus air temperature (Ta) is essential to study the water status of a crop, relating Tc-Ta to productivity and crop water requirements. Other studies compared

the measured canopy temperature to that of a well-watered reference plot (Tr) as an indicator of water stress (Fuchs and Tanner, 1966), representing by Tc-Tr (Sepulcre-Canto et al., 2006). Moran et al., (1994) found that vegetation cover assessed by vegetation indices can be negatively correlated with canopy temperature, because the soil background can influence canopy temperature measurements. It was also found that evapotranspiration and field water deficit can be estimated using remotely sensed measurements of surface temperature (crop + soil) and reflectance (red and near infrared spectrum) with limited on-site meteorological data (net radiation, vapor pressure deficit, wind speed and air temperature). It is challenging to separate the plant water stress from N stress (Zhu et al., 2011, Clay et al., 2006) and also separate soil factors such as texture and others nutrients from N deficiency (Zillmann et al., 2006). Knowing that several factors can influence the assessment of crop water status using canopy temperature measured by IRTs, due to interferences and calibration of the equipments, there were initiatives for complex variable rate irrigation systems that relied on canopy temperature measurement to manage water in center pivots with success (Sadler et al., 2002 and O'Shaughnessy et al., 2010).

In the early 2000's, active optical crop canopy sensors have been used to manage in-season variable N fertilization to match the plant demand that occurs mid-season, increasing efficiency compared to broadcast N applications (Stone et al., 1996; Raun et al, 2005; Tubana et al., 2008, Schmidt et al., 2009). There were also initiatives of using ultrasonic sensors to measure plant height on-the-go for N application (Sui et al., 2006) and plant height measurement during the season to estimate evapotranspiration and crop water demand (Sammis et al., 1988), but no studies have integrated optical, ultrasonic

and canopy temperature sensors for on-the-go crop water stress assessment. The objective of this chapter is to evaluate crop water status using infrared thermometry integrated with optical and ultrasonic sensors. Specifics objectives are: (i) evaluate corn canopy temperature under different previous crop, N rates and irrigation levels; (ii) test a procedure for water stress measurement using the integration of sensors, (iii) correlate plant based sensor measurements (N status, plant height and canopy temperature) with grain yield, soil attributes and detailed topographical features, and (iv) study the spatial dependence of canopy temperature.

MATERIAL AND METHODS

Research Fields

This study was conducted on small plots at the South Central Agriculture Laboratory (SCAL) (MS10), near Clay Center, Nebraska and on three producer's fields in 2010 (BR10, HU10 and BL10). The BL10 field was near Brule, Nebraska, and the other (BR10 and HU10) near Aurora, Nebraska. All fields were sprinkler-irrigated to provide enough water for high yielding corn production. The hybrids, starter fertilization and water management were selected by each farmer and similar hybrids were selected for the small plots at SCAL. Soil characteristics and other management practices and related information are presented in Chapter 2.

Sensor Platform

One optical sensor, two ultrasonic sensors and one infrared temperature sensor (IRT) were mounted in an aluminum apparatus designed to keep enough distance between sensors to avoid interference and close enough to measure the same target. The aluminum bar was painted black around the infrared thermometer to avoid interference of the aluminum surface. For the small plot field, sensors were installed on a bicycle and integrated with a differential global navigation satellite system (DGPS) to gather data in the same location. For the producer fields the sensors were installed on the boom of a high clearance sprayer. All sensors were adjusted to make measurements over the corn row, to have minimum bare soil interference in the readings.

Sensors Descriptions

The optical sensor was an active light reflectance sensor that emits and receive canopy reflectance in the near infrared (NIR) and visible spectrum regions. The Crop Circle 470 (CC470) (Holland Scientific, Lincoln, NE) was used. The CC470 is a three band active sensor that measures NIR at 760nm and the red and red-edge bands at 670 and 720nm, respectively. These spectral bands were used to calculate a vegetation index. From the results obtained in the Chapter 1, the MTCI was chosen as vegetation index.

For plant height measurements we used an ultrasonic distance sensor that measures the sound pulse and scattering from the canopy back to the sensor. The model

used was a TSPC-30S1 (Senix, Bristol, VT) that has a maximum range of 4.3 meters and optimum range of 0.10 to 3 meters, with a field of view less than 5 cm at 1 meter height from the target. It is waterproof and temperature-compensated. Output data was calibrated in the laboratory and converted to distance in centimeters. Plant height was determined by the difference of the sensor height and the distance from the top of the canopy to the sensor.

Canopy temperature was measured using an non-contact infrared temperature sensor (IRT) model PSC SSS – LT02H (Process Sensors Corp., Milford, MA), that has a lower limit temperature of 0 ºC and a upper limit of 500 ºC, with a 2:1 field of view, and accuracy of 0.5 ºC at object temperatures > 20ºC for the target temperature. The sensor was oriented at nadir position and kept from about 1 meter above crop canopy. The sensor was calibrated in the factory. IRT also measures the temperature of the instrument box and the tip of the sensor. The selection of this sensor allowed the use of the tip or box temperature as the ambient temperature (Ta) that is required in most of canopy temperature studies for calculation of the difference of canopy temperature (Tc) minus the ambient temperature (Ta), related to water status of the crop. Details about the (Tc-Ta) theory can be found in Jackson et al. (1981) and Idso et.al. (1978). To calculate the Tc-Ta it we used the ambient temperature measured on site with automated weather stations due to variations of the temperature recorded by either box or tip temperature. For on-the-go purposes it is required to measure the Ta in real time to calculate the Tc-Ta, so attempts were made to calculate a similar approach using the tip temperature (Tc-Tt), where Tt was the tip temperature measured at the same time as the target temperature or canopy temperature (Tc).

Experimental Design and Data Analysis

Small Plots

The small plot experiment consisted of two irrigation levels (70 and 100% of evapotranspiration – ET), two previous crop schemes (corn after corn – CC and corn after soybean – CS), and four N rates (0, 75, 150, 225 kg N ha^{-1}) with three replications. Canopy temperature was measured from R2 until R6 growth stages. Soil moisture sensor probes were installed to monitor hourly the soil available water during the growing season. The experimental design was a randomized complete block split-split plot, with irrigation levels as main plot, previous crop as subplot, and fertilizer N rate as sub-sub plots. Analysis of variance was done to evaluate treatment effects on canopy temperature (Tc-Ta) and means separation using the Duncan Multiple Range Test ($p<0.05$). Irrigation level, previous crop and replications were considered random effects. Time-repeated measures analysis was used with PROC MIXED to evaluate Tc-Ta at different growth stages (R2, R3, R4 and R6).

On-Farm Research Sites

At producer's fields, three long strips across the field were for a non-limited N treatment with 250 kg N ha^{-1}. These strips were used to calculate the nitrogen sufficiency index (NSI) for the optical and plant height sufficiency index (HSI) for the ultrasonic

sensors and also to have a reference canopy temperature where N and water were not limiting. To evaluate plant water availability at the time of sensing, data were collected from two sets of soil moisture probes (Watermarks, Irrometer Co, Riverside, California) measuring at 30, 60, 92 and 121 cm soil depth installed in two locations inside the reference strip in each field at the beginning of the growing season. These locations consisted of low and high elevation areas in the field where one of three reference strips were located. These regions were used to calculate a reference canopy temperature, considered to be non-water stressed plants (Tc-Tr), where Tr is the canopy temperature of a non-stressed crop measured by IRT. This method was used by Sadler et al. (2002) in corn and Sepulcre-Canto et al. (2006) assessing olive tree canopy temperatures. Next to those reference strips, continuous georeferenced sensor measurements were taken at side-dress (V11 growth stage) in about 10 hectares in each field.

The procedure to be tested consisted of the main assumption that water stress measured with canopy temperature is the major factor affecting the grain yield. To evaluate this assumption two zones in each farmers fields were created: (i) Non-water stressed (NonS) and (ii) Water stressed (S). To delineate these zones the Raster Calculator in ArcGIS was used considering the following criteria:

$$NonS = NSI \text{ and } HSI > 0.95 \text{ and } Tc\text{-}Tr < 0$$

$$S = NSI \text{ and } HSI > 0.95 \text{ and } Tc\text{-}Tr > 0$$

Where:

NSI is the nitrogen sufficiency index calculated using the average MTCI calculated from three replications of the N-rich strips; HSI is the height sufficiency index calculated using the average plant height measured

using ultrasonic sensors from the N-rich strips; Tc – Tr is the canopy temperature minus the average canopy temperature from the N-rich strips where soil matric potential measured by soil moisture sensors indicated non water-limited crop at time of sensing.

The criteria of 0.95 was selected based on previous studies (Varvel et al., 2007 and Solari et al., 2010) where an SI greater than 0.95 can be considered N sufficient. Similarly as observed in Chapter 4, a HSI of 0.95 is also a good indicator of N sufficiency corn plant.

After the two zones were delineated, all points inside these zones were used to compare the means of the variables using pairwise comparison with Tukey's test at $p < 0.05$. To perform a balanced comparison a number of points were randomly excluded from some fields to have the same number for every zone.

Correlations between Canopy Temperature, Topographic Features and Soil Attributes

Previous to the reference strip implementation on the producer's fields, apparent electrical conductivity (EC) was mapped using a Veris (Veris Technologies, Salina, KS) and grid soil sampling was done to map organic matter and other soil nutrients. Detailed elevation was measured using a real kinematic (RTK) GPS associated with the EC mapping. To delineate topographical features (concave and convex areas) it was used the Focal Statistics procedure from the Spatial Analyst package of ArcGIS 9.3 (ESRI, Redlands, CA). Using focal statistics it was calculated the difference in elevation from one pixel (5x5 meters) in the raster elevation map and the average elevation inside a

radius of 10 meters of that pixel (Focal20m). Focal20m = pixel – (average elevation of 10 m radius from that pixel). In the resulting map, negative values in meters represent concave areas and the positive convex areas, considering one region of influence in the pixel of 20m diameter. It is expected that concave areas and lower relative elevation have less water stress and lower canopy temperatures compared to convex and relatively high elevation areas. All variables (NSI, HSI, Tc-Tr, grain yield, ECsh, OM, pH, P, NO_3, RTK elevation, Focal20m, Tc-Tr) were correlated using Spearman rank correlations to analyze spatial relationships between these variables inside zones (NonS and S). As reported by Kitchen et al. (2003) if correlation analysis is used to compare large datasets, such as these collected using sensors, the results should be viewed subjectively and mainly used as an indicator of those factors to be included in more scrutinizing analyses. With large datasets statistically significant correlations are common. However, a variable could be found to be significant even with a quite low correlation. For this reason it was decided to analyze the data also using zones comparisons. Then, the Focal20m data was used as input for clustering in Management Zone Analyst 1.0.1 (MZA) (USDA-ARS and University of Missouri, Columbia, MO) (Fridgen et al., 2004) to delineate homogeneous zones of concave and convex areas, and evaluate yield, Tc-Tr and Focal20m values averaged inside each zone. Two performance indices are calculated with the software to determine the number of zones within each field. The Normalized Classification Entropy (NCE) measures the disorganization created by dividing the data into classes. The Fuzziness Performance Index (FPI) is a measure of membership sharing (fuzziness) among classes. The optimum number of zones or classes is when NCE and FPI are minimized.

Spatial Dependence of Crop Canopy Temperature

Tc-Ta in the producer's fields was evaluated using geostatistical analysis basically to determine if the maximum distance between passes was adequate for this experiment, and also an indicator on how far we can sample for Tc-Ta and generate a confident kriged map. The semivariograms to determine the model and range were calculated using GS+ (Gamma Design Software, Plainwell, MI), and the models were adjusted and validated using cross validation.

RESULTS AND DISCUSSION

Comparing Ambient and Sensor Tip Temperatures

In the beginning of this project about on-the-go canopy temperature measurements, it was expected that the temperature measured by the tip of the IRT (Tt) could be used as a substitute of Ta for Tc-Ta calculations, but variations obtained during the course of the day were high compared to Ta (Figures 1, 2, 3 and 4). For the small plots experiment where the collection time varied from 3 to 6 hours, the Tt variation was a big concern. For the producer's fields where the data gathering was done in one or two hours, the Tt also varied. When air temperatures are not available, the adjustment used by Evans et al. (2000) can be used, which entails the regression of temperature against time, subtracting the trend, and adding back the average. For this study to calculate the Ta

diurnal variations for each Tc reading in different positions (to obtain Tc-Ta for each position), we was used an equation regressing the time and the hourly data available from an automated weather station near the sites, using the same method proposed to obtain the corrected Ta. The hourly air temperature information was downloaded from the High Plains Regional Climate Center. For the small plot study hourly temperatures were recorded on site, and for the producer's fields we used the closest weather station. For the producer's sites the diurnal Ta variation was also a concern for corrections, even with collection in 2 hour interval (Figure 2, 3 and 4). For the BR10 field where the measurements were done early evening, the Ta dropped faster than the crop temperature (Figure 2). To be able to compare results from this study with previous studies, we used Ta estimated from the hourly data from weather stations to calculate Tc-Ta.

Another difficulty encountered in the canopy temperature data was the filtering process for outliers caused by several issues, e.g. soil background interference, gaps in the plots and inter-row sensing due to inadequate sensor orientation. These outliers can be observed in Figures 1 to 4. Fortunately, the optical measurements and plant height could be used to help this filtering process. Basically, most of the outliers were filtered using the following criteria: Exclude the temperature data when the reflectance was lower than the value at 15% percentile in the check plot (0 kg N ha^{-1}) ; plant height lower than the smallest plant inside the plot (excluding the buffer), and temperatures with coefficient of variation higher than 200% in each plot.

Small Plots

The 2010 growing season had good early season rainfall delaying the irrigation for the small plot area compared to other years. The canopy measurements started at V7, but the irrigation commenced around V15. Thus only later stages of corn were selected for statistical analysis to study canopy temperature effects. Analysis of variance of canopy temperature showed significant correlations for irrigation level and N rates, but no interaction terms were observed (Table 1). Irigation levels affected the Tc-Ta similarly for both previous crops, and significant differences were observed at R3 and R4 growth stages (Table 2). When soybean was the previous crop, differences in canopy temperature were also observed at R6 (Table 2), perhaps due to higher leaf density in vigorous plants. However, Hatfield (1983) observed in wheat that non-transpiring panicles above the canopy can confound canopy temperature measurements. There are chances in the R6 stage that the tassel or other dry material may have interfered with readings. Analyzing N rates effects on canopy temperature across growth stages and previous crop, there were differences between the check plot (0 kg N ha^{-1}) and the other N rates (Table 3). Carefully attention was given during the filtering process to exclude plot alley ways and extremely low plants using the plant height measured by ultrasonic sensors, but as observed by Moran et al. (1994) and Heilman et al. (1981), soil temperature can still be interfered with canopy temperature with low vegetation cover. During sensing it was observed that the CS had higher plants than CC, but the ANOVA didn't indicate significant differences in canopy temperature between previous crops. The growth stage

R4 was the best stage to sense water stress as shown in Figure 2, with pronounced differences in Tc-Ta between irrigation levels. At this stage the highest N rate had the lowest temperature also for 100 % ET. This experiment showed that differences from 0.5 to 3 ºC can be detected when different irrigation levels were used across previous crop and N rates. Overall the experiment showed that intensive data collection of canopy temperature can be viable to detect small differences in irrigation levels across previous crop and N rates.

On-Farm Research Sites

All producer fields had adequate soil moisture at the time of sensing for the reference strip, as assured by measurements taken with soil moisture sensors (Table 4). Normally, in practical situations the trigger point to start irrigation for corn planted reference is around 85 cB, to have enough time for a safe and complete irrigation event. This moisture threshold will change with soil type, clay content and others soil physical properties, but the soil matric potential at all sites were generally very low, indicating sufficient available soil water content. The highest measurements for the soil moisture sensors in the BR10, HU10 and BL10 fiels were 15, 61 and 32 cB, respectively (Table 4), so enough moisture was observed in all reference strips, either in the low or high elevation areas of the field. Based on these measurements, the calculation of an average reference temperature (Tr) from these strips was a good representation of a non-water limited crop, and the Tc-Tr approach can be used as an indicator of crop water stress for the producer fields. As observed in Chapter 2, local variations can still have effect when a

reference value is adopted for SI, and certainly soil spatial variability can also affect Tc-Tr, but variability in Tr was not evaluated in this study.

On those areas with SI higher than 0.95 we observed considerable zones with low and high Tc-Tr, in this case represented by negative and positive numbers (Figure 6). The white areas in the maps represent NSI and HSI < 0.95, and these were not considered in the analysis to determine zones with water stress, because the canopy temperature can be influenced by N deficient plants. All these producer's sites (BR10, HU10 and BL10) had enough N applied before the sensor measurements were conducted (over 180 kg N ha^{-1}). Analyzing the NonS and S zones, significant grain yield differences were observed between zones in 2 of 3 fields (Table 5). For the BR10 and HU10 sites the differences in grain yield caused by water stress were around 840 kg ha^{-1} on average; but BL10 difference was only 45 kg ha^{-1} and not statistically significant. The Tc-Tr and Tc-Ta also showed significant differences between the zones, indicating that the crop canopy temperature was higher for water-stressed plants, as expected.

Soil fertility between zones were not different, though lower nitrate in the beginning of the season was observed for HU10 and BL10. After starter N fertilizer and N sidedressing it was not a concern for these zones because average SI was higher than 0.96 in all zones (Table 5). Organic matter, pH and P were similar in all fields.

The spatial variability observed in Figure 7 for the BR10 field showed that NSI, HSI, Tc-Tr and grain yield had similar spatial patterns when all data was used. On the East side of the field higher yields were observed and in the Tc-Tr map two different zones of canopy temperatures were noted even with high NSI and HSI. For the HU10 field the spatial patterns were not delineated with as large zones as BR10, but it can be

seem that lower yields were obtained in areas with higher Tc-Tr (Figure 8). In the BL10 field the spatial pattern was similar for NSI, HSI and yield, but for canopy temperature it seems that the visual correlations were low. In general the procedure proposed to delineate zones of water stress could identify zones in the producer's field where water stress can still be a yield limiting factor even with irrigation.

Correlations between Canopy Temperature, Topographic Features and Soil Attributes

Inside the zones where NSI and HSI were higher than 0.95, water stress played a major role, because low correlations between plant height (HSI), plant N status (NSI) and canopy temperature (Tc-Tr) were found, indicating that the canopy temperature had more influence from water stress than vegetation cover (Table 7, 9 and 11). Negative correlations between NSI, HSI and Tc-Tr were observed, indicating that taller plants with adequate N nutrition can have lower temperatures, though Moran et al., (1994) showed that vegetation indices can be negatively correlated with canopy temperature, because the soil background can influence canopy temperature measurements.

In the BR10 field (sandy site) moderate correlations between yield and NSI were noted (r=0.61), indicating that even in zones with SI > 0.95, N nutrition was important to achieve higher yields (Table 6 and Figure 10). Generally the spatial patterns showed in Figure 10, indicated that elevation, EC shallow and OM were high correlated, but Table 7 also showed correlations of concave and convex areas with grain yield (r=-0.579), where lower yield was observed in convex zones.

At the HU10 and BL10 fields there were low correlations between N status and plant height with yield, indicating again that water stress was the major yield limiting factor on those zones used to study the water stress effect measured by IRTs (Table 7). For BR10 field the visual correlation of the procedure to determine concave and convex areas (Focal 20 m) had high correlation with EC shallow, but the Spearman rank correlation was non-significant (Table 9). Grain yield was negatively correlated with RTK elevation, with the same trend for BR10. For the BL10 field elevation was positively correlated with yield and EC shallow (r = 0.22 and 0.20). Generally canopy temperature was not correlated with yield or NSI on those fields, indicating that the water stress measured by IRT integrated with the plant N status and height can be a good approach to isolate water effects on the corn canopy.

In 2 of 3 fields (BR10 and HU10) the concave and lower elevation areas had higher yields compared to convex and higher elevation areas. These fields also had higher Tc-Tr at high elevation zones where the OM was lower.

In general, soil fertility (pH, P, NO_3, OM) was not correlated with yield as expected, since nutrients were supplied in adequate amounts for the crop (Table 5).

The entire dataset for the three producer fields were analyzed using MZA, clustering zones of Focal20m to compare topographical features (concave or convex areas) in terms of grain yield and canopy temperature. MZA indicated an optimum number of zones as 3 for all sites, minimizing the NCE and FPI (Fridgen et al., 2004). As observed in Figure 13, the lower the Focal20m (concave areas) and Tc-Tr, the higher the yield for all fields. This is a strong indicator that the procedure for zone delineation (Focal20m) in concave and convex areas can be a good tool for delineation of zones to be

considered in variable rate irrigation systems. These zones are spatial and temporally stable and likely will behave similarly in terms of water demand and consequently canopy temperature. Zone 1 was the lowest yielding zone across fields, with yields around 7000, 12500 and 9000 kg ha^{-1} for BR10, HU10 and BL, respectively, and zone 3 had the highest yields (Figure 13). Zones 1 and 3 had a difference of 4000 kg ha^{-1} for the BR10 field and 1000 kg ha^{-1} for the BL10 field, indicating that the zones were very different in terms of yield and canopy temperature. At all sites even including the areas with NSI and HSI < 0.95, the zones (which can introduce a bias in the interpretation of canopy temperature as a water stress indicator, because N is the main factor) lower yields were found when the canopy temperature was higher compared to the reference and that concave areas were beneficial in all fields (Figure 14, 15 and 16). This finding confirms that the Focal20m could be a good approach to refine irrigation optimizing the use of water and could be an important layer to use with optical and ultrasonic sensors for site-specific N management to discriminate water effects from plant N demand.

Spatial Dependence of Crop Canopy Temperature

The spatial dependence of canopy temperature determined by semivariogram analysis was over 65 meters across farmer sites, with varying ranges of 65, 80 and 210 meters for HU10, BL10 and BR10, respectively, showing that commercial high clearance applicator's swath width was detailed enough to obtain accurate kriged maps during canopy temperature mapping (Figure 17). The resultant maps showed consistent spatial patterns (Figures 7, 8 and 9) compared to other measurements made for NSI, HSI and

yield. For the BR10 field, the model had very low semivariance at small distances indicating that the canopy temperature in this field had low variability at small scales, different from the other sites where the semivariance was much higher (higher intercept) at small distances. These effects can be observed in the cross validation where BR10 had the best prediction model with low standard error (SE) and higher r^2. Even with a higher intercept for the HU10 and BL10 sites, the maps represent well the spatial variability of Tc-Ta. For both sites, the model used for interpolation underestimated canopy temperature, showing that for several estimated points the actual canopy temperature was much higher, almost double (Figure 18 and 19). These high temperatures could be error during mapping where the sensors "see" the inter-row or deficient plant stand with long gaps between plants, as observed on those fields. Maybe increasing the IRT field of view angle from nadir to slightly oblique can ameliorate these interferences, but also acute angles can introduce differences of 3 to 5ºC into canopy temperature measurements (Paw E et al., 1989).

SUMMARY AND CONCLUSIONS

In this chapter we evaluated the use of on-the-go canopy temperature measured by infrared sensors integrated with plant N status measured with optical sensors and plant height measured with ultrasonic sensors for crop water status assessment. In the small plot experiment the effect of different irrigation levels, previous crop and N rates were evaluated on canopy temperatures. We found that canopy temperature was influenced by irrigation level and N rate. Small differences between 70 and 100% irrigation levels could

be detected using IRTs and small plants with lower N supply had the highest canopy temperatures. On-farm research plots were mapped and the procedure proposed (using optical and ultrasonic sensors, the criteria of NSI and HSI > 0.95 as a filter for IRT evaluation of water stress) could identify zones in the field where water stress was the major yield-limiting factor, showing differences of about 840 kg ha^{-1} due to water deficit even with irrigation. Correlations between plant, soil, topographical features and canopy temperature in zones where water was the major yield-limiting factor indicated that canopy temperature was important to delineate zones prone to water stress, but plant N status still affected grain yield simultaneously. The delineation of zones using the Focal20m procedure could identify great differences in yield, and showed that concave areas had cooler plants. It is likely that measurements taken with the IRT used in this study can be used in commercial high clearance machines to map canopy temperature. The integration of plant N status, plant height and canopy temperature was beneficial to detect water stressed zones in the field, affecting yield and possibly promising to delineate stable zones for variable rate irrigation. Opportunities can be foreseen also for on-the-go N fertilization using integration of sensors because is likely that water stress can be confounded with N supply during the growing season and in different zones of the field. More studies should be done to investigate the integration of these sensors with detailed topography to fine tune in-season N variable rate fertilization.

REFERENCES

Aston, A.R., Van Bavel, C.H.M. 1972. Soil surface water depletion and leaf temperature. AgronJ. 64(3): 368-373

Clay, D.E., Kim, K.-I., Chang, J., Clay, S.A., Dalsted, K. 2006. Characterizing Water and Nitrogen Stress in Corn Using Remote Sensing. Agron. J. 98: 579-587.

Fuchs, M., Tanner, C.B., 1966. Infrared thermometry of vegetation. Agronomy J. 58, 597–601.

Fridgen, J.J., N.R. Kitchen, K.A. Sudduth, S.T. Drummond, W.J. Wiebold, C.W. Fraisse. 2004. Management zone analyst (MZA): Software for subfield management zone delineation. Agron. J. 96:100–108.

González-Dugo, M.P., Moran, M.S., Mateos, L., Bryant, R. 2006. Canopy temperature variability as an indicator of crop water stress severity. Irrigation Science 24, 233-240.

Hatfield, J.L. 1983. Remote sensing estimators of potential and actual crop yield. Remote Sens. Environ. 13:301–311.

Hatfield, J.L., Gitelson, A.A., Schepers, J.S., Walthall, C.L. 2008. Application of Spectral Remote Sensing for Agronomic Decisions. Agron. J. 100, 117-131.

Heilman, J.L., W.E. Heilman, and D.G. Moore. 1981. Remote sensing of canopy temperature at incomplete cover. Agron. J. 73:403–406.

Howell, T.A., Hatfield, J.L., Yamada, H., Davis, K.R. 1984. Evaluation of Cotton Canopy Temperature to Detect Crop Water Stress. Transactions Of The Asabe 27: 5-9.

Idso, S.B., Jackson, R.D., Reginato, R.J. 1978. Remote sensing for agricultural water management and crop yield prediction. 299-310.

Idso, S.B. 1982. Non-water-stressed baselines: a key to measuring and interpreting plant water stress. Agricultural Meteorology. 27: 59-70.

Idso, S.B., Jackson, R.D., Reginato, R.J. 1978. Extending the "Degree Day " Concept of Plant Phenological Development to Include Water Stress Effects. Ecology 59, 431-433.

Jackson, R.D., Reginato, R.J., Idso, S.B. 1977. Wheat canopy temperature: a practical tool for evaluating water requirements, Water Resource Research. 13: 651-656.

Jackson, R.D., Idso, S.B., Reginato, R.J., Pinter, P.J. 1981. Canopy temperature as a crop water stress indicator. Water Resources Research 17, 1133-1138.

Kitchen, N.R., Drummond, R.D., Lund, E.D., Sudduth, K.A., Buchleiter, G.W. 2010. Ground-Based Canopy Reflectance Sensing for Variable-Rate Nitrogen Corn Fertilization. Agron. J. 102, 71: 483-495.

Moran, M.S., Clarke, T.R., Inoue, Y., Vidal, A. 1994. Estimating Crop Water Deficit Using the Relation between Surface-Air Temperature and Spectral Vegetation Index. Remote Sensing of Environment 246-263.

O'Saughnessy, S., Evett, S., Howell, T. 2011. Irrigation management with infrared thermometry. Resource September/October, p. 15.

O'Shaughnessy, S., Hebel, M.A., Evett, S.R., Colaizzzi, P.D. Evaluation of a wireless infrared thermometer with a narrow field of view. 2010. Computers and Electronics in Agriculture 76:59-68.

Paw U, K.T., Ustin, S.L., Zhang, C.A. 1989. Anisotropy of thermal infrared exitance in sunflower canopies. Agric. Forest Meteorol. 48:45–58.

Raun, W. et al. Optical Sensor-Based Algorithm for Crop Nitrogen Fertilization. 2005. Communications in Soil Science and Plant Analysis 36, 2759-2781.

Sammis, T.W., Smeal, D., Williams, S. 1988. Predicting Corn yield under limited irrigation using plant height. Transactions Of The Asabe 31: 830-838.

Sadler, E.J., Camp, C.R., Evans, D.E., Millen, J.A. 2002. Corn canopy temperatures measured with a moving infrared thermometer array. Transactions of the ASAE, 45: 581-591.

Sepulcre-Cantó, G., Zarco-Tejada, P.J., Jiménez-Muñoz, J.C., Sobrino, J.A., Miguel, E. De, Villalobos, F.J. 2006. Detection of water stress in an olive orchard with thermal remote sensing imagery. Agricultural and Forest Meteorology 136, 31-44.

Schmidt, J.P., Dellinger, A.E., Beegle, D.B. 2009. Nitrogen Recommendations for Corn: An On-The-Go Sensor Compared with Current Recommendation Methods. Agron. J. 101, 916-924.

Solari, F., Shanahan, J.F., Ferguson, R.B. & Adamchuk, V.I. 2010. An Active Sensor Algorithm for Corn Nitrogen Recommendations Based on a Chlorophyll Meter Algorithm. Agronomy Journal 102: 1090-1098.

Stone, M.L., Solie, J.B., Raun, W.R., Whitney, R.W., Taylor, S.L., Ringer, J.D. 1996. Use of spectral rediance for correcting in-season fertilizer nitrogen deficiencies in winter wheat. Transactions of the ASABE. 39:1623-1631.

Sui, R. and Thomasson, J.A. 2006. Ground-based sensing system for cotton nitrogen status determination. Transactions Of The Asabe 49: 1983-1991.

Tubana, B.S., Arnall, D. B., Walsh, O., Chung, B., Solie, J. B., Girma, K., Raun, W. R. 2008. Adjusting Midseason Nitrogen Rate Using a Sensor-Based Optimization Algorithm to Increase Use Efficiency in Corn. Journal of Plant Nutrition 31: 1393-1419.

Varvel, G.E., Wilhelm, W.W., Shanahan, J.F., Schepers, J.S. 2007. An Algorithm for Corn Nitrogen Recommendations Using a Chlorophyll Meter Based Sufficiency Index. Agronomy Journal 99, 701-706.

Zhu, J., Tremblay, N., Liang, Y. 2011. Corn Nitrogen Status Indicator Less Affected by Soil Water Content. Agron. J. 103, 890.

Zillmann, E., Graeff, S., Link, J., Batchelor, W.D., Claupein, W. 2006. Assessment of Cereal Nitrogen Requirements Derived by Optical On-the-Go Sensors on Heterogeneous Soils. Agron. J. 98: 682-690.

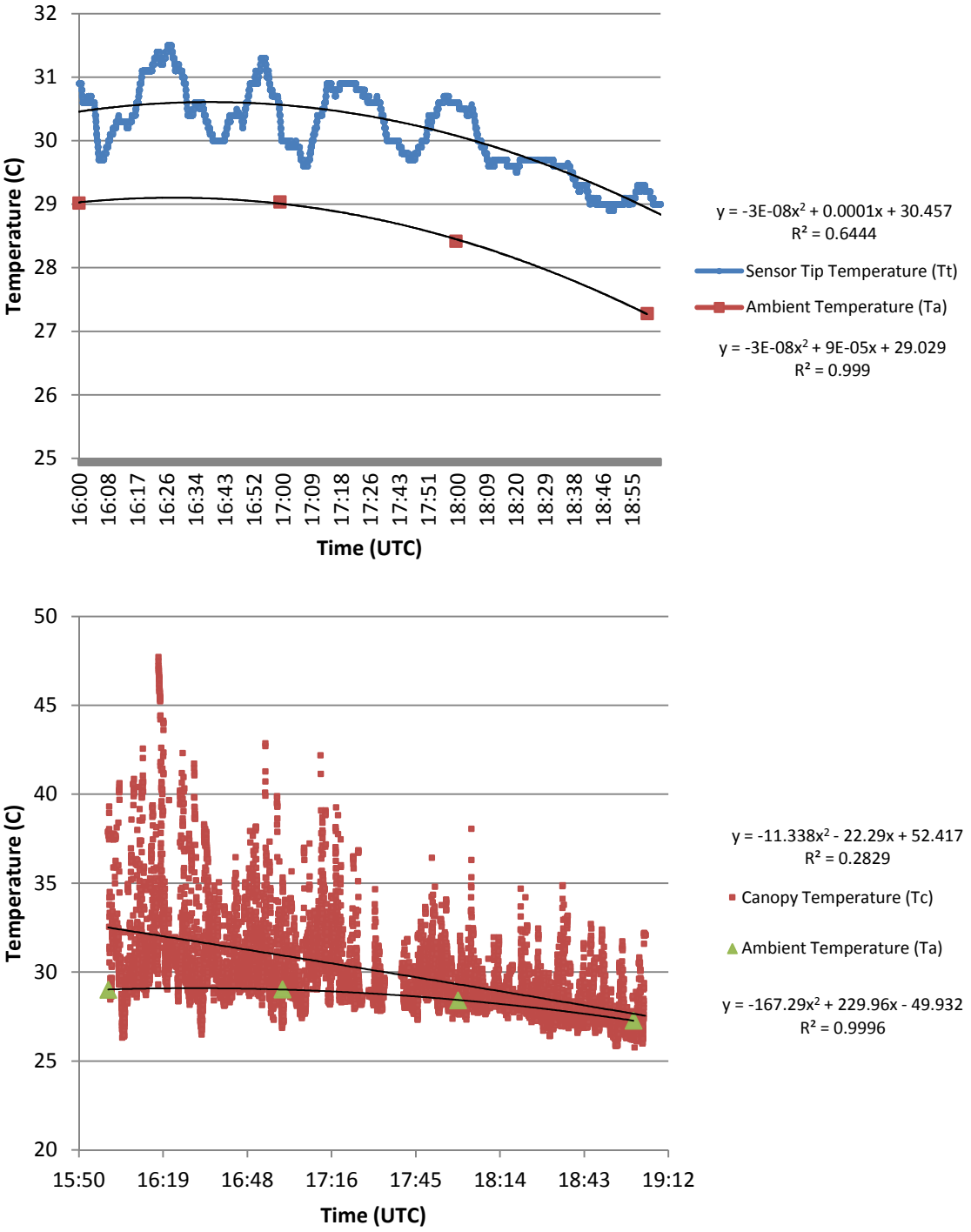

Figure 1. Diurnal temperature variations in the IRT sensor tip (Tt) and ambient temperature (Ta) for the small plots area. Ta was acquired using the onsite automated weather station at the MS field in July1st, 2010.

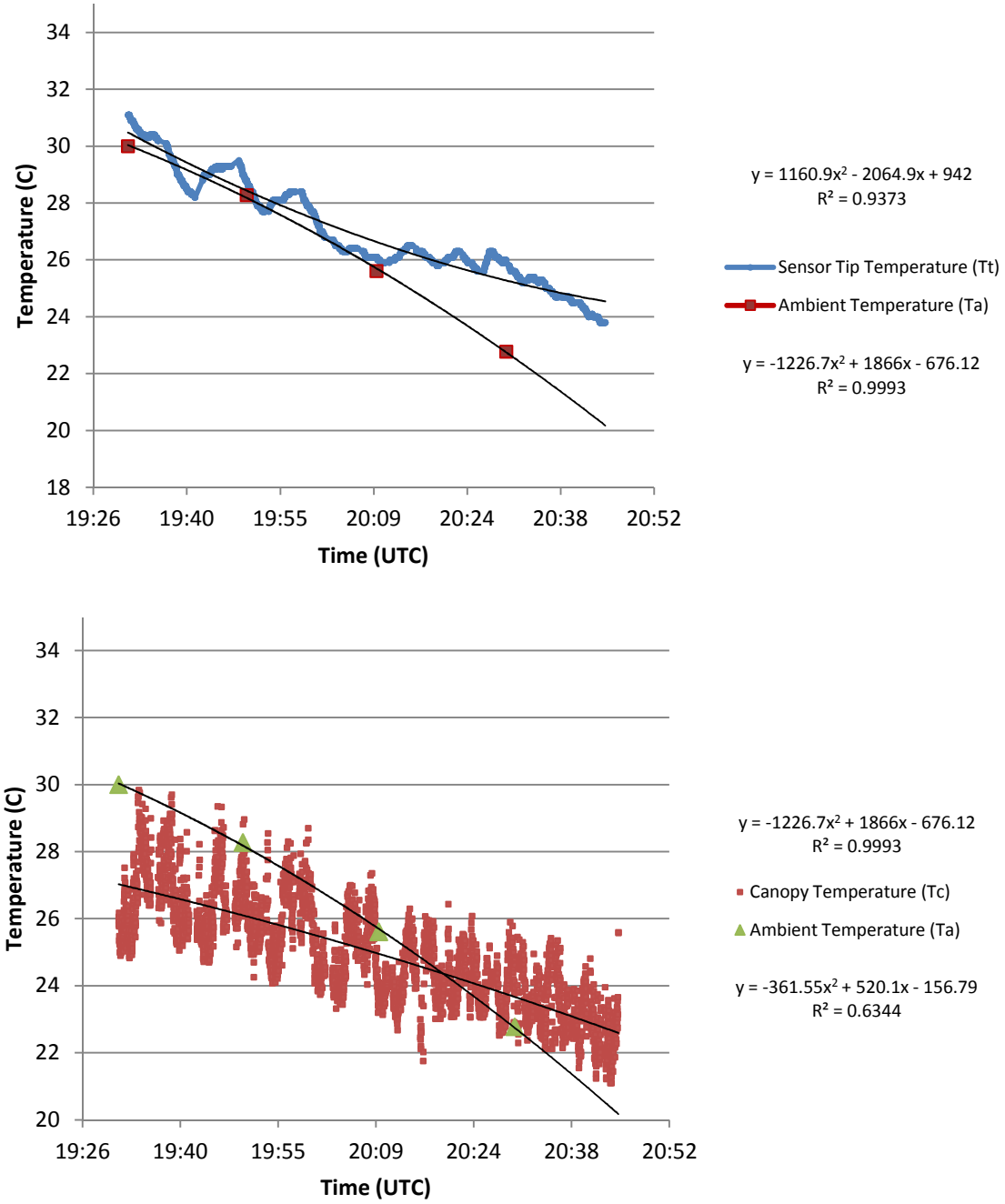

Figure 2. Temperature variations in the IRT sensor tip (Tt), canopy (Tc) and ambient (Ta) for the BR10 field. Ta from High Plains Regional Climate Center in June 28th, 2010.

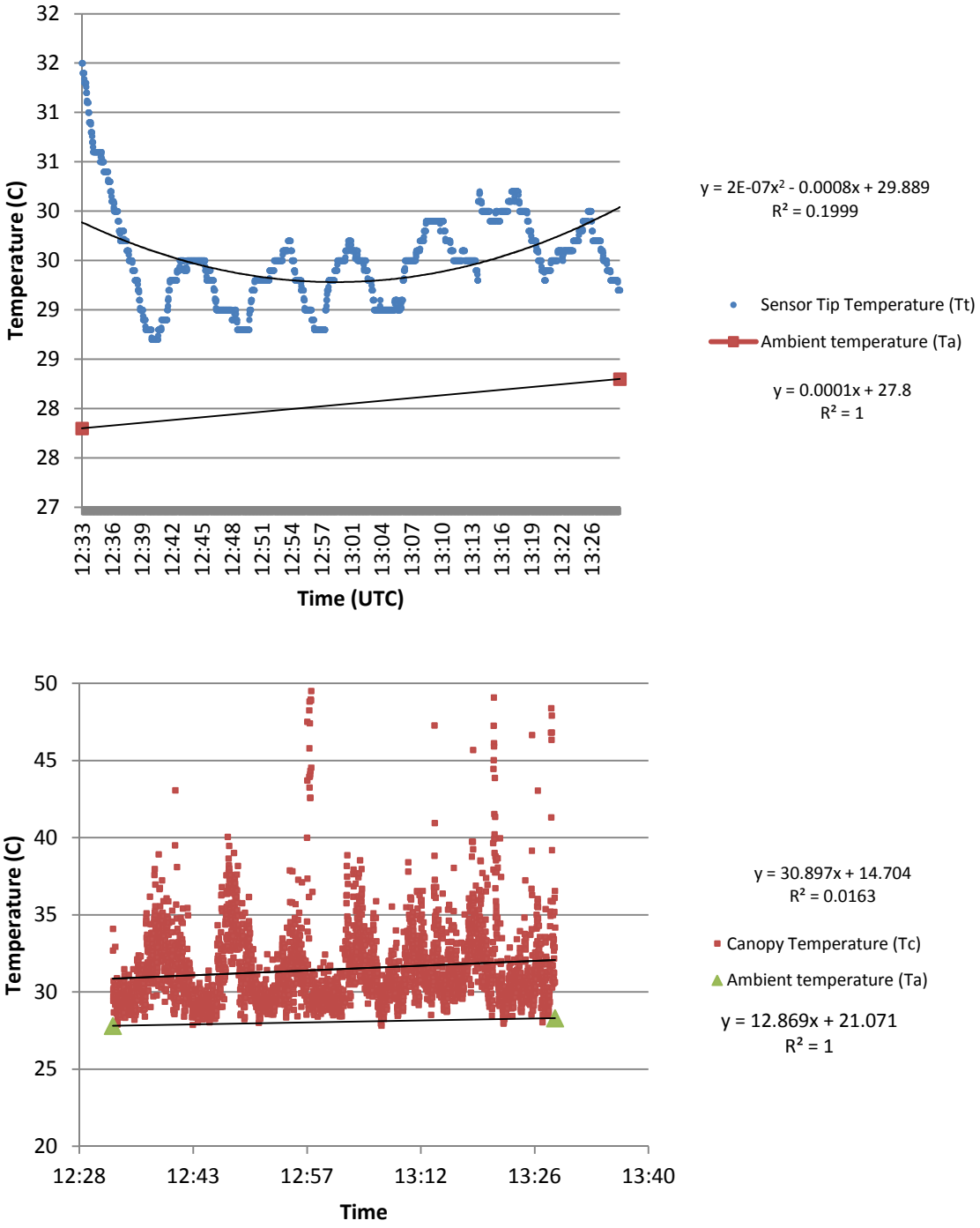

Figure 3. Temperature variations in the IRT sensor tip (Tt), canopy (Tc) and ambient (Ta) for the HU10 field. Ta from High Plains Regional Climate Center in June 30th, 2010.

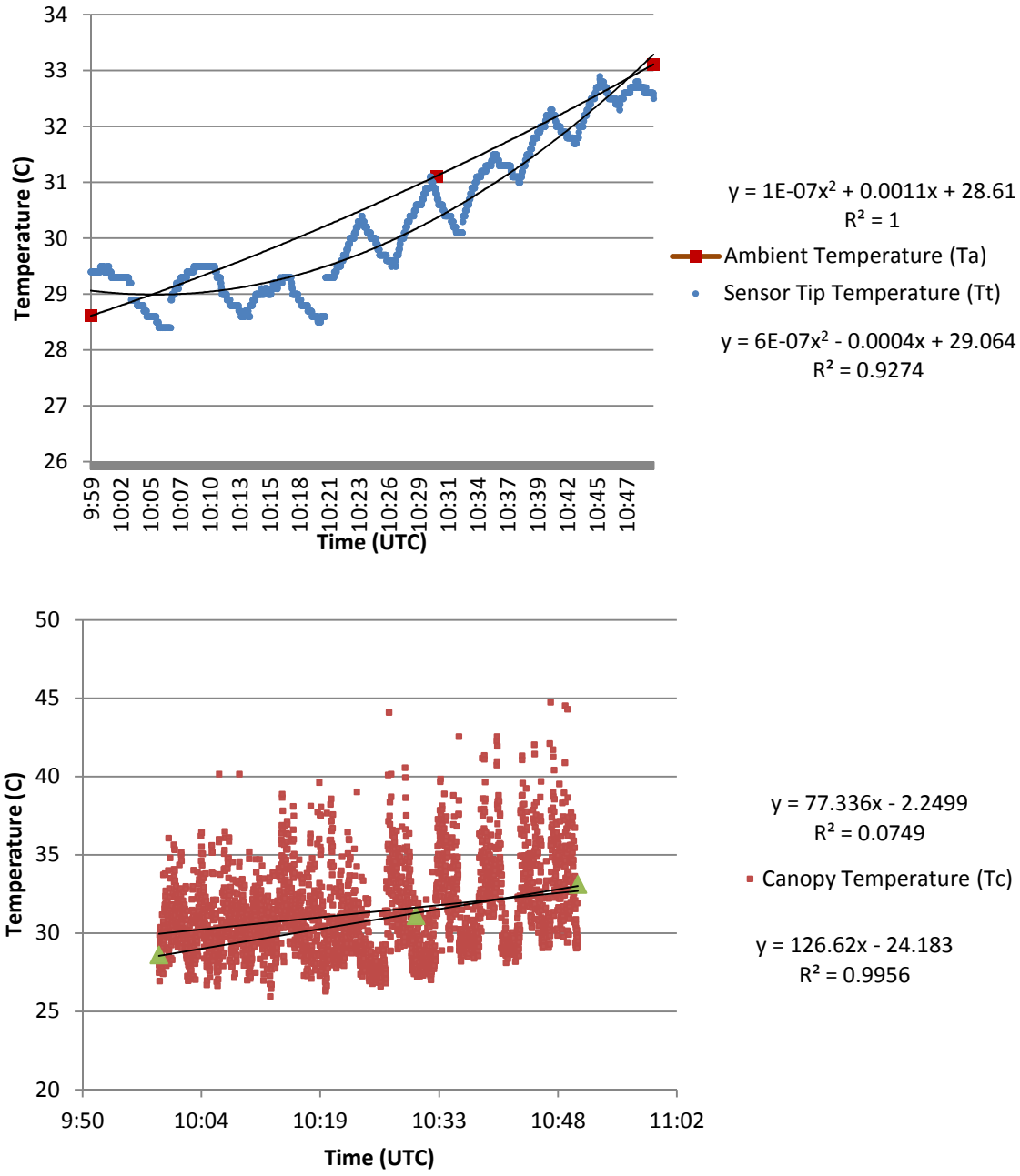

Figure 4. Diurnal temperature variations in the IRT sensor tip (Tt) and ambient temperature (Ta) for the BL10 site. Ta from High Plains Regional Climate Center in July 13th, 2010.

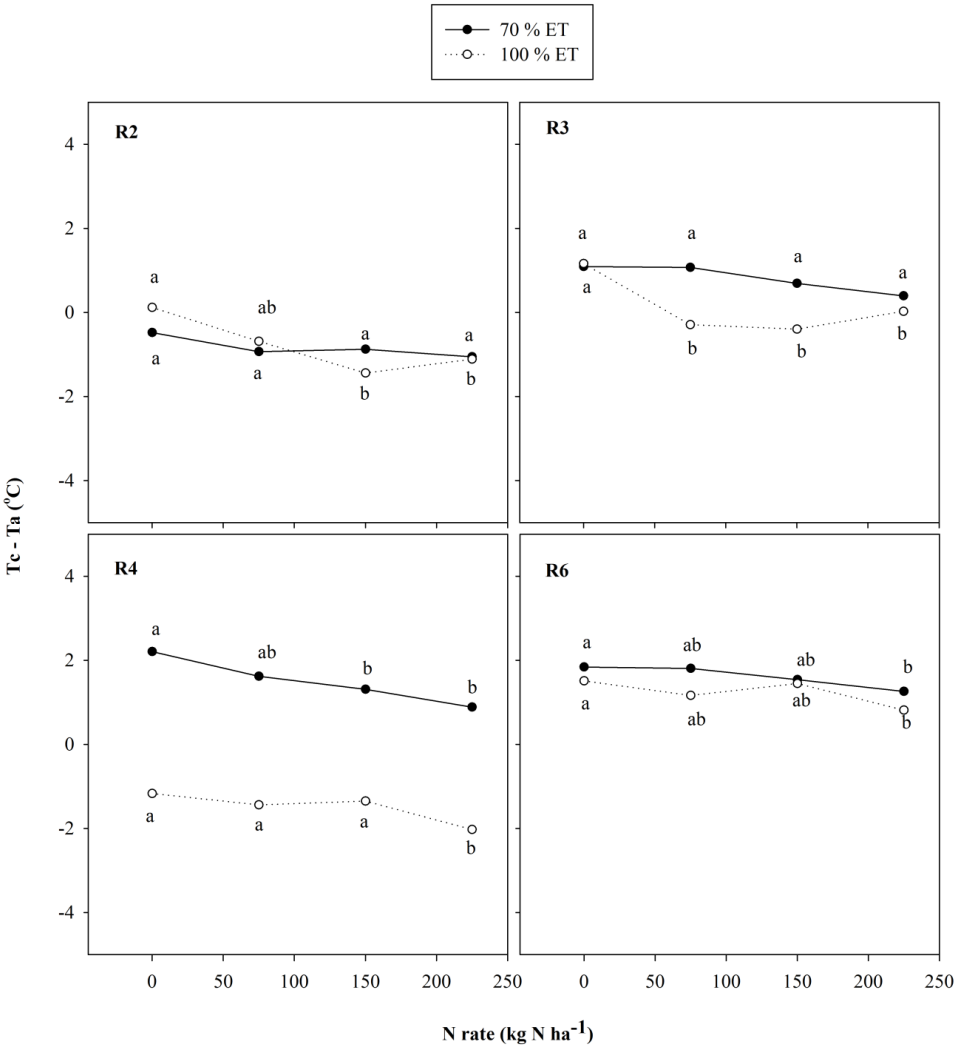

Figure 5. Effects of N rates on Tc-Ta under different irrigation levels and growth stages (R2 – R6) for MS site.

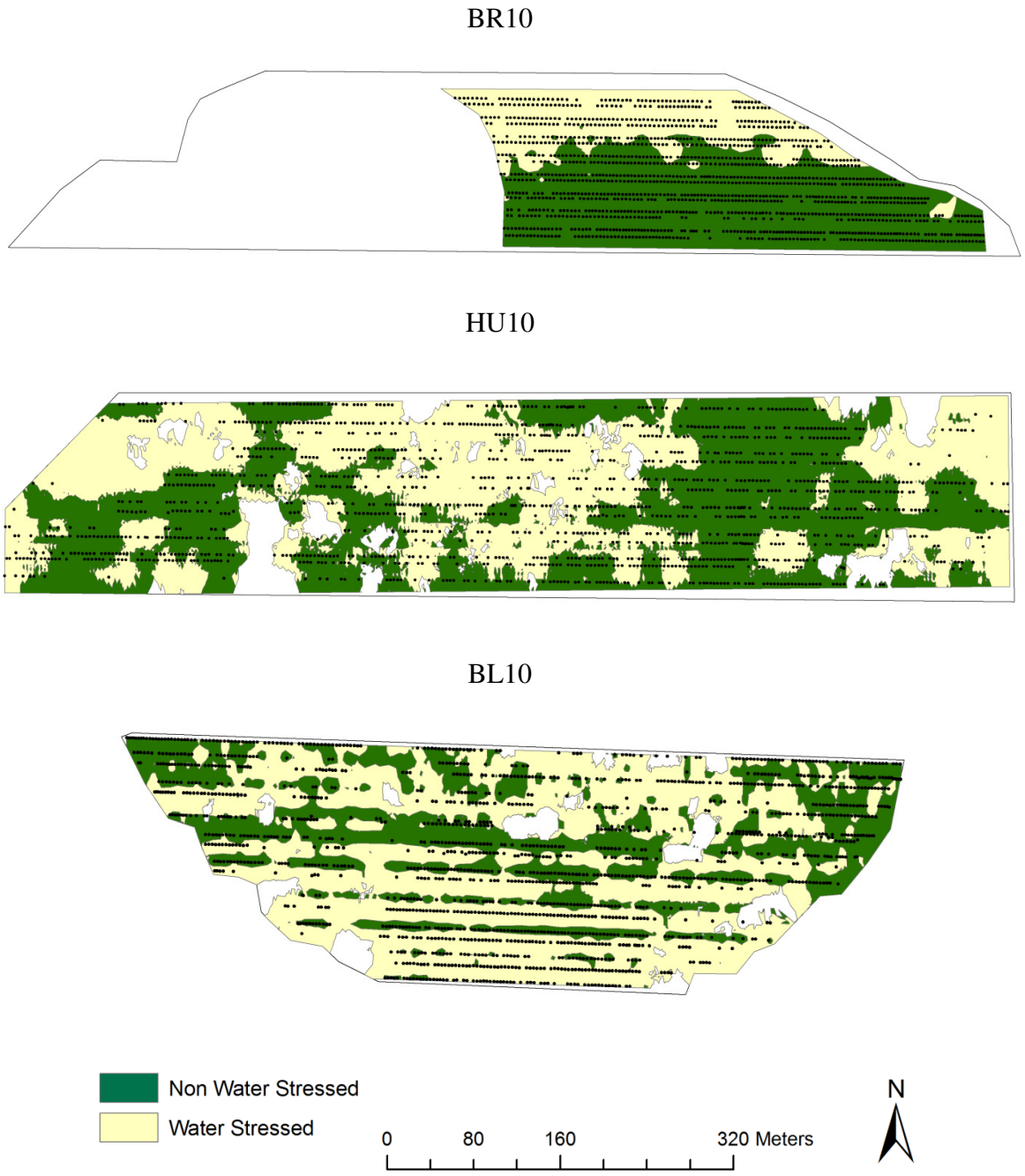

Figure 6. Zones delineated indicating water status based on the procedure proposed. Inside the zones where NSI and HSI > 0.95 the Tc-Tr > 0 represent water-stressed zone and Tc-Tr < 0 non water-stressed zone.

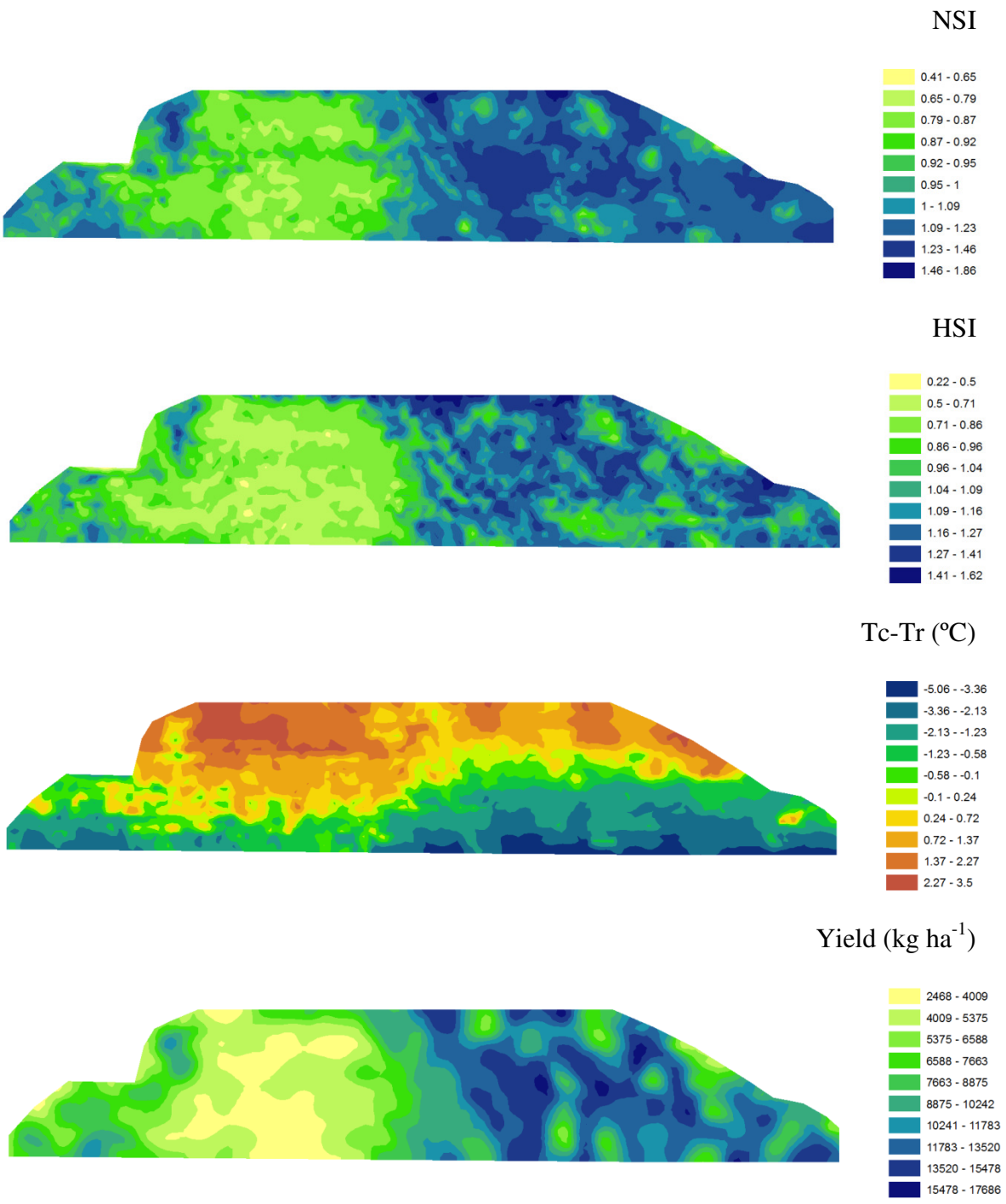

Figure 7. Interpolated maps of NSI, HSI, Tc-Tr and yield for the BR10 field.

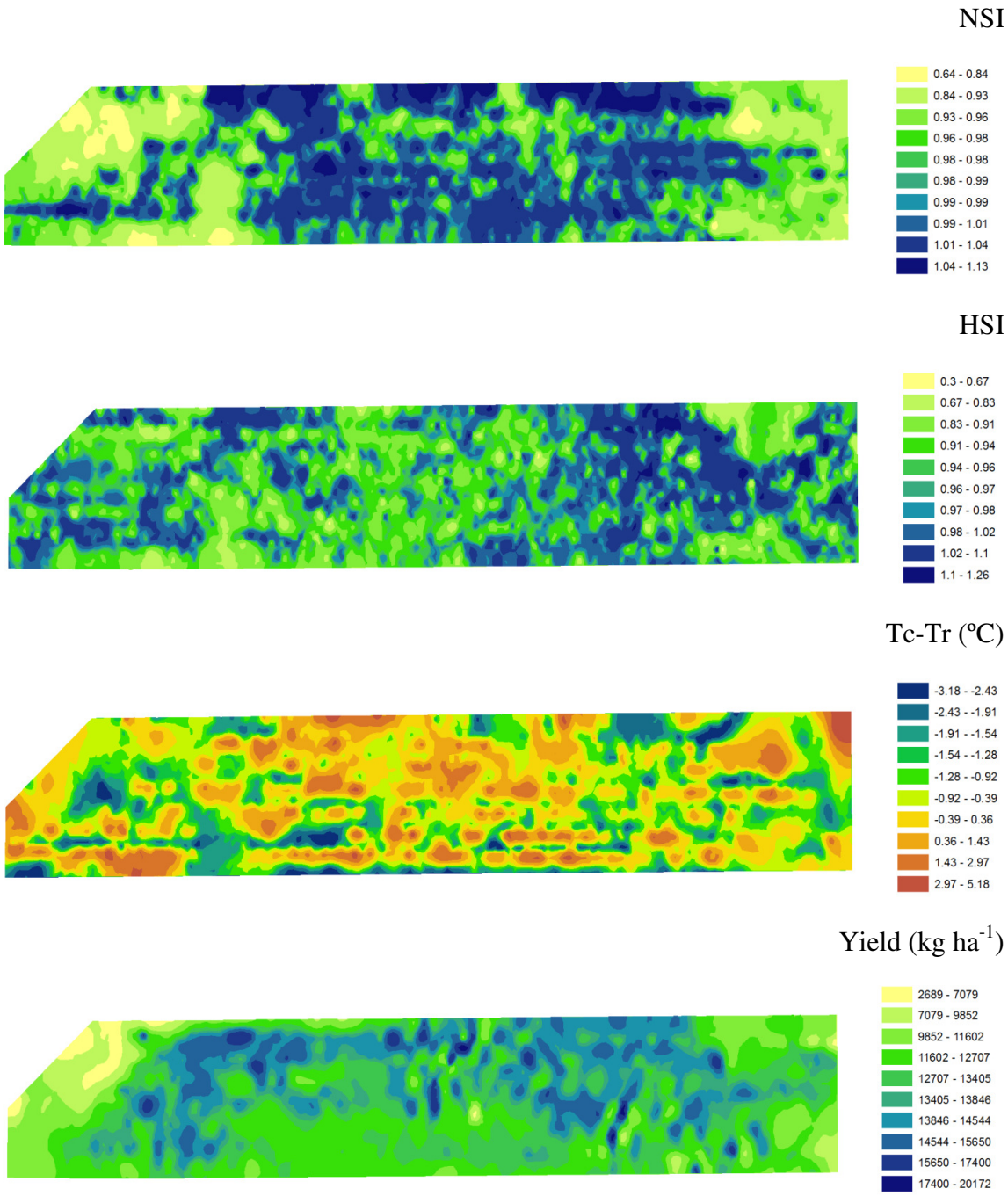

Figure 8. Interpolated maps of NSI, HSI, Tc-Tr and yield for the HU10 field.

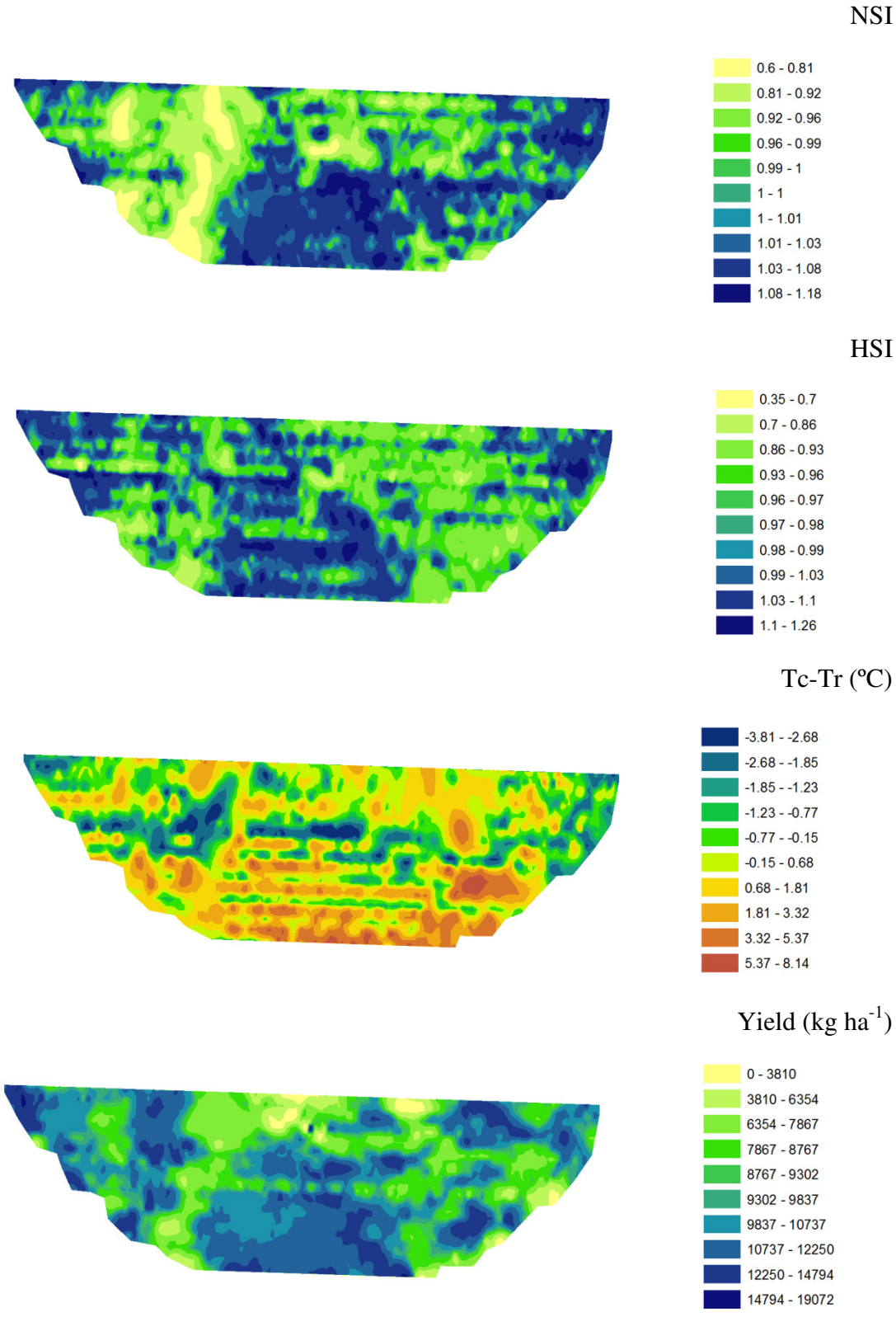

Figure 9. Interpolated maps of NSI, HSI, Tc-Tr and yield for the BL10 field.

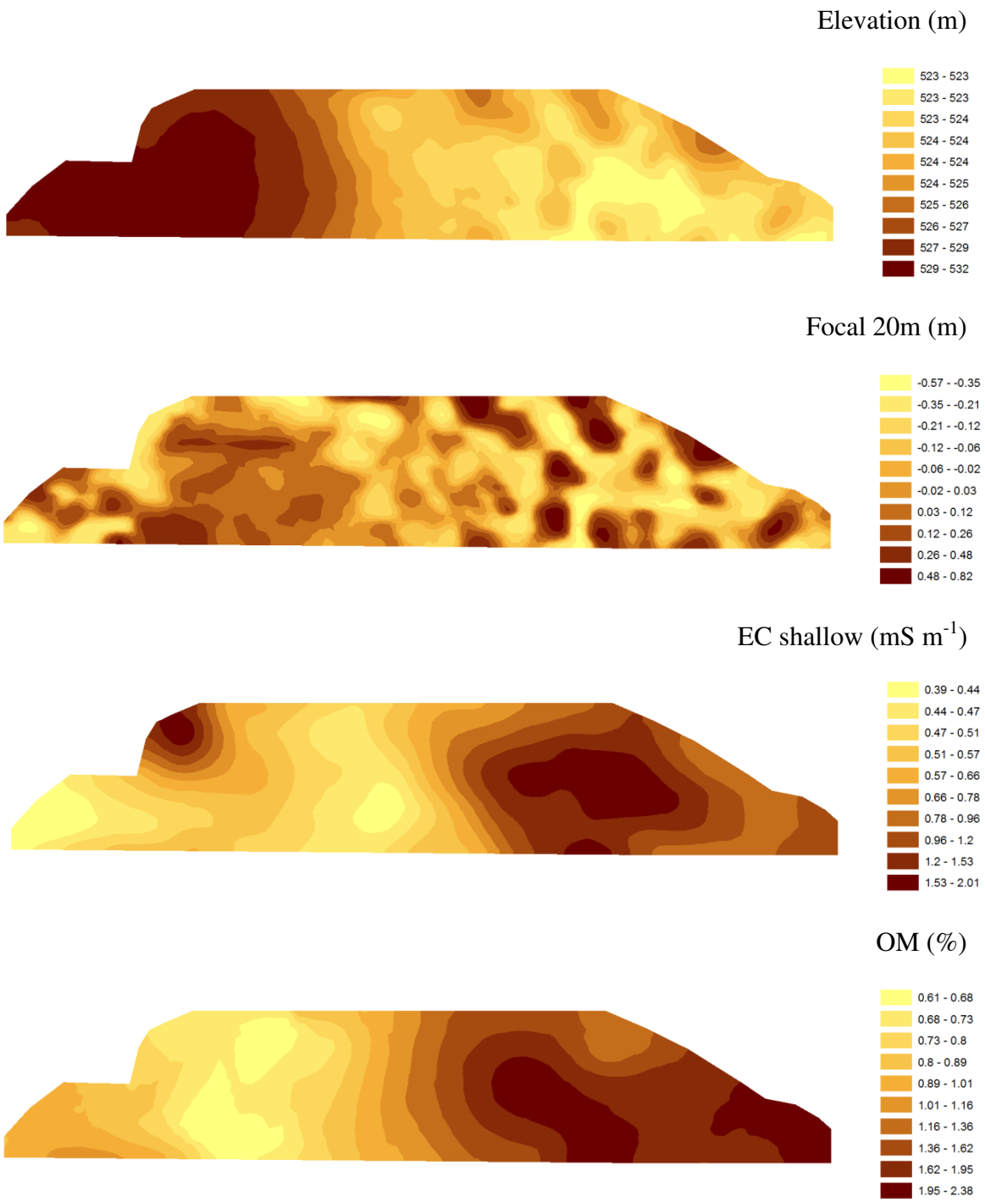

Figure 10. Soil attributes and topographical features for the BR10 field.

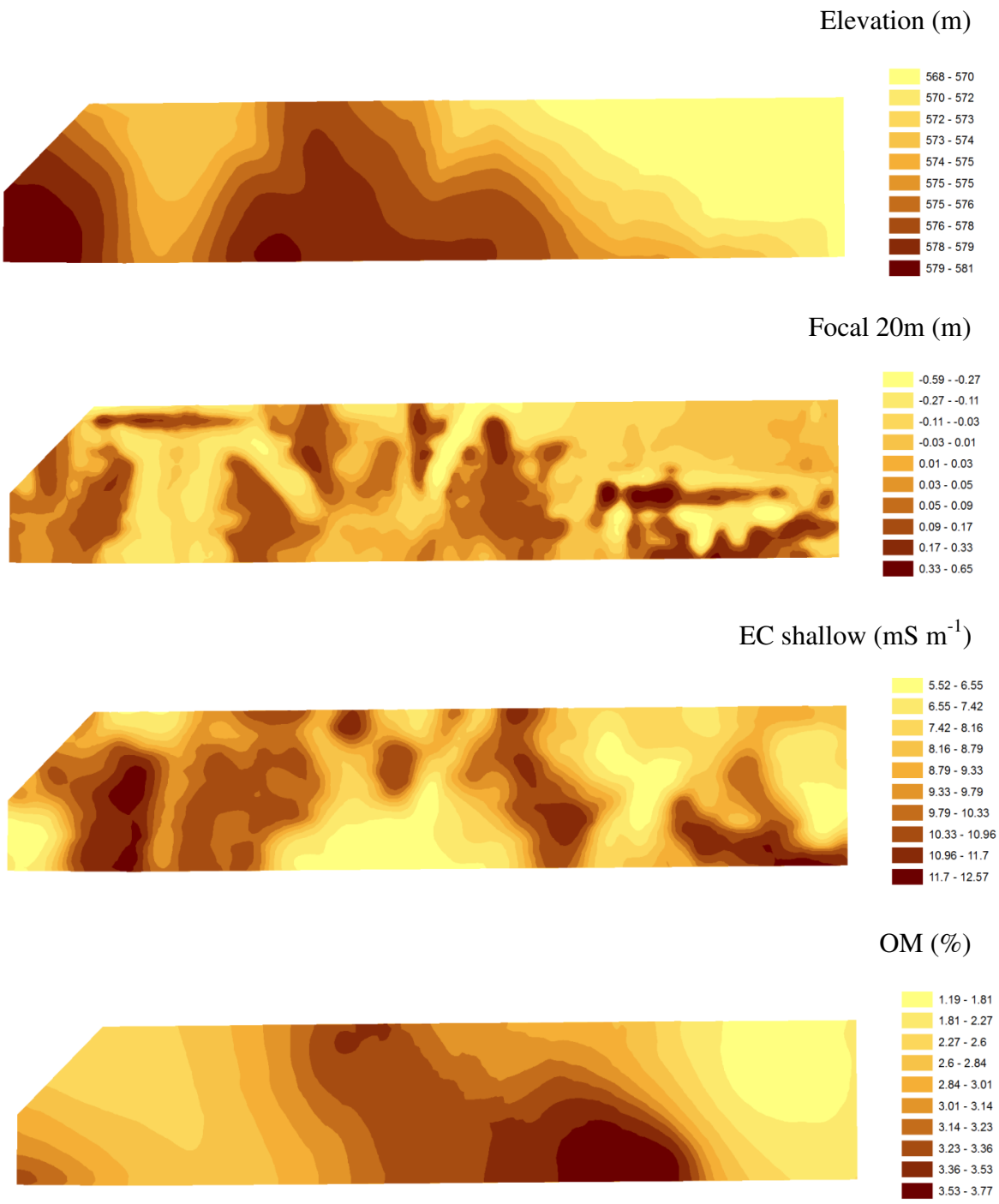

Figure 11. Soil attributes and topographical features for the HU10 field.

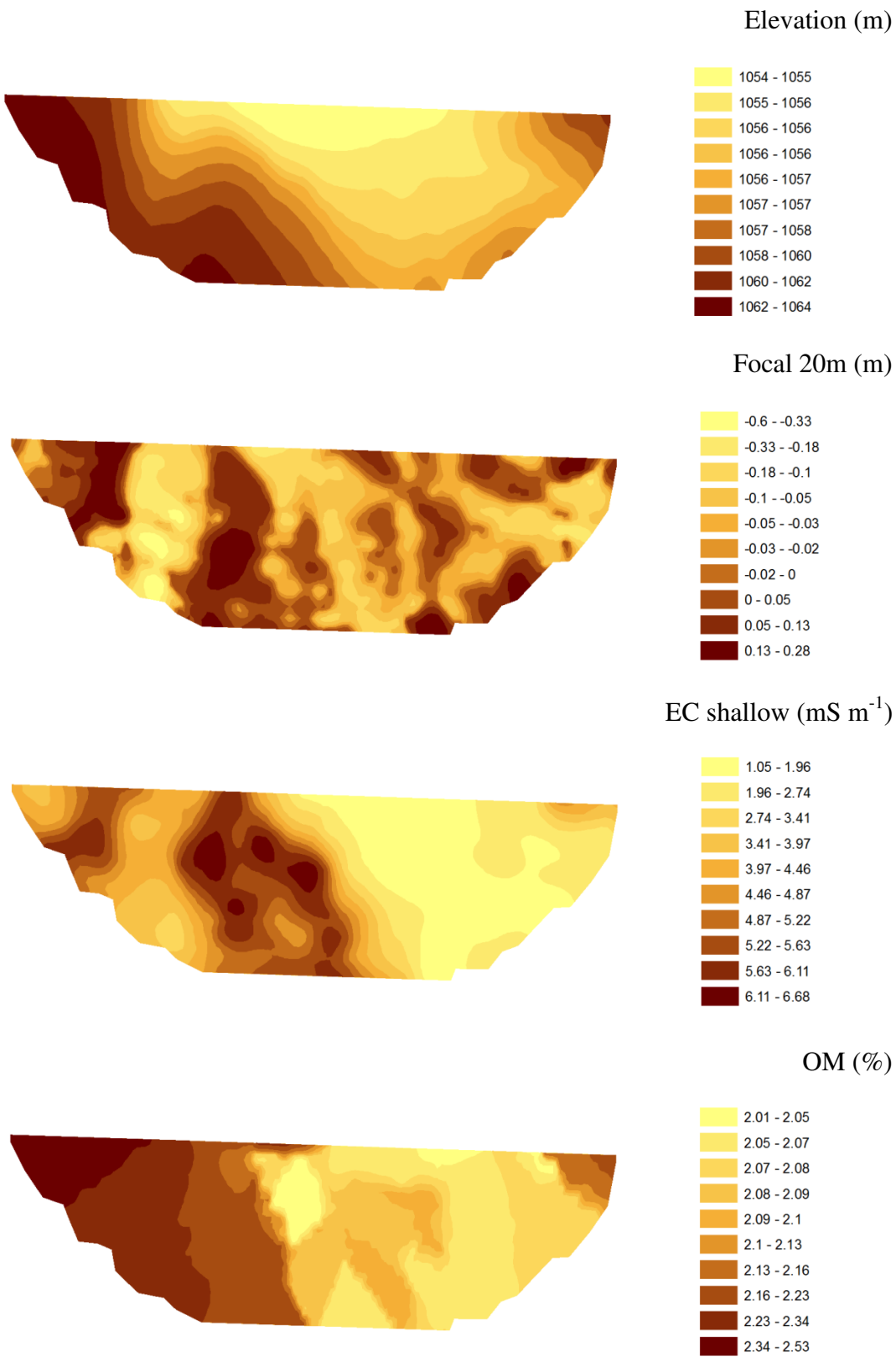

Figure 12. Soil attributes and topographical features for the BL10 field.

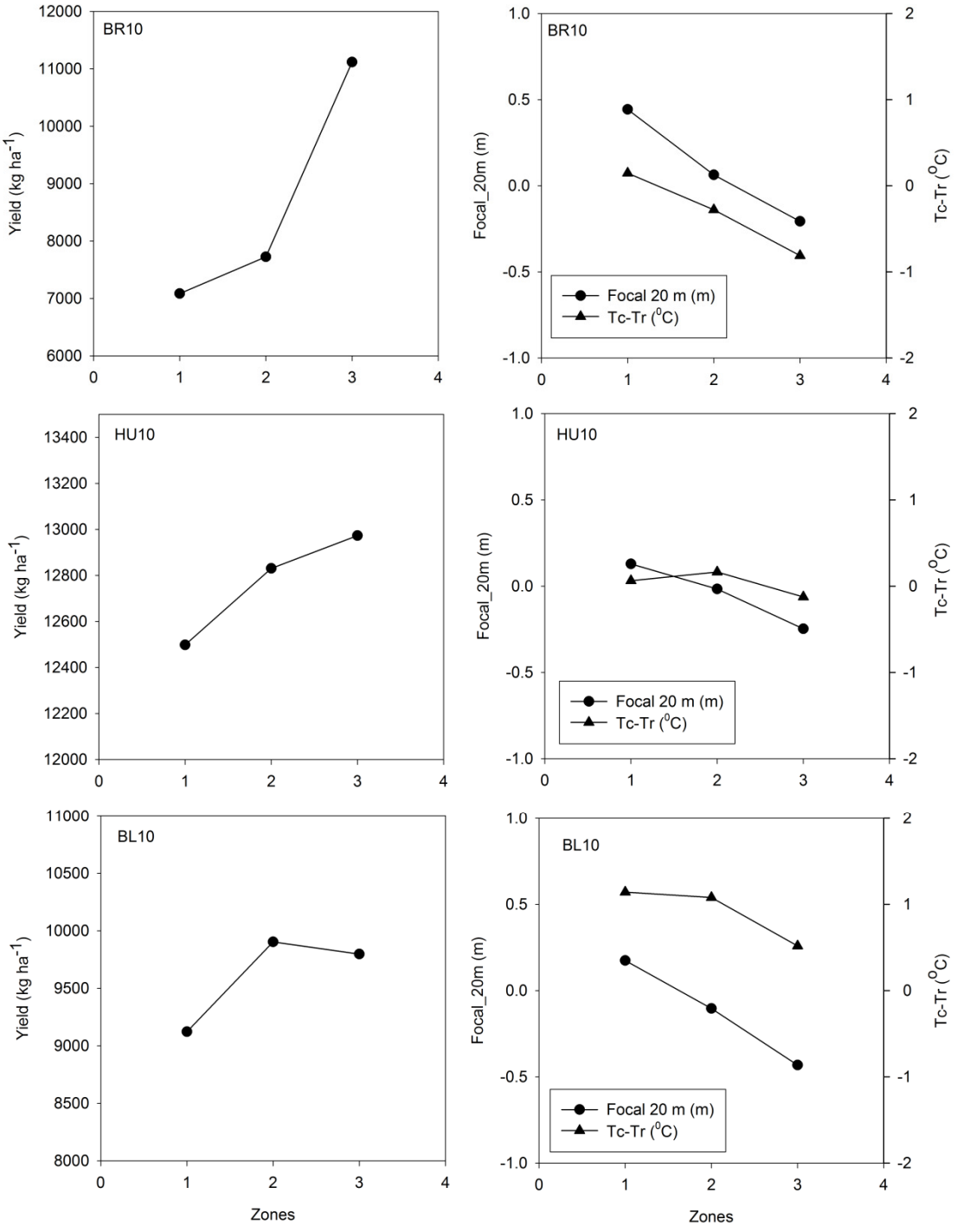

Figure 13. Grain yield, Focal 20 m and Tc-Tr average inside each zone delineated with Focal20m that represents concave and convex areas in the field.

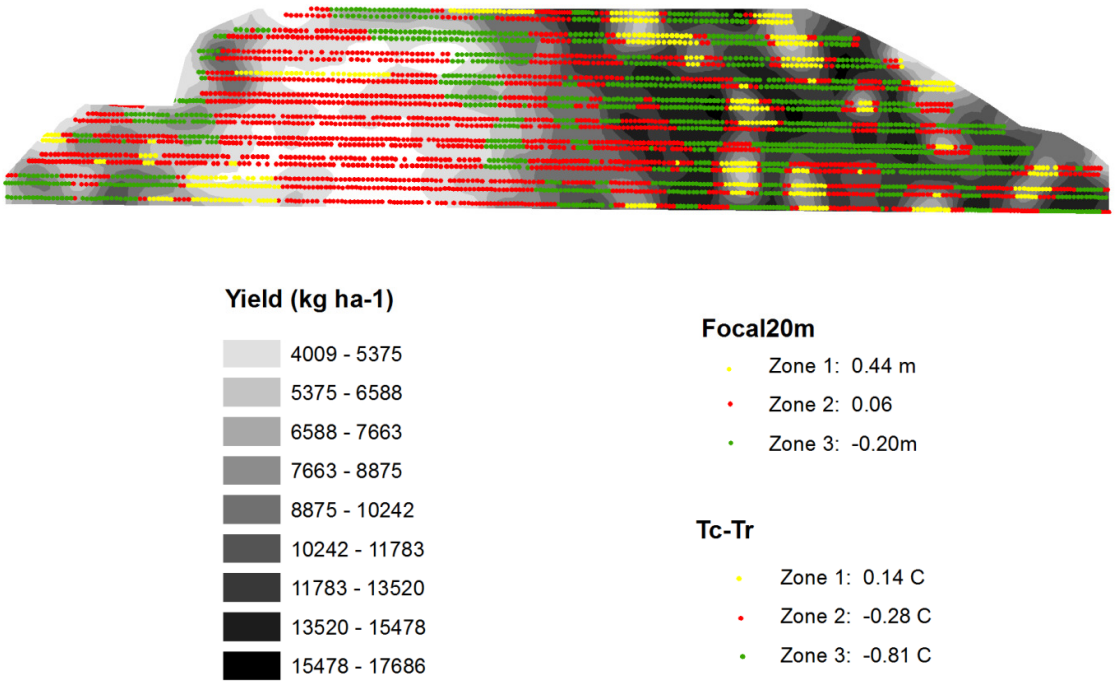

Figure 14. Average of Tc-Tr (ºC) and concave and convex areas in each zone delineated by Focal20m, overlaying yield map (kg ha^{-1}) for the BR10 field. Zones 1,2 and 3 were classified in three zones of different Focal20m values using MZA. For each zone was calculated the average value of Focal 20m and Tc-Tr.

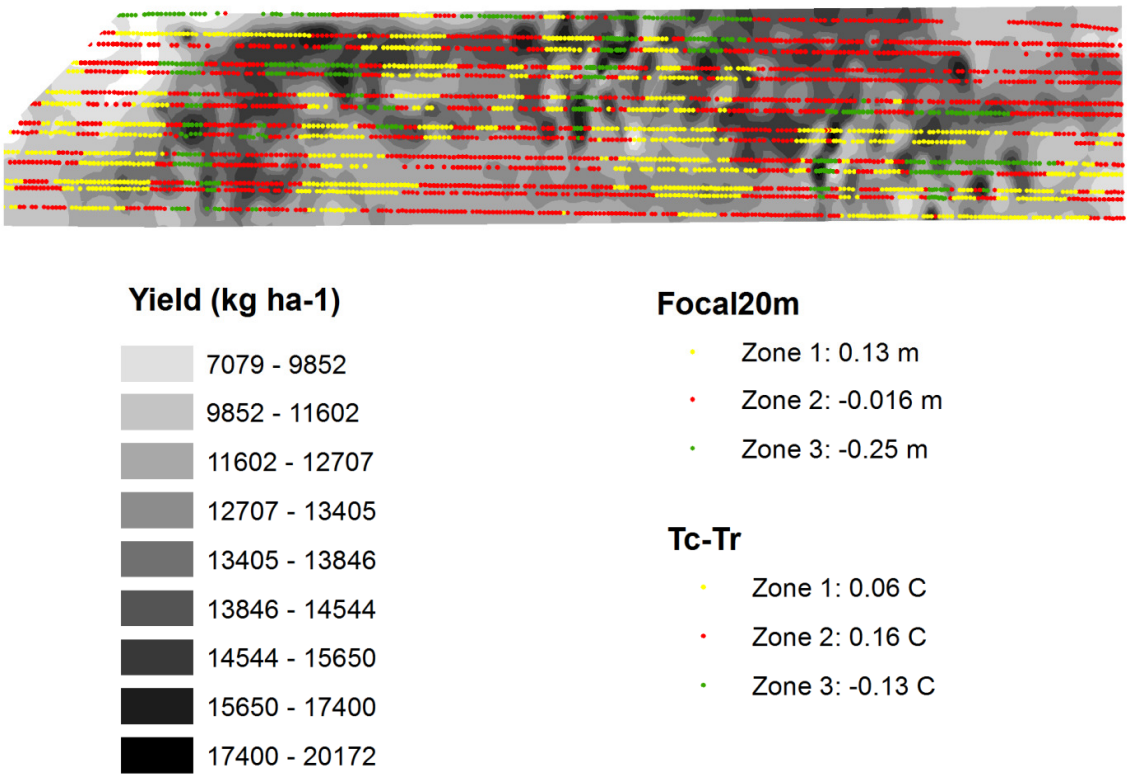

Figure 15. Average of Tc-Tr (ºC) and concave and convex areas in each zone delineated by Focal20m, overlaying yield map (kg ha^{-1}) for the HU10 field. Zones 1,2 and 3 were classified in three zones of different Focal20m values using MZA. For each zone was calculated the average value of Focal 20m and Tc-Tr.

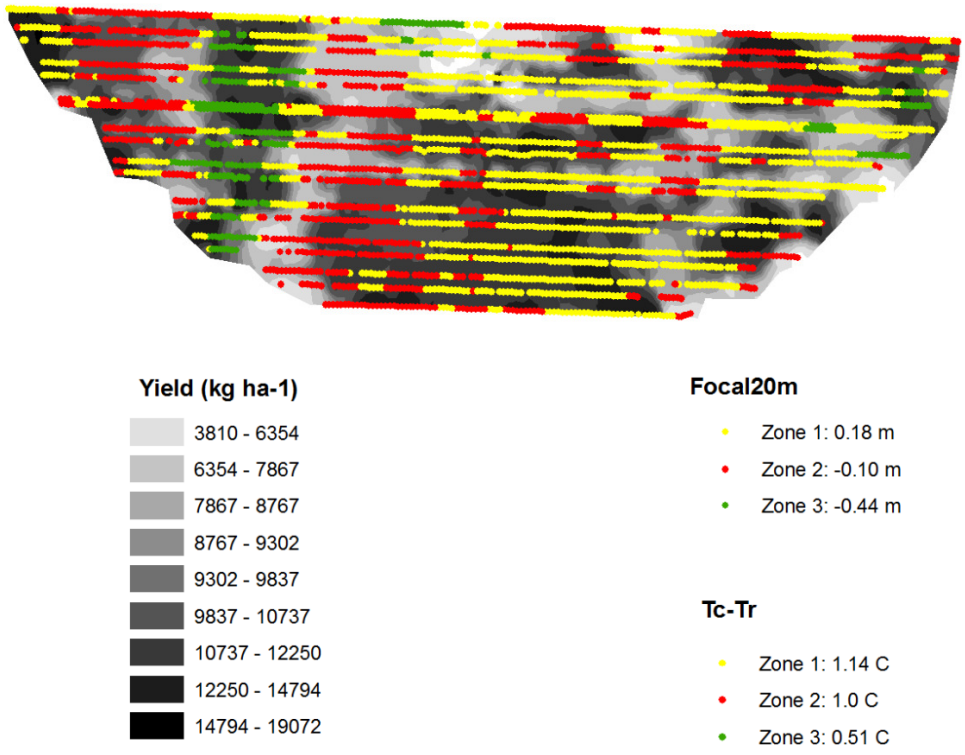

Figure 16. Average of Tc-Tr (ºC) and concave and convex areas in each zone delineated by Focal20m, overlaying yield map (kg ha^{-1}) for the BL10 field. Zones 1,2 and 3 were classified in three zones of different Focal20m values using MZA. For each zone was calculated the average value of Focal 20m and Tc-Tr.

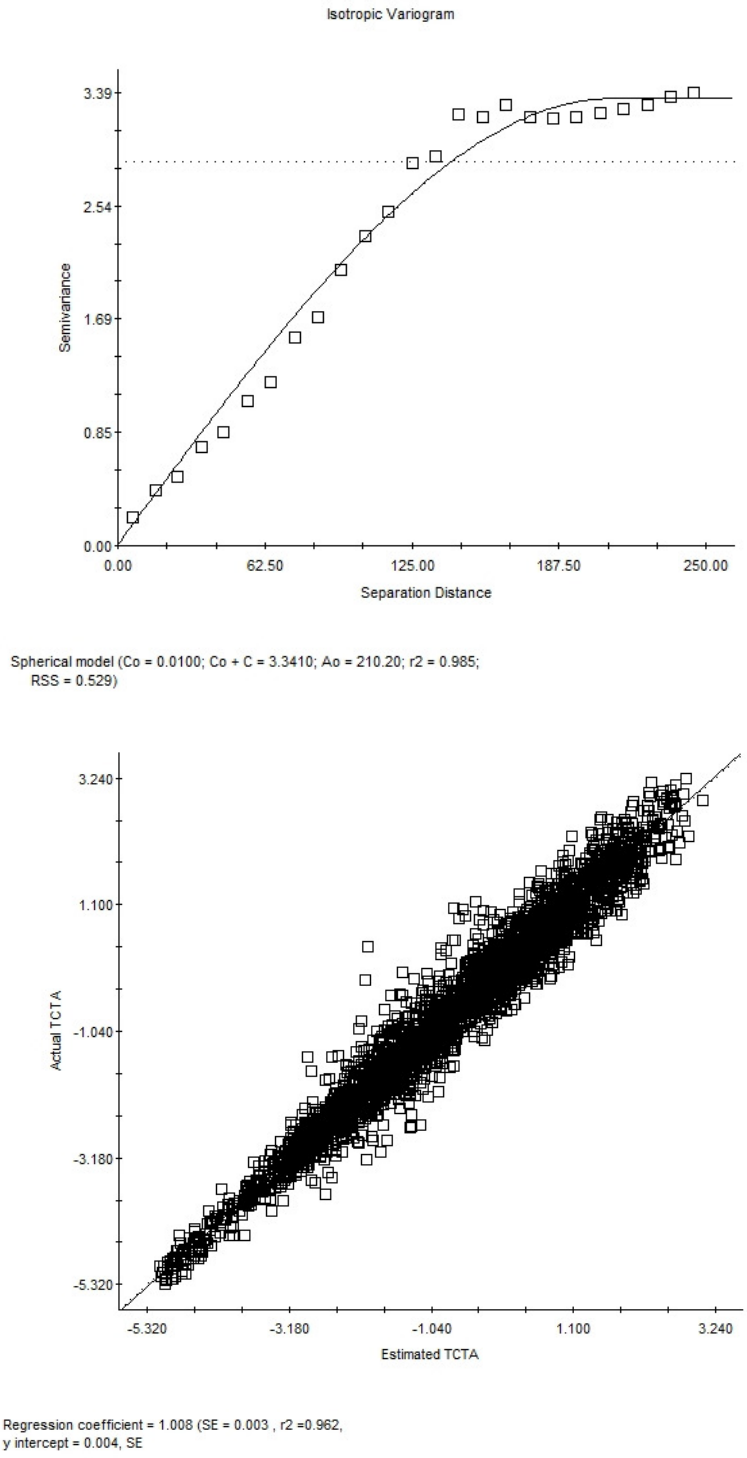

Figure 17. Semivariograms and cross validation for the canopy temperature (Tc-Tr) measured with IRT for the BR10 field.

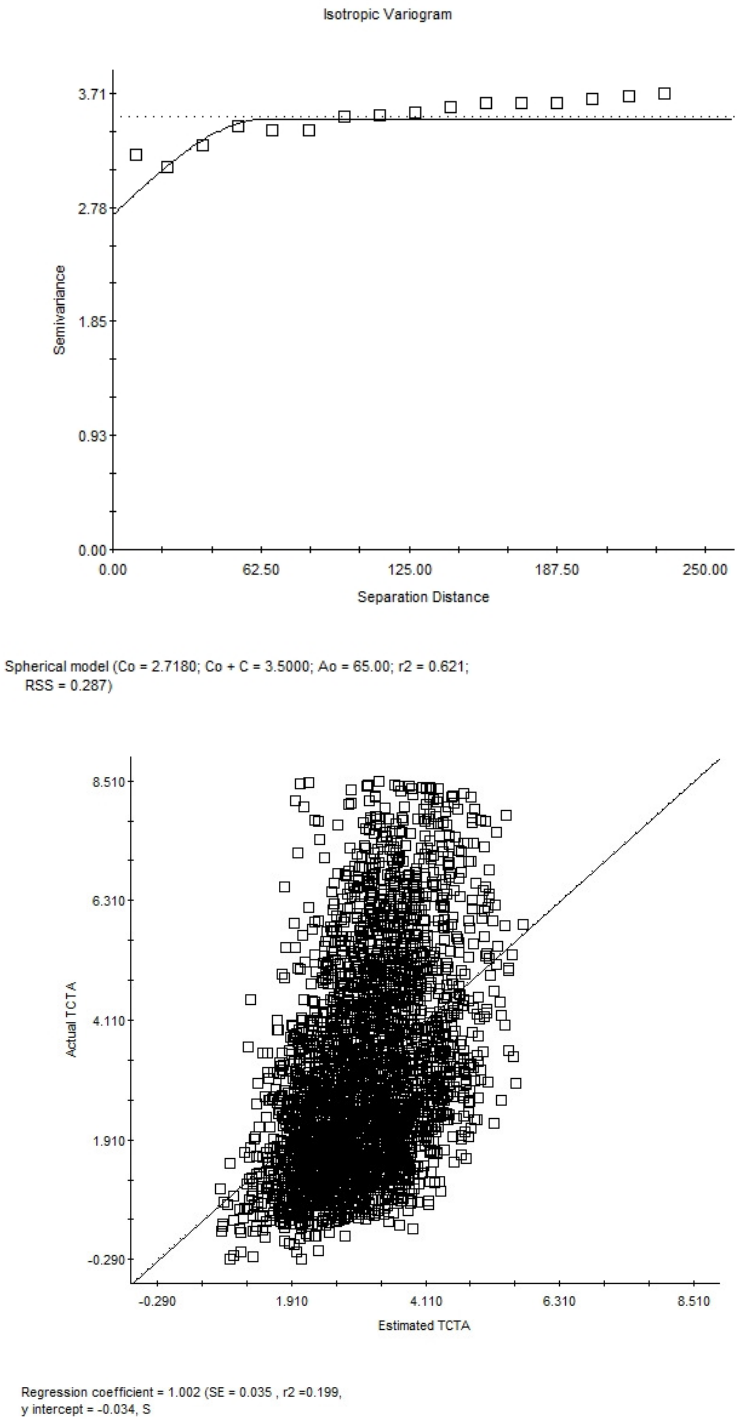

Figure 18. Semivariograms and cross validation for the canopy temperature (Tc-Tr) measured with IRT for the HU10 field.

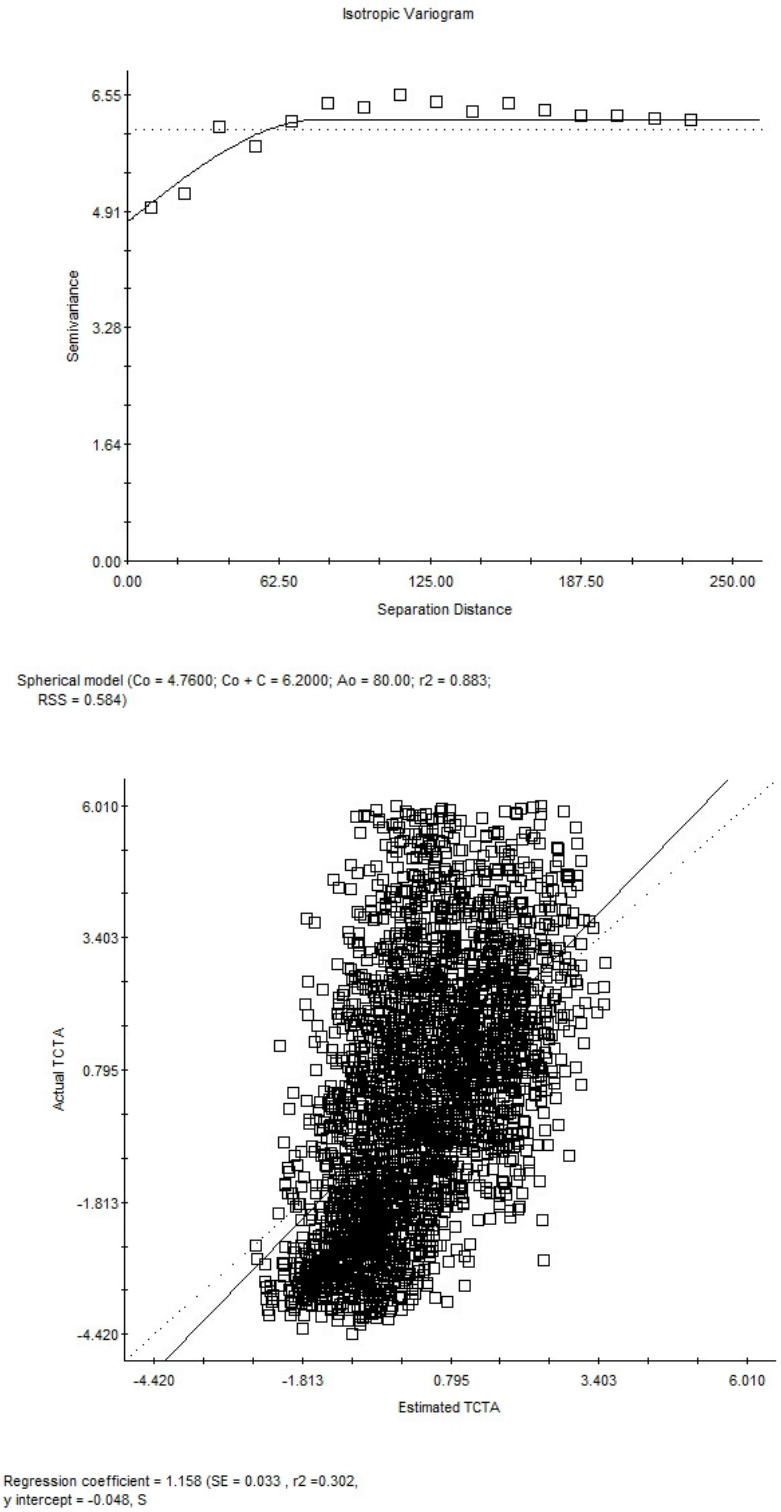

Figure 19. Semivariograms and cross validation for the canopy temperature (Tc-Tr) measured with IRT for the BL10 field.

Table 1. Analysis of variance calculated for canopy temperature (Tc) minus ambient temperature (Ta) obtained using infrared temperature sensors (IRT) at different irrigation levels (70 and 100 % ET), different previous crop (CC and CS) and nitrogen rates between growth stages R2 and R6 for the MS site.

Source of variation Effect	Num DF	Den DF	F Value	Pr > F
Irrigation Level	1	34.9	4.53	0.0404
N	3	174	4.38	0.0053
Irrigation Level*N	3	174	0.29	0.8308
Previous Crop	1	174	3.32	0.0703
Irrigation Level*Previous Crop	1	174	3.19	0.0757
N*Previous Crop	3	174	0.19	0.9047
Irrigation Level*N*Previous Crop	3	174	0.21	0.8869

Table 2. Tc-Ta at different irrigation levels, previous crop (corn after corn – CC and corn after soybeans – CS) and growth stages of corn (R2 to R6) for the MS site.

Tc-Ta (ºC)	Previous Crop			
	CC		**CS**	
			Irrigation Levels	
Growth stage	**70% ET**	**100% ET**	**70% ET**	**100% ET**
R2	-0.66a	-0.39a	-1.01a	-1.16a
R3	0.81a	0.68b	0.80a	-0.44b
R4	1.50a	-1.31b	1.50a	-1.68b
R6	1.46a	1.40a	1.75a	1.06b

* Letters in the rows indicate treatment mean differences in canopy temperature between irrigation levels (70 and 100% ET) inside the same previous crop, either CC or CS, using Duncan's Multiple Range Test ($p<0.05$).

Table 3. Treatment mean differences for Tc-Ta measured at different N rates across growth stages, irrigation levels and previous crops. Duncan Multiple Range Test ($p<0.05$) for MS site.

Differences of TRT Least Squares Means						
N	**N**	Estimate	Standard Error	DF	t Value	Pr > |t|
0	**75**	0.6301	0.3027	32	2.08	0.0454
0	**150**	0.9773	0.3027	32	3.23	0.0029
0	**225**	0.9025	0.3027	32	2.98	0.0054
75	**150**	0.3472	0.3027	32	1.15	0.2599
75	**225**	0.2724	0.3027	32	0.9	0.3749
150	**225**	-0.07476	0.3027	32	-0.25	0.8065

Table 4. Soil matric potential (cB – centibars) measured with soil moisture sensors (Watermark) installed in high and low elevation areas delineated from elevation inside the N-rich strip in each of the producer fields at the day of sensing.

Elevation	Depth (cm)	Soil Matric Potential (cB)		
High		BR10	HU10	BL10
	30	15	61	15
	60	12	50	20
	92	10	43	23
Low				
	30	15	13	18
	60	3	8	32
	92	3	4	30

Table 5. Zonal average for the points inside each non water-stressed (NonS) and water-stressed (S) zones delineated for each producer field.

Variable	BR10		HU10		BL10	
	NonS	**S**	**NonS**	**S**	**NonS**	**S**
Yield (kg ha^{-1})	11915*	10850*	13089*	12476*	9883	9838
NSI	1.16	1.11	0.99	0.96	1.01	0.98
HSI	1.15	1.13	0.98	0.95	1.00	0.98
Tc-Tr (ºC)	-1.70*	0.80*	-0.82*	0.90*	-1.39*	2.47*
Tc-Ta (ºC)	-1.96*	0.54*	2.16*	3.83*	-1.80*	1.74*
pH	6.50	6.53	7.23	7.14	7.11	7.24
P (mg kg^{-1})	15.99	16.83	16.31	17.34	17.48	16.93
NO_3 - N (µg g^{-1})	5.26	6.21	1.87	1.86	1.88	1.89
OM (g kg^{-1})	1.83	1.51	2.88	2.85	2.16	2.15
RTK (m)	523.38	523.84	573.76	574.51	1057.63	1057.39
ECsh (mS m^{-1})	1.22	1.05	8.83	8.99	3.84	3.66
Focal (m)	-0.05*	0.02*	-0.02*	0.01*	-0.03	-0.02

* Pairwise comparisons between NonS and S zones in the field using Tukey-test significant at $p < 0.05$

Table 6. Descriptive statistics for the variables measured in the BR10 field

Variable	N	Mean	Std Dev	Median	Minimum	Maximum
NSI	1448	1.17	0.10	1.19	0.95	1.42
HSI	1448	1.18	0.12	1.17	0.95	1.54
Tc-Tr	1448	-1.01	1.37	-1.18	-3.71	2.51
Yield	1448	11861	2155	12111	6400	17686
OM	1448	1.74	0.29	1.83	0.88	2.38
RTK_elevation	1448	523.49	0.36	523.49	522.65	524.91
EC_shallow	1448	1.18	0.37	1.14	0.46	2.01
Focal 20 m	1448	-0.05	0.21	-0.07	-0.57	0.73
P	1448	16.25	1.46	15.96	13.47	20.18
pH	1448	6.51	0.04	6.49	6.45	6.61
NO_3	1448	5.48	2.50	5.80	1.68	9.80

Table 7. Spearman rank correlations between variables for the BR10 field

Spearman Correlation Coefficients, N = 1448

Prob > |r| under H0: Rho=0

	NSI	**HSI**	**Tc-Tr**	**Yield**	**OM**	**RTK_elev**	**EC_sh**	**Focal20m**	**P**	**pH**	**NO_3**
NSI	1.000	0.478	-0.188	0.610	0.243	-0.411	0.356	-0.435	-0.177	-0.145	-0.133
HSI	0.478	1.000	-0.002*	0.294	0.000*	-0.141	0.087	-0.297	-0.103	-0.005*	-0.009*
Tc-Tr	-0.188	-0.002*	1.000	-0.138	-0.373	0.505	-0.066	0.053	0.044*	0.255	0.209
Yield	0.610	0.294	-0.138	1.000	0.249	-0.587	0.495	-0.579	-0.212	-0.174	-0.207
OM	0.243	0.000*	-0.373	0.249	1.000	-0.357	0.531	-0.011*	-0.261	-0.147	-0.190
RTK_elev	-0.411	-0.141	0.505	-0.587	-0.357	1.000	-0.528	0.616	0.209	0.226	0.217
EC_sh	0.356	0.087	-0.066	0.495	0.531	-0.528	1.000	-0.171	-0.212	-0.268	-0.315
Focal20m	-0.435	-0.297	0.053	-0.579	-0.011*	0.616	-0.171	1.000	0.153	-0.016*	-0.077
P	-0.177	-0.103	0.044*	-0.212	-0.261	0.209	-0.212	0.153	1.000	-0.307	-0.337
pH	-0.145	-0.005*	0.255	-0.174	-0.147	0.226	-0.268	-0.016*	-0.307	1.000	0.850
NO_3	-0.133	-0.009*	0.209	-0.207	-0.190	0.217	-0.315	-0.077	-0.337	0.850	1.000

* Correlations were not significant at $p < 0.05$

Table 8. Descriptive statistics for the variables measured in the HU10 field

Variable	N	Mean	Std Dev	Median	Minimum	Maximum
NSI	1461	0.97	0.01	0.97	0.95	1.00
HSI	1461	0.81	0.04	0.80	0.75	1.00
Tc-Tr	1461	2.80	1.61	2.40	0.00	8.63
Yield	1461	13234	1572	13321	3012	20172
OM	1461	2.97	0.49	3.09	1.31	3.77
RTK_elevation	1461	574.07	3.37	574.18	568.22	580.88
EC_shallow	1461	8.75	1.62	8.82	5.52	12.16
Focal20m	1461	-0.01	0.14	0.01	-0.59	0.65
P	1461	20.51	3.32	19.90	14.99	26.54
pH	1461	5.95	0.12	5.91	5.81	6.43
NO_3	1461	17.58	1.36	17.33	14.78	20.43

Table 9. Spearman rank correlations between variables for the HU10 field

Spearman Correlation Coefficients, N = 1461

Prob > |r| under H0: Rho=0

	NSI	**HSI**	**Tc-Tr**	**Yield**	**OM**	**RTK_elev**	**EC_sh**	**Focal20m**	**P**	**pH**	**NO_3**
NSI	1.000	0.118	-0.341	0.042*	0.041*	0.013*	-0.054	0.003*	0.101	0.080	0.009*
HSI	0.118	1.000	-0.198	0.099	-0.236	-0.304	-0.070	-0.159	0.007*	-0.053	0.043*
Tc-Tr	-0.341	-0.198	1.000	0.000*	0.127	0.142	0.082	0.043*	-0.048*	-0.052	-0.013*
Yield	0.042*	0.099	0.000*	1.000	-0.118	-0.295	0.153	-0.230	0.052	0.005*	-0.024*
OM	0.041*	-0.236	0.127	-0.118	1.000	0.469	-0.093	0.246	-0.114	0.046*	-0.013*
RTK_elev	0.013*	-0.304	0.142	-0.295	0.469	1.000	0.087	0.410	-0.060	0.066	-0.039*
EC_sh	-0.054	-0.070	0.082	0.153	-0.093	0.087	1.000	0.034*	0.013*	0.010*	-0.038*
Focal20m	0.003*	-0.159	0.043*	-0.230	0.246	0.410	0.034*	1.000	0.031*	0.009*	0.006*
P	0.101	0.007*	-0.048*	0.052	-0.114	-0.060	0.013*	0.031*	1.000	0.665	-0.571
pH	0.080	-0.053	-0.052	0.005*	0.046*	0.066	0.010*	0.009*	0.665	1.000	-0.482
NO_3	0.009*	0.043*	-0.013*	-0.024*	-0.013*	-0.039*	-0.038*	0.006*	-0.571	-0.482	1.000

* Correlations were not significant at $p < 0.05$

Table 10. Descriptive statistics for the variables measured in the BL10 field

Variable	N	Mean	Std Dev	Median	Minimum	Maximum
NSI	1570	1.03776	0.04506	1.0365	0.95007	1.18475
HSI	1570	1.03542	0.05714	1.02633	0.9502	1.2558
Tc-Tr	1570	0.38879	2.34457	-0.13	-3.805	8.14
Yield	1570	10242	2105	10448	62.3354	16852
OM	1570	2.15452	0.10902	2.09146	2.01096	2.53076
RTK_elevation	1570	1058	2.5039	1057	1054	1064
EC_shallow	1570	3.89199	1.52492	4.16693	1.0496	6.67878
Focal20m	1570	-0.02584	0.11194	-0.02643	-0.60461	0.27698
P	1570	16.68864	4.42243	15.86671	10.24663	27.39797
pH	1570	7.19001	0.18274	7.1985	6.80091	7.50846
NO_3	1570	1.88149	0.4291	1.72011	0.80253	3.05766

Table 11. Spearman rank correlations between variables for the BL10 field

Spearman Correlation Coefficients, N = 1570

Prob > |r| under H0: Rho=0

	NSI	HSI	Tc-Tr	Yield	OM	RTK_elev	EC_sh	Focal20m	P	pH	NO_3
NSI	1.000	0.246	-0.124	0.128	-0.088	-0.033*	-0.086	-0.086	-0.019*	0.188	0.041*
HSI	0.246	1.000	-0.133	0.118	0.191	0.168	0.214	-0.025*	0.012*	-0.034*	0.006*
Tc-Tr	-0.124	-0.133	1.000	0.147	-0.082	0.030*	0.096	0.104	-0.361	-0.266	-0.359
Yield	0.128	0.118	0.147	1.000	0.109	0.222	0.208	-0.011*	-0.264	0.047*	-0.135
OM	-0.088	0.191	-0.082	0.109	1.000	0.701	0.408	0.292	-0.100	-0.077	0.143
RTK_elev	-0.033*	0.168	0.030*	0.222	0.701	1.000	0.562	0.438	-0.307	0.114	0.005*
EC_sh	-0.086	0.214	0.096	0.208	0.408	0.562	1.000	0.322	-0.122	-0.006*	-0.113
Focal20m	-0.086	-0.025*	0.104	-0.011*	0.292	0.438	0.322	1.000	-0.078	-0.032*	0.097
P	-0.019*	0.012*	-0.361	-0.264	-0.100	-0.307	-0.122	-0.078	1.000	0.035*	0.354
pH	0.188	-0.034*	-0.266	0.047*	-0.077	0.114	-0.006	-0.032*	0.035*	1.000	0.178
NO_3	0.041*	0.006*	-0.359	-0.135	0.143	0.005*	-0.113	0.097	0.354	0.178	1.000

* Correlations were not significant at $p < 0.05$

GENERAL SUMMARY AND FUTURE SUGGESTIONS

The main objective of this research was to develop and validate strategies for in-season N fertilization using integration of plant-based canopy sensors, considering spatial variability and detailed topographical features.

The first experiment was conducted to compare different vegetation indices for on-the-go N assessment with different soil N residual from previous crop and irrigation levels. We found that some vegetation indices are less susceptible to the effects of irrigation and more reliable for N estimation in the corn plant. This is a good indication that the selection of index is very important depending on particular purposes.

The second experiment showed that local variations should be considered if the N-rich concept is used, due to local variations across agricultural fields. We also generated a database for yield linked with a sufficiency index response for diverse soil types, crop systems, topographical features, weather conditions, and locations in Nebraska. This database can be used for future algorithm development and simulations.

The third experiment showed that the correlation between optical and ultrasonic sensors were strong and that the integration of both sensors to measure the plant N status improves the use of on-the-go systems for N assessment.

These correlations were strong between both sensors and, in the fourth experiment, encouraged the development of a first approximation of an algorithm for in-season N fertilization based on the use of plant height information. It is important to note that plant height varies in response to several sources of stress other than N derived, so the algorithm is limited for some conditions.

The last experiment used on-the-go infrared thermometry in association with optical and ultrasonic sensors to study the spatial variability of crop water stress and the effects on grain yield. We were able to isolate the potential water stress with the integrated use of sensors and detailed topographical features, showing great differences in yield between zones delineated based on canopy temperature. This bodes well for improving the ability of sensors to make better decisions in real-time, considering the benefits of the integration of plant-related information.

Future research possibilities complementing this study include the use of local variations embedded in systems that can update the sufficiency index information on-the-go in commercial cornfields. Another complementary line of research would involve the development of optical sensors with the ability to sense water and nitrogen content in crops simultaneously. In more complex situations normally encountered in producers' fields (e.g., differing hybrids, plant population, crop history, and fertilization history), the integrated use of sensors and detailed layers of information should be beneficial. Certainly the area size and production system adopted will be of great importance when deciding the best strategy and conditions for the use of these technologies.

APPENDIX

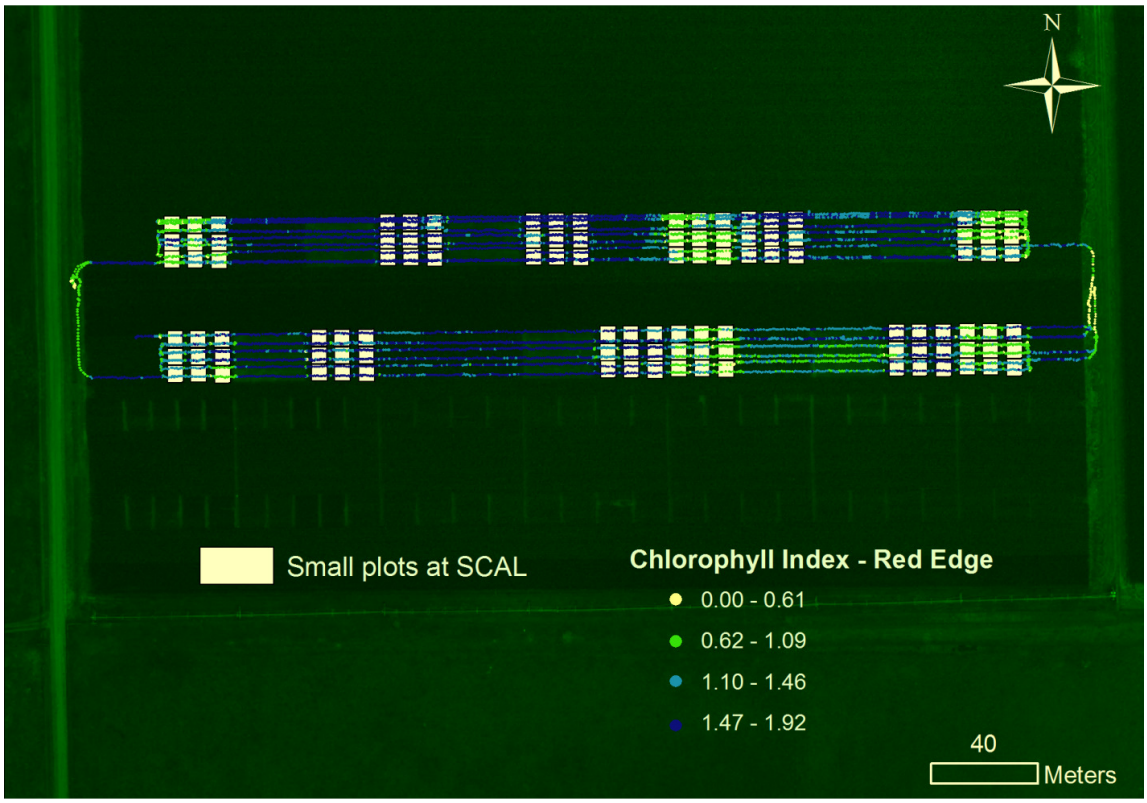

Appendix 1.1. Example of data collection using sensors with the bicycle platform in the MS field.

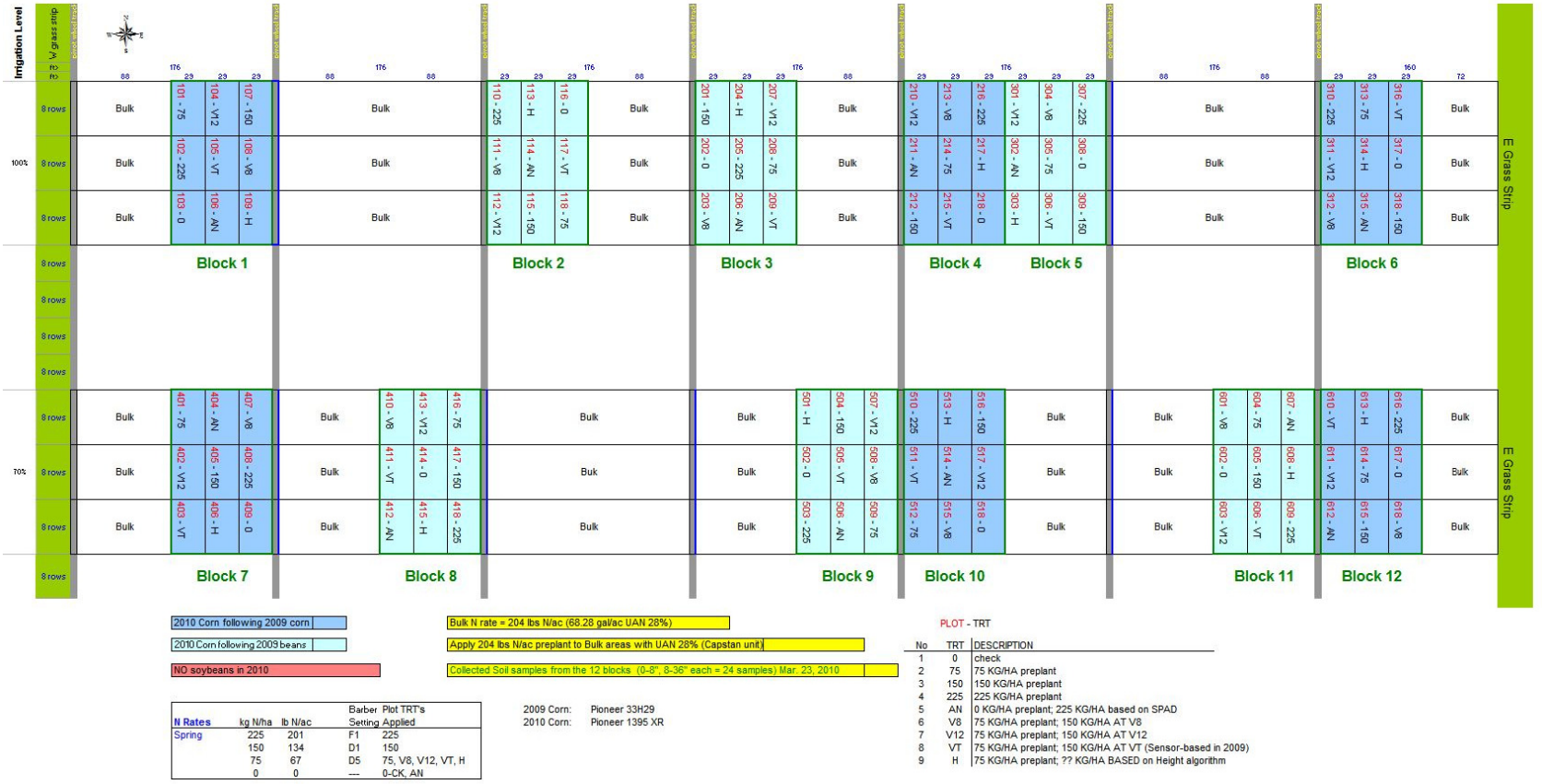

Appendix 1.2. Experimental design for the MS Study, that accommodates in parts data used for chapters 1, 2, 3, 4. Source: adapted from Glen Slater record keeping.

Appendix 2.1. Example of data collection using sensors with the bicycle platform in the BN field.

Appendix 3.1. High clearance machine used to take sensor readings and the sensor attachment to the spray boom.

Appendix 3.2. Real Time Kinematic GPS base station and equipment to measure EC (Veris). Source: (ARS/USDA server).

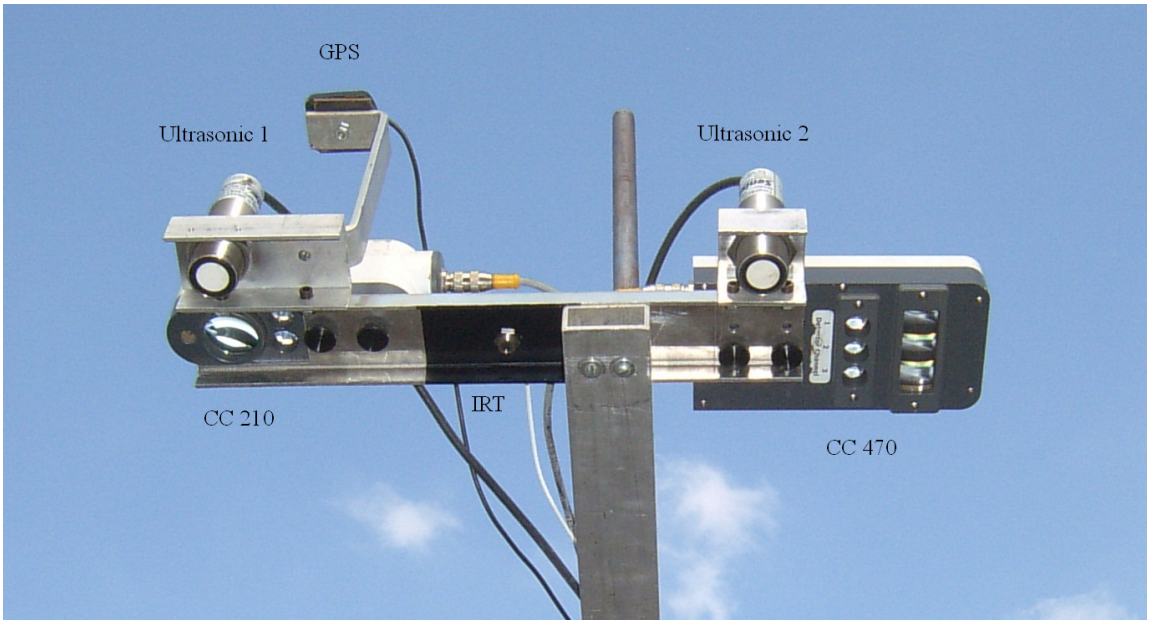

Appendix 3.1, 4.1. and 5.1. Apparatus designed to accommodate sensors in the bicycle platform or in the boom of high clearance sprayers. CC210 – Crop circle sensor, model 210 (2 bands – 880nm and 590 nm), CC470 – Crop Circle 470 (3 bands – 760nm, 720nm and 670nm), IRT – infrared thermometer for canopy temperature measurements.